

תל אביב

THE 14<sup>TH</sup> INTERNATIONAL SYMPOSIUM ON  
COMPUTER METHODS  
IN BIOMECHANICS AND  
BIOMEDICAL ENGINEERING

ABSTRACT BOOK

TEL AVIV, ISRAEL  
20 - 22 SEPTEMBER 2016  
[WWW.CMBBE2016.COM](http://WWW.CMBBE2016.COM)

# CONTENT

<b>Plenary Lectures</b>	3
<b>Session 1 - Advances in modelling and simulations of biological soft matter</b>	13
<b>Session 2 - Skin bioengineeringi</b>	18
<b>Session 3 - Patient specific computational modelling and tissue properties</b>	23
<b>Session 4 - Patient specific computational modelling and tissue properties 2</b>	26
<b>Session 6 - Computational modelling in cardiovascular diseases and therapies 1</b>	33
<b>Session 7 - Computational modelling in cardiovascular diseases and therapies 2</b>	39
<b>Session 8 - Computational respiratory mechanics and flows 1</b>	46
<b>Session 9 - Computational respiratory mechanics and flows 2</b>	49
<b>Session 10 - Computational approaches in synthetic biology, biomedical informatics, and molecular genetics</b>	54
<b>Session 11 - Dental biomechanics</b>	58
<b>Session 12 - Neural engineering and injuries to the brain, central nervous system, and eyes 1</b>	64
<b>Session 14 - Multiscale computer modelling in rehabilitation biomechanics</b>	70
<b>Session 15 - Neural engineering and injuries to the brain, central nervous system, and eyes 2</b>	76
<b>Session 16 - Reproductive biomechanics</b>	78
<b>Session 16 - Computational biomedical image-analysis and simulation 1</b>	80
<b>Session 17 - Modelling and simulations of vascular diseases</b>	82
<b>Session 18 - Models of drug transport and nano-medicine</b>	88
<b>Session 19 - Biomaterials and modelling</b>	93
<b>Session 20 - Computer modelling of tissue engineering processes</b>	98
<b>Session 21 - Interfaces in medicine and biology: from fracture to adhesion 1</b>	101
<b>Session 22 - Interfaces in medicine and biology: from fracture to adhesion 2</b>	107
<b>Session 23 - Tissue engineering scaffolding: Computer-aided design and 3D printing</b>	112
<b>Session 24 - Modelling mechanical and frictional interactions of tissues and cells 1</b>	117
<b>Session 25 - Modelling mechanical and frictional interactions of tissues and cells 2</b>	121
<b>Session 26 - Mathematical models in injury and disease</b>	126
<b>Session 27 - Knee joint</b>	131
<b>Session 28 - Mechanical interactions of cells with their environment 1</b>	137
<b>Session 29 - Modelling fluctuations in active matter</b>	142
<b>Session 30 - Mechanical interactions of cells with their environment 2</b>	147
<b>Session 31 - Tissue elastograph</b>	150
<b>Session 32 - Biomechanics for computer assisted medical interventions</b>	156
<b>Session 33 - Computer methods in vascular bioengineering</b>	162
<b>Session 34 - Biomechanics of movement foot and gait 2</b>	167
<b>Session 35 - Modelling soft tissue damage and healing</b>	170
<b>Session 36 - Biomechanics of movement foot and gait</b>	177
<b>Session 37 - Spine biomechanics, imaging and therapeutics 1</b>	182
<b>Session 38 - Spine biomechanics, imaging and therapeutics 2</b>	187
<b>Session 39 - Computational biomedical image-analysis and simulation 2</b>	191

## PLENARY LECTURES



### Mechanisms of pediatric TBI – Integrating computational and experimental approaches to understanding brain injury

14:00 – 14:50; 20 September 2016

Meeting room: Israel A

#### Prof. Susan Margulies

*School of Engineering and Applied Science  
 University of Pennsylvania  
 Pennsylvania, USA*

**Abstract:** The overall goal of my research program is to determine the mechanical thresholds associated with functional and structural injury in the brain and lung, ultimately to open avenues for injury prevention, intervention and treatment. Our lab pioneered functional and structural injury threshold measurement in the brain and lung to identify mechanisms of traumatic brain and lung injury. The research thrusts are united by a common, integrated approach consisting of experiments to measure cell or tissue function/structure under carefully controlled loading conditions (deformations or forces), complemented by computational models that extend these microscopic findings to a broad range of real-world, macroscopic environments. By integrating across scale and species and across computational and experimental approaches in our novel interdisciplinary platform, we translate basic research to clinical injury prevention and treatment strategies.

In traumatic brain injury (TBI), we integrate animal experiments, tissue and surrogate tests, clinical studies, and computational models to define biomechanical and molecular cascades, assess outcomes, and develop TBI interventions and treatments for children. By increasing our understanding of how head injuries occur in children, this crucial information enables engineers to design safer protective equipment (e.g. car seats, helmets) for children and provides physicians with tools to assist them in the diagnosis and treatment of head injuries in children.

**Short biography:** Dr. Margulies received her BSE in Mechanical and Aerospace Engineering from Princeton and MSE and PhD in Bioengineering from University of Pennsylvania. She is a Professor in Bioengineering, in the School of Engineering and Applied Science at the University of Pennsylvania, with over 30 years of experience in the area of traumatic brain injury research, and over 25 years in pulmonary biomechanics. Dr. Margulies is a Fellow of the American Society of Mechanical Engineers, Biomedical Engineering Society, and American Institute for Medical and Biological Engineering. With funding from NIH, NSF, CDC, and the Department of Transportation, she has trained 25 post-doctoral clinicians, engineers, and scientists, 26 graduate students, and dozens of undergraduates in her laboratory to translate basic research findings to improve clinical outcomes. mann Institute, Rehovot, Israel.



## Computational models of angiogenesis: relevance for tissue engineering and relation to cell mechanics

08:30 – 09:15; 21 September 2016

Meeting room: Israel A

### Prof. Hans van Oosterwyck

*Biomechanics section  
University of Leuven  
Belgium*

**Abstract:** Angiogenesis is the formation of new blood vessels from preexisting ones. As most tissues in our body require blood vessels for oxygenation and nutritional transport, angiogenesis plays a major role in their regeneration. We have previously developed a multiscale model of angiogenesis and integrated it into a computational model of bone regeneration. The model focuses on the interplay between oxygen, pro-angiogenic signaling and blood vessel formation on the one hand, and oxygen-mediated cell fate decisions during bone formation on the other hand. I will show examples on how model simulations can support the development of cellular and tissue engineering therapies that aim at enhancing bone regeneration, and how modelling can be used in combination with biofabrication technologies to improve the design of tissue engineering constructs.

In our multiscale model, endothelial cells that make up new blood vessels are represented as a single agent that can migrate according to directional cues, such as chemotactic and haptotactic signals. In reality cell migration in a three-dimensional matrix requires matrix degradation, cell adhesion and the application of cell-generated protrusive and contractile forces, which in the context of angiogenesis are all modulated by pro-angiogenic signals, like Vascular Endothelial Growth Factor (VEGF). Having computational models of angiogenesis that explicitly incorporate cell-matrix mechanics and mechano-chemical feedback would enable to explore the importance of cell mechanical principles for making new blood vessels, which is an aspect that we could not address by our previous models. We have recently built cell and matrix mechanical models, based on particle-based, meshless methods, and have coupled them into a model of cell migration. I will discuss some methodological advances and their comparison to experimental data, such as Traction Force Microscopy (TFM) data

**Short biography:** Hans Van Oosterwyck (DOB 02.02.1972) is a professor and the chair of the Biomechanics section (Mechanical Engineering Department) at KU Leuven, where he is heading the Mechanobiology and Tissue Engineering research group. He holds an MSc degree in Materials Engineering (1995) and a PhD degree in Engineering (2000), both obtained at KU Leuven (Leuven, Belgium). He has been a postdoctoral fellow at the AO Research Institute (Davos, Switzerland) in 2004-2005 and a visiting scientist at the University of Zaragoza (Spain) in 2009. He is a member of Prometheus, the Leuven R&D Division for Skeletal Tissue Engineering. In 2012 he was awarded an ERC Starting Grant on the role of cell-matrix interaction in angiogenesis ('MAtrix: In silico and in vitro Models of Angiogenesis: unraveling the role of the extracellular matrix'). His research focuses on the development of quantitative tools for unraveling the role of the microenvironment for cell fate, in particular the development of multiscale computational models for studying the importance of mechanics and mass transport for angiogenesis and bone regeneration. His research group is strongly interdisciplinary and combines computational modelling with experimental techniques, adopted from various fields, such as cell and tissue mechanics, cell biology, biomaterials and biophysics.

Hans Van Oosterwyck has been a Council Member of the European Society of Biomechanics (ESB) since 2006. He has been the President of the ESB between 2012-2014.



## Growth-induced mechanobiological processes are determinants of adult tissue structure and mechanics – a multi-scale multi-phase analysis

13:45 – 14:30; 21 September 2016

Meeting room: Israel A

### Prof. Yoram Lanir

*Faculty of Biomedical Engineering  
Technion – Israel Institute of Technology  
Israel*

**Abstract:** Biological tissues have the unique ability to grow and remodel (G&R) under altered mechanical environment by changing their size, shape, structure and mechanical properties. Adaptation occurs since in order to survive and proliferate, tissue cells strive for a homeostatic mechanical environment by adapting their extracellular matrix (ECM) via turnover (production and/or degradation) of ECM constituents. In the present study a mechanistic structural computational simulation was developed for soft tissues G&R based on the local biological processes involved. The framework incorporates the specific mechanical and turnover properties of each constituent. The resulting predictions are compatible with the evolution of adult tissue structure and mechanical properties. Specifically, the theory predicts the evolution of well-known soft tissues features such as the non-uniform undulation of collagen fibers and associated tissue non-linear convex strain-stress relationship, the evolution of growth-induced pre-strain and pre-stress, the dominance of non-remodelling elastin fibers in load bearing at low strain and the switch to collagen dominance at high strain levels, and the onset of significant anisotropy in tissues structure and mechanical properties.

**Short biography:** Dr. Lanir earned his PhD degree from the Technion and did his post-doctoral training in UCSD. He joined the Technion in 1973 as a faculty member in Biomedical Engineering. In 1974-1975 he served as the department head. In 1990 he was a founding member of the World Congress in Biomechanics and served in its council till 1998. In 1995-1999 he initiated and led the establishment of the new Technion undergraduate program in Biomedical Engineering, the first in Israel. In 1998-2008 he held the Technion Marcus Reiner chair in Rheology till his retirement. He served as an associate editor of the ASME Journal of Biomechanical Engineering in 2005-2010. Dr. Lanir experimental and theoretical studies are in two fields of Biomechanics: the underlying molecular, micro-structural, transport and mechano-biological aspects of tissues mechanics and of their evolution under growth and remodelling, and the coronary flow and its regulation.

Dr. Lanir won twice the Henri Gutwirth Research Award (1982,1985), the Lee Silver Friedman Award in Biomedical Engineering (1992) and the 2003 Richard Skalak Best Paper Award, by the Bioengineering Division, American Society of Mechanical Engineering.



## Physical theories of cell mechanics

14:00 – 14:50; 22 September 2016

Meeting room: Israel A

### Prof. Sam Safran

*Department of Materials and Interfaces  
The Weizmann Institute  
Israel*

**Abstract:** Cell contractility at either the coarse-grained level of an entire cell or at the sub-cellular level of individual acto-myosin fibers, can be understood using the concept of elastic force dipoles. These dipoles interact via their mutual deformations of the surrounding elastic medium which can be either the extra-cellular matrix (in the case of cells modeled as dipoles) or the internal, cellular cytoskeleton (in the case of acto-myosin fibers within the cell). The theory of these elastically mediated interactions combined with the unique "living" nature of cells (implying that the activity of these dipoles is non-equilibrium and energy consuming) allows us to understand the organization and order of acto-myosin fibers within the cytoskeleton of a single cell or among contractile cells in systems of non-motile and adherent cells. We present the general theory of elastic interactions in the context of acto-myosin activity with examples that demonstrate its utility in understanding experiments on cytoskeletal alignment in stem cells that differentiate into muscle cells, the structure and beating of cardiomyocytes, very long-ranged cell-cell interactions in fibrous elastic matrices, and elastically controlled diffusion of biomolecules that trigger development in embryos.

**Short biography:** Safran received his Ph.D. in Physics from MIT, followed by a postdoctoral position at Bell Laboratories. From 1980-1990 he served as a Senior Staff member in the Complex Fluids Physics group of Exxon Research and Engineering in New Jersey. Prof. Safran joined the faculty of the Weizmann Institute of Science in 1990 as a Professor in the Department of Materials and Interfaces. He has served as Dean of the Graduate School and as Vice President of the Weizmann Institute. His current research interests in the theory of soft and biological matter focus on cellular response to mechanical stress and domain ("raft") formation in charged and multicomponent membranes. The latter extends his earlier work on surfactant membranes that unified their mesoscale structures, phase behavior and dynamics. Recent honors include the de Gennes Lecture Award of the European Physical Journal and the Beller Lectureship of the American Physical Society. He is the author of a graduate level text on the physics of surfaces, interfaces and membranes, translated into Japanese and Chinese.

## ABSTRACTS OVERVIEW ACCORDING TO SESSION

### Session 1 - Advances in modelling and simulations of biological soft matter

- Computational analysis of x-ray data and high-resolution modelling of self-assembled bio-structures; *Uri Raviv*
- Large-scale coarse-grained simulations of biomembranes using meshless membrane model and lattice monte MC model; *Hiroshi Noguchi*
- Accurate discrete-time isothermal and isobaric molecular dynamics; *Niels Grønbech-Jensen*
- Influence of periodic boundary conditions on lateral diffusion in membranes; *Frank Brown*
- Numerical simulations for the determination of chemical gradients induced in collagen and fibrin hydrogels; *Mar Córdor*

### Session 2 - Skin bioengineering

- Evaluating skin mechanics and ageing features with digital image correlation; *Kemal Levi*
- Comparison of anisotropic models to simulate the mechanical response of facial skin; *Cormac Flynn*
- In vivo quantification of skin tension and stiffness using surface wave propagation; *Aisling Ni Annaidh*
- On the mechanics of skin wrinkles: the role of skin microrelief; *Georges Limbert*
- Modelling skin mechanics under shear deformation in 3D; *Jibbe Soetens*

### Session 3 - Patient specific computational modelling and tissue properties

- Personalized FEA may reduce unnecessary prophylactic surgeries in femurs with metastatic tumors - a clinical study; *Zohar Yosibash*
- Topology optimization for design of porous scaffolds for bone tissue engineering; *Oded Amir*
- The generic modelling fallacy: is it happening in your lab?; *Daniel Robertson*

### Session 4 - Patient specific computational modelling and tissue properties 2

- Characterization of irreversible physio-mechanical processes in stretched fetal membranes; *Yulia Marom*
- Patient-specific modelling in the absence of materials property data: Combining experimental and computational techniques to gain insights; *Douglas Cook*
- About unloading control at leg orthotics; *Il'ya Dashevskiy*
- A database of pelvis finite element models for a high-throughput pipeline of dynamic, biofidelic, sideways fall impact simulations; *William Enns-Bray*
- Patient-specific model generation for foot pressure ulcer prevention; *Antoine Perrier*
- Prediction of subject specific cartilage degeneration within the knee and comparison to experiments: data from the osteoarthritis initiative; *Mika Mononen*
- Contact pressure variation between eight subject-specific finite element models of the first metatarsophalangeal joint; *Jennifer Boyd*

### Session 6 - Computational modelling in cardiovascular diseases and therapies 1

- Quantifying the effect of in vivo alginate injections on healthy myocardial tissue structure; *Kevin Sack*
- On solution of the cox (1968) problem; *Raz Hechter*
- Coherent structures govern white blood cell transport in cerebral aneurysms; *Mark Epshtein*
- Fluid-structure interaction bio-mechanical models of bicuspid aortic valves; *Karin Lavon*
- Fluid-structure simulation of a transcatheter aortic valve implantation: Potential application to patient specific cases; *Francesco Migliavacca*
- Computational fluid dynamics for intracranial aneurysm rupture prediction & post treatment hemodynamic analysis; *Albert Einstein George*

### Session 7 - Computational modelling in cardiovascular diseases and therapies 2

- A multi-resolution analysis of the mitral valve geometry for the development of personalized models; *Michael Sacks*
- Mechanical stress-strain relations of pig's myocardium, experiments and constitutive models; *Avihai Spizzichino*
- A fun-g-type exponential constitutive model accurately captures and differentiates between strain- and remodelling-induced stiffening in conduit pulmonary arteries; *Mark Golob*
- Stress analysis of normal and pathological arteries with residual stress; *Shaoxiong Yang*

- Comparison of different strain-based parameters to identify human left ventricular myocardial infarct: a three-dimensional finite element study; **Gerardo Kenny Rumindo**
- Patient-specific simulations of aortic valve flows; **Arnas Kačeniauskas**
- Validation of a four chamber porcine model; **Brian Baillargeon**

### Session 8 - Computational respiratory mechanics and flows 1

- The instantaneous stokes number for aerosol transport and deposition in the respiratory airways; **Laura Nicolaou**
- Fate of inhaled aerosols in heterogeneous pulmonary acini; **Josue Sznitman**
- Recruitment and derecruitment in a comprehensive computational lung model; **Wolfgang A. Wall**

### Session 9 - Computational respiratory mechanics and flows 2

- Distribution of nano-and micro-particle depositions in a murine pulmonary acinar model; **Toshihiro Sera**
- In silico assessment of mouth-throat effects on regional deposition in the conducting human airways; **Stavros Kassinos**
- Respiratory flow behavior in bronchial airways: evolution from childhood to adulthood; **Katrin Bauer**
- Multi-D models for respiration and aerosol in health and disease; **Irene Vignon-Clementel**
- Chest wall kinematics using triangular cosserat point elements in helathy and neuromuscular subjects; **Dana Solav**

### Session 10 - Computational approaches in synthetic biology, biomedical informatics, and molecular genetics

- Reliable analog and digital computation in living cells; **Ramez Daniel**
- What can mutation patterns observed in antibody sequences tell us about antibody-antigen interactions, and about the dynamics of the adaptive immune response?; **Gur Yaari**
- Following the footsteps of the ribosome throws light on protein evolution and the design principles of gene expression engineering; **Renana Sabi**
- Yeast response to multiple carbon sources: a case study of combinatorial signal integration, **Yonatan Savir**

### Session 11 - Dental biomechanics

- How and why do dental implant fracture; **Keren Shemtov-Yona**
- Biomechanical evaluation of pre and post – bilateral sagittal split mandibular osteotomy on 3D models for obstructive sleep apnea using finite element analysis; **Aishwarya Srinivasan**
- Studying implant osseointegration in the sika deer antler; **Christoph Bourauel**
- Influence of tooth dimension on the initial mobility – a numerical study; **Cornelius Dirk**
- Numerical analysis of a combined implant-residual tooth supported prosthesis after tooth hemisection - Influence of residual root number and bone density; **Ludger Keilig**
- Numerical modelling of dental implant-bone interface; **Raouf Korabi**

### Session 12 - Neural engineering and injuries to the brain, central nervous system, and eyes 1

- Brain injury metric based on computed axon strains; **Remy Willinger**
- Dynamic micro indentation of animal neural tissue; **David MacManus**
- Integration of finite element analysis with MR imaging for estimation of in vivo brain deformation; **Brittany Coats**
- Development of a physical brain-skull model for the study of neurosurgical brain shift; **Matthew Potts**
- Evaluation of a mechanically-coupled reaction-diffusion model for macroscopic brain tumor growth; **Daniel Abler**
- Development of a computational model to aid prediction of neurosurgical brain shift; **Nicholas Bennion**

### Session 14 - Multiscale computer modelling in rehabilitation biomechanics

- Computational models of foot and ankle for foot support design; **Ming Zhang**
- Multiphysics modelling of the effects of toxic biowastes from mechanically damaged muscle cells on the damage propagation of deep tissue injury; **Arthur Mak**
- Inverse analysis of biaxial tensile testing on human skin; **Jibbe Soetens**

- Finite-element analysis and experimental investigation of grooved and porous collar in inducing extra-cortical bone growth for mechanical fixation; **Vee San Cheong**
- A preliminary study on the influence of cadence on path optimized handle-based propulsion for wheelchairs; **Margit Gföhler**
- Investigation of the biomechanical behavior of the urethra duct in relation with lumen occlusion; **Arturo Natali**

### Session 15 - Neural engineering and injuries to the brain, central nervous system, and eyes 2

- 3D FE head modelling: Techniques and solutions for impact analysis; **Philippe Young**
- Theoretical analysis of the potential ultrasonic neuromodulation mechanisms; **Michael Plaksin**

### Session 16 - Reproductive biomechanics

- Transitional hemodynamics and gas exchange in premature postpartum adaptation: Delayed vs. immediate cord clamping; **Kerem Pekkan**
- Patient-specific biomechanical simulations of pregnancy; **Andrea Westervelt**

### Session 16 - Computational biomedical image-analysis and simulation 1

- Statistical shape models to reconstruct whole femur surface from pelvic radiographs; **John O'Connor**
- Image-based transport modeling in human placental terminal villi; **Romina Plitman Mayo**

### Session 17 - Modelling and simulations of vascular diseases

- High-Fidelity numerical simulations of vortical structures and cardiovascular disease; **Steven Frankel**
- Patient-specific numerical model of calcific aortic stenosis and its treatment by balloon-expandable transcatheter aortic valve: Effect of positioning on the anchorage; **Gil Marom**
- Pulmonary arterial biaxial tissue mechanics in PAH; **Daniela Valdez-Jasso**
- Modelling and computational simulation of hemodynamically induced atherosclerosis; **Pinhas Bar-Yoseph**
- Modelling of microstructure and mechanics of healthy and aneurysmatic abdominal aortas; **Justyna Niestrawska**
- Results of in-vitro tests on a 2:1 prototype of a percutaneous ventricular assist device; **Alen Karabegovic**

### Session 18 - Models of drug transport and nano-medicine

- Computer simulation of electroporation and drug transport through membranes; **Nenad Filipovic**
- Targeted delivery in upper airways using inhaled magnetic particles; **Yan Ostrovski**
- Multifunctional Nanoconstructs for cancer theranosis: from in silico to preclinical models; **Paolo Decuzzi**
- Designing shear responsive nano-medicine for targeted drug delivery; **Netanel Korin**
- Drug-eluting implants: Release mechanisms and models; **Meital Zilberman**

### Session 19 - Biomaterials and modelling

- Simulation of protein folding based on statistical knowledge; **Simcha Srebnik**
- Molecular modelling of biomaterials used in drug delivery systems; **Dafna Knani**
- Computational modelling of cellular bodies in high elastic deformation; **Hayley Wyatt**
- Mechanical flexure behavior of bio-inspired collagen-reinforced thin sheet composites; **Mirit Sharabi**
- Development of an adaptive bone remodelling model driven by mechanical and biological stimuli for implant analysis; **Vee San Cheong**

### Session 20 - Computer modelling of tissue engineering processes

- Neotissue growth in a perfusion bioreactor system: a multiscale multiphysics model; **Hans van Oosterwyck**
- Combining an in silico model with in vitro experiments to create a framework for process optimization. Case study: Optimizing the production of aggregates in a micro-well; **Maxim Cuvelier**
- Computational analysis of flow and biochemical transport in a multichamber bioreactor; **Laura Iannetti**

### Session 21 - Interfaces in medicine and biology: from fracture to adhesion 1

- An isogeometric finite element model for the mechanics of lipid bilayer membranes; **Roger Sauer**

- Multiscale moving contact line theory and simulation of cell motility; *Shaofan Li*
- Simulating contact phenomena in dental biomechanics; *Christoph Bourauel*
- Manufacturability of custom endosteal dental implants by selective laser melting; *Eric Wagnac*
- Preclinical analysis to assess aseptic loosening of orthopaedic implants; *Heidi-Lynn Ploeg*
- Measuring the biomechanical properties of the bone-implant interface: a multiphysical approach; *Guillaume Haiat*

### Session 22 - Interfaces in medicine and biology: from fracture to adhesion 2

- Mechanobiology of bone-implant interface; a mixed theoretical and experimental approach; *Pascal Swider*
- Wave propagation in generalized continua in presence of interfaces; *Giuseppe Rosi*
- Tunable porous biomaterial to reduce stress-shielding in total hip arthroplasty; *Damiano Pasini*
- Improving acetabular reaming quality for total hip arthroplasty using a serrated blade reamer; *Yvan Petit*
- Computer modelling of the spine to support next generation of prevention and intervention injuries and pathologies; *Pierre-Jean Amoux*

### Session 23 - Tissue engineering scaffolding: Computer-aided design and 3D printing

- Design and fabrication of a site specific bioresorbable cage for tibial tuberosity advancement in dogs; *Paulo Fernandes*
- Biomanufacturing as an effective route for skeletal tissue regeneration; *Marco Domingos*
- A new multiscale micromechanical model of vertebral trabecular bones; *Eyass Massarwa*
- Graph based over-segmentation of bone porous micro-structure; *Yizhak Ben-Shabat*
- Computer-aided tissue engineering of a novel bone-ligament-bone multistructured construct; *Laurent Cedric*

### Session 24 - Modelling mechanical and frictional interactions of tissues and cells 1

- Adhesive, contractile, and resistive forces during cancer cell invasion in connective tissue; *Ben Fabry*
- Artificial hydrogels to study cell-matrix-mechanics; *Florian Rehfeldt*
- Mechanical and molecular mechanisms driving intercellular communication during collective cell migration; *Assaf Zaritsky*
- Two distinct actin networks mediate traction oscillations to confer mechanosensitivity of focal adhesions; *Jian Liu*

### Session 25 - Modelling mechanical and frictional interactions of tissues and cells 2

- Physics of adhesion regulation: The case of cadherin; *Ana Suncana Smith*
- Force application model for defining mechanical mechanisms of metastatic invasion; *Martha Alvarez*
- Theoretical analysis of stress distribution and cell polarization surrounding a model wound; *Yonit Maroudas-Sacks*
- Mechanotransduction during cell adhesion: Numerical analysis of the influence of substrate topology; *Maxime Vassaux*
- Micromechanics, wrinkling formation, and wave propagation in soft matrix-fiber and layered biological tissues; *Stephan Rudykh*

### Session 26 - Mathematical models in injury and disease

- Mathematical modelling of burns; *Fred Vermolen*
- Agent-based multi-level simulations of drug-induced liver damage and regeneration: from data to models and back; *Dirk Drasdo*
- Modelling fibroblast populated collagen lattice contraction; *John Dallon*
- A robust and efficient adaptive multigrid solver for the optimal control of phase field formulations of geometric evolution laws; *Anotida Madzvamuse*
- Implications of anomalous kinetics on the course of wound contraction and closure; *Etelvina Javierre*

### Session 27 - Knee joint

- The effect of non-surgical realignment therapies upon knee contact mechanics; *Howard Hillstrom*
- Application of validated computational knee model to predict improved joint reconstruction; *Rajshree Mootanah*
- Simulation of coupled neuromuscular coordination and knee joint mechanics during movement; *Colin Smith, Darryl Thelen*
- UKA component fatigue test development using DOE and FEA; *Danny Levine*
- Soft tissues loadings on healthy knee at different physiological flexions: A coupled experimental-numerical approach; *Woo Suck Han*
- Effect of weight loss on cartilage stresses in obese subjects: Data from the osteoarthritis initiative (OAI); *Olesya Kleis*

## Session 28 - Mechanical interactions of cells with their environment 1

- Nonlinear elasticity in the interaction of living cells with their mechanical environment; *Yair Shokef*
- Mechanics of cell adhesion: principles of symmetry breaking and self-polarization; *Assaf Zemel*
- Shape regulation generates elastic interaction between active force dipoles; *Roman Golkov*
- Cellular mechanosensitivity: Cell reorientation under cyclic stretching; *Eran Bouchbinder*
- Model of cell-cell mechanosensing in non-linear fibrous matrix; *Ayelet Lesman*

## Session 29 - Modelling fluctuations in active matter

- Active contraction of biological fiber networks; *Pierre Ronceyay*
- Broken detailed balance at mesoscopic scales in active biological systems; *Chase Broedersz*
- A chemo-mechanical free-energy-based approach to model durotaxis and extracellular stiffness-dependent contraction and polarization of cells; *Vivek Shenoy*
- Fluctuations spectrum in active gels; *Yael Roichman*
- Quantitative characterization of the nuclear refractive index; *Mirjam Schürmann*

## Session 30 - Mechanical interactions of cells with their environment 2

- Migration, force generation and mechanosensing of tumour cells in 3-dimensional environments; *Ben Fabry*
- Proximity of metastatic cells strengthens the mechanical interaction with their environment; *Yulia Merkher*
- Isothermal Langevin dynamics in systems with power-law spatially-dependent friction; *Shaked Regev*

## Session 31 - Tissue elastography

- Integrating cardiac biomechanics and MR elastography; *David Nordsletten*
- Magnetic resonance elastography of the brain; *Katharina Schregel*
- Paediatric liver viscoelastic properties differ from adults: A multifrequency MR elastography study; *Lynne Bilston*
- Functional changes in the shear modulus of the mouse brain cortex observed with electrical stimulation of the hind limb using magnetic resonance elastography (MRE); *Samuel Patz*
- Investigating the performance of a new ultrasonic elastography technique for cardiac stiffness assessment through finite element simulations; *Pascal Verdonck*
- Impacting cancer cells via mechanical waves: Can we change cellular behavior?; *Marties Hoelzl*

## Session 32 - Biomechanics for computer assisted medical interventions

- Breast biomechanical modelling for compression optimization in digital breast tomosynthesis; *Anna Mira*
- Coronary atherosclerotic plaque elasticity reconstruction methods based on in vivo intravascular ultrasound strain measurements; *Jacques Ohayon*
- An integrated and non-intrusive computational approach to uncertainty quantification and statistical inverse problems for soft tissue biomechanics: Towards model selection; *Paul Hauseux*
- Improving patient safety through real-time numerical simulation; *Stephane Cotin*
- Peri-prosthetic fractures simulation for minimal invasive surgery; *Daniel Baumgartner*
- Novel model for load carriage ergonomics optimization; *Amir Hadid*

## Session 33 - Computer methods in vascular bioengineering

- A predictive multiscale model for simulating platelets activation in shear flows; *Danny Bluestein*
- Computational modelling of embolus transport in the inferior vena cava; *Keefe Manning*
- High resolution pressure drop for combined functional and biomechanical assessment of coronary stenoses – a validated numerical study; *Oren Rotman*
- Sensitivity of pulmonary outflow patch reconstruction with respect to the native and artificial tissue properties; *Kerem Pekkan*
- Physiologic modelling and surgical optimization in single ventricle congenital heart defects; *Alison Marsden*

### Session 34 - Biomechanics of movement foot and gait 2

- The effect of knee osteoarthritis on gait variability and equilibrium ability; **Rita Kiss**
- A Key Dataset for the Comprehensive Assessment of the Musculoskeletal System: The CAMS-Knee Project; **William R. Taylor**
- A compute biomechanical gait analysis comparison using walking sticks and walker in adult scoliosis patients; **Ram Haddas**

### Session 35 - Modelling soft tissue damage and healing

- Damage of soft biological tissues: Continuum model and FE implementation; **T. Christian Gasser**
- Finite element reconstruction of acute subdural haematoma cadaver experiments; **Zhao Ying Cui**
- The effect of strains and stresses on collagen reorientation in intact and injured cartilage; **Petri Tanska**
- Biomechanical evaluation of the (un)reinforced ross procedure; **Heleen Fehervary**
- Microstructural models of ligament and tendon elasticity and viscoelasticity; **Tom Shearer**
- Investigation of the state of stress generated by high loads in the ovine lumbar intervertebral disc using a new anisotropic hyperelastic model; **Gloria Casaroli**
- Effect of natural honey treatment and external stretching on kinematics of cell migration during gap closure; **Daphne Weihs**

### Session 36 - Biomechanics of movement foot and gait

- Foot type biomechanics: A matter of structure, function and flexibility; **Howard Hillstrom**
- Biomechanics of foot with total ankle arthroplasty; **Yan Wang**
- The effect of the ground reaction force manipulation on the COP with emphasis on the shear forces; **Hadar Shaulian**
- Influence of muscle strength on hip contact forces following total hip arthroplasty with a minimal direct anterior approach; **Enrico De Pieri**
- Force transmission through the wrist during performance of pushups on a hyperextended and a neutral wrist; **Olga Polovinets**

### Session 37 - Spine biomechanics, imaging and therapeutics 1

- Patient-specific simulation of spine deformity correction based on biplanar radiographic images; **Fabio Galbusera**
- UltraSpine: Minimally invasive fractionation of degenerate intervertebral disc nucleus pulposus by ultrasound and its replacement by an injectable hydrogel; **Constantin Coussios**
- Understanding cerebrospinal fluid flow in the spinal subarachnoid space and perivascular fluid transport into the spinal cord: The role of CSF pressure pulse shape; **Lynne Bilston**
- Finite element analysis of pre and post lumbar fusion for scoliosis patients; **Ram Haddas**
- Novel injectable biomimetic glycosaminoglycan analogues for intervertebral disc regeneration: Replacing like with like; **Sarit Sivan**

### Session 38 - Spine biomechanics, imaging and therapeutics 2

- Vertebral loading during daily living activities estimated from measured spinal kinematics: Elderly vs. young subjects; **Dominika Ignasiak**
- Biomechanics of implant failure after PSO: Influence of the hardware configuration through a finite element analysis; **Tomaso Villa**
- Finite element analysis based lumbosacral revision surgery using an individual navigation template; **Peter E. Eltes**
- Biomechanical gait assessment on a patient undergoing surgical correction of kyphosis from severe ankylosing spondylitis - A case study; **Ram Haddas**

### Session 39 - Computational biomedical image-analysis and simulation 2

- Generation of anatomical models for biomechanical simulation of transeptal puncture; **Joao Tavares**
- Computational modeling of electromagnetic and (focused-) ultrasound thermal therapies: Application to applicator design, personalized treatment planning/optimization, and therapeutic innovation; **Esra Neufeld**
- New method for radiographic spinal reconstruction using probabilistic principal component analysis (PPCA); **Olivier Moal**
- Prediction of alignment after surgical treatment of adult spinal deformity (ASD) with probabilistic principal component analysis; **Olivier Moal**
- Statistical shape modeling to analyse the talus in pediatric clubfoot; **Heidi-Lynn Ploeg**

## COMPUTATIONAL ANALYSIS OF X-RAY DATA AND HIGH-RESOLUTION MODELING OF SELF-ASSEMBLED BIO-STRUCTURES

**Uri Raviv**<sup>1</sup>

<sup>1</sup> Institute of Chemistry, The Hebrew University of Jerusalem, Jerusalem, Israel

Using SAXS, in combination with Monte Carlo simulations, and our unique solution x-ray scattering data analysis program, we resolved at high spatial resolution, the exact manner by which wtSV40 packages its 5.2kb circular DNA about 20 histone octamers in the virus capsid. This structure, known as a mini-chromosome, is highly dynamic and could not be resolved by any microscopy methods (1). Using time-resolved solution SAXS, stopped-flow, and flow-through setups the assembly process of VP1, the major capsid protein of the SV40 virus, with RNA or DNA to form virus-like particles (VLPs) was studied in msec temporal resolution. By mixing the nucleotides and the capsid protein, virus-like particles formed within 35 msec, in the case of RNA that formed T=1 particles, and within 15 seconds in the case of DNA that formed T=7 particles, similar to wt SV40. The structural changes leading to the particle formation were followed in detail (2). We also solved the high-resolution structure of the nanodrug Doxil, which encapsulates doxorubicin in PEGylated liposomes (3).

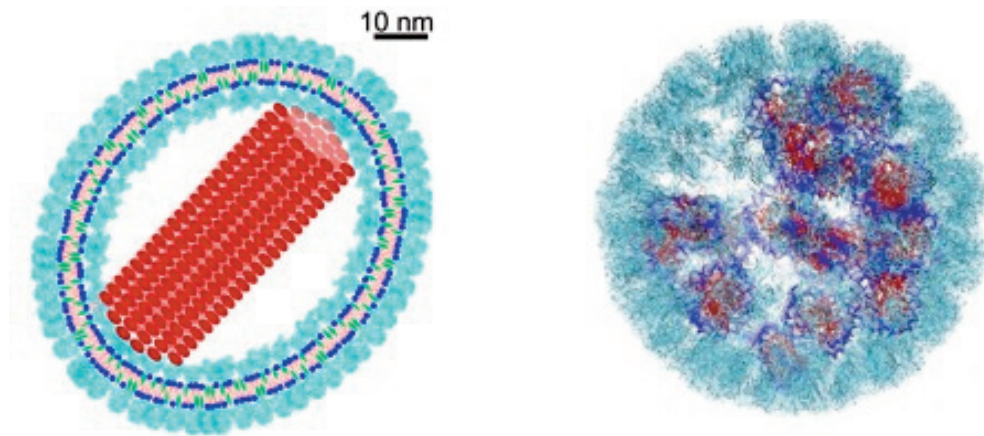


Figure Caption: High-resolution structure of Doxil (left) and atomic model of wt SV40 (right).

### Acknowledgments:

We thank ISF, BSF, the Israel ministry of science and the chief scientist of the ministry of Israel ministry of economy for financial support

### References:

1. *Nucleic Acid Research*, 41, 1569, 2013.
2. *J. Am. Chem. Soc.* 134, 8823, 2012.
3. *BBA - General Subject*, 1860, 108, 2016.

# LARGE-SCALE COARSE-GRAINED SIMULATIONS OF BIOMEMBRANES USING MESHLESS MEMBRANE MODEL AND LATTICE MONGE MC MODEL

**Hiroshi Noguchi<sup>1</sup>**

*<sup>1</sup>Institute for Solid State Physics, University of Tokyo, Kashiwa, Japan*

Various types of coarse-grained models have been developed to simulate lipid membranes. The models of bilayer membranes can be classified into two groups, depending on whether the bilayer structure is explicitly or implicitly taken into account. In my talk, I will focus on the second group, in which the continuum membrane surface is discretized by mesh or meshless (particle-based) methods in simulations.

I will introduce our meshless membrane models and present our recent application to membrane shape deformation by banana-shaped protein rods [1]. Membrane-mediated interactions between the rods induce rod assembly coupled with membrane shape changes such as protrusion of membrane tubules (see Fig. 1) and formation of a polygonal tube, polyhedral vesicle, and vesicle rupture into a high-genus vesicle and membrane inversion.

For mesh methods, a triangular mesh is widely employed. I will present a Monge lattice Monte Carlo simulation for a quasi-flat membrane [2]. To treat the exact nonlinear Helfrich Hamiltonian, measure correction for the excess entropy of the Monge gauge is required. Three types of surface tensions can be defined for lipid membranes: the internal tension conjugated to the real membrane area, the mechanical frame tension conjugated to the projected area, and the fluctuation tension obtained from the fluctuation spectrum of the membrane height. Our results for the relation between internal and frame tensions agrees well with the previous theoretical prediction based on a Gaussian approximation. However, the fluctuation tension coincides the frame tension within an accuracy of our simulation. If the Gaussian approximation is used and the measure correction is not accounted, the fluctuation tension becomes close to the internal tension. Hence, the previous discrepancy on the fluctuation tension is due to the approximations.



*Figure Caption: Sequential snapshots of tubulation from a flat membrane by bending of (red) protein rods.*

## References:

- [1] H. Noguchi, *EPL* 108, 48001 (2014); *J. Chem. Phys.* 143, 243109 (2015); *Sci. Rep.* 6, 20935 (2016); *arXiv:1602.04569*.
- [2] H. Shiba, H. Noguchi, and J.-B. Fournier, *Soft Matter* 12, 2373 (2016).

# ACCURATE DISCRETE-TIME ISOTHERMAL AND ISOBARIC MOLECULAR DYNAMICS

**Niels Grønbech-Jensen<sup>1</sup>, Oded Farago<sup>2</sup>**

*<sup>1</sup> Department of Mathematics, Department of Mechanical and Aerospace Engineering, University of California, Davis, United States*

*<sup>2</sup> Ben Gurion University of the Negev, Beer Sheva, Israel*

Numerical simulations of atomic and molecular ensembles by Molecular Dynamics always involve discretization of time, and as the time step is increased the discrete-time behavior becomes increasingly different from that of the anticipated continuous-time dynamics. Adding to this is a much overlooked problem; namely that the velocity variable does not produce the conjugate momentum to the position in discrete time [2]. Thus, time-step errors are inconsistently different in velocity and position. This results in a number of potentially severe issues if the time step is challenged. For example, isothermal ensembles that are guided by kinetic temperature will inevitably lead to erroneous configurational sampling. Another example is diffusion, which cannot be precisely measured by velocity autocorrelations in discrete time.

Our aim is improve simulation techniques for systems in thermal equilibrium. We briefly review our stochastic algorithm [1] for proper configurational sampling. The resulting method has been numerically tested on both low-dimensional nonlinear systems as well as more complex molecular ensembles [3,4]. In light of the fundamental artifacts introduced by discrete time, we provide a simple intuitive picture of the unique benefits of our algorithm.

We then introduce a companion algorithm for controlling pressure in molecular ensembles; i.e., a barostat for so-called NPT simulations [2]. Drawing on the idea of Andersen, we consider a global variable (a virtual piston) for the dynamics of the volume. However, our description of the discrete-time dynamics is defined differently from previous work and leads to a very simple set of equations that is easily implemented in existing MD codes. We discuss the core feature of separating the dynamics of the particles from the dynamics of the geometry, and we allude to applications of hybrid methods between Molecular Dynamics and Monte Carlo techniques.

## References:

- [1] Grønbech-Jensen & Farago, *Molecular Physics* Vol.111, 983 (2013).
- [2] Grønbech-Jensen & Farago, *Journal of Chemical Physics* 141, 194108 (2014).
- [3] Grønbech-Jensen, Hayre, & Farago, *Computer Physics Communications*, Vol.185, 524 (2014).
- [4] Arad, Farago, & Grønbech-Jensen, *arXiv:1602.05321* (2016).

# INFLUENCE OF PERIODIC BOUNDARY CONDITIONS ON LATERAL DIFFUSION IN MEMBRANES

**Frank Brown**<sup>1</sup>

*<sup>1</sup> University of California, Department of Chemistry, Santa Barbara, United States*

The Saffman-Delbruck hydrodynamic model for lipid-bilayer membranes is easily modified to account for the periodic boundary conditions commonly imposed in molecular simulations. The resulting predictions suggest that lateral diffusion coefficients for membrane-embedded solid bodies are sensitive to box shape and converge slowly to the limit of infinite box size, raising serious doubts for the prospects of using detailed simulations to accurately predict membrane transport properties. Coarse-grained simulations support the findings of the hydrodynamic model.

# NUMERICAL SIMULATIONS FOR THE DETERMINATION OF CHEMICAL GRADIENTS INDUCED IN COLLAGEN AND FIBRIN HYDROGELS

Mar C3n3dor<sup>1</sup>, Oihana Moreno-Arotzena<sup>2</sup>, Jos3 Manuel Garc3a-Aznar<sup>1</sup>

<sup>1</sup> Aragon Institute of Engineering Research (I3a), University of Zaragoza, Zaragoza, Spain,

<sup>2</sup> Department of Applied Mathematics, University of the Basque Country Upv/Ehu, San Sebastian, Spain

Microfluidic devices allow for the production of physiologically relevant cellular microenvironments by including biomimetic hydrogels and generating controlled chemical gradients. During transport, the biomolecules interact in distinct ways with the fibrillar networks: as purely diffusive factors in the soluble fluid or bound to the matrix proteins. These two main mechanisms may regulate distinct cell responses in order to guide their directional migration: caused by the substrate bound chemoattractant gradient (haptotaxis) or by the gradient established within the soluble fluid (chemotaxis) [1, 2].

In this work we present a numerical model based on a reaction-diffusion transport model, in combination with ELISA assays, to predict the distribution of different growth factor as PDGF-BB and TGF- $\beta$ 1 across collagen and fibrin gel. This model yields an accurate prediction of the experimental results (Fig.1), confirming that diffusion and binding phenomena are established within the microdevice [3].

At the same time we present a Web application for showing the numerical results provided by the model to characterize the chemical gradients generated within the microfluidic devices. This application allows the user to define online the geometrical parameters that characterize these devices (hydrogel height and width, among others); as well as the input parameters of the diffusion case: the growth factor (PDGF-BB and TGF- $\beta$ 1), the initial concentration, the type of matrix (collagen or fibrin) or the time to simulate.

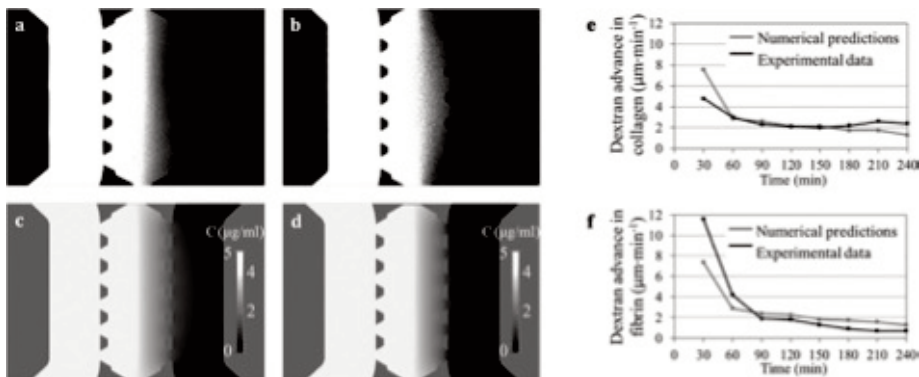


Fig.1. In vitro and in silico images of the diffusive gradient of dextran in collagen (a),(c) and fibrin (b),(d) hydrogels, after 4 h since addition. The development in terms of dextran speed for collagen (e) and fibrin (f) [3].

## Acknowledgments:

This study is supported by the European Research Council (ERC) through project ERC - 2012 - StG 306751, the Spanish Ministry of Economy and Competitiveness (DPI2015-64221-C2-1-R) and the Government of Aragon (C126/2015).

## References:

1. Aznavoorian, S., et al., *J Cell Biol*, 1990. 110(4): p. 1427-38.
2. Daub, J.T., et al., *Bull Math Biol*, 2013. 75(8): p. 1377-99.
3. Moreno-Arotzena, O., et al., *Biomechanics*, 2014. 8(6).

## EVALUATING SKIN MECHANICS AND AGEING FEATURES WITH DIGITAL IMAGE CORRELATION

**Kemal Levi**<sup>1</sup>, **Pelin Kefel**<sup>2</sup>, **Arved Kaltwasser**<sup>3</sup>, **Juergen Keller**<sup>3</sup>

*1 Bio-X Consulting, Inc., Mountain View, United States,*

*2 Bio-X Consulting, Inc., Mountain View, United States,*

*3 Bio-X Technologies GmbH, Berlin, Germany*

The adverse effects of ageing are increasingly the focus of medical and scientific communities, and the role of applying a materials science & mechanical framework in studying these is increasingly recognized as a critically important lens in finding new and improved ways to diagnose and treat skin conditions. In addition, the non-invasive nature of available mechanical measurement techniques provides unique opportunities for monitoring treatment efficacy over time. A very promising non-invasive technique is digital image correlation (DIC). We will present various case studies where DIC is used both in vivo and in vitro to measure treatment efficacy, monitor surgical and healing processes, study mechanical behavior of skin, monitor performance of medical devices on skin, and how all of these are affected by the change in the mechanical properties of the tissue with ageing. We will demonstrate how the ability to quantify skin deformation using DIC enables us to determine thresholds of skin damage following exposure to various ageing factors; understand how the propensity for skin damage varies for different skin types and evaluate how cosmetics and treatments change the mechanical homeostasis of the tissue. In addition, we will also show how surgical intrusions and wound closure are affected by skin mechanics and how ageing impacts these. Ageing has a significant impact on the directionality of the mechanical properties of skin, yet surgical incisions performed on the elderly population do not take into account the perturbed mechanics of the aged skin. We will then showcase how the results of this research can be utilized to design and develop next generation approaches and therapies to prevent and repair skin damage and redefine how cosmetic products are formulated in the future with more precise values of effectiveness.

# COMPARISON OF ANISOTROPIC MODELS TO SIMULATE THE MECHANICAL RESPONSE OF FACIAL SKIN

**Cormac Flynn<sup>1</sup>, Andrew Taberner<sup>2</sup>, Sid Fels<sup>3</sup>, Poul Michael Fonss Nielsen<sup>4</sup>**

*1 Wintec, Hamilton, New Zealand,*

*2 Auckland Bioengineering Institute, Department of Engineering Science, University of Auckland, Auckland, New Zealand,*

*3 Department of Electrical and Computer Engineering, University of British Columbia, Vancouver, New Zealand,*

*4 Auckland Bioengineering Institute, Department of Engineering Science, Auckland University, Auckland, New Zealand*

“Physically-realistic models of the face can be applied in a wide range of domains, including biomedicine, computer animation, and forensics. There has been significant improvement in the anatomical accuracy of face models with better representation of the mimetic muscles, and realistic contact and attachments between soft and bony tissues [1,2]. Face simulations can also benefit from improved constitutive models of the skin layer. For example, better representation of the mechanical properties of facial skin can lead to improved predictions of deformations as a result of maxillofacial surgical procedures.

The objective of this work is to compare and evaluate constitutive models’ ability to simulate the mechanical response of facial skin subjected to a rich set of deformations using a probe.

We developed a finite element model to simulate the facial skin experiments of Flynn et al [3]. Several anisotropic constitutive equations were tested for their suitability to represent facial skin, including models proposed by Gasser et al [4], and Tong and Fung [5]. To represent in vivo tension, we applied a prestress to the model prior to simulating the full set of deformations. The reaction forces due to the displaced probe were calculated. A non-linear optimization procedure determined model parameters and in vivo tensions that best fit the model reaction forces to the measured experimental reaction forces.

The finite element model simulated the force-displacement response of facial skin under a rich set of deformations. Use of an anisotropic constitutive law in place of an isotropic law resulted in a better fit between the models and experiments. For example, using the Gasser et al [4] anisotropic material model results in a 0.87 variance accounted for compared to 0.79 variance using an isotropic Ogden material model [3].

Future developments include the incorporation of the structure inferior to the skin in the model. We believe this will have the most significant effect on the model performance.”

## References:

[1] Flynn et al. *Comput Methods Biomech Biomed Eng*, 18: 571-582, 2015

[2] Wu et al. *IEEE Trans Vis Comput Graph*, 20:1519-1529, 2014

[3] Flynn C et al. *J Mech Behav Biomed Mater*, 28: 484-494, 2013.

[4] Gasser T et al. *J R Soc Interface*, 3: 15-35, 2006.”

[5] Tong, P and Fung Y-C. *J Biomech*, 9: 649-657, 1976”

## IN VIVO QUANTIFICATION OF SKIN TENSION AND STIFFNESS USING SURFACE WAVE PROPAGATION

**Aisling Ní Annaidh**<sup>1</sup>, **Antonia Trotta**<sup>1</sup>, **Claire Deroy**<sup>1</sup>, **Michel Destrade**<sup>2</sup>

<sup>1</sup> University College Dublin, Dublin, Ireland,

<sup>2</sup> National University of Ireland Galway, Galway, Ireland

In this study, we measure the speed of propagation of an elastic disturbance on the skin of the forearm, using a commercial device called a Reviscometer®. By taking measurements in different orientations we can see a marked anisotropy which increases with the age of the volunteer. We have shown experimentally, via an animal model, that this anisotropy corresponds to the orientation of Langer lines (the lines of maximum skin tension) and have determined that the Reviscometer® can identify the orientation of Langer Lines in the skin non-destructively and non-invasively.

Flavin (1963) has shown that, for the Neo-Hookean case, a Rayleigh wave propagating over a uniformly pre-stressed half space travels at a speed  $v$ , given by:

By measuring the speed of propagation at two different loading conditions, the Young's modulus,  $E$ , and the in vivo skin tension in the two principle directions,  $\lambda_1$  and  $\lambda_2$ , can be evaluated directly and non-invasively. This has implications for the identification of Langer Lines and the prediction of skin tension levels, both important factors in preoperative planning for cosmetic surgeries.

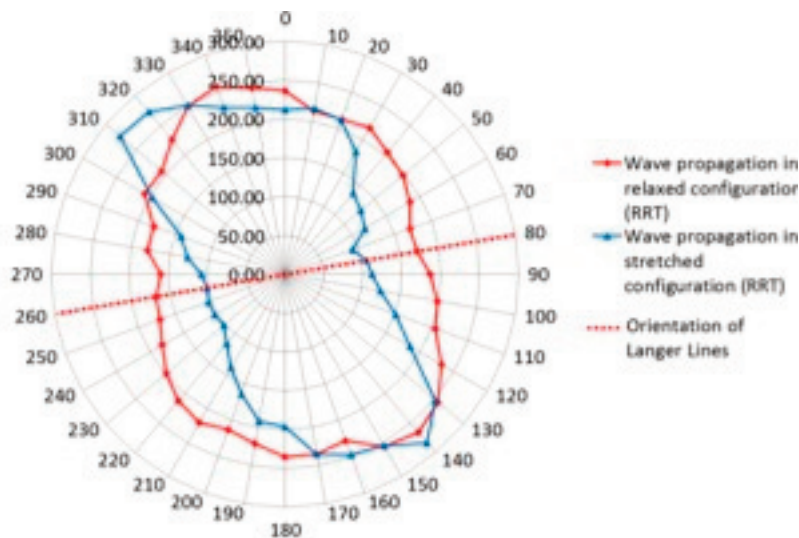


Figure Caption: Wavespeed measurement of human skin at in vivo tension and at elevated tension levels in 10° increments from 0-360°. The minimum resonance running time (RRT), and therefore greater wave speed, corresponds to the direction of maximum skin tension.

### References:

Flavin, J.N., Surface Waves in a pre-stressed Mooney material. *Q.J. Mech. Appl. Math.*, 16:441-449, 1963.

# ON THE MECHANICS OF SKIN WRINKLES: THE ROLE OF SKIN MICRORELIEF

**Georges Limbert<sup>1</sup>**

*<sup>1</sup> National Centre for Advanced Tribology, Faculty of Engineering and the Environment, University of Southampton, UK, Biomechanics and Mechanobiology Laboratory, Department of Human Anatomy, Faculty of Health Sciences, University of Cape Town, South Africa, Southampton, United Kingdom*

## Introduction:

During intrinsic and extrinsic ageing, the formation and evolution of wrinkles alter the physical properties of the skin surface. Besides these cosmetic effects, unveiling the underlying mechanical principles that condition the morphologies and patterns of wrinkles are essential in predicting how an aged skin interacts with its environment. From the view point of physics, wrinkles are the result of a complex interplay between adaptive material and structural properties as well as boundary and loading conditions the skin is subjected to over a life time. The objective of the present study was to develop a computational toolbox and an anatomical mechanobiological multi-layer skin model capable of simulating the effects of ageing and the subsequent formation of wrinkles.

## Methods:

A parametric 3D finite element multi-layer skin model was developed from 3D laser profilometry of a silicone replica of a patch of human skin surface. Equations describing the change in material properties and volume (e.g. dehydration) of the different skin layers as a function of ageing were implemented in a customised computational environment. Compression-induced and ageing-induced wrinkles were simulated.

## Results:

Simulations confirmed the strong dependency of wrinkle morphology on the characteristics of primary and secondary lines in both type of wrinkles. The ratio between material and structural properties of each skin layer was also key in shaping the characteristics of the induced wrinkling instabilities. Due to the structural characteristics of skin microrelief limited straining of the stratum corneum layer during in-plane compression of the skin was observed. It was also demonstrated that microrelief inhibits large wrinkle wave lengths.

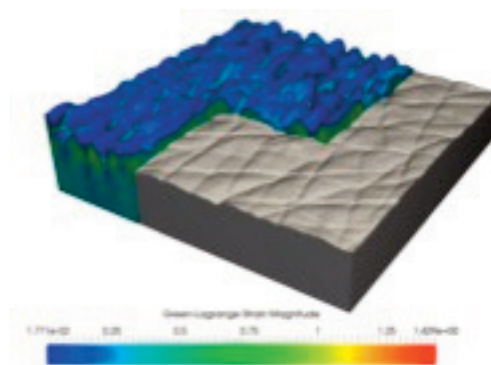


Figure 1: Colour plot of strain magnitude of a 3D skin patch after in-plane compression in the undeformed and deformed configuration.

## Conclusion:

The modular computational platform has proven to be robust to simulate the highly non-linear mechanics of wrinkle formation and allowed the testing of various hypotheses about the genesis of ageing-induced wrinkles. On-going work is looking at increasing the fidelity of the geometry of each skin layer.

## MODELING SKIN MECHANICS UNDER SHEAR DEFORMATION IN 3D

**Jibbe Soetens<sup>1</sup>, Christine Obbink-Huizer<sup>1</sup>, Gerrit Peters<sup>1</sup>, Cees Oomens<sup>1</sup>**

<sup>1</sup> Eindhoven University of Technology, Eindhoven, Netherlands

Skin is the largest organ of the human body and functions as a barrier with the external environment. However, the mechanical balance of the skin can be threatened. Therefore, skin mechanics is important for various fields of research. This includes research into the development of pressure ulcers and the interaction between skin and devices or materials. For this research, prediction of mechanical response of skin is essential.

Skin is a three-layered tissue that has non-linear viscoelastic, anisotropic and heterogeneous properties. From a mechanical point of view, however, skin should be considered as a highly dynamic and complex composite. Because of this complexity, its mechanical response is difficult to understand and predict. Therefore the aim of this work was to develop a 3D finite element material model that is based on experimental evidence and captures the complex material properties of skin.

Skin is modelled as a fiber-reinforced matrix, with an elastic fibrous component and an isotropic, non-linear visco-elastic matrix. The fibers only contribute in extension and provide anisotropic properties. For the matrix, the deformation is split into a change in volume and in shape. Both contribute independently to the stress. All elastic components are non-linear, providing non-linear viscoelastic behavior. The model is implemented in the Marc/Mentat software package using a user subroutine (HYPELA2).

Large amplitude oscillatory shear (LAOS) experiments on ex-vivo human skin were performed, which showed that the mechanical properties of the skin layers varied as a function of depth. Larger deformations were present for increasing skin depth. To validate the model and obtain an estimate of the material parameters, the response of the model to oscillatory shear was fitted to the LAOS data.

The simulated stress-strain response is similar to the experimental stress-strain response (figure 1). Also, the spatial distribution of the deformation in both simulation and experiment match. Regarding these results, the newly developed model is promising tool to simulate skin mechanics and to improve understanding of the mechanical behavior of human skin under various circumstances.

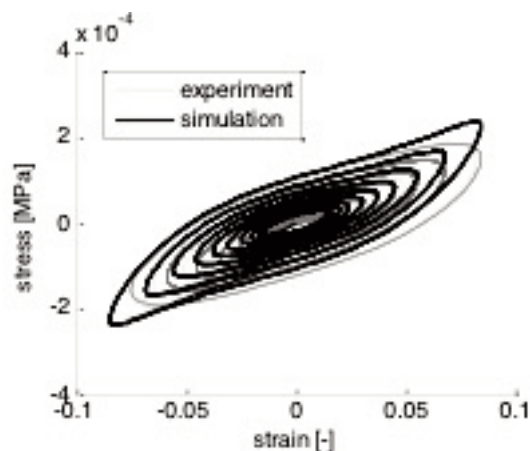


Figure Caption: Stress-strain response of oscillatory shear in experiment and model

## PERSONALIZED FEA MAY REDUCE UNNECESSARY PROPHYLACTIC SURGERIES IN FEMURS WITH METASTATIC TUMORS - A CLINICAL STUDY

**Zohar Yosibash<sup>1</sup>, Nir Trabelsi<sup>2</sup>, Moshe Salai<sup>3</sup>, Amir Sternheim<sup>4</sup>**

*1 Dept of Mechanical Engineering, Ben Gurion University of the Negev, Beer-Sheva, Israel,*

*2 Dept of Mechanical Eng, Shamoon Engineering College, Beer-Sheva, Israel,*

*3 Orthopaedic DIV, Sourasky Medical Center , Tel Aviv, Israel, 4 Orthopaedic DIV, Sourasky Medical Center, Tel Aviv, Israel*

Patient-specific QCT-based high-order finite element models (p-FEMs) well predict in ex-vivo experiments the mechanical response of femurs, including the risk of fracture [1,2]. They account for the exact geometry and inhomogeneous material properties, are created in a semi-automated manner from QCT scans and validated on a large cohort of fresh frozen femurs.

The use of QCT-based p-FEMs was extended to femurs with bone metastasis [3] and femurs with a prosthesis following a total-hip-replacement procedure. The first part of the talk addresses the methodology to semi-automatically generate the femurs' FEM from CT scans, assign material properties and apply the stance position load.

The methodology was applied in clinical practice. We performed a retrospective clinical trial on 31 patients with metastatic tumors to their femur on whom prophylactic surgery was performed. CT-scans of the femurs done prior to surgery were analyzed. We questioned whether the risk of fracture necessitated an operation. For example, in Figure 1 a radiograph and a p-FEA of the femurs of a 43 y.o. patient with breast cancer metastatic tumor to the right femur is shown - the performed prophylactic surgery, although performed, was most probably unnecessary. The second part of the presentation will present such cases analyzed during the clinical trial and the potential use of p-FEA in clinical practice.

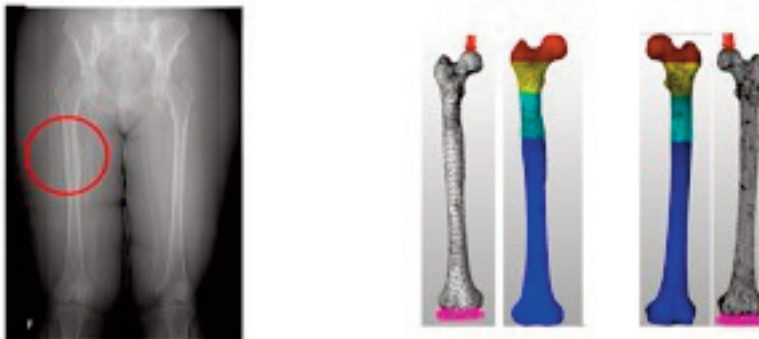


Figure 1. Left: Radiograph of a 43 y.o. patient with metastatic tumors in the right femur. Right: p-FEA of the femurs representing a stance position (colors - vertical displ).

### References:

[1] N. Trabelsi et al. Patient-specific finite element analysis of the human femur - a double-blinded biomechanical validation. *J. Biomech.*, 44:1666-1672, 2011.

[2] Z. Yosibash, et al. Predicting the yield of the proximal femur using high order finite element analysis with inhomogeneous orthotropic material properties. *Phyl. Tran. of the Roy Soc.: A*, 368:2707-2723, 2010.

[3] Z. Yosibash, et al. Predicting the stiffness and strength of human femurs with realistic metastatic tumors. *Bone*, 69:180-190, 2014.

# TOPOLOGY OPTIMIZATION FOR DESIGN OF POROUS SCAFFOLDS FOR BONE TISSUE ENGINEERING

**Oded Amir<sup>1</sup>, Liron Reuveny<sup>1</sup>, Anath Fischer<sup>1</sup>, Pinhas Bar-Yoseph<sup>1</sup>**

*<sup>1</sup> Technion - Israel Institute of Technology, Haifa, Israel*

Topology optimization is a computational method aimed at optimizing the distribution of one or several materials in a given design domain. The method is nowadays well integrated into the design process of structural components in the automotive and aircraft industries. Typically, the computational procedure seeks the best trade-off between weight and stiffness. Significant research effort is invested in further development of the method for utilization in other engineering disciplines and more complex design trade-offs. In the context of bio-medical engineering, topology optimization has been shown to be a promising tool for the design of bone replacements such as porous scaffolds for tissue engineering [1].

The current research addresses the integration of medical imaging, geometric meshing, finite element analysis (FEA) and topology optimization, for the design of porous scaffolds and internal bone supports. The proposed approach consists of the following stages:

- a) Acquisition of a micro-CT image of the bone, providing the current state with respect to fracture, damage and degradation;
- b) Geometrical reconstruction and meshing of a computational model of the bone;
- c) Topology optimization iterations, based on FEA and gradient-based optimization algorithms, for finding the best porous scaffold structure with respect to the functional requirements.

One of the main factors that enable this computational design approach is the recent development of efficient procedures for high resolution FEA and topology optimization. These exploit the power of parallel computing and facilitate the solution of problems where the material distribution is represented by up to hundreds of millions of voxels.

In this talk, we will focus on the challenges in the design of bone scaffolds, and on how these can be overcome by utilizing topology optimization. In particular, we will show how the design of the scaffold can be tailored according to various functional requirements, such as porosity, stiffness, and strength. Furthermore, avoiding damage of the host tissue in the interface with the scaffold can also be considered via design constraints.

## References:

- [1] Hollister, S. J. (2005). Porous scaffold design for tissue engineering. *Nature Materials*, 4(7), 518-524.
- [2] Podshivalov, L., Fischer, A., Bar-Yoseph, P. Z. (2011). 3D hierarchical geometric modeling and multiscale FE analysis as a base for individualized medical diagnosis of bone structure. *Bone*, 48(4), 693-703.
- [3] Reuveny, L. (2015). *Design of 2D Porous Micro Structures by using Geometric Meshing, Finite Element Analysis and Topology Optimization*, M.Sc. thesis, Faculty of Mechanical Engineering, Technion.
- [4] Podshivalov, L., Fischer, A., Bar-Yoseph, P. Z. (2014). On the road to personalized medicine: multiscale computational modeling of bone tissue. *Archives of Computational Methods in Engineering*, 21(4), 399-479.

# THE GENERIC MODELING FALLACY: IS IT HAPPENING IN YOUR LAB?

**Daniel Robertson<sup>1</sup>, Douglas Cook<sup>2</sup>**

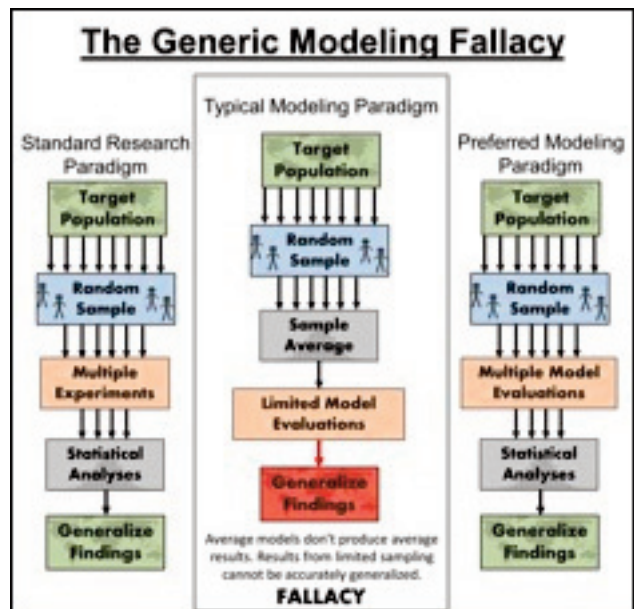
<sup>1</sup> New York University - Abu Dhabi, Abu Dhabi, United Arab Emirates,

<sup>2</sup> New York University Abu Dhabi, Abu Dhabi, United Arab Emirates

Computational models based on nominal or average input parameters are often assumed to produce average results that are representative of a target population. However, this assumption has never been fully investigated. To investigate the effects of average input parameters on biomechanical models a stochastic Monte Carlo analysis of two common model archetypes was conducted. Consistent discrepancies were found between the behavior of average models (i.e. models which utilized average input parameters) and the average behavior of the population from which the average model's input parameters were derived. Furthermore, multiple sets of non-average input parameters were found to produce average behaviors. In other words, average models did not produce average behavior, but multiple non-average models did produce average behavior. Mathematical arguments which explain and prove this phenomena will be presented. In particular, it will be shown that average inputs to nonlinear biomechanical models cannot produce average behavior. To facilitate further discussions on this topic the authors have termed this phenomena the "generic modeling fallacy".

The above findings have implications for the interpretation and execution of computational modeling studies. In particular, these results demonstrate the necessity of analyzing the behavior of multiple patient specific models when generalizing results from computational studies to real world populations of interest. However, many patient specific models still make use of some average input parameters and may therefore be subject to the ill effects of the generic modeling fallacy. The authors will discuss how to avoid this pitfall.

*Figure Caption: The typical modeling paradigm (center) of evaluating an average model and generalizing its results to a target population is vulnerable to the generic modeling fallacy. The preferred modeling paradigm (right) is to conduct modeling studies in accordance with the standard research paradigm (left). This requires multiple model evaluations statistical analysis of model results.*



# CHARACTERIZATION OF IRREVERSIBLE PHYSIO-MECHANICAL PROCESSES IN STRETCHED FETAL MEMBRANES

**Yulia Marom**<sup>1</sup>, **Shlomit Goldman**<sup>2</sup>, **Eliezer Shalev**<sup>3</sup>, **Doron Shilo**<sup>4</sup>

*1 Department of Mechanical Engineering, Technion, Haifa, Israel,*

*2 Laboratory for Research in Reproductive Sciences, Department of Obstetrics and Gynecology, Emek Medical Center, Afula, Israel,*

*3 Faculty of Medicine, Israel Institute of Technology, Laboratory for Research in Reproductive Sciences, Department of Obstetrics and Gynecology, Emek Medical Center, Haifa, Israel,*

*4 Department of Mechanical Engineering, Technion, Haifa, Israel*

We perform bulge tests on live fetal membrane (FM) tissues that simulate the mechanical conditions prior to contractions. Experimental results reveal an irreversible mechanical behavior that appears during loading and is significantly different than the mechanical behavior that appears during unloading or in subsequent loading cycles. The irreversible behavior results in a residual strain that does not recover upon unloading and remains the same for at least 1 hour after the FM is unloaded. Surprisingly, the irreversible behavior demonstrates a linear stress-strain relation.

We introduce a new model for the mechanical response of collagen tissues, which accounts for the irreversible deformation and provides predictions in agreement with our experimental results. Fittings of calculated and measured stress-strain curves reveal a well-defined single-value property of collagenous tissues, which is related to the threshold strain  $\epsilon_{th}$  for irreversible transformation. Further discussion of several physio-mechanical processes that can induce irreversible behavior indicate that the most probable process, which is in agreement with our results for  $\epsilon_{th}$ , is a phase transformation of collagen molecules from an  $\alpha$ -helix to a  $\beta$ -sheet structure. A phase transformation is a manifestation of a significant change in the molecular structure of the collagen tissues that can alter connections with surrounding molecules and may lead to critical biological changes, e.g. an initiation of labor.

## PATIENT-SPECIFIC MODELING IN THE ABSENCE OF MATERIALS PROPERTY DATA: COMBINING EXPERIMENTAL AND COMPUTATIONAL TECHNIQUES TO GAIN INSIGHTS.

Douglas Cook<sup>1</sup>, Daniel Robertson<sup>2</sup>

<sup>1</sup> New York University Abu Dhabi, Abu Dhabi, United Arab Emirates, <sup>2</sup> New York University - Abu Dhabi, Abu Dhabi, United Arab Emirates

Patient-specific modeling almost always requires that models are created based on incomplete information. But how does the lack of information influence our models and their predictive power? Furthermore, how can a model itself be used to make intelligent choices about how to deal with missing information? This study utilized a model system to investigate these questions. Maize (corn), has a cross-sectional profile very similar to that of human bone, suffers from stalk failure, and is much easier to obtain and test than bone. A subject-specific model of a maize stalk was created and simulated to determine the influence geometric and material parameters. As in modeling bone, a finite element model of the maize stalk was developed based on geometric data acquired from quantitative computed tomography (QCT) scanning, and CT intensity was used to infer local material properties.

Sensitivity analysis was performed to investigate relationships between model inputs (geometry, material properties) and model outputs (stress). Perturbation of geometric and material parameters resulted in a total of 17 unique finite element models. Each model was subjected to four orthogonal bending loads, with a total of 68 simulations performed. Figure 1 depicts the nominal model with and without applied loading. The locations of maximum stresses predicted by the finite element models correlated well with field observations of naturally lodged stalks (Robertson et al., 2015).

Geometric parameters were found to have a much greater influence on stress levels than material properties. This finding was validated by laboratory experiments (n = 1000) in which geometric variables were observed to account for the vast majority variation in stalk strength.

Sensitivity analysis techniques can be used to provide valuable information, even when patient-specific data is not available. In this case, sensitivity analysis was used to determine the relative effects of material vs. geometry, and provide information on which material properties are most influential.

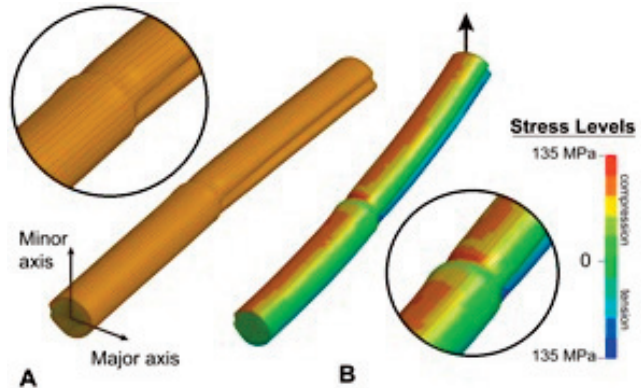


Figure Caption: A finite element model of maize stalk. A - unstressed and B - under bending load. The arrow depicts the direction of displacement of the corresponding face. Colors in B represent stress levels.

### Acknowledgments:

This research was supported by the Core Technology Platform Resources at New York University Abu Dhabi and funding from the National Science Foundation, award #1400973.

### References:

Robertson, D. J., Julias, M., Gardunia, B. W., Barten, T., & Cook, D. D. (2015). Corn Stalk Lodging: A Forensic Engineering Approach Provides Insights into Failure Patterns and Mechanisms. *Crop Science*, 55(6), 2833-2841.

## ABOUT UNLOADING CONTROL AT LEG ORTHOTICS

***Il'ya Dashevskiy***<sup>1</sup>

*<sup>1</sup>Institute for Problems in Mechanics of the Russian Academy of Sciences , Moscow, Russian Federation*

In [Dashevskiy & Nikitin, 2016] an idea was formulated of programmed control of limb unloading coefficient (CU) through change of the orthosis lateral compression when tightening. With regard to the shin the hypothesis was that due to circumferential compression the shin will be "pushed" out of the orthosis up, its contact with the sole be weakened, and the load be redistributed from the shin on the orthosis case.

Measurements of CU using under the orthosis both cotton and special slippery synthetic stockings were conducted. For cotton stockings no dependence of CU on compression was found, for slippery stockings in walking - as well, while in statics recorded was a sharp rise in CU with an increase of compression on the left side of the curve and the stabilization in the right part of it. For the simulation of unloading in orthotics measured were friction coefficients of pairs of skin-stockings and stocking-orthosis for cotton (0.48 and 0.57, respectively) and for synthetic stockings (0.42 and 0.16).

A model was considered of rough rigid cone (the shin), covered by a conformal expandable rigid holder (orthosis sleeve) and loaded with vertical force (weight) and belt-like load (lateral compression). The requirement of orthosis slip with respect to the limb led to the condition for the friction coefficient between them  $k < \sim 0.25$ . Thus, for cotton (respectively, synthetic) stockings, conditions are realized of limb cohesion (respectively, slippage) relative to the orthosis, and lateral compression can not affect (respectively, change) the unloading level.

Models of leg-orthosis system considering the deformability of soft tissues were studied numerically: conical models - based on the method of boundary integral equations, models of real forms - by FEM using specially made for the purpose computer tomograms of the shin in vivo. It was found that on the shin-orthosis contact surface slip areas arise. For a cotton stocking with a coefficient of friction between the shin and the orthosis  $k = 0.48$  their size are strongly dependent on the geometry adopted, for synthetic stocking with  $k = 0.16$  in all cases they are significant.

Participation of M. Perelmuter, and P. Shushpannikov is gratefully acknowledged.

Dashevskiy I.N., Nikitin S.E. Biomechanics of lower limbs unloading at orthotics. Russian J. of Biomechanics, 2016 (In press). 16 pp.

# A DATABASE OF PELVIS FINITE ELEMENT MODELS FOR A HIGH-THROUGHPUT PIPELINE OF DYNAMIC, BIOFIDELIC, SIDEWAYS FALL IMPACT SIMULATIONS

**William Enns-Bray<sup>1</sup>, Ingmar Fleps<sup>1</sup>, Stefan Anthamatten<sup>1</sup>, Sigurður Sigurðsson<sup>2</sup>, Tamara Harris<sup>3</sup>, Vilmundur Gudnason<sup>2</sup>, Stephen J. Ferguson<sup>1</sup>, Benedikt Helgason<sup>1</sup>**

<sup>1</sup> Eth Zurich, Institute for Biomechanics, Zurich, Switzerland,

<sup>2</sup> The Icelandic Heart Association Research Institute, Kopavogur, Iceland,

<sup>3</sup> Laboratory of Epidemiology and Population Sciences, Bethesda, MD, United States

## Introduction:

Quasi-static finite element (FE) models of the femur are insufficient for predicting patient specific fracture risk in large clinical retrospective studies because they lack important information about the patient specific loads. The impact energy stored by the femur during the injury also depends on the energy stored by the surrounding tissues such as the pelvis, cartilage, and soft tissue. However, it is not always possible to construct a CT-based FE model of the pelvis from a clinical scan due to a limited field of view that only includes the proximal femur, which reduces the radiation dose. This study developed a method for matching a suitable pelvis model from a database of different subjects to a patient specific model of the proximal femur from a clinical study.

## Methods:

CT scans of the pelvis were acquired from the Virtual Skeleton Database (VSD), while CT scans of the femur were acquired from the Age Gene/Environment Susceptibility Reykjavik Study (AGES-RS). Image segmentation and material mapping were performed using open source software (MITK-GEM, <https://simtk.org/home/mitk-gem/>). VSD pelvises were parameterized based on landmarks visible in both VSD and AGES-RS scans, specifically pelvic width (W), depth (D), and femoral head radius (R). Two models were constructed using femur models of the AGES-RS patient with the largest pelvis (defined as  $W \cdot D$ ): the first model used the best matching VSD pelvis model (in terms of  $W \cdot D$ ), the second used the smallest available VSD pelvis model to test differences in extremely mismatched pelvises. The distal limb and soft tissue surrogates were constructed in ANSA, and designed such that the impact energies in both models were identical. Dynamic simulations were solved using LS-DYNA with an initial velocity of 3 m/s at the point of hip impact [1].

## Results and Discussion:

Combining different VSD pelvises with AGES-RS femurs resulted in different maximum force and impact energy stored in the femur (Fig. 1). In vitro testing has predicted that the femur can only absorb 5-20 J before fracture [2]. The difference of approximately 2 J stored by the femur between the matched pelvis and small pelvis models suggests that selecting the correct pelvis surrogate could be important for accurately predicting patient specific fracture risk. The total kinetic energy at the moment of impact was approximately 127 J. Since only a small fraction of this energy was stored by the femur, clearly the surrounding tissues play an important role in determining the patient specific loads on the femur during impact. Future work will focus on enlarging the pelvis database and further investigating soft tissue properties. A database of pelvis models will enable future cohort studies to test dynamic full hip models with only proximal femur information.

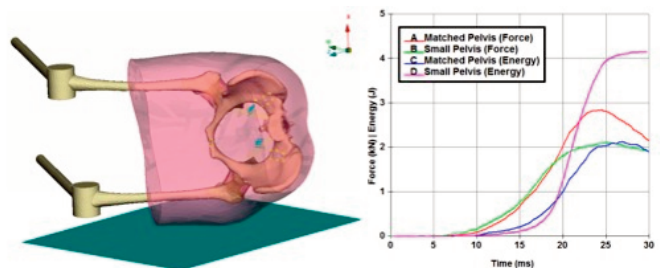


**Figure 1:** Fully constructed FE model of sideways fall on the hip using a VSD pelvis and AGES-RS femur (left), and the resulting impact energy and force stored by the femur (right).

## References:

[1] F. Feldmann et al., J Biomech 40(12), 2612-2618, 2007. [2] O. Ariza et al., J Biomech 48(2), 224-232, 2015.

## PATIENT-SPECIFIC MODEL GENERATION FOR FOOT PRESSURE ULCER PREVENTION

Marek Bucki<sup>1</sup>, Vincent Luboz<sup>1</sup>, Antoine Perrier, 2, Nicolas Vuillerme<sup>3</sup>, Yohan Payan<sup>4</sup>

<sup>1</sup> Texisense, Montceau-Les-Mines, France,

<sup>2</sup> Texisense, Ageis, Université Grenoble Alpes, Montceau-Les-Mines, France,

<sup>3</sup> Ageis, Université Grenoble Alpes, Grenoble, France,

<sup>4</sup> Univ. Grenoble Alpes, Chrs, La Tronche, France

Deep pressure ulcers (PU) appear internally when pressures applied on the foot create high internal strains nearby bony structures. Monitoring tissue strains on a patient-specific basis is therefore important for efficient PU prevention. To generate a biomechanical foot model adapted to patients' morphology and where strains can be monitored, our method deforms a foot atlas to conform it to the contours of the patients' feet in segmented medical images [Bucki]. Our atlas is a model composed of rigid bones, joined by ligaments and muscles, and surrounded by a Finite Element mesh representing the soft tissues. Three new patient models were created from the registration of our atlas with three datasets. The maximal Von Mises strains and "cluster volumes" (i.e. volumes of contiguous elements with strains above a given threshold) were measured within eight functionally meaningful foot regions after simulating these foot models during unipodal stance. This regionalization is automated for enhanced clinical interpretation of the simulations. The figure shows the variability of these two criterions in terms of location among the three patients. The results also confirm the influence of the foot anatomy on the risk of PU.

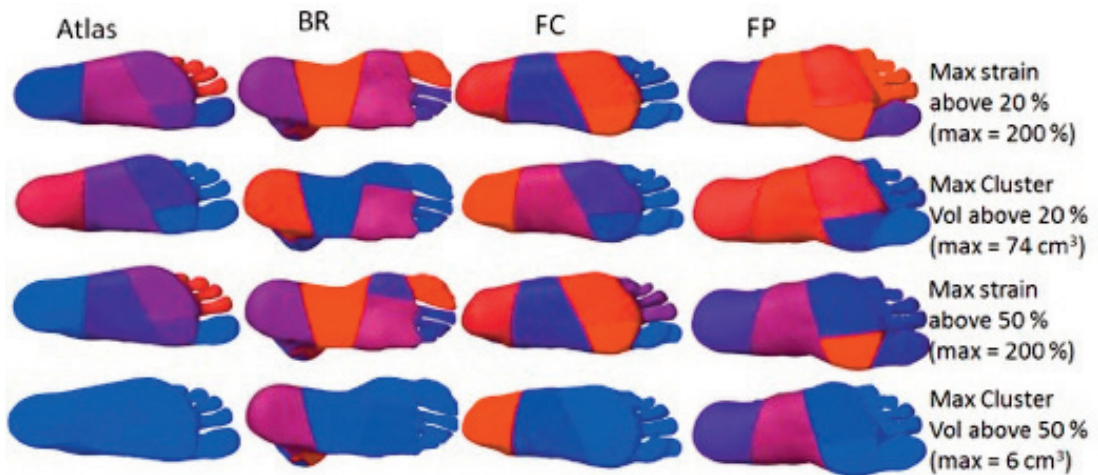


Figure Caption: Maximum VM strain and maximum cluster volume repartition for each anatomical region and for each patient, according to the strain thresholds of 20 and 50% [Loerakker]. For the strains, red colors mean strains above 200%. For cluster volume, red colors mean volume above 74cm<sup>3</sup> for strains above 20%, and volume above 6cm<sup>3</sup> for strains above 50%.

### References:

Bucki et al., *Clinical workflow for personalized foot pressure ulcer prevention*, Med. Eng. & Phys. 2016.

Loerakker et al., *The effects of deformation, ischaemia and reperfusion on the development of muscle damage*. J. App. Phys. 2011.

# PREDICTION OF SUBJECT SPECIFIC CARTILAGE DEGENERATION WITHIN THE KNEE AND COMPARISON TO EXPERIMENTS: DATA FROM THE OSTEOARTHRITIS INITIATIVE

Mika Mononen<sup>1</sup>, Petri Tanska<sup>1</sup>, Rami Korhonen<sup>2</sup>

<sup>1</sup> Department of Applied Physics, University of Eastern Finland, Kuopio, Finland,

<sup>2</sup> Department of Applied Physics, University of Eastern Finland, Diagnostic Imaging Center, Kuopio University Hospital, Kuopio, Finland

One of the first signs of cartilage degeneration in osteoarthritis is collagen fibrillation, causing tissue softening. It is suggested that excessive and cumulative loadings due to overweight are the most prominent factors causing collagen damage and osteoarthritis in cartilage tissue [1-4]. Thus, our objective was to test the ability of our recently developed degeneration algorithm [5] to predict subject specific collagen fibril degeneration within the knee joint.

Knee joint geometries were constructed from MRI data obtained from the Osteoarthritis Initiative (OAI) for ten subjects with intact knee joints (Kellgren-Lawrence (KL) grade = 0) at the baseline. Subjects were initially classified into three different groups (KL0, KL2 and KL3) according to 4-year follow-up KL grades. In KL0 group (N=3), KL grade remained unchanged (healthy), whereas in KL2 (N=3) and KL3 groups (N=4), KL grades increased from 0 to 2 and 3, respectively, indicating different levels of osteoarthritis progression. Age range of the subjects was within 48-63 years, whereas the average body mass index (BMI) range in the KL0, KL2 and KL3 subject groups varied between 20.7–24.6, 29.6–36.6 and 30.3–38.4, respectively. Recently developed cartilage degeneration algorithm, based on excessive and cumulatively accumulated stresses of collagen fibrils within knee joint cartilage during physiological gait loading [5], was implemented into each knee joint geometry (Fig. 1a). Based on the earlier study [5], the threshold stress T for the onset and development of collagen degeneration was set to 7 MPa (maximum principal stress of the tissue). Finally, subject specific cartilage degeneration was simulated with 100 iterations for each subject.

The highest fibril degeneration was predicted in the KL3 group with the algorithm, whereas in the KL0 group, almost negligible fibril degeneration occurred (Fig. 1b). Furthermore, substantial differences were observed in the fibril degeneration between the KL2 and KL3 groups.

The cartilage degeneration algorithm showed a great potential to sensitively predict different levels of cartilage degeneration between different subjects.

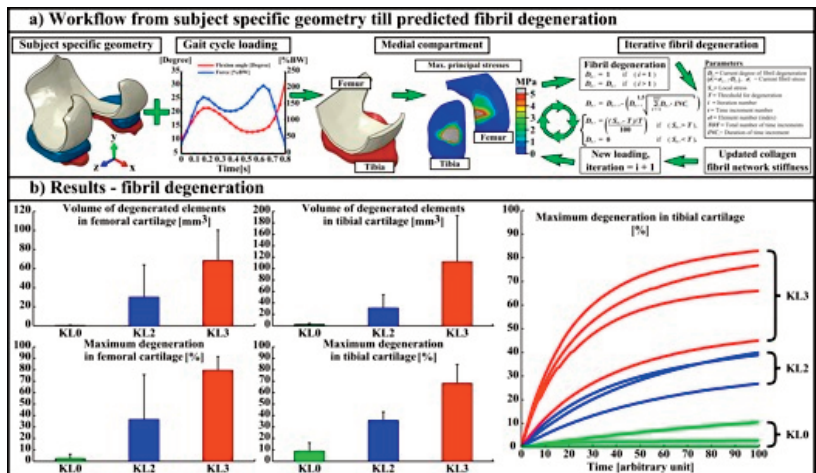


Figure 1: (a) Study workflow to predict subject specific fibril degeneration of cartilage and (b) predicted fibril degenerations in different subject groups (mean±SD, left; all subjects, right)

## References:

1. Buckwalter JA, Clin Symp 1995
2. Horisberger M, J Orthop Res 2013
3. Radin EL, Nature 1970
4. Seedhom BB, Rheumatology 2006
5. Mononen ME, Sci Rep 2016

# CONTACT PRESSURE VARIATION BETWEEN EIGHT SUBJECT-SPECIFIC FINITE ELEMENT MODELS OF THE FIRST METATARSO-PHALANGEAL JOINT

Jennifer Boyd<sup>1</sup>, Oliver Morgan<sup>1</sup>, Matthew F Koff<sup>2</sup>, Howard J Hillstrom<sup>2</sup>, Rajshree Mootanah<sup>3</sup>

<sup>1</sup> Anglia Ruskin University, Chelmsford, United Kingdom,

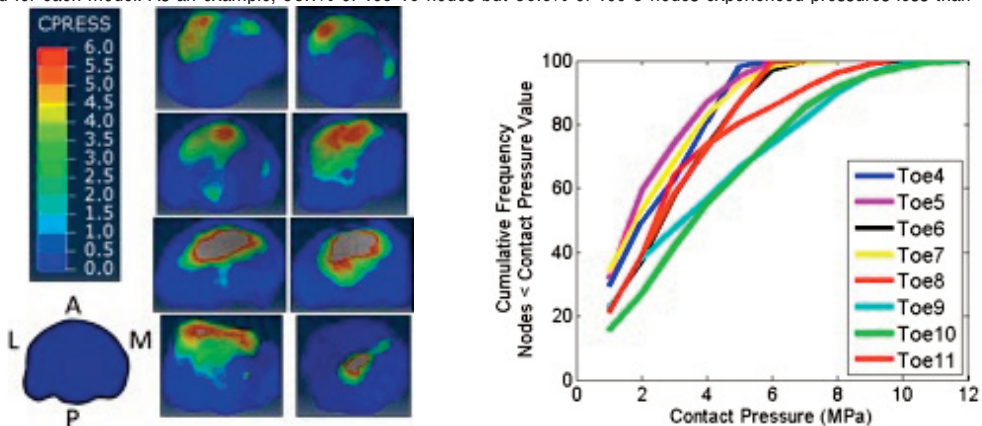
<sup>2</sup> Hospital for Special Surgery, New York City, United States,

<sup>3</sup> Anglia Ruskin University, Hospital for Special Surgery, Chelmsford, United Kingdom

Osteoarthritis in the 1st metatarso-phalangeal [MTP] joint affects 35%-60% of adults 60+ years old [1]. The cause of the disease is unknown but is hypothesised to be linked to high contact pressures within the joint. Joint contact pressures cannot be non-invasively measured in vivo but can be computed by finite element (FE) models. Subject-specific FE models can calculate pressures within an individual's joint, which is useful for personalized medicine, yet time-consuming to create. This study investigates if subject-specific models are necessary for describing 1st MTP joint contact mechanics or whether generic models would suffice. We created subject-specific FE models of eight cadaveric 1st MTP joints and compared the variability of the contact pressures between the models.

Each FE model was created using the same previously-validated model creation method. Models included the metatarsal, proximal phalanx, sesamoids, and hallux bones as well as associated cartilage, plantar fascia, and 14 tension-only "wire" ligaments. Each tissue geometry was derived from 3T MRI scans. Identical loads, material properties, and contact and boundary conditions were applied to each model. Contact pressures on the proximal phalanx's articulating surface (typical location of osteoarthritis) were then compared. Qualitatively, pressure distributions on this surface were compared. Quantitatively, cumulative frequencies of the percentages of nodes at or below threshold values (1MPa, 2MPa, 3MPa, etc) were calculated.

Unique pressure distributions, magnitudes (maximum pressures ranged from 5.5MPa to 11.4MPa), and cumulative frequencies were calculated for each model. As an example, 55.1% of Toe 10 nodes but 86.9% of Toe 5 nodes experienced pressures less than 4MPa.



This study highlights the importance of creating subject-specific FE models, especially for personalized medical treatments.

Figure Caption: (left) Distribution of contact pressure magnitudes and (right) cumulative frequencies of contact pressures on the articulating surface of the proximal phalanx. Note: All figures use the same colour threshold and are in the same orientation (shown in left panel)

## Acknowledgments:

Jonathan Deland, MD, Scott Ellis, MD, for clinical guidance.

## QUANTIFYING THE EFFECT OF IN VIVO ALGINATE INJECTIONS ON HEALTHY MYOCARDIAL TISSUE STRUCTURE

**Kevin Sack**<sup>1</sup>, **Eric Aliotta**<sup>2</sup>, **Daniel Ennis**<sup>2</sup>, **Susy Choy**<sup>3</sup>, **Ghassan Kassab**<sup>3</sup>, **Thomas Franz**<sup>4</sup>

<sup>1</sup> University of Cape Town, Observatory, South Africa,

<sup>2</sup> University of California, Los Angeles, Los Angeles, United States,

<sup>3</sup> California Medical Innovations Institute, San Diego, United States,

<sup>4</sup> University of Cape Town, Dept of Human Biology, Observatory, South Africa

Significant interest has arisen in intra-myocardial biomaterial injections as therapy for patients with myocardial infarctions (MI). These injections have shown promise pre-clinically [1-2] promoting improvements to cardiac function and wall mechanics that aim to inhibit post-MI remodeling which often leads to heart failure. However, further research is needed to understand the specific mechanisms that will enable optimal treatment efficacy. Of 12 healthy porcine hearts, 4 hearts received alginate injections and 8 hearts served as control. Alginate was delivered in 12 injections (0.3 mL each) ~ 15 mm apart in circumferential rows 10 mm above and below the midline between the base and the apex of the left ventricle (LV) from the anterior to the posterior wall. The animals were sacrificed 8-weeks post injection; the hearts were excised and underwent T1 and T2 weighted magnetic resonance imaging (MRI) at 0.33 x 0.33 x 0.7 mm spatial resolution, and diffusion tensor MRI (DT-MRI) with  $b = 1000$  s/mm<sup>2</sup>, 30 diffusion encoding directions, and 1 x 1 x 2 mm spatial resolution. Geometrically detailed finite element (FE) meshes of the LV and biomaterial injections were reconstructed from MRI data (see Figure) and morphometrically analyzed employing LV regions proposed by the American Heart Association (AHA). The injections present as discrete ellipsoids with retention of  $72.0 \pm 8.1\%$  of the injected volume. Gel ellipsoids were generally orientated circumferentially and located at  $59.7 \pm 13.7\%$  of the wall depth from the endocardium. The absence of local bulging in proximity of the injections and consistent inter-group wall thickness in AHA regions ( $16.2 \pm 2.5$  mm injected vs.  $18.2 \pm 3.2$  mm control) suggest longitudinal, rather than radial, displacement or averaging phenomena of surrounding tissue, or both. DT-MRI data demonstrated consistent regional myofibre angle distributions between the groups. Myofibre tractography (see Figure) supported these findings indicating that alginate injections do not disrupt regional myocardial structure.

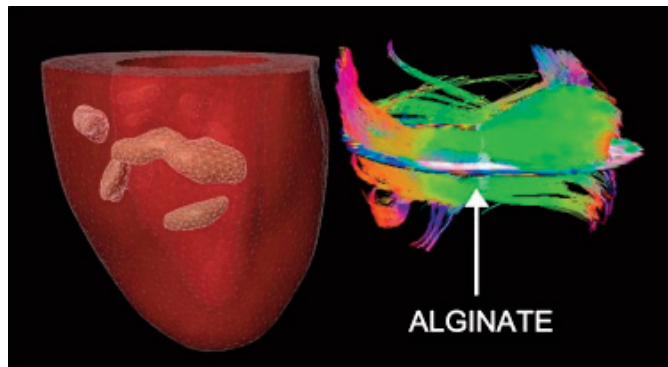


Figure Caption: FE mesh of LV with alginate injections (left) and short-axis slice with myofibre tractography data surrounding one injection (right).

### Acknowledgments:

Funding was provided by NIH grant R01HL118627, the Oppenheimer Memorial Trust and the National Research Foundation of South Africa.

### References:

1. Plotkin, M., et al., The effect of matrix stiffness of injectable hydrogels on the preservation of cardiac function after a heart attack. *Biomaterials*, 2014. 35(5): p. 1429-38.
2. Dobner, S., et al., A Synthetic Non-degradable Polyethylene Glycol Hydrogel Retards Adverse Post-infarct Left Ventricular Remodeling. *Journal of Cardiac Failure*, 2009. 15(7): p. 629-636.

## ON SOLUTION OF THE COX (1968) PROBLEM

**Raz Hechter<sup>1</sup>, Alex Yakhot<sup>2</sup>**

*1 Ben-Gurion University of the Negev, Rishon Le-Zion, Israel,*

*2 Ben-Gurion University of the Negev, Beer Sheva, Israel*

In Cox (1968), the problem of viscous incompressible unsteady flow in a viscoelastic tube has been solved. The problem was modeled as a simplification of blood flow through a large artery. The study was aimed at characterizing wave propagation through the fluid. About 50 years ago, the implementation of the Cox68 solution for analyzing the viscoelastic tube compliance was difficult as the solution is quite cumbersome for the then available computational resources. As a result, a comprehensive description of flow in a viscoelastic tube could not be attained. In attempts to apply the Cox68 solution for analyses of wall-movements, we encountered certain difficulties. Thus, the Cox68 solution needed to be revised and expanded.

In this study, we approach the Cox68 problem using the computational tools available nowadays. We reformulated the Cox-68 problem in a nondimensional form, that includes five nondimensional groups: ratio of the internal and external tube radii at rest ( $b/a$ ), ratio of fluid and elastic wall densities ( $\rho/\rho_w$ ), the Reynolds number ( $(2a\rho U_0)/\mu$ ), the Womersley number ( $a\sqrt{\rho\omega}/\mu$ ) and the complex modulus of rigidity normalized by a characteristic dynamic stress ( $\mu^*(\rho_w a^2 \omega^2)$ ). The model was expanded to accommodate arbitrary inlet flow rates. The Cox68 formulation was found to yield nonphysical axial motions, and modifications that address these were examined.

Based on the obtained solution, we developed an easy-to-use “computational lab” in MATLAB environment to determine the sensitivity of the solution to nondimensional parameters. In addition, the developed computational lab can be utilized to formulate the inverse elasticity problem that might enable deduction of arterial mechanical properties from medical imaging and measurements.

### References:

Cox, R. H. (1968). Wave propagation through a Newtonian fluid contained within a thick-walled, viscoelastic tube. *Biophysical Journal*, Vol. 8, 691.

# COHERENT STRUCTURES GOVERN WHITE BLOOD CELL TRANSPORT IN CEREBRAL ANEURYSMS

**Mark Epshtein**<sup>1</sup>

<sup>1</sup> Technion-Iit, Technion-Iit, Haifa, Israel

Aneurysms are blood filled sac like bulges in the wall of a blood vessel, which commonly develop around blood vessel bifurcations or weakened areas in a blood vessel wall. It has been long known that cerebral aneurysms are characterized by certain hemodynamic structures - namely, separated and circulatory flows. Of which coherent flow structures such as vortices are pivotal to the understanding of the initiation and progression of the disease. However, most of current work on aneurysm hemodynamics focus on the subject of wall shear stress and little work has been performed on coherent hemodynamic structures in cerebral aneurysm research.

As inflammation is a dominant mechanism in aneurysm progression as well as in promoting aneurysm rupture, it is important to understand the transport of white blood cells (WBC) into the inflamed region. Coherent hemodynamic structures such as vortices and flow separation are not common mechanisms of WBC transport, however, these structures are common at aneurysm sites. In this work, with the aid of computational fluid dynamics (CFD), we show that such structures may entrap WBCs in the vortices and transport them deep into the aneurysm. Additionally, as the vortices are dynamic in nature and are transient both in time and location, we examine the temporal and spatial features of the coherent structures and their role on WBCs transport.

Altogether, this study reviews what coherent structures in hemodynamics are and elucidate their role in the mechanism driving WBC transport at sites of cerebral aneurysm.

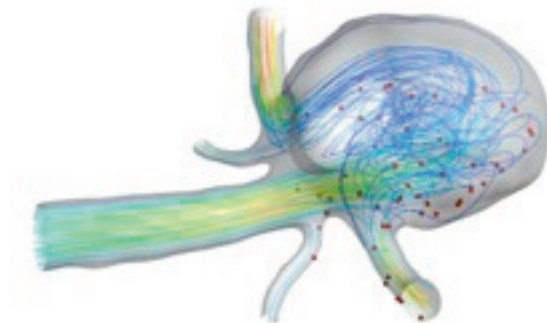


Figure 1: CFD simulations illustrating the transport of WBC at an aneurysm site.

## FLUID-STRUCTURE INTERACTION BIO-MECHANICAL MODELS OF BICUSPID AORTIC VALVES

**Karin Lavon<sup>1</sup>, Rotem Halevi<sup>2</sup>, Gil Marom<sup>3</sup>, Sagit Ben Zekry<sup>4</sup>, Ehud Raanani<sup>5</sup>, Rami Haj-Ali<sup>2</sup>**

*1 School of Mechanical Engineering, Tel Aviv University, Tel Aviv, Israel,*

*2 School of Mechanical Engineering, Faculty of Engineering, Tel Aviv University, Tel Aviv, Israel,*

*3 Biomedical Engineering Department, Stony Brook University, Ny, United States,*

*4 Echocardiography Laboratory, Chaim Sheba Medical Center, Tel Hashomer, Israel,*

*5 Department of Cardio- Thoracic Surgery, Chaim Sheba Medical Center, Tel Hashomer, Israel*

### Objective

The bicuspid aortic valve (BAV) is the most common type of congenital heart disease, occurring in 0.5-2% of the population, where the aortic valve has only two rather than the three normal cusps. BAV is associated with valvular complications, the most common of which are aortic regurgitation and aortic stenosis, which develop more rapidly than tricuspid aortic valves (TAVs). A possible cause for these complications is related to a non-optimal geometry of the valve.

The aim of this study is to provide a new Fluid-Structure Interaction (FSI) modeling approach of BAVs that can be used to investigate the influence of different geometric parameters on their functionality from the structural and hemodynamic aspects.

### Methods

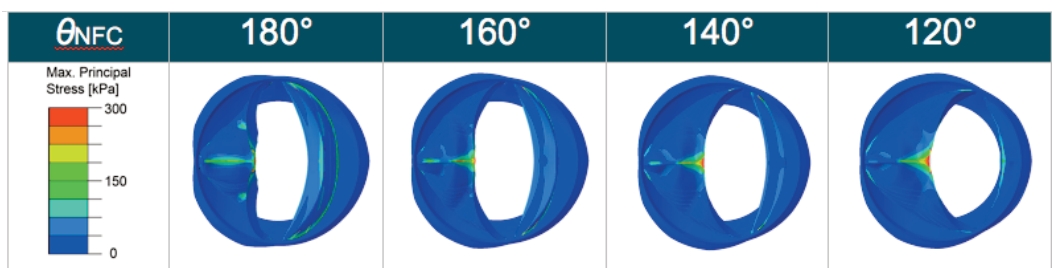
Parametric FSI models of BAVs were generated with four common BAV geometries. These included the most common BAV configuration with one raphe and different non-fused cusp (NFC) angles, which varied from 120° to 180°. The FSI simulations were based on fully-coupled structural and fluid dynamic solvers and corresponded to physiologic response values; the tissue properties in the structural model demonstrate hyper-elastic behavior. Also, “dry” (without fluid) structural finite element (FE) BAV models were simulated, and compared to the FSI cases. Echocardiography (echo) data from patients with BAVs were used to correlate with the present model results.

### Results

The simulated model results imply on a tradeoff between the increased effective orifice area (in smaller NFC angles) and the centered jet flow direction (in larger NFC angles). The measured echo results support this predicted opening pattern. As the NFC angle increased, the stresses during diastole on this cusp increased as well. Also, concentrated flow shear stress (FSS) was found in BAVs with decreased NFC angles, which can initiate calcification.

### Conclusions

The predicted biomechanical behavior in the form of jet flow patterns (hemodynamics) and stresses could help assess the functionality and durability of BAVs. High stress regions on the leaflets can explain the initiation of calcification, while asymmetric flow jet can be a major cause for aortic dilatation. The present computational model is a step forward towards patient specific simulation for future BAV repair.



Maximum principal stress distribution on the four models during peak systole

## FLUID-STRUCTURE SIMULATION OF A transcatheter AORTIC VALVE IMPLANTATION: POTENTIAL APPLICATION TO PATIENT SPECIFIC CASES

Wei Wu<sup>1</sup>, Desiree Pott<sup>2</sup>, Claudio Chiastra<sup>1</sup>, Lorenza Petrini<sup>1</sup>, Giancarlo Pennati<sup>1</sup>, Gabriele Dubini<sup>1</sup>, Ulrich Steinseifer<sup>2</sup>, Simon Sonntag<sup>2</sup>, Maximilian Kütting<sup>3</sup>, **Francesco Migliavacca**<sup>1</sup>

<sup>1</sup> Politecnico DI Milano, Milan, Italy,

<sup>2</sup> RWTH Aachen University, Aachen, Germany,

<sup>3</sup> RWTH Aachen University, Aachen, Germany

Transcatheter aortic valve (TAV) implantation is a mini-invasive procedure adopted in the treatment of valve diseases. The behavior of a TAV is influenced by the mechanics of the aortic root, the leaflets, the stent frame, and the fluid passing through the site where the valve is implanted. This work presents a fluid-structure interaction (FSI) model for the evaluation of TAVs. A TAV [1], after it was used in an in vitro mock loop, was virtually implanted in a reconstructed aortic root simulating in vivo conditions. The Nitinol TAVs are equipped with polyurethane leaflets and the model was built according to their dimensions (Fig.1a). All material properties of the valve were acquired through experimental tests. As boundary conditions, the typical ventricular and aortic pressure curves were applied to the inlet and outlet sections, respectively. The leaflets and compartment were coupled to the domain during the simulation. The commercial explicit finite element solver LS-DYNA was used to run the FSI simulation. The mean strain and strain amplitude of the valve predicted by FSI simulation considering the aortic root, if compared to a case where the valve is implanted in a silicon cylindrical compartment for accelerated fatigue tests [1], showed higher strains potentially dangerous for the fatigue behaviour. This study shows the feasibility of performing accurate simulations able to capture the main behavior of a TAV both from structural and fluid dynamic points of views. The application of this methodology to patient-specific cases enhance the capability to perform a correct surgical planning.

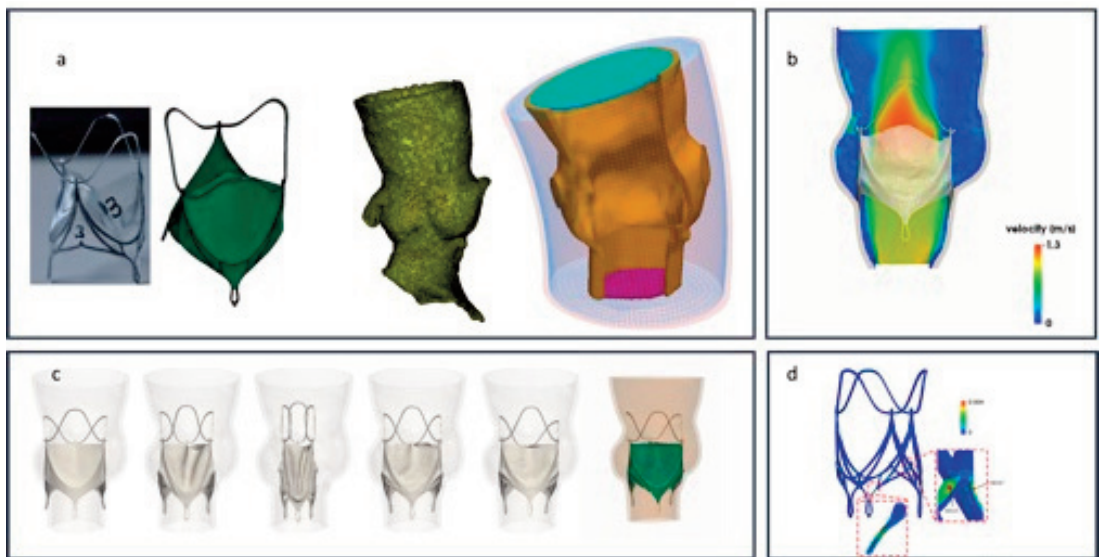


Figure 1: a) valve with leaflets and corresponding model; aortic root and FSI model; b) velocity pattern during valve opening; c) implantation of the valve into the aortic root; d) strain amplitude of the stent frame during the cycle.

### References:

[1] Wu W, et al. *Ann Biomed Eng.* 2016;44:590-603.

# COMPUTATIONAL FLUID DYNAMICS FOR INTRACRANIAL ANEURYSM RUPTURE PREDICTION & POST TREATMENT HEMODYNAMIC ANALYSIS

**Albert Einstein George<sup>1</sup>, Sreeja V<sup>2</sup>, Aishwarya Srinivasan<sup>2</sup>, Aradhana S<sup>2</sup>**

<sup>1</sup> Einnel Technologies, Chennai, India,

<sup>2</sup> Einnext Biosciences, Chennai, India

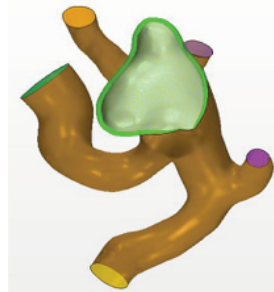
Intracranial aneurysm is a cerebrovascular disorder that weakens the intima of the cerebral artery or vein causing a local dilation of the blood vessel after which the blood vessel becomes thin and ruptures without warning. The resultant bleeding into the space around the brain is called subarachnoid hemorrhage (SAH). The incidence of intracranial aneurysm varies from 0.75 - 10.3% in India, out of which approximately 0.2 - 3% of the people suffering from intracranial aneurysm may suffer from Subarachnoid Hemorrhage per year[1].

In this context, there is an urgent need for early aneurysm rupture prediction that could save numerous human lives. Computational Fluid Dynamics (CFD) has proved to be potent enough for the prediction of intracranial aneurysm rupture. The computational analysis along with the expertise in numerical methods for the virtual prediction of complicated life threatening medical disorders is essential to be focused for the betterment of society.

In this research, we aimed to predict the rupture of intracranial aneurysm through different morphological parameters of the aneurysm and changes in hemodynamics obtained from CFD. The various treatment options for intracranial aneurysm involves endovascular clipping, coiling and both coiling and stenting. We demonstrated quantitatively and qualitatively the hemodynamic changes (velocity, pressure and wall shear stress-WSS) in artery after stent implantation and coiling into the 3D reconstructed patient-specific artery model, taking into consideration the non-Newtonian characteristics of blood using Finite Element approach. We also performed a comparison between scenarios of with aneurysm and normal artery without aneurysm, which showed considerably high WSS, pressure and velocity values in the model with aneurysm. The possible treatment options for the case were also computationally analyzed which showed stenting and coiling considerably reduced the WSS on the aneurysm dome. It was speculated that low WSS at the tip of the aneurysm and high WSS on the aneurysm dome is responsible for the rupture of aneurysm.



**(i) CFD aneurysm model**



**(ii) After coiling**



**(iii) After both coiling and stenting**

## References:

[1] Prevalence and Risk of Rupture of Intracranial Aneurysms, A Systematic Review, Gabriel J. E. Rinkel, MD; MamukaDjibuti, MD; Ale Algra, MD; J. van Gijn, MD

## A MULTI-RESOLUTION ANALYSIS OF THE MITRAL VALVE GEOMETRY FOR THE DEVELOPMENT OF PERSONALIZED MODELS

Mitral Valve (MV) regurgitation is the most common heart valve disorder, afflicting more than 2.5 millions of people in the U.S. alone. Unfortunately, the current treatment options have a high failure rate and low event-free survival. It is strongly believed that the complex Mitral Valve (MV) structure and tissue remodeling play a significant role on the valvular response to MV repair. Computational models have proven to provide powerful predictive tools to improve treatment planning and design. In this work, we have developed a full pipeline to build anatomically accurate image-based models of the full MV. We imaged three ovine MVs obtained from an USDA approved abattoir in the open and closed states using micro computed tomography (Fig. 1). The images were then segmented and processed to acquire geometric data on the MV leaflets from open and chordae tendineae from closed scans. This allowed us to fully resolve the fine features and geometric details of both leaflets and the chordal tendineae. To analyze the leaflets, we decomposed the geometry into two models: (1) a superquadric shape primitive and (2) the spectral representation of geometric details. Next, we used skeletonization filters to extract a curve-skeleton representation of the MV chordal structure enriched with dimensional information such as the cross-sectional area. We developed multi-resolution models of the MV leaflets (Fig. 1) by controlling the level of detail in geometry reconstruction using digital filtering in the frequency domain. In addition, the chordal structure was reconstructed in the curve-skeleton framework (Fig 1) enriched with registered cross-sectional area values. Another important feature of the proposed model is that our parametric representation provides smoothness of leaflet reconstruction and smoothness. High-level of smoothness allows to build high-fidelity FE models using high-order Lagrangian and novel isogeometric formulations.

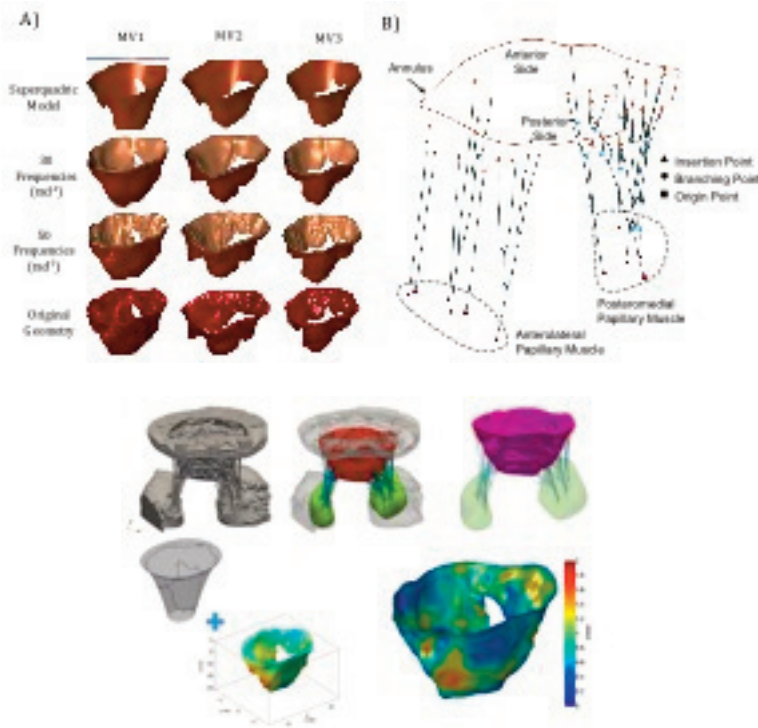


Figure 1. (A) multi-resolution reconstruction of three MV leaflets, (B) the chordae tendineae reconstruction using cubic splines. (C) shows the final results for the mitral valve, with the chordae removed for clarity.

## MECHANICAL STRESS-STRAIN RELATIONS OF PIG'S MYOCARDIUM, EXPERIMENTS AND CONSTITUTIVE MODELS

**Avihai Spizzichino<sup>1</sup>, Jacob Bortman<sup>1</sup>, Ravit Ohana<sup>2</sup>**

<sup>1</sup> Ben-Gurion University of the Negev, Be'er Sheva, Israel,

<sup>2</sup> Department of Mechanical Engineering, Be'er Sheva, Israel

This research focuses on establishing stress-strain relations via experiments and to reevaluate the parameters in constitutive models of myocardium. During the research we performed over than 50 experiments with pig myocardium tissues.

New Bi-axial test machine which is focused on the clamping method, image analysis, alignment process and control software was developed. In addition, protocol that defines the procedure for performing repetitive experiments was set.

Moreover, three sets of experiments were conducted. The first was with pig's hearts sacrificed by injection which is the preferred method by scientific literature, the second was with pigs sacrificed by electric shock which conventional method, and the third was with engineering tissues which are recently been developed.

Finally, parameters for four different models were calculated using: Holzapfel model, Horowitz & Lanir model, Guccione model and Hunter - Pole Zero model. The experimental results include strain stress relationship graphs.

It was shown that the tissue has an exponential behavior as expected. The different constitutive models were examined using the experimental results and it was found that Holzapfel, Lanir and Guccione models have better level of fitting.

In addition, we observed that pcECM have similar stiffness as pig sacrificed by injection or electric shock. Furthermore, studies about the level of fitness for global parameters show low level of fitness. That means that each tissue might have different material properties and when these parameters are implemented in material modeling, it should be taken into account to determine the specific parameters for each tissue.

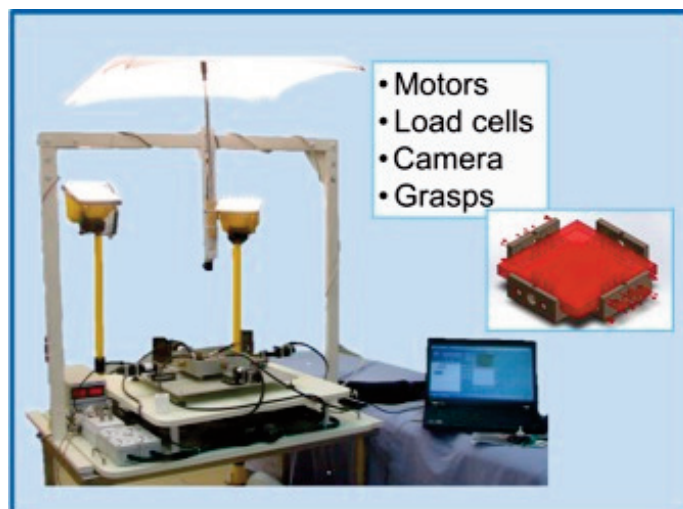


Figure 1- Experimental system, Bi-axial stretch device

# A FUNG-TYPE EXPONENTIAL CONSTITUTIVE MODEL ACCURATELY CAPTURES AND DIFFERENTIATES BETWEEN STRAIN- AND REMODELING-INDUCED STIFFENING IN CONDUIT PULMONARY ARTERIES

Mark Golob<sup>1</sup>, Omid Forouzan<sup>2</sup>, Ashley Mulchrone<sup>2</sup>, Heidi Kellihan<sup>3</sup>, Naomi Chesler<sup>4</sup>

<sup>1</sup> 2145 Engineering Centers, Madison, United States,

<sup>2</sup> 2143 Engineering Centers, Madison, United States,

<sup>3</sup> 1153 Veterinary Medicine Building, Madison, United States,

<sup>4</sup> 2146 Engineering Centers, Madison, United States

Pulmonary arterial hypertension (PAH) is a debilitating pulmonary vascular disease that changes pulmonary vascular mechanical properties, affecting hemodynamics and right ventricular function. Conduit pulmonary artery (PA) stiffening is a robust predictor of mortality in PAH. Previously, we demonstrated that acute PAH caused PA stiffening due to arterial nonlinear elasticity, termed strain-induced stiffening [1,2]. Clinically, the distinct contributions of strain- and remodeling-induced stiffening may be relevant to the predictive power of PA stiffening in PAH. Here, we investigated the ability of a four parameter 2D Fung-type exponential constitutive model [3] to differentiate between strain- and remodeling-induced PA stiffening using a chronic canine model of PAH. Chronic thromboembolic pulmonary hypertension (CTEPH) was generated in male dogs using a previously established protocol [4] with IACUC approval. After euthanasia, circumferential and axial strips (Fig. 1A) of conduit PAs were mounted in a uniaxial mechanical setup, preconditioned, and strained at a rate of 20% length/s until non-linear behavior was observed. The square of the difference between model and experimental stresses was calculated using constraints previously established [5]. Parameters were assessed using a student's t-test with a two-sided p-value < 0.05 indicating statistical significance between aged-matched controls and the CTEPH group. The model fit the data well for both groups (fitting error, Control,  $e=0.05$ ; CTEPH,  $e=0.19$ ), demonstrating strain-induced stiffening in both groups. Furthermore, the parameter associated with the slope of the mechanical response was increased with CTEPH (Fig. 1B), demonstrating that remodeling-induced stiffening was also captured by the model. We conclude that this four parameter constitutive model can account for and differentiate between strain- and remodeling-induced arterial stiffening. Application of this model to in vivo PA pressure-diameter data may yield insight into the predictive power of PA stiffening in PAH outcomes.

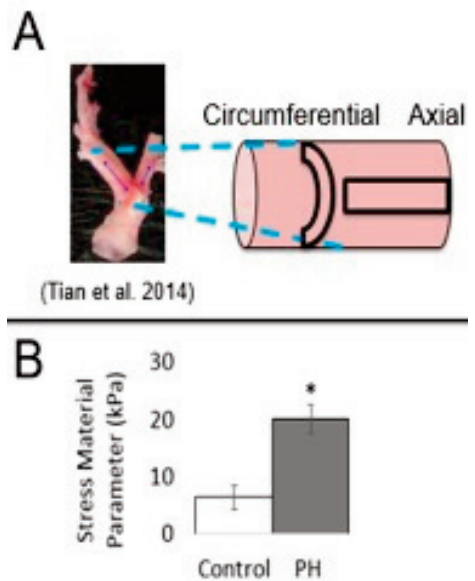
Figure 1: A) PA tissue strip orientations used for mechanical testing; B) model fit stress parameter. (Control,  $n=5$ ; CTEPH,  $n=4$ ;  $p=0.005$ ).

## ACKNOWLEDGMENTS:

This work was supported by NIH grant R01-HL105598 (NCC). The authors thank Dr. Tim Hacker and Allison Brodbeck for help with harvesting tissues, Dr. Lian Tian for constitutive modeling advice, Eric Dinges for guidance during software development, and Chandler Benjamin and Greg Wolf for assistance with mechanical testing.

## References:

- [1] Bellofiore A, et al. 2013. *Ann Biomed Eng*, 41(1):195-204.
- [2] Tian L, et al. 2014. *J Biomech*, 47: 2904-2910.
- [3] Hu JJ, et al. 2007. *J Biomech*, 40(11): 2559-2563.
- [4] Hori Y, et al. 2012. *Vet J*, 194(2): 215-221.
- [5] Holzapfel GA, et al. 2000. *J Elast Phys Sci Sol*, 61(1-3): 1-48.



## STRESS ANALYSIS OF NORMAL AND PATHOLOGICAL ARTERIES WITH RESIDUAL STRESS

Zonglai Jiang<sup>1</sup>, Shaoxiong Yang<sup>2</sup>, Yunqiao Liu<sup>2</sup>, Xiaobo Gong<sup>2</sup>

*1 Institute of Mechanobiology and Biomedical Engineering, School of Life Sciences and Biotechnology, Shanghai Jiao Tong University, Shanghai, China,*

*2 Moe Key Laboratory of Hydrodynamics, Department of Engineering Mechanics, School of Naval Architecture, Ocean and Civil Engineering, Shanghai Jiao Tong University, Shanghai, China*

The change of the stress in arteries often induces remodeling of arterial tissues, and causes severe diseases such as the aneurysm and atherosclerosis due to the local excessive stress. However, there is still short of methods to measure the stress onsite in vivo. Therefore, predicting the mechanical behaviors of arteries with computer aids becomes valuable for estimating the stress variations. In the present work, a three-dimensional finite element model of an artery was constructed for stress analysis, in which the residual stress was taken into account based on volumetric tissue growth. As a further application of the present model, the stress distribution of the atherosclerotic plaque was evaluated in a stressed hyperelastic artery for the study of plaque rupture. Dealing the residual stresses by the volumetric tissue growth, overcomes the numerical discontinuity of stress distribution arising from the co-localization of meshes comparing with the conventional opening-angle method, and avoids the large deformation calculation which may cause convergence difficulties as well. The present analysis shows that the deformation behaviors of the artery model with residual stress match other classical results. The numerical simulation of atherosclerosis suggests that stenosis plays a more dominant role in plaque rupture, and emphasizes that the present finite element analysis can be used to predict the complex three-dimensional stress distribution in pathological arteries conveniently. The present study helps doctors to gain more useful information to determine the most effective treatment for vascular diseases. Keywords— Arteries, Stress analysis, Residual stress, Volumetric tissue growth, Plaque rupture

### Acknowledgments:

The presentation of this work is supported by National Natural Science Foundation of China (11372191 and 11232010).

# COMPARISON OF DIFFERENT STRAIN-BASED PARAMETERS TO IDENTIFY HUMAN LEFT VENTRICULAR MYOCARDIAL INFARCT: A THREE-DIMENSIONAL FINITE ELEMENT STUDY

**Gerardo Kenny Rumindo<sup>1</sup>, Jacques Ohayon<sup>2</sup>, Magalie Viallon-Croisille<sup>3</sup>, Matthias Stuber<sup>4</sup>, Pierre Croisille<sup>3</sup>, Patrick Clarysse<sup>5</sup>**

<sup>1</sup> Univ Lyon, Insa - Lyon, Université Lyon 1, Ujm-Saint Etienne, Cnrs, Inserm, Creatis Umr 5220, U1206, Lyon, France,

<sup>2</sup> Laboratory Timc-Imag/Dyctim, Ujf, Cnrs, Umr 5525, In3s, Grenoble, Polytech Annecy-Chambéry, University of Savoie Mont-Blanc, Le Bourget du Lac, Grenoble, France,

<sup>3</sup> Univ Lyon, Insa - Lyon, Université Lyon 1, Ujm-Saint Etienne, Cnrs, Inserm, Creatis Umr 5220, U1206, Saint-Etienne, France,

<sup>4</sup> Department of Radiology, University Hospital and University of Lausanne, Center for Biomedical Imaging and Center for Cardiovascular Magnetic Resonance Research, University of Lausanne, Lausanne, Switzerland,

<sup>5</sup> Univ Lyon, Insa - Lyon, Université Lyon 1, Creatis Cnrs Umr 5220, Inserm U1206, Insa Batiment Blaise Pascal, Lyon, France

Assessment of post-ischemic myocardial damage is important to obtain an accurate long-term prognosis after myocardial infarction. Myocardial strains have been shown to be good indicators of the myocardial viability [1]. Strain analysis has been used to identify dysfunctional regions, and several strain-based parameters have been proposed to detect regions of infarct: fractional anisotropy [2], principal strain [3], and local directional strains [1]. In this study, these parameters were used to detect synthetically generated infarct lesions on left ventricles. In addition, effective strain, and stretch-dependent invariance in fiber, sheet, and sheet-normal directions were also tested. The parameters were investigated on ten virtual three-dimensional cases based on healthy human left ventricles extracted from MRI examinations [4]. Realistic infarcts were generated for each virtual case with different locations, shapes, sizes and stiffer materials. Diastolic virtual strain data were obtained via finite-element simulations using widely implemented passive constitutive law [4] and rule-based myofiber orientation. This simulation-based approach enables a definite ground truth for the quantitative assessment of each tested parameter. Our preliminary results show that in comparison with the other tested parameters, the stretch-dependent invariance in fiber direction is able to better delineate the infarct in pathological hearts.

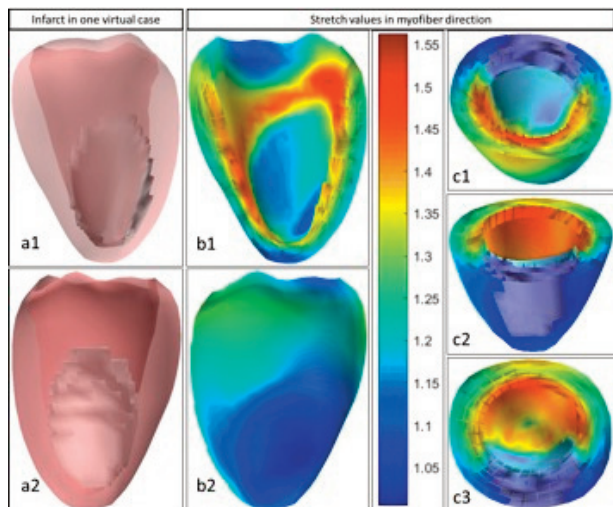
*Figure Caption: Visualization of one virtual case at end-diastole. The left ventricle (red) and the synthetic infarct (grey) in posteromedial (a1) and anterolateral (a2) views. Color map of the stretch-dependent invariance in fiber direction: endocardial cross-section (b1) and epicardium (b2) views. Lateral (c1,c2) and axial (c3) cross-section views, with superimposed synthetic infarct (grey).*

## Acknowledgments:

This project has received funding from the European Union's Horizon 2020 research and innovation programme under the Marie Skłodowska-Curie agreement No 642612.

## References:

1. MJW Götte et al. Quantification of regional contractile function after infarction: strain analysis superior to wall thickening analysis in discriminating infarct from remote myocardium. *J Am Coll Cardiol.* 2001.
2. S Soleimanifard et al. Identification of myocardial infarction using three-dimensional strain tensor fractional anisotropy. *Proc IEEE Int Symp Biomed Imaging.* 2010
3. WN Lee et al. Preliminary validation of angle-independent myocardial elastography using MR tagging in a clinical setting. *Ultrasound Med Biol.* 2008
4. M Genet et al. Distribution of normal human left ventricular myofiber stress at end diastole and end systole: a target for in silico design of heart failure treatments. *J Appl Physiol.* 2014

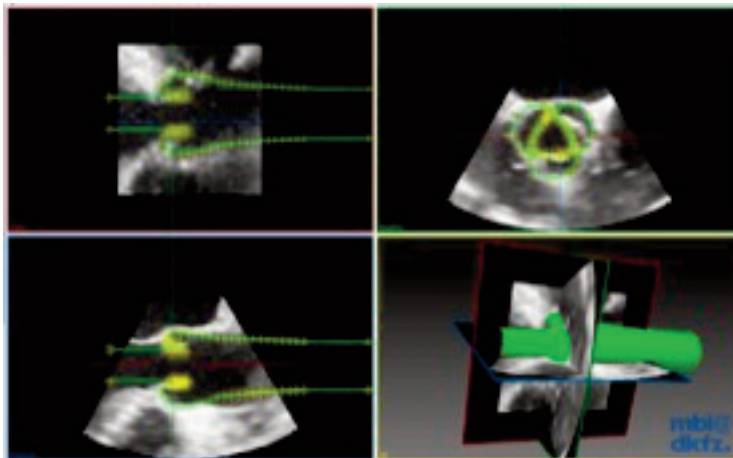


## PATIENT-SPECIFIC SIMULATIONS OF AORTIC VALVE FLOWS

**Arnas Kačeniauskas<sup>1</sup>, Vadimas Starikovičius<sup>1</sup>, Algirdas Maknickas<sup>1</sup>, Eugenius Stupak<sup>1</sup>, Giedrius Davidavičius<sup>2</sup>**  
*1 Vilnius Gediminas Technical University, Vilnius, Lithuania, 2 Vilnius University Hospital "santariškių Klinikos", Interventional, Adult Cardiology, Vilnius, Lithuania*

The emergence of a hemodynamic theory of aortic valve calcification has motivated the investigation of aortic valve hemodynamics. CFD computations based on the geometry extracted from medical images seem to be well suited for patient-specific analysis and is compatible with clinical routine [1]. The geometry of the aortic valve was obtained from electrocardiographically gated 4D images that were acquired by using the Philips iE33 ultrasonographic system. The MITK was employed to obtain the geometric parameters of aortic valve. A 3D geometric model was constructed from NURBS surfaces in Blender software according to the extracted geometric parameters. Fig. 1 shows the geometrical model defined by control points that can be adjusted in the MITK environment. Pulsatile blood flow through the aortic valve was described by incompressible Navier-Stokes equations solved by the finite volume method. Different types of boundary conditions were considered to investigate their influence to the numerical solution. The systolic phase of the cardiac cycle was analyzed by applying at the inlet a pulsatile plug flow based on the clinical Doppler measurements and analytic approximations. At the outflow the prescribed pressure and zero velocity gradient normal to the boundary were applied. The time-dependent pressure values were defined by using the three-element Windkessel model. Several sets of model parameters were examined to imitate human arterial systems characterized by Stergiopoulos et al [2]. The computed pressure fields were compared with the results obtained specifying the alternative traction-free boundary conditions at the outlet in terms of the pressure gradient, which is extremely valuable in assessing of aortic valve stenosis.

*Figure Caption: Processing of the patient-specific geometry in the MITK environment*



### Acknowledgments:

The research is supported by the Research Council of Lithuania (AVALVE project, MIP-052/2014).

### References:

1. ChnafaC, MendezS, NicoudF. 2012. Image-based patient-specific simulation: a computational modelling of the human left heart haemodynamics. *Comput. Methods Biomech. Biomed. Eng.* 15:1-3.
2. StergiopoulosN, WesterhofBE, Westerhof N. 1999. Total arterial inertance as the fourth element of the windkessel model. *American Journal of Physiology.* 276:H81-88.

## VALIDATION OF A FOUR CHAMBER PORCINE HEART MODEL

**Brian Baillargeon**<sup>1</sup>

*<sup>1</sup> Dassault Systèmes Simulia Corp, Fremont, Ca, United States*

Pre-clinical research relies on animal models as using humans as research subjects is not feasible. Building on the established methodology of a four chamber human heart finite element model previously developed, a complete porcine heart model was created using ex-vivo diffusion tensor MRI. The Abaqus multiphysics simulation combines electrical, mechanical and blood flow responses to provide a complete representation of the electromechanical function of the heart. The computational response of the tissue in the left and right ventricles is validated using in-vivo wall motions, as well as left ventricle strains measured using "tagged" MRI as comparator.

# THE INSTANTANEOUS STOKES NUMBER FOR AEROSOL TRANSPORT AND DEPOSITION IN THE RESPIRATORY AIRWAYS

Laura Nicolaou<sup>1</sup>, Tamer Zaki<sup>2</sup>

<sup>1</sup> Imperial College London, London, United Kingdom,

<sup>2</sup> Johns Hopkins University, Baltimore, United States

Prediction of aerosol deposition in the respiratory system is important in the optimisation of inhaled drug delivery for lung disease. Deposition is typically described as a function of a global Stokes number,  $St_{kref}$ , based on a reference flow timescale which is evaluated from a characteristic flow velocity and length scale. Scatter in the deposition data versus Stokes number exists due to the qualitative differences in the flow at different flow rates, and across subjects as a result of geometric variation [1]. A dependence on Reynolds number was observed for deposition in an idealised mouth-throat geometry, and an empirical Reynolds number correction,  $Re^{0.37}$ , was derived [2]. The physical significance of this correction was later explained via examination of the flow fields in a number of realistic mouth-throat geometries [1].

The dependence of deposition on Reynolds number highlights the effect of the flow on particle transport. The reference Stokes number, and Reynolds number correction, do not take into account the varying flow timescales that particles experience as they are advected through the flow. In order to gain a better understanding of the particle transport and deposition we propose the use of an instantaneous Stokes number based on the local properties of the flow field. We define the effective Stokes number,  $St_{keff}$ , as the time-average of the instantaneous value. This effective Stokes number thus encapsulates the flow history and geometric variability, and provides a more detailed representation of the particle's trajectory in the flow. Our results demonstrate that the effective Stokes number can deviate significantly from the reference value. In addition,  $St_{keff}$  shows a clear correlation with deposition efficiency and can therefore be used to determine optimal aerosol release locations for enhanced pulmonary drug delivery.

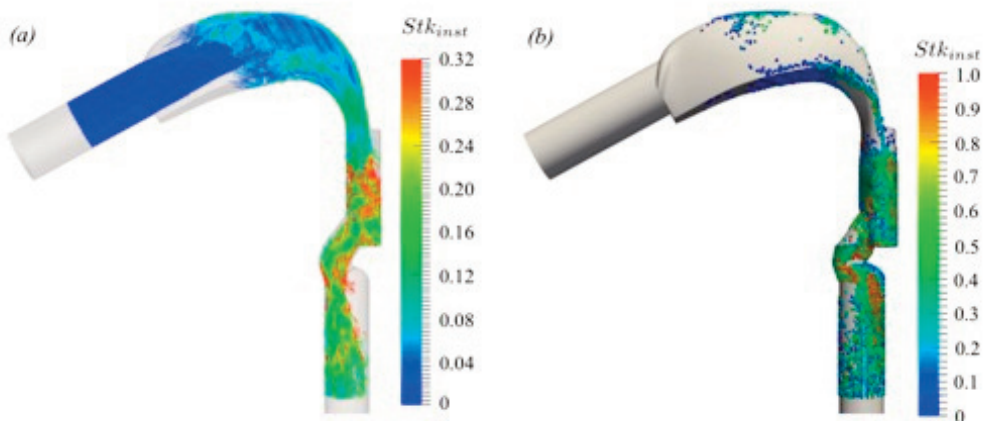


Figure Caption:  $6\mu\text{m}$  particles ( $St_{kref} = 0.012$ ) in the extrathoracic airways. (a) Trajectories, and (b) deposited particles coloured by instantaneous Stokes number.

## References:

[1] Nicolaou L, Zaki TA. Direct numerical simulations of flow in realistic mouth- throat geometries.

*J Aerosol Sci* 2013, 57:71-87.

[2] Grgic et al. Regional aerosol deposition and flow measurements in an idealized mouth and throat.

*J Aerosol Sci* 2004, 35: 21-32.

## FATE OF INHALED AEROSOLS IN HETEROGENEOUS PULMONARY ACINI

Philipp Hofemeier<sup>1</sup>, Kenichiro Koshiyama<sup>2</sup>, Shigeo Wada<sup>2</sup>, Josue Sznitman<sup>3</sup>

<sup>1</sup> Department of Biomedical Engineering, Technion - Israel Institute of Technology, Haifa, Israel,

<sup>2</sup> Graduate School of Engineering Science, Osaka University, Toyonaka, Japan,

<sup>3</sup> Technion - Israel Institute of Technology, Dept. of Biomedical Engineering, Haifa, Israel

Inhaled (ultra)fine aerosols are widely acknowledged to reach and deposit in the lung's acinar regions. Particle transport, and ultimately deposition outcomes, are intrinsically coupled with the local shape and morphology of the airways and alveolar cavities. Previous studies in bifurcating acinar models have been mostly restricted to generic geometrical models that do not capture the dense heterogeneous acinar morphology. Recently, Koshiyama and Wada introduced an algorithm to randomly generate space-filling heterogeneous alveolar structures that mimic realistic in vivo environments. Here, we utilize such acinar models as the basis for numerical simulations of respiratory acinar flows and particle transport. By generating and modeling various heterogeneous multi-generation acinar models, we shed light on the role of spatial acinar heterogeneity on particle deposition fate, as a function of inhaled particle size and breathing maneuvers.

Here, we analyze various domain sizes, up to a characteristic sub-acinus, as well as differences in local topology including gravity orientations. Figure 1 (left) exemplifies an acinar domain combined with the bifurcating tree structure. Using these physiologically-realistic topologies, computational simulations of the airflow and particle transport are performed. Actuating the fluid and thereby, the airborne particles, cyclic expansions of the domain are imposed to mimic breathing motion. Particles are injected during the second half of the inhalation to account for the travel time of the particles through the dead space. Particle diameters ( $0.001\text{-}5\ \mu\text{m}$ ) spanning the whole size range acknowledged to potentially reach the acinar region (Fig. 1, right). Accordingly, particles sizes covering three orders of magnitude in diameter were modeled featuring a variety of governing transport mechanisms, i.e. diffusion, sedimentation and convection.

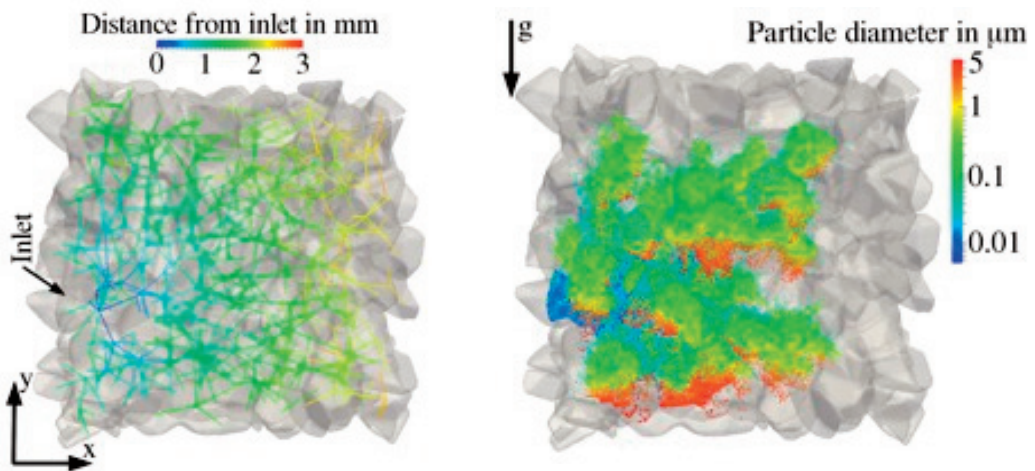


Figure 1: Left: Domain and bifurcation structure with 881 airspaces. Right: Particle locations at the end of inhalation ( $t = 0.5 T$ ); color-coding indicates particle diameter.

### Acknowledgments:

This work was supported in part by the Israel Science Foundation (ISF grant nr. 992)

### References:

Hofemeier P and Sznitman J, *J Appl Physiol*, 118: 1375-1385 2015.

Koshiyama K and Wada S, *Comput Biol Med*, 62:25-32, 2015.

## RECRUITMENT AND DERECRUITMENT IN A COMPREHENSIVE COMPUTATIONAL LUNG MODEL

**Wolfgang A. Wall<sup>1</sup>, Christian J. Roth<sup>1</sup>, Tobias Becher<sup>2</sup>, Inèz Frerichs<sup>3</sup>, Norbert Weiler<sup>4</sup>**

<sup>1</sup> Institute for Computational Mechanics, Technical University of Munich, Garching, Germany,

<sup>2</sup> Department of Anesthesiology and Intensive Care Medicine, Christian Albrechts University Kiel, Kiel, Germany,

<sup>3</sup> Klinik für Anästhesiologie und Operative Intensivmedizin, Universitätsklinikum Schleswig-Holstein, Campus Kiel, Kiel, Germany,

<sup>4</sup> Klinik für Anästhesiologie und Operative Intensivmedizin, Universitätsklinikum Schleswig-Holstein, Campus Kiel, Kiel, Germany

Using recruitment maneuvers [1] to re-open collapsed regions of the lung in patients suffering from respiratory dysfunction includes an inherent risk of ventilator-induced barotrauma. Here, we extend a comprehensive computational lung model with an approach to computationally predict advances and risks of potential reopening maneuvers before applying them in practice.

Our approach is integrated into a comprehensive computational lung model [2] based on medical imaging data. In regions where collapse or fluid filling is identified, all airways are collapsed and the dynamics of reopening and collapse are evaluated following [3].

For a reopening pressure of 40cmH<sub>2</sub>O in line with clinical standards there is good accordance between computationally predicted reopening and clinical measurement (see Figure 1). Computations show that the required reopening pressure for our patient is 75cmH<sub>2</sub>O and that the associated risk for barotrauma overbalances the benefit of derecruitment in this particular setting.

We hope that this computational prediction of reopening pressure and barotrauma risk will help clinicians to evaluate advances and risk of potential recruitment maneuvers and to improve patient-tailored protective mechanical ventilation in future.

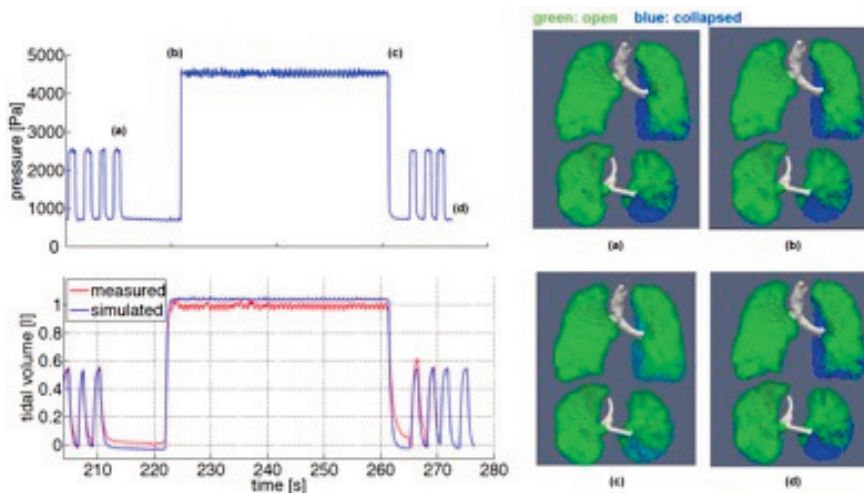


Figure 1: Comparison of tidal volume and recruitment behavior between simulation and clinical measurement for the applied pressure.

### References:

[1] P. J. Papadakos and B. Lachmann, *Crit. Care Clin.*, 23:241-50, 2007.

[2] C. J. Roth, M. Ismail, L. Yoshihara and W. A. Wall, *Int. J. Numer. Method Biomed. Eng.*, submitted.

[3] B. Ma and J. H. T. Bates, *Ann. Biomed. Eng.*, 38:3466-77, 2010.

## DISTRIBUTION OF NANO-AND MICRO-PARTICLE DEPOSITIONS IN A MURINE PULMONARY ACINAR MODEL

**Toshihiro Sera**<sup>1</sup>, **Ryosuke Higashi**<sup>2</sup>, **Yuri Inagaki**<sup>3</sup>, **Gaku Tanaka**<sup>3</sup>, **Masao Tanaka**<sup>4</sup>

<sup>1</sup> Department of Mechanical Engineering, Kyushu University, Fukuoka, Japan,

<sup>2</sup> Department of Mechanical Science and Bioengineering, Graduate School of Engineering Science, Osaka University, Toyonaka, Japan,

<sup>3</sup> Department of Mechanical Engineering, Chiba University, Chiba, Japan,

<sup>4</sup> Department of Mechanical Science and Bioengineering, Graduate School of Engineering Science, Osaka University, Toyonaka, Japan

We quantitatively investigate nano- and micro-particle deposition (density: 1.0 g/cm<sup>3</sup>, diameter: 0.2–1.0  $\mu$ m) in a pulmonary acinus during a deep breathing. Particle transport and deposition are simulated using computational fluid dynamics with expansion and contraction of the acinar model, the volume changing sinusoidally with time as the boundary conditions. In particular, we base the acinar model and volume change on a synchrotron micro-computed tomography of a mammalian lung (1), and evaluate the distribution of particle depositions through acinar generation. In this study, functional residual capacity (FRC) was defined as the lung volume at euthanasia, and the lung airway pressure was 0 cm H<sub>2</sub>O. And, Total lung capacity (TLC) was defined as the lung volume at 1.0-ml air inflation and a pressure of 25.0 cm H<sub>2</sub>O. The acinar volumes at FRC and TLC (VFRC and VTLC) were  $4.94 \times 10^{-11}$  m<sup>3</sup> and  $1.87 \times 10^{-10}$  m<sup>3</sup>, respectively. Under self-similar and sinusoidal deformation to achieve volume change between VFRC and VTLC, the maximum Reynolds numbers (Re) at the inlet (generation 1) and terminal alveoli (generation 12) were 0.191 and  $1.93 \times 10^{-3}$ , respectively. With Brownian force, particle deposition is strongly affected, except for the 1.0- $\mu$ m particle. The deposition fraction of the 0.2- $\mu$ m particle is approximately 70 % and 17 % with and without Brownian force, respectively. And, with Brownian force, 50% of 0.2- $\mu$ m deposited particles are deposited at the terminal alveoli. The deposition fraction per segment for the 1.0- $\mu$ m particle reaches 30% around the inlet (generation 10), owing to sedimentation after the beginning of inflation. We find that the particles are deposited at terminal alveoli during a deep breathing and that the deposition is enhanced by gravity, Brownian force, and the complex acinar geometry, despite the small terminal velocity.

### REFERENCES:

(1) Sera, T., Yokota, H., Tanaka, G., Uesugi, K., Yagi, N., Schroter, R.C., 2013. Murine pulmonary acinar mechanics during quasi-static inflation using synchrotron refraction-enhanced computed tomography. *J. Appl. Physiol.* 115, 219–228.

# IN SILICO ASSESSMENT OF MOUTH-THROAT EFFECTS ON REGIONAL DEPOSITION IN THE CONDUCTING HUMAN AIRWAYS

Pantelis Koullapis<sup>1</sup>, Laura Nicolaou<sup>2</sup>, Stavros Kassinos<sup>1</sup>

<sup>1</sup> Computational Sciences Laboratory (Ucy-CompSci), Department of Mechanical and Manufacturing Engineering, University of Cyprus, Nicosia, Cyprus,

<sup>2</sup> Imperial College London, London, United Kingdom

## Introduction

Quantifying regional lung deposition of therapeutic aerosols is important for developing customized or targeted therapies for classes of patients. Yet, the in vivo measurement of lung deposition is expensive, time-consuming process and carries risks to human subjects. As result there has been a search for in vivo – in vitro correlations that provide a link between in vivo drug deposition in the human lung and in vitro predictions. In the current pharmacoepial state of the art, assemblies of validated inlet throat models are often mounted on cascade impactors to produce estimates of total lung deposition. Yet, such in vitro methods cannot produce reliable estimates of regional deposition, especially for classes of patients with diseased airways. The purpose of this study is to assess the possibility of using volume-matched model inlet throats for the in silico assessment of regional lung deposition for classes of patients.

## Method

Large Eddy Simulations (LES) were used to assess the detailed regional aerosol deposition in complete patient airway geometry (mouth to 7th bronchial generation) derived from a patient CT-scan. Then, the actual patient mouth-throat section was replaced by three validated mouth-throat models derived from CT-Scans [1,2] and LES was again used to assess regional deposition in the conducting airways under the same inflow conditions. Regional deposition in the complete patient geometries and in the merged geometries are compared in detail.

## Results

Large-scale LES studies are currently in progress and will be completed in the coming months. At the time of the presentation, we will be in position to report the relative errors in regional deposition estimates introduced by the replacing the actual patient mouth-throats by validated inlet throat models.

## References:

[1] Grgic, B., Finlay, W. H., Burnell, P. K. P. and Heenan, A. F. 2004. In vitro intersubject and intrasubject deposition measurements in realistic mouth-throat geometries. *Journal of Aerosol Science* 35:1025-1040

[2] Nicolaou, L. and Zaki, T. A. 2013. Direct numerical simulations of flow in realistic mouth-throat geometries. *Journal of Aerosol Science* 57:71-87

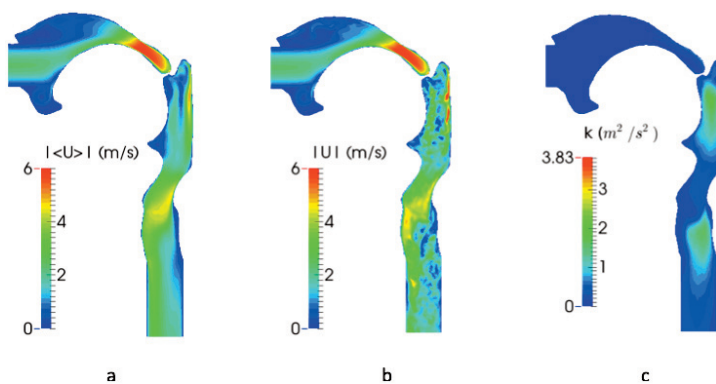


Figure Caption: Contours of (a) the mean velocity, (b) the instantaneous velocity and (c) the turbulent kinetic energy in one of the model mouth-throat geometries.

# RESPIRATORY FLOW BEHAVIOR IN BRONCHIAL AIRWAYS: EVOLUTION FROM CHILDHOOD TO ADULTHOOD

**Katrin Bauer<sup>1</sup>, Josue Sznitman<sup>2</sup>**

<sup>1</sup> TU Bergakademie Freiberg, Institute of Mechanics and Fluid Dynamics, Freiberg, Germany,

<sup>2</sup> Technion - Israel Institute of Technology, Dept. of Biomedical Engineering, Haifa, Israel

## Introduction:

Premature babies are particularly prone to suffer from lung diseases due to their underdeveloped lungs. Frequently they require mechanical ventilation that can eventually lead to lung injuries and chronic lung diseases. Hence, special effort has to be taken to protect the lungs during mechanical ventilation. One ventilation strategy often adopted to protect the premature lungs from overdistension (volutrauma) is High Frequency Oscillatory Ventilation (HFOV). Under HFOV, oscillatory frequencies are increased by a factor of about 10 while the tidal volume is decreased to about 1-2ml/kg bodyweight. Despite widespread clinical use of HFOV, there is no broad consent on the ideal settings. In adults it has been recently shown that HFOV might even damage more than it helps (Ferguson, 2014). The question arises as how does respiratory flow behavior fundamentally change from childhood to adulthood, under normal breathing as well as HFOV conditions.

## Methods:

A 3D model of the upper bronchial tree from the trachea down the 6th generation was constructed. Since the formation of the conductive airways is accomplished around the 17th week of gestation, an adult geometry of the large airways can be scaled down to match the size of a neonate as a first approximation. Special care needs to be taken for the boundary conditions. Not only the tidal volume and breathing frequency have to be adjusted accordingly but also the large change in compliance and resistance have to be taken in consideration. Physiological flow conditions matching normal ventilation as well as HFOV are applied by matching Reynolds and Womersley numbers. Oscillatory flow simulations are carried out using OpenFoam and the evolving flow patterns are investigated in detail.

## Results:

Preliminary results suggest similar flow patterns for babies and adults. However, local shear rates, captured here by vorticity decrease by a factor of about 5 from childhood to adulthood.

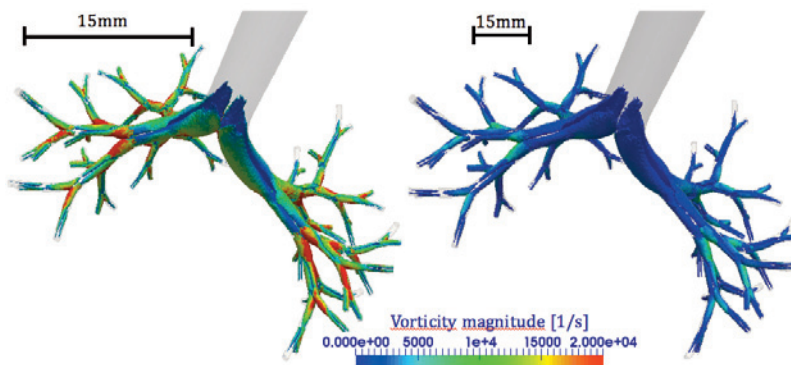


Figure Caption: Respiratory flow patterns during inspiration in a neonatal (left) and adult (right) upper airway geometry. Shown are contours of the helicity with color-coded vorticity magnitude.

## References:

Ferguson, N. D. (2014). High-frequency oscillatory ventilation in adults: handle with care.

Critical Care (London, England), 18(4), 464.

# MULTI-D MODELS FOR RESPIRATION AND AEROSOL IN HEALTH AND DISEASE

## **Vignon-Clementel<sup>1</sup>**

*<sup>1</sup> Inria, Paris, France, Upmc Universite Paris 6, Laboratoire Jacques-Louis Lions, France, Paris, France*

Computational modeling has become a powerful tool to investigate ventilation and aerosol spread in the lung in health and disease, such as asthma or emphysema. For respiration, our simulations range from global OD models for parameter estimation from data [1], to extensive OD models if airway tree information is available, and 3D models for more regional representation for the airways [2] and/or the lung tissue. The selection of one or the other, or their coupling, depend on the biomedical to be addressed, the heterogeneity of the disease [2], and the available data. Moreover, aerosol spread in the lung cannot be currently imaged in a dynamic way. Simulations can provide insights about such dynamics. We have built multi-dimensional tools to study differences between lobes, inspiration versus expiration, and disease versus healthy states [3].

## **Acknowledgments:**

This work has been supported by ANR, NIH, NSF, Burroughs Wellcome Funds, INRIA international grant, University of California Presidential Postdoctoral Fellowship, Whitaker International Scholarship, Israel Science Foundation.

## **References:**

1. JM Oakes, AL Marsden, C Grandmont, SC Shadden, C Darquenne, IE Vignon-Clementel. *Airflow and Particle Deposition Simulations in Health and Emphysema: From In Vivo to In Silico Animal Experiments*, *Annals of Biomedical Engineering*, 42 (4), pp.899-914, 2014.
2. JM Oakes, AL Marsden, C Grandmont, C Darquenne, and IE Vignon-Clementel. *Distribution of aerosolized particles in healthy and emphysematous rat lungs: Comparison between experimental and numerical studies*. *Journal of Biomechanics*, 48:1147-1157, 2015.
3. JM Oakes, Ph Hofemeier, IE Vignon-Clementel, and J Sznitman. *Aerosols in healthy and emphysematous in silico pulmonary acinar rat models*. *Journal of Biomechanics*, 2016.

# CHEST WALL KINEMATICS USING TRIANGULAR COSSERAT POINT ELEMENTS IN HEALTHY AND NEUROMUSCULAR SUBJECTS

**Dana Solav<sup>1</sup>, Henri Meric<sup>2</sup>, Frédéric Lofaso<sup>3</sup>, Alon Wolf<sup>1</sup>**

<sup>1</sup> Technion, Haifa, Israel,

<sup>2</sup> Upvd Département Staps, Font-Romeu, France,

<sup>3</sup> Université de Versailles Saint-Quentin-En-Yvelines, Versailles, France

Optoelectronic plethysmography (OEP) has shown to be a reliable and accurate method for measuring lung volume changes during breathing in various positions and conditions. OEP enables the detection of asynchronous and asymmetric movements between the Chest Wall (CW) compartments [1]. Typically, OEP is used to measure of volume variations of up to six CW compartments. The objective of this study is to enrich the kinematical description of the CW and thus enhance the clinical interpretation of pulmonary function tests. The kinematical methods used here are based on the Triangular Cosserat Point Element (TCPE) method [2], previously developed for bone pose estimation.

3 groups were examined; 10 healthy subjects, 10 patients with Duchenne muscular dystrophy (DMD), and 9 with Pompe disease. The positions of 52 markers attached to the anterior CW in anatomical positions [1] were recorded in the supine position during spontaneous breathing. A mesh of 78 triangles was defined by the markers (Fig.1a). Each triangle was characterized by a TCPE, and the non-rigid kinematics of each TCPE was described by 4 scalar parameters ( $P_i$ ). Attention will be given here to the outward translation parameter (PT) only. In addition, the volume variations of the CW ( $V_{cw}$ ) were computed by applying the Gauss divergence theorem. The phase angles  $\Theta(PT, V_{CW})$  were computed from the Lissajou figures obtained by plotting  $V_{cw}$  versus PT. In this method,  $\Theta=0^\circ / \Theta=\pm 180^\circ$  represent complete synchrony/asynchrony, respectively [3].

Fig.1b shows a characteristic pattern of  $\Theta(PT, V_{CW})$  for each group. Healthy: values close to zero over the entire CW (mean:  $-2^\circ \pm 10^\circ SD$ ). DMD: negative values ( $-45^\circ \pm 22^\circ$ ) in the medial CW and positive ( $-40^\circ \pm 18^\circ$ ) in the lateral and abdominal CW. Pompe: large negative values ( $-90^\circ \pm 47^\circ$ ) in the abdominal CW and positive values in the thoracic CW ( $80^\circ \pm 43^\circ$ ). Neuromuscular disease typically causes progressive respiratory muscle weakness. In particular, diaphragm weakness is evident in Pompe patients, which causes asynchrony and low contraction, and causes an abdominal paradoxical motion. In this study, PT appears as a good tool to analyze the kinematical pattern over the CW and distinguish the paradoxical motion.

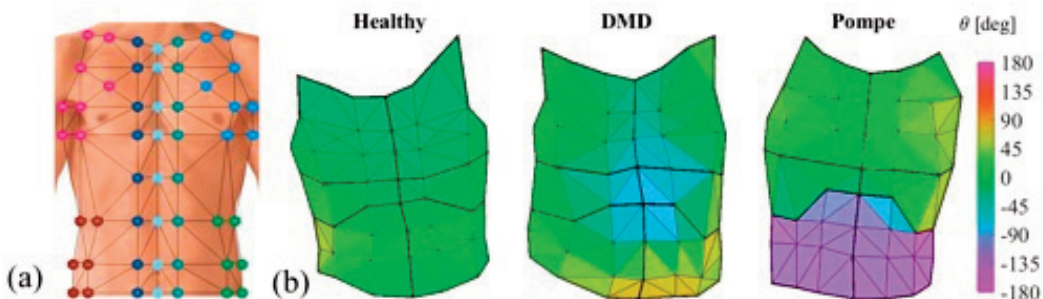


Fig.1: (a) Anatomical marker placement. (b) A characteristic patterns of the values of  $\theta(P_i, V_{CW})$  for each group of subjects.

## REFERENCES:

- Boudarham et al, *Chest*, 2013.
- Solav et al, *Ann Biomed Eng*, 2015.
- Aliverti et al, *Eur Respir J*, 2009.

# RELIABLE ANALOG AND DIGITAL COMPUTATION IN LIVING CELLS

**Ramez Daniel**<sup>1</sup>

*<sup>1</sup> Technion - Israel Institute of Technology, Haifa, Israel*

Biomolecular computing, encompassing computations performed by molecules, proteins and DNA, is a central area of focus in Synthetic Biology research and development, which attempt to apply engineering design principles in living cells. Two major computation paradigms have been implemented so far in living cells - analog paradigm that computes with a continuous set of numbers and digital paradigm that computes with two-discreet set of numbers. Here, we analyze the biophysical and technological limits of large-scale gene networks created based on analog and digital computation in living cells. More specifically, we calculate the precision of analog systems and the noise margin of digital systems in living cells. We conclude that both systems are challenging to operate with low protein levels. To overcome this challenge, we show that analog systems should operate with a Hill coefficient smaller than 1 and digital systems should be buffered. An analytical description of a biophysical model recently developed for positive feedback linearization circuits and used in analog synthetic biology, is presented. Furthermore, we argue that, compared to digital design, analog computation is very efficient in its use of synthetic parts, however, embedded digital systems can operate reliably with low molecular counts. For example, we show that synthetic analog gene circuits can be engineered to execute sophisticated computational functions in living cells using just three transcription factors. Such synthetic analog gene circuits exploit graded positive feedback to implement logarithmically linear sensing, addition, subtraction, and ratio-metric computations. In addition, they exploit negative feedback to implement power laws. Finally, we suggest new directions for engineering biological circuits capable of computation.

## WHAT CAN MUTATION PATTERNS OBSERVED IN ANTIBODY SEQUENCES TELL US ABOUT ANTIBODY-ANTIGEN INTERACTIONS, AND ABOUT THE DYNAMICS OF THE ADAPTIVE IMMUNE RESPONSE?

**Gur Yaari**<sup>1</sup>

*<sup>1</sup> Faculty of Engineering, Bar Ilan University, Ramat Gan, Israel*

What can mutation patterns observed in antibody sequences tell us about antibody-antigen interactions, and about the dynamics of the adaptive immune response?

Our immune system's ability to adapt to ever evolving threats, and remember these threats for many years, crucially relies on the diversity of antibody repertoires. Recent advances in high-throughput sequencing have boosted our ability to sequence antibody repertoires in an unprecedented scale. Together with the great promises that these technologies bring with them, they also pose many nontrivial challenges for us, i.e. to be able to extract valuable biological information from the large datasets they produce. For this reason, we and others have developed specific computational methods tailored for antibody repertoire analyses. In this talk I will describe how we can apply these tools to antibody repertoire sequencing data, and reveal a more complete picture of the dynamics of the adaptive immune response in various clinical conditions. I will give two examples of these computational tools' applicability in the context of multiple sclerosis and celiac disease, and demonstrate how the mutation patterns observed in antibody sequences guide us to the antibody-antigen interaction sites.

# FOLLOWING THE FOOTSTEPS OF THE RIBOSOME THROWS LIGHT ON PROTEIN EVOLUTION AND THE DESIGN PRINCIPLES OF GENE EXPRESSION ENGINEERING

**Renana Sabi<sup>1</sup>, Tamir Tuller<sup>1</sup>**

<sup>1</sup> Tel Aviv University, Tel Aviv, Israel

Gene expression is a key process in all living organisms in which the information encoded in the DNA is converted into proteins. Gene translation is the major stage of gene expression in which the ribosome, a large macromolecular particle, translates a sequence of nucleotides (messenger RNA) into a functional protein. As the new protein is being synthesized, it departs from the ribosome through a narrow exit tunnel (figure 1). Specific sequences within the nascent protein may undergo stalling interactions with the tunnel and affect the efficiency of gene translation. By analyzing genomic data and large-scale measurements of the movement of ribosomes in the baker's yeast (e.g. see [1, 2]), we identify short protein sequences that lead to ribosome stalling and demonstrate that they tend to be under/over represented in the proteome [3]. The study includes a comprehensive analysis of the amino acid content and the biochemical properties of these short peptides. Our findings throw light on protein evolution and open the door to various biomedical and biotechnological applications such as gene expression/protein modeling and engineering.

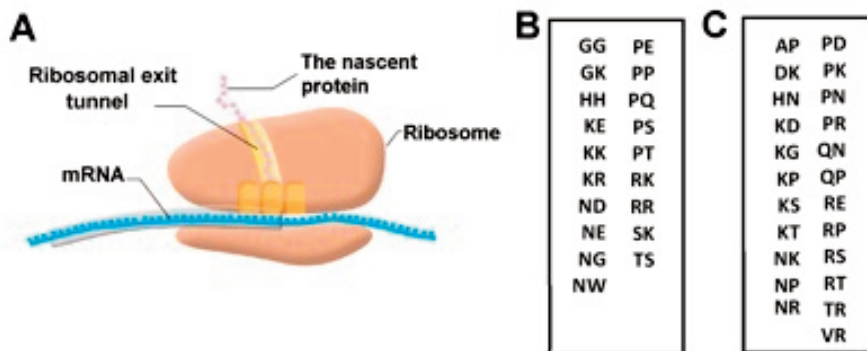


*Figure caption: Figure 1. (A) An illustration of the ribosome during translation elongation. The ribosome moves along the messenger RNA (mRNA in blue) and adds amino acids (depicted by pink circles) to the nascent protein which leaves the ribosome through the ribosomal exit tunnel. When specific short peptides appear in the nascent protein they may interact with the ribosome exit tunnel and slow down its movement. (B) Stalling dipeptides that are overrepresented in the proteome of baker's yeast. (C) Stalling dipeptides that are underrepresented in the proteome of baker's yeast.*

## Acknowledgments:

This study was supported in part by a fellowship from the Edmond J. Safra Center for Bioinformatics at Tel-Aviv University.

## References:

1. Sabi R, Tuller T: A comparative genomics study on the effect of individual amino acids on ribosome stalling. *BMC genomics* 2015, 16(Suppl 10):S5.
2. Ingolia NT, Ghaemmaghami S, Newman JR, Weissman JS: Genome-wide analysis in vivo of translation with nucleotide resolution using ribosome profiling. *Science* 2009, 324(5924):218-223.
3. Sabi R, Tuller T: Evidence of Positive and Negative Selection of Short Peptides that Interact with the Ribosomal Exit Tunnel. Under Review.

# YEAST RESPONSE TO MULTIPLE CARBON SOURCES: A CASE STUDY OF COMBINATORIAL SIGNAL INTEGRATION

**Yonatan Savir**<sup>1</sup>

*<sup>1</sup> Dept. of Physiology, Biophysics and Systems Biology, Rappaport Faculty of Medicine, Technion, Haifa, Israel*

A major determinant of the fitness of biological systems is their ability to integrate multiple cues from the environment and coordinate their metabolism and regulatory networks accordingly. While much is known about the response to a single stimulus, our understanding of combinatorial integration of multiple inputs is still limited. As a model system, we studied how yeast responds to hundreds of mixtures of preferred carbon source, glucose, and a less preferred one, galactose. Many of the components of this response, known as catabolite repression, are conserved from yeast to human. We found that, in contrast to the textbook view, instead of simply inhibiting galactose utilization when glucose is above a threshold concentration, individual cells respond to the ratio of glucose and galactose, and based on this ratio determine whether to induce genes involved in galactose metabolism. We investigate the genetic architectures that can result in a ratio sensing and how these architectures provide a fitness advantage which could have shaped the evolution of this property.

## HOW AND WHY DO DENTAL IMPLANT FRACTURE

**Keren Shemtov-Yona**<sup>1</sup>, **Daniel Rittel**<sup>2</sup>

<sup>1</sup> Technion, Haifa, Israel.

<sup>2</sup> Technion Institute of Technology, Haifa, Israel

With the growing use of dental implants, so grows the incidence of implants' failures. Late treatment complications, after reaching full osseointegration and functionality, include mechanical failures, such as fracture of the implant and its components. Those complications are deemed severe in dentistry, albeit usually considered as rare, and therefore seldom addressed in the clinical literature.

The introduction of dental implants into clinical practice fostered a wealth of research on their biological aspects. By contrast, mechanical strength and reliability issues were seldom investigated in the open literature, so that most of the information to date remains essentially with the manufacturers.

Over the years, dental implants have gone through major changes regarding the material, the design, and the surface characteristics aimed at improving osseointegration. Did those changes improve the implants' mechanical performance?

This talk will present our results on various aspects of the mechanical integrity and failure of dental implants. The concept of fatigue failure will be presented in its aspects of identification (failure analysis), causes (surface condition), and working environment (loads, intraoral atmosphere).

A novel in-vitro approach to fatigue functional performance of dental implants will be briefly discussed.

# BIOMECHANICAL EVALUATION OF PRE AND POST – BILATERAL SAGITTAL SPLIT MANDIBULAR OSTEOTOMY ON 3D MODELS FOR OBSTRUCTIVE SLEEP APNEA USING FINITE ELEMENT ANALYSIS

Albert Einstein George<sup>1</sup>, Sreeja V<sup>2</sup>, Aishwarya Srinivasan<sup>2</sup>, Aradhana S<sup>2</sup>

<sup>1</sup> Einnel Technologies, Chennai, India,

<sup>2</sup> Einnext Biosciences, Chennai, India

Obstructive Sleep Apnea syndrome (OSA) is the hindrance of upper airway during sleep, associated with curtailment in blood oxygen saturation. It is characterized by subdual flow of oxygen to vital organs causing irregular heart rhythms. One of the triumphant surgeries to treat OSA is Maxillo mandibular advancement (MMA) which is found to be 90% successful for OSA patients [1]. In MMA, the lower jaw and the mid face is progressed to augment the posterior airway space facilitating trouble-free breathing.

In this research, we attempted to contemplate the von Mises stresses due to mastication in normal and osteotomed 3D models and identify the maximum stress that can be tolerated by the mandible using Finite Element Analysis (FEA). FEA has been extensively used to solve complex problems in dentistry and researchers have found a high correlation between FEA simulation results and in vitro measurements for mandibular specimens [2]. The location of screws and miniplate fixation in the 3D osteotomed models was determined by Champy's lines in order to ensure stable fixation [2]. We first evaluated the extent of movement of the posterior airway space that is mandatory for the OSA patients to breathe normally. It was evident that the airway constriction was corrected in the upper respiratory tract by advancement of the mandible. The von Mises stress and displacement in the mandible before and after MMA by applying two different loads, incisal and contra lateral compressive molar loads were analyzed to rule out the fixation and orthognathic issues. The stress distributions during mastication were furthermore compared for mandibular osteotomy models with two distinct lengths of advancement. In addition, the deflection by virtue of mastication on molars, incisors and canines were also assessed.

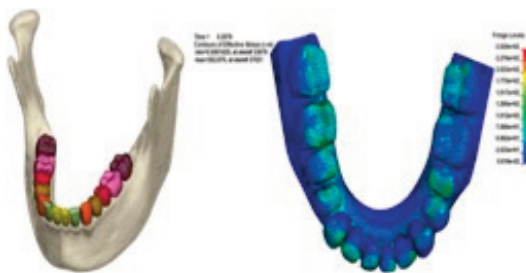


Figure 1(a) Normal mandible . Figure 1(b) von Mises stress distribution in normal mandible

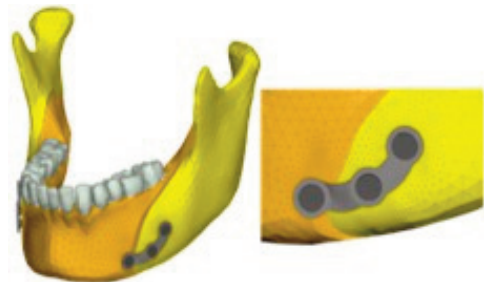


Figure 2 3D osteotomed model

## Reference:

[1] Phee, Brian L., "Clinical Outcomes of Maxillo mandibular Advancement Surgery for the Treatment of Obstructive Sleep Apnea" (2015). *Electronic Thesis and Dissertation Repository Paper 2654*

[2] Erkmen E, Simsek B, Yücel E, Kurt A: Three-dimensional finite element analysis used to compare methods of fixation after sagittal split ramus osteotomy: setback surgery-posterior loading. *Br J Oral Maxillofac Surg* 2005, 43:97-104

# STUDYING IMPLANT OSSEOINTEGRATION IN THE SIKA DEER ANTLER

**Christoph Bourauel<sup>1</sup>, Istabrak Hasan<sup>2</sup>, Yun He<sup>3</sup>, Ludger Keilig<sup>2</sup>, Gerhard Wahl<sup>4</sup>**

*1 Endowed Chair of Oral Technology, Dental School, Rheinische Friedrich-Wilhelms University Bonn, Bonn, Germany,*

*2 Endowed Chair of Oral Technology and Department of Prosthetic Dentistry, Preclinical Education and Materials Science, Dental School, Rheinische Friedrich-Wilhelms University Bonn, Bonn, Germany,*

*3 Department of Oral and Maxillofacial Surgery, Hospital of Stomatology, Luzhou Medical College, Luzhou, China,*

*4 Department of Oral Surgery, Dental Clinic, University of Bonn, Bonn, Germany*

## Introduction:

Bone remodelling processes around immediate loaded dental implants have been investigated in several conventional animal studies. However, these experiments are problematic and controversial. The use of Deer antlers offers the possibility to study remodelling processes around implants without sacrificing the animal. The aim of the present study was to develop an alternative animal model for studying bone remodelling under various loading conditions.

## Methods:

Straumann® implants were inserted in the antlers of four male Sika Deer and loaded immediately via a self-developed loading device [1] (Figures below). After 2, 3, 4, and 5 weeks, implants and surrounding tissue were explanted, specimens scanned by  $\mu$ CT, and FE models generated. As in the animal experiment, vertical loads of 10 N were applied to the implant. Immediate loading by defining frictional contact and osseointegrated state were simulated.

*Insertion of an implant (arrow) into the antler.  
Middle: An animal with the loading device on the left and the control electronics on the right antler. Right: Longitudinal section of the numerical model.*



## Results and Discussion:

During the healing time after insertion of the implant, the bone mineral density (BMD) and Young's modulus around the implant increased significantly (Table below). Minimum and maximum implant displacements (min: 0.2  $\mu$ m, max: 16  $\mu$ m), stress in the implant (0.2, 7 MPa) and bone (0.1, 3 MPa), and strain in the bone (80, 9,000  $\mu$ strain) were observed in 1-week and 5-week models. For each model, higher values of the displacement, stress and strain were obtained in the model with friction contact compared to osseointegrated condition. Currey et al. [2] measured Young's modulus for Red Deer antlers in wet (7.3 GPa) and dry condition (17.5 GPa). Compared to their study, Young's modulus of the antler tissue in our study was relatively low 2 weeks after implant insertion, but increased to 16 GPa in 5 weeks which is similar to human cortical bone (14 GPa).

Time	BMD (g/cm <sup>3</sup> )	Young's Modulus (GPa)
2 W	0.31±0.01	0.11±0.01
3 W	0.92±0.23	1.6±0.1
4 W	1.54±0.40	6.6±0.1
5 W	2.00±0.53	16.2±2.0

*Table 1: BMD and Young's modulus of the bone around implants in different healing periods.*

## References:

[1] Rahimi A et al., *J Biomech* 2009 15:2415-2418

[2] Currey JD et al., *Annals of Anatomy* 2012,194:518-523

# INFLUENCE OF TOOTH DIMENSION ON THE INITIAL MOBILITY – A NUMERICAL STUDY

**Cornelius Dirk**<sup>1</sup>, **Martin Hartmann**<sup>2</sup>, **Susanne Reimann**<sup>3</sup>, **Ludger Keilig**<sup>4</sup>, **Christoph Bourauel**<sup>5</sup>

<sup>1</sup> Oralmedizinische Technologie, Bonn, Germany,

<sup>2</sup> Endowed Chair of Oral Technology, Bonn, Germany,

<sup>3</sup> Endowed Chair of Oral Technology, Department of Orthodontics, Bonn, Germany,

<sup>4</sup> Endowed Chair of Oral Technology and Department of Prosthetic Dentistry, Preclinical Education and Materials Science, Dental School, Rheinische Friedrich-Wilhelms University Bonn, Bonn, Germany,

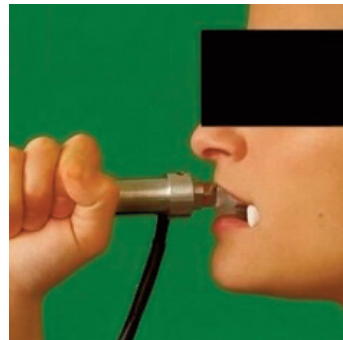
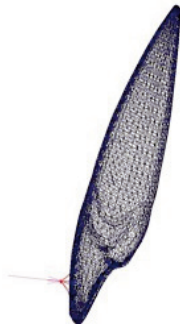
<sup>5</sup> Endowed Chair of Oral Technology, Dental School, Rheinische Friedrich-Wilhelms University Bonn, Bonn, Germany

## Introduction:

Initial tooth mobility is an important factor for planning all kinds of orthodontic tooth movement. Obviously, tooth dimensions have an influence on force-induced displacements. Getting a better understanding of the underlying mechanics was aim of this study.

## Methods:

Force/displacement characteristics of 21 upper incisors were measured in a clinical study (Ethical Committee, University of Bonn, 181/13). The teeth were loaded using a self-developed device [1, 2] to determine the material properties of the periodontal ligament (PDL). Patients' scaled X-rays were used to measure the length and thickness of the roots, and plaster casts to get the thickness and width of the crowns. Corresponding to the determined variations, numerical models of an upper incisor with its PDL, compact and spongy bone were generated with length from 11 to 17 mm, width from 6 to 10 mm and thickness from 7 to 9 mm. The models were loaded with forces of 10 N in palatal direction (according to figure 1) and torques of 10 Nmm around the labial-palatal axis.



Left: FE-Model of the tooth with direction and point of force application. Right: Clinical application of the intraoral loading-device.

## Results and Discussion:

Total displacements decreased with increasing root volume: Smallest, thinnest and slimmest teeth had a total displacement of 0.14 mm at the incisal edge while longest, widest and thickest teeth were displaced by 0.10 mm. Changes in the width had the greatest influence on the displacement, changes in the thickness the least. The position of the centre of resistance is located between 37 % and 43 % of the root length down to the apex. The centre of resistance of longer roots is closer to the incisal edge, while the influence decreases with thicker and wider roots.

## References:

[1] Drolshagen et al. Development of a novel intraoral measurement device to determine the biomechanical characteristics of the human periodontal ligament. *J Biomech* 2011;44:2136-43

[2] Keilig et al. In vivo measurements and numerical analysis of the biomechanical characteristics of the human periodontal ligament. *Ann Anat* 2015; in press

# NUMERICAL ANALYSIS OF A COMBINED IMPLANT-RESIDUAL TOOTH SUPPORTED PROSTHESIS AFTER TOOTH HEMISECTION - INFLUENCE OF RESIDUAL ROOT NUMBER AND BONE DENSITY

**Ludger Keilig<sup>1</sup>, Yun He<sup>2</sup>, Istabrak Hasan<sup>1</sup>, Junliang Chen<sup>2</sup>, Christoph Bourauel<sup>3</sup>**

*1 Endowed Chair of Oral Technology and Department of Prosthetic Dentistry, Preclinical Education and Materials Science, Dental School, Rheinische Friedrich-Wilhelms University Bonn, Bonn, Germany,*

*2 Department of Oral and Maxillofacial Surgery, Hospital of Stomatology, Luzhou Medical College, Luzhou, China,*

*3 Endowed Chair of Oral Technology, Dental School, Rheinische Friedrich-Wilhelms University Bonn, Bonn, Germany*

## Introduction:

For multirouted teeth, a hemisection may offer ways to preserve part of the natural tooth if one root is damaged while the remaining roots are healthy. It was the aim of this study to analyse the influence of the number of the residual roots as well as the bone density on the loading distribution of a combined implant/residual tooth restoration after tooth hemisection using finite element methods (FEM).

## Materials and Method:

Computer tomography data of the mandibular right first molar from two clinical cases were used as a data basis. In the first case the molar had one distal root, in the second case the molar had two distal roots. One implant was placed in the location of the missing root(s). For each case, two FE models were created: a combined crown over implant and residual tooth, and separate crowns for the implant and the residual tooth. For all four resulting models, two different densities for the trabecular bone were assumed, a lower density bone with 800 MPa, and a higher density bone with 1,370 MPa. A vertical load of 100 N was applied on the crowns.

## Results:

The results showed that the magnitude of all biomechanical parameters decreased in the models with two remaining distal roots. In the same way the models with low trabecular bone density showed higher strains upon loading. The highest strains in trabecular bone of up to 9,000  $\mu$ strain were observed in small regions around the implant of the model with only one distal root, low trabecular bone density, and a combined crown on implant and residual tooth.

## Conclusion:

A single crown placed on the implant and distal half of the molar or two separate crowns seem to be an acceptable treatment option in cases when two residual roots exist, regardless of the bone density. If there is one residual root and the bone density is low, restorations combining implant and residual root cannot be recommended.

## NUMERICAL MODELING OF DENTAL IMPLANT-BONE INTERFACE

**Raouf Korabi**<sup>1</sup>, **Avraham Dorogoy**<sup>2</sup>, **Keren Shemtov-Yona**<sup>2</sup>, **Daniel Rittel**<sup>3</sup>

<sup>1</sup> Technion, Mechanical Engineering, Haifa, Israel,

<sup>2</sup> Technion, Haifa, Israel, <sup>3</sup> Technion, Mechanical Engineering, , Haifa, Israel

Dental implants are widely used as a substitute for missing teeth for dentate and edentulous people. Despite their high success rates, dental implants may still fail mechanically. In order to better understand the implant-bone interaction, reliable numerical models must be constructed.

In this talk, a realistic finite element model will be presented, to study the interaction of the bone-implant system. The model is based on a commercially used dental implant system together with a CT-scan reconstruction of a mandible bone section. In this model, the bone tissue distinguishes between cortical and cancellous bone regions. The cortical bone is modeled as fully anisotropic with spatially varying properties, while the cancellous bone is modeled as a homogenous isotropic material.

Moreover contact interaction is included between all parts in the model, while the coefficient of friction (C.O.F.) between the implant system parts is set as constant, the latter can be varied methodically for the bone-implant interaction, thus providing quantitative information on the stress development developing in the bone system. Lastly, the bone-implant interface will be systematically investigated by using an interfacial failure criterion for cohesive elements of variable properties.

The outcome of this study is a physically-based numerical model of the bone-implant system, with special emphasis on the bone mechanics, such as to better understand and eventually optimize the interaction between the bone and the implant.

# BRAIN INJURY METRIC BASED ON COMPUTED AXON STRAINS

**Remy Willinger<sup>1</sup>, Deck Caroline<sup>2</sup>, Sahoo Debasis<sup>2</sup>**

*1 University Strasbourg, Ucube-Cnrs, Strasbourg, France,*

*2 University Strasbourg, Strasbourg, France*

## Introduction

DAI is characterized by dynamic tensile elongation of axonal fibers and consequential fiber rupture and yielding retraction balls of 30  $\mu\text{m}$  in diameter [1]. Based on these models and head trauma simulations, brain stress and strain have been proposed as possible criteria to predict DAI [2].

Multiscale computation of axon elongation by using finite element head model in numerical simulation can enlighten the DAI mechanism and help to establish advanced head injury criteria.

## Methods

A state-of-the-art FE head model was used for this study. The FEHM was enhanced by incorporating DTI data (fractional anisotropy and fiber orientation) and new constitutive brain law by [3]. The material parameters are obtained from [4] and the model was validated against all available data by [3]. A total of 109 well-documented real world head trauma cases were replicated using this enhanced FEHM. Statistical analysis was performed to obtain the best suitable parameters to predict DAI and finally the threshold for model based criteria.

## Results

From the results from 109 head traumas maximum of axon strain have been computed. Range of axon strain is 0.02-0.43, with a smooth evolution from non-injured to injured. Based on statistical analysis, axon strain presents the highest R2 value of 0.876.

## Discussion and Conclusion

The proposed tolerance limit in terms of axonal elongation (15% for a 50% risk) is in very good accordance with the experimental studies based on cell culture shown in Fig.3. It is believed that this study provides a key way for a realistic novel injury metric for DAI.

The authors acknowledge the ANR-12-EMMA-0026-0 (SUFEHM-13) for their support.

## References:

[1] Arfanakis et al., 2002. *AJN* 23: 794-802.

[2] Deck et al., 2008. *IJ Crash* 13(6): 667-678.

[3] Sahoo et al., 2013. *JMBBM* 33 :24-42.

[4] Chatelin et al., 2013. *J.Biorheology*27(1-2) :26-37.

## DYNAMIC MICRO INDENTATION OF ANIMAL NEURAL TISSUE

David Macmanus<sup>1</sup>, Baptiste Pierrat<sup>2</sup>, Jeremiah Murphy<sup>3</sup>, Michael Gilchrist<sup>1</sup>

<sup>1</sup> School of Mechanical & Materials Engineering, University College Dublin, Dublin, Ireland,

<sup>2</sup> Ecole Nationale Supérieure des Mines, St. Etienne, France,

<sup>3</sup> Department of Mechanical & Manufacturing Engineering, Dublin City University, Dublin, Ireland

The brain is a complex organ made up of many different functional and structural regions consisting of different types of cells and complex geometries. It is hypothesized that the different regions of the brain exhibit significantly different mechanical properties. The regional mechanical properties of animal brain tissue under dynamic indentation are presented and discussed in the context of traumatic brain injury. The experimental data obtained from micro-indentation measurements were fit to three hyperelastic material models using the inverse Finite Element method. The cortex elicited a stiffer response than the cerebellum, thalamus, and medulla. The thalamus was found to be the least sensitive to changes in velocity, and the medulla oblongata was most compliant. The results show that different regions of the mouse brain possess significantly different mechanical properties, and a significant difference also exists between the in vitro and in situ brain (MacManus, 2016).

Following the characterization of the hyperelastic properties of mouse brain tissue, a viscoelastic analysis of brain tissue was performed on mouse and pig brain regions. The viscoelastic properties of brain tissue are determined using linear and nonlinear viscoelastic models. Figure 1 presents the mean  $\pm$  standard deviation of the shear moduli for the mouse and pig brain regions investigated. Significant differences were found between the medulla oblongata, thalamus, and cortical grey matter, of the two animals.

The findings from dynamic micro-indentation experiments on animal brain tissue will be presented and discussed in detail. The time and frequency domain response of brain tissue will be highlighted and differences between the mechanical properties of animal models will be discussed.

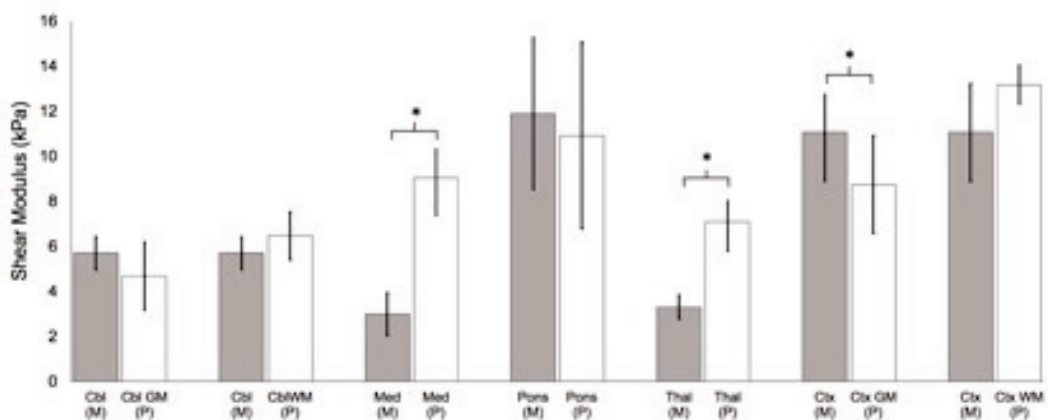


Figure Caption: Comparison of the linear shear modulus of mouse and pig brain regions under micro-indentation. Cbl = cerebellum, Med = medulla oblongata, Thal = thalamus, Ctx = cerebral cortex, WM = white matter, GM = grey matter, (M) = mouse, and (P) = pig. \* = statistically significant difference, determined by ANOVA with post-hoc test.

### References:

MacManus D.B. et al. Mechanical characterization of the P56 mouse brain under large-deformation dynamic indentation, *Sci. Rep.* 6, 21569; doi: 10.1038/srep21569 (2016).

## INTEGRATION OF FINITE ELEMENT ANALYSIS WITH MR IMAGING FOR ESTIMATION OF IN VIVO BRAIN DEFORMATION.

Arnold D. Gomez<sup>1</sup>, Gregory Scott<sup>2</sup>, Boston Terry<sup>2</sup>, Brittany Coats<sup>2</sup>

<sup>1</sup> Johns Hopkins University, Baltimore, MD, United States,

<sup>2</sup> University of Utah, Salt Lake City, Ut, United States

"MRI is a versatile tool for investigating soft-tissue mechanics in vivo because one can collect anatomical, structural, and dynamic information before and after injury in controlled experimental animal studies. However, technical challenges include (1) a need for high resolution given the small cranium of the animal and (2) detecting non-injurious small deformations. The objective of this work was to demonstrate an integrated finite element (FE) and imaging analysis strategy capable of overcoming these challenges and capturing subtle changes in brain deformation in a mild traumatic brain injury (TBI) piglet model.

An MRI-compatible apparatus was built to generate small coronal head rotations leading to measureable brain/skull displacement at accelerations far below injurious levels. A high-resolution CINE-MRI scan was performed on anesthetized immature piglets while the device rotated the animals head through a 60° arc. Imaging on two animals was performed immediately prior to and 24 hours after a mild TBI. Region-specific elastic image registration was applied to each image set using the Hyperelastic Warping (HW) plugin extension for the FEBio software suite. HW used image data to deform a finite element model by means of body forces arising from material point comparisons in reference and deformed images. Image information also provided loading and boundary conditions. Relative displacement of the cortex with respect to the base of the brain was used to evaluate deformation changes before and after injury.

In one animal, the displacement post-injury was greater in a focal region lateral to the sagittal sinus. The difference in motion patterns and displacements were not as clearly identifiable in the second animal. These results demonstrate the ability to use combined imaging-FE methodology to estimate brain deformation changes from TBI. The subject variability could be explained by absence of injury in the second animal, or a lack of signal in the areas of interest. This can be improved by optimizing imaging parameters. While the sample size in this study was small, the finding of a detectable change in cortical brain deformation in one the animals is promising and will be explored in a larger data set."

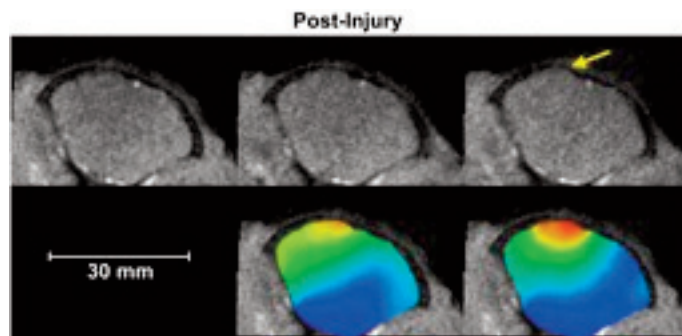


Figure Caption: "Elastic registration compared all frames of the head rotation to those acquired at rest (left column). The analysis showed a unique cortical deformation pattern visible through the head rotation (middle column) and at impact (right column) that wasn't seen before injury."

### Acknowledgments:

"The authors would like to thank the Primary Children's Medical Center Foundation for their financial support. Special thanks to the Small Animal Imaging Core and Musculoskeletal Research Laboratories at the University of Utah."

## DEVELOPMENT OF A PHYSICAL BRAIN-SKULL MODEL FOR THE STUDY OF NEUROSURGICAL BRAIN SHIFT.

**Matthew Potts**<sup>1</sup>, **Nicholas Bennion**<sup>2</sup>, **David Marshall**<sup>3</sup>, **Stephen Anderson**<sup>4</sup>, **Sam Evans**<sup>5</sup>

<sup>1</sup> School of Engineering, Cardiff University, Cardiff, United Kingdom,

<sup>2</sup> School of Engineering, Cardiff University, Cardiff, United Kingdom,

<sup>3</sup> School of Computer Science and Informatics, Cardiff University, Cardiff, United Kingdom,

<sup>4</sup> Renishaw Plc., New Mills, Wootton-Under-Edge, United Kingdom,

<sup>5</sup> School of Engineering, Cardiff University, Cardiff, United Kingdom

Surgery of the brain is a delicate procedure that requires meticulous planning and exceptional accuracy if it is to be successful. For many surgeries, surgical trajectories are planned using preoperative MRI images and a stereotactic frame is attached to the skull and used to set the correct surgical trajectory relative to the skull. The brain, however, is soft and moves around during and after the various surgical procedures that occur following the acquisition of the preoperative images, affecting the accuracy with which particular features can be targeted intra-operatively (Mohammadi et al. 2015).

In order to develop a computational model of neurosurgical brain shift, a means of model validation is required. With current technology, however, a comprehensive measurement of intra-operative brain shift is not possible without putting the patient at increased risk (e.g. from increased surgery duration). For this reason, a realistic mechanical model of the brain-skull system to which the computational model can be validated against is required.

Presented here is the preliminary work done towards creating such a model, including the design and manufacturing of a three part brain-skull model (generated from anatomically realistic geometries segmented from MR images) and the initial measures taken to validate it. Particular focus is given here to the computational methods used to design and optimise the synthetic surrogate for the brain-skull tethering tissues, including the geometry design and finite element modelling of the surrogate in FEBio.

The initial steps taken towards validating the brain-skull model, comprising the comparison of brain deformation patterns between the synthetic brain of the model presented here and the biological brain of a human subject (measured by MRI) under gravity loading, show the model to respond mechanically in a similar way to that of the biological structure under this type of loading.

### References:

Mohammadi, A. et al. 2015. Estimation of intraoperative brain shift by combination of stereovision and doppler ultrasound: phantom and animal model study. *International Journal of Computer Assisted Radiology and Surgery* 10, pp. 1753-1764.

# EVALUATION OF A MECHANICALLY-COUPLED REACTION-DIFFUSION MODEL FOR MACROSCOPIC BRAIN TUMOR GROWTH

**Daniel Ablner**<sup>1</sup>, **Philippe Büchler**<sup>2</sup>

<sup>1</sup> University of Bern, Institute for Surgical Technology & Biomechanics (Istb), Bern, Switzerland,

<sup>2</sup> University of Bern, Institute for Surgical Technology & Biomechanics (Istb), Bern, Switzerland

Macroscopic growth of brain tumors has been studied by means of different computational modeling approaches. Glioblastoma multiforme (GBM), the most frequent malignant histological type, is commonly modeled as a reaction-diffusion type system, accounting for its invasive growth pattern, e.g. [1]. Purely mechanical models have been proposed to represent the mass-effect caused by the growing tumor, e.g. [2]. Only few models, such as [3], consider both effects in a single 3D model.

We report first results of a comparative study that evaluates the ability of a simple computational model to reproduce the shape of pathologies and healthy tissue deformations found in patients.

We use the finite element method (FEM) for simulating GBM invasion into brain tissue and the mechanical interaction between tumor and healthy tissue components. Cell proliferation and invasion is modeled as a reaction-diffusion process; the simulation of the mechanic interaction relies on a linear-elastic material model. Both are coupled by relating local increase in tumor cell concentration to the generation of isotropic strain in the corresponding tissue element. The model accounts for multiple brain regions with values for proliferation, isotropic diffusion and mechanical properties derived from literature.

Tumors were seeded at multiple locations in FEM models derived from publicly available human brain atlases. Simulation results for a given tumor volume were compared to patient images, using a metric that takes into account extent and shape of the tumor, as well as healthy tissue deformation. Model parameterizations resulting in simulated tumors most similar to real-world pathologies were identified by systematic variation of seed location and relative magnitude of diffusion and mechanical coupling.

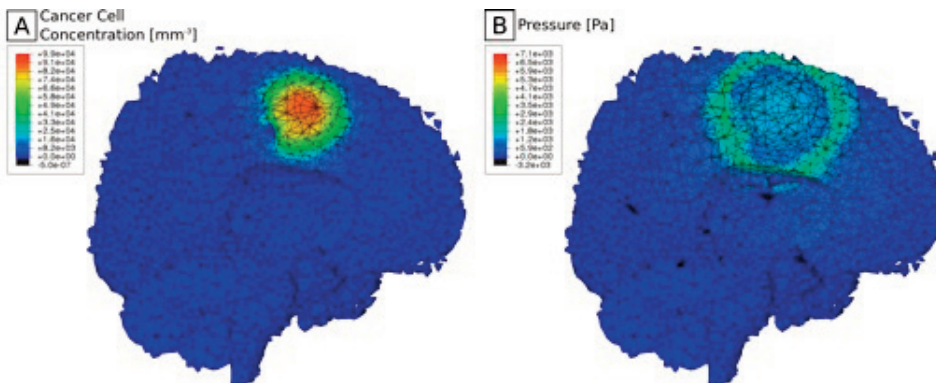


Figure Caption: Cross-section through FEM model of the human brain: (A) concentration of cancer cells in grown tumor, (B) resulting pressure distribution.

## Acknowledgments:

The research leading to these results has received funding from the European Union Seventh Framework Programme (FP7/2007-2013) under grant agreement n° 600841.

## References:

1. Swanson et al., *J. Neurol. Sci.*, 216 (1):1-10, 2003.
2. Hogeia et al., *Phys. Med. Biol.*, 52 (23):6893-6908, 2007.
3. Clatz et al., *IEEE Trans. Med. Imag.*, 24 (10):1334-1346, 2005.

# DEVELOPMENT OF A COMPUTATIONAL MODEL TO AID PREDICTION OF NEUROSURGICAL BRAIN SHIFT.

**Nicholas Bennion<sup>1</sup>, Matthew Potts<sup>2</sup>, David Marshall<sup>3</sup>, Stephen Anderson<sup>4</sup>, Sam Evans<sup>5</sup>**

<sup>1</sup> School of Engineering, Cardiff University, Cardiff, United Kingdom,

<sup>2</sup> School of Engineering, Cardiff University, Cardiff, United Kingdom,

<sup>3</sup> School of Computer Science and Informatics, Cardiff University, Cardiff, United Kingdom,

<sup>4</sup> Renishaw Plc., New Mills, Wootton-Under-Edge, United Kingdom,

<sup>5</sup> School of Engineering, Cardiff University, Cardiff, United Kingdom

## Introduction:

Stereotactic neurosurgical procedures are planned and carried out according to preoperative medical images in a fixed reference frame. As the operation is carried out, a variety of factors lead to a non-rigid movement of the brain within the skull, known as brain shift. Currently, brain shift is attributed mainly to a loss of cerebrospinal fluid (Elias et al. 2007), however incomparability of patient groups means that the mechanisms behind brain shift are still debated. As definitive prediction is not currently possible, other methods to account for the effects of brain shift are used, adding time and complexity to the operation (Jimenez-Shahed et al. 2014).

## Aims:

To develop a computational model of the brain and surrounding structures in order to give a better understanding of the mechanical processes of brain shift and improve surgical accuracy.

## Methods:

Medical images were imported to Simpleware Scan IP in order to segment the desired structures. These were exported to Abaqus CAE for meshing. Analysis was carried out in FEBio, allowing wide range of constitutive models to be applied to the different tissues within the skull. Inclusion of different structures and material models for these was undertaken to identify which have the most important mechanical role in brain shift.

## Conclusion:

Although still in the early stages, results have suggested that the tethering effect of the meninges plays an important role in brain shift, especially when loss of cerebrospinal fluid is limited. In these cases, initial results suggest that a preoperative adjustment to account for brain shift may be possible, however a patient specific model is a considerably more complex task. Regardless of this, identification of the generic mechanisms opens the door to future work in reducing brain shift in conjunction with accounting for it.

## Acknowledgments:

This work has been funded by the EPSRC and Renishaw Plc. through an iCase studentship.

The authors acknowledge the contributions of Rob Harrison, Renishaw Plc.

## References:

- Elias, W. J., Fu, K. M. and Frysinger, R. C. 2007. Cortical and subcortical brain shift during stereotactic procedures. *Journal of Neurosurgery*. 107 (5), pp. 983-988.
- Jimenez-Shahed, J., York, M., Smith-Gloyd, E.M., Jankovic, J., Viswanathan, A.; MER vs. MRI guidance in placement of DBS electrodes for Parkinson's disease [abstract]. *Movement Disorders* 2014;29 Suppl 1 :1202

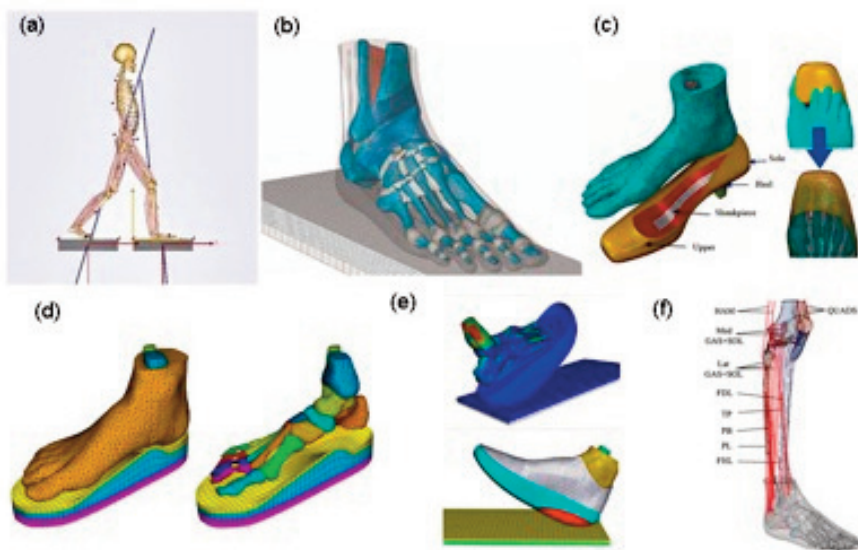
# COMPUTATIONAL MODELS OF FOOT AND ANKLE FOR FOOT SUPPORT DESIGN

**Ming Zhang<sup>1</sup>, Yan Wang<sup>1</sup>, Duo Wai-Chi Wong<sup>1</sup>**

*<sup>1</sup> Interdisciplinary Division of Biomedical Engineering, The Hong Kong Polytechnic University, Kowloon, Hong Kong*

Special foot supports are often used for persons with physical disability in rehabilitation engineering. Footwear should be able to provide a comfortable environment for foot, to protect foot from injury and to enable foot to function as support and to facilitate locomotion in varied surface conditions. At the same time, proper alignment of the knee-ankle-foot structures to prevent the extra loads on joint structures should be considered. Different shoe design philosophies may have different functional aspects for different groups of people. No matter what design philosophy, it is useful to have a platform which can provide biomechanical information on how the footwear changes the load distribution within the foot structures and at the foot-shoe interface and joint loading during locomotion and sport activities. Such information can help for evaluation and optimal design of the footwear.

This presentation will report our development on the computational biomechanical models of the lower extremity including foot-ankle and knee joints which can accurately simulate the biomechanical response of the lower limb to different foot supports (1, 2). A full-featured foot/ankle and knee model including the bones, the key ligaments, muscles and soft tissues was developed. The computational model was validated through comparison with experimental data, such as foot plantar pressure, knee joint pressure and ligament/muscle forces. Parametrical analyses provide the effects of various designs of foot support using the validated computational models for understanding the alignment mechanisms and establishing design guidelines for footwear.



## Acknowledgments:

This project was supported by Hong Kong Research Grant Council GRF (PolyU152216/14E, PolyU152002/15E) and NSFC (11272273, 11120101001)

## References:

- 1) Cheung JTM, Zhang M, Leung AKL and Fan YB, Three-dimensional finite element analysis of the foot during standing - a material sensitivity study, *J Biomech* 2005, 38(5): 1045-54.
- 2) Wang Y; Wong DWC, Zhang M, Computational models of the foot and ankle for pathomechanics and clinical applications - A review, *Annals of Biomedical Engineering, Annals of Biomedical Engineering*, , 2016, 44(1): 213-21.

# MULTIPHYSICS MODELING OF THE EFFECTS OF TOXIC BIOWASTES FROM MECHANICALLY DAMAGED MUSCLE CELLS ON THE DAMAGE PROPAGATION OF DEEP TISSUE INJURY

Yifei Yao<sup>1</sup>, Lucas Ong<sup>2</sup>, Xiaotong LI<sup>1</sup>, Arthur Mak<sup>1</sup>

<sup>1</sup> Division of Biomedical Engineering, The Chinese University of Hong Kong, Shatin, Hong Kong,

<sup>2</sup> Department of Biomedical Engineering, National University of Singapore, Singapore, Singapore

Deep tissue injuries occur in muscle tissues around bony prominences under mechanical loading, and can lead to severe pressure ulcers. Tissue compression can potentially compromise lymphatic transport and cause accumulation of metabolic biowastes, which may cause further cell damage under continuous mechanical loading.

In vitro, we applied long-term low compressive stress and short-term high compressive stress on myoblasts to cause cell damage and collected the biowastes secreted by the damaged cells. We found that biowastes collected from cells damaged under long-term low compressive stress were more toxic and could compromise the capability of the otherwise normal myoblasts to resist compressive damage, as compared to those collected from cells damaged under short-term high compressive stress.

In silico, we used the solid mechanics module and the transport of diluted species module in COMSOL to simulate the stress distribution and the diffusion of biowastes in a finite element model of a buttock (Linder-Ganz, 2009). We assumed the mechanically damaged muscles, as predicted by the compressive stress - duration damage threshold (Yao, 2015), would release biowastes that could diffuse to the surrounding tissues and potentially lower their damage threshold in a binary manner as observed in-vitro. The damage propagation with and without the effects of toxic biowastes were presented in Fig1, showing the importance of biowastes in the development of deep tissue ulcers under long-term compression.

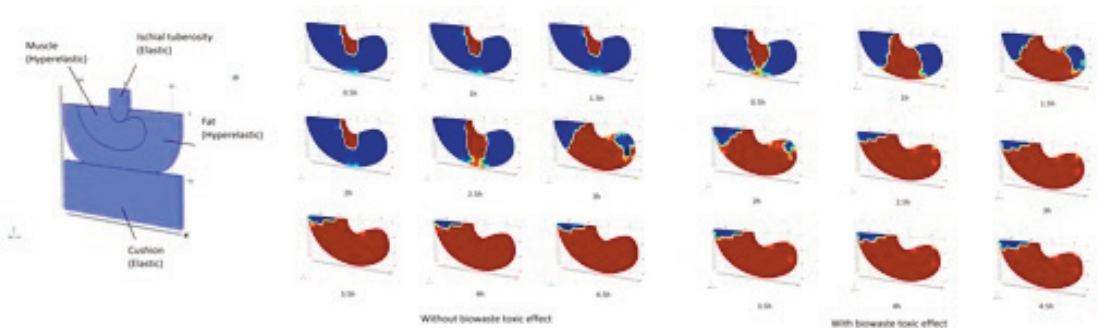


Fig 1. Damage evolution in muscles with and without the toxic effects of biowastes

## References:

Linder-Ganz, E. et al., 2009. *Ann Biomed Eng* 37, 387-400.

Yao, Y. et al., 2015. *Ann Biomed Eng*, 43(2), 287-296.

## INVERSE ANALYSIS OF BIAXIAL TENSILE TESTING ON HUMAN SKIN

**Jibbe Soetens<sup>1</sup>, Marc van Vijven<sup>1</sup>, Gerrit Peters<sup>1</sup>, Cees Oomens<sup>1</sup>**

*<sup>1</sup> Eindhoven University of Technology, Eindhoven, Netherlands*

Skin mechanics is important for various fields of research. This includes research into the development of pressure ulcers and the interaction between skin and devices or materials such as shaving appliances, prosthetic liners and bed linens. For this research, prediction of mechanical response of skin is essential.

From a macroscopic point of view, skin is a three layered tissue that has non-linear viscoelastic, anisotropic and heterogeneous properties. These mechanical properties, however, are determined by skin components on a microscopic scale. For instance the presence and distribution of collagen and elastin fibers in the dermal skin layer provide anisotropic properties. Therefore, the focus of this study is on the contribution of dermal fiber distribution and stiffness on the mechanical behavior of skin. In order to achieve this, inverse analysis using a recently developed 3D finite element material model of human skin was used.

The Marc/Mentat software package was used for the implementation of this skin model. In the HYPELA2 user subroutine the skin is modelled as a fiber-reinforced matrix, with an elastic fibrous component and an isotropic, non-linear visco-elastic matrix. The fibers only contribute in extension and provide anisotropic properties. All elastic components are non-linear, providing non-linear viscoelastic behavior.

Biaxial tensile tests were performed on ex-vivo human skin, combined with digital image correlation to determine local displacements of the skin. Subsequently, the in-plane fiber distribution of each specific skin sample was determined histologically and used as a model parameter. Finally, inverse analysis in Matlab was applied for deformation mapping of the finite element simulation with the experimental results from the biaxial tensile tests. The aim was to obtain an optimized value for the fiber stiffness by using this as the variable parameter in the inverse analysis.

By applying the inverse method in coupling the experiments and model, an accurate estimation of the fiber stiffness could be obtained. It is shown that microscopic fiber components influence the macroscopic mechanical behavior of human skin. The newly developed material model is thus considered to be a promising tool to simulate skin mechanics.

# FINITE-ELEMENT ANALYSIS AND EXPERIMENTAL INVESTIGATION OF GROOVED AND POROUS COLLAR IN INDUCING EXTRA-CORTICAL BONE GROWTH FOR MECHANICAL FIXATION

**Vee San Cheong<sup>1</sup>, Melaine J Coathup<sup>1</sup>, Aadil Mumith<sup>1</sup>, Paul Fromme<sup>2</sup>, Gordon Blunn<sup>1</sup>**

*1 John Scales Centre for Biomedical Engineering, Institute of Orthopaedics and Musculoskeletal Science, University College London, Middlesex, United Kingdom,*

*2 Department of Mechanical Engineering, University College London, London, United Kingdom*

The successful osteointegration of massive prostheses to treat bone cancers is critical to ensure their long-term survival, but mechanical fixation among patients is difficult to predict [1]. The use of a hydroxyapatite-coated grooved collar has been demonstrated to encourage extra-cortical bone formation, improve fixation and implant survival [2]. It is hypothesized that the use of porous collars could provide a better scaffold for bone ingrowth. There is a need to develop computational tools for optimizing the design of porous collars, reducing the requirement for pre-clinical testing in animals.

The geometry and material properties from two ovine tibiae were obtained from computed tomography (CT) scans and used to develop Finite Element (FE) models of the tibiae implanted with different collar designs. The bones were assigned inhomogeneous, transversely isotropic material properties based on the CT grey values and typical walking load conditions were applied. A bone remodeling algorithm based on strain energy density combined with a new concept of bone connectivity was used as the bone adaptation criteria, where the rate of bone adaptation is controlled by the difference in the current strain energy against the reference value [3]. The bone adaption results for the grooved collar designs were first verified against experimental studies at different time stages and shown to match the process of bone growth (Figure 1). Thereafter, the bone formation process for the porous collar was predicted before an experimental study was undertaken to verify the computational results. This computational tool thus shows potential to be developed further for the optimization of collar designs.

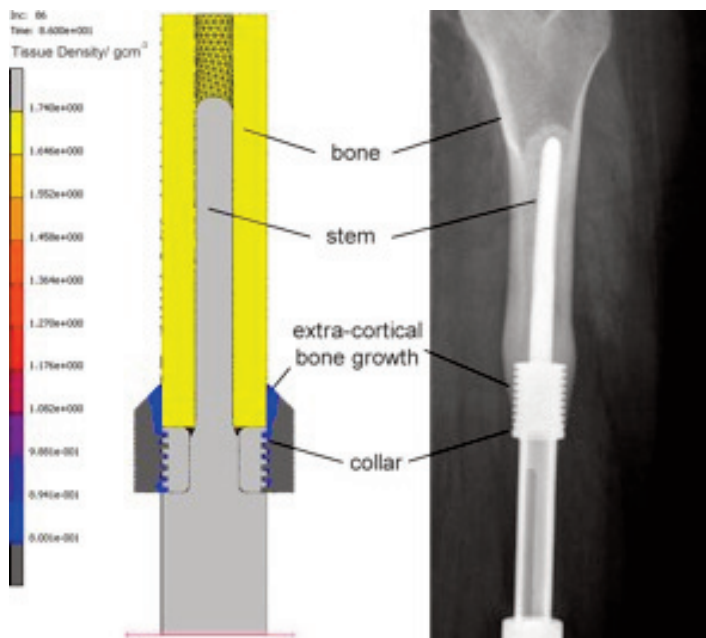
Figure 1: The bone modeling results (left) showing good correspondence with X-ray images (right) of hydroxyapatite collar with good osteointegration taken 12 years after implantation.

## Acknowledgments:

This work is funded by a grant from the Orthopaedic Research UK.

## References:

- [1] McDonald, D. *Bone Joint Surg Am.* 2013 Sep 4;95(17):e1281-2.
- [2] Coathup, M, et. al. *Clin Orthop Relat Res.* 2015 Apr;473(4):1505-14
- [3] Huiskes, R., et. al. *J Biomech.* 1987;20(11-12):1135-50.



## A PRELIMINARY STUDY ON THE INFLUENCE OF CADENCE ON PATH OPTIMIZED HANDLE-BASED PROPULSION FOR WHEELCHAIRS

Nithin Babu Rajendra Kurup<sup>1</sup>, Margit Gföhler<sup>2</sup>

<sup>1</sup> Institute for Engineering Design and Logistics Engineering-Machine Design and Rehabilitation Engineering Division, Vienna University of Technology, Vienna, Austria,

<sup>2</sup> Technische Universität Wien, Vienna, Austria

Wheelchairs are used extensively for daily mobility by the elderly and lower extremity injured patients [1]. A great number of daily wheelchair users prefer the conventional hand-rim propulsion mechanism even though it's proved to be least efficient and leading to injuries due to discontinuous upper arm movements and physical strains.

The aim of this study is to optimize a continuous wheelchair propulsion movement by a continuous handle movement in a parasagittal plane and to determine the influence of cadence variation. At each cadence (40, 50 and 60 rpm) the shape of the handle path will be optimized for maximum net propulsion power using forward dynamic simulation and optimization.

An upper extremity model was selected with major muscle groups, and the hand segment was linked to the handle part of the propulsion mechanism in the parasagittal plane with origin C and based on inputs of the shape parameters the handle part connected to the origin C was allowed to translate with respect to C within upper and lower bounds. For this study the propulsion mechanism was prescribed at above mentioned constant angular velocities. Then using forward simulation and dynamic optimization, muscle excitations for the musculotendon actuators and the shape factors of the handle path were optimized at each rpms. The preliminary results of the study are as shown in Fig.1. Taking into consideration the normal propulsion rate of 50 rpm a maximum power of 36.82 Watts was obtained at an aspect ratio (AR) of 1.359. Further investigations need to be done to validate the results and also the need to verify the joint torques and reaction forces at higher propulsion speeds. Furthermore, emphasis will be given to achieve a global optimum solution for the best suited propulsion path [2].

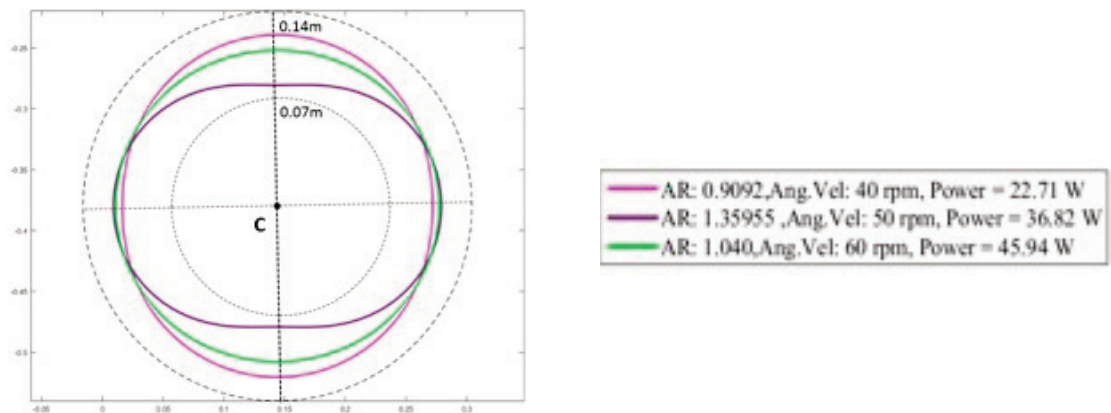


Figure 1: Optimized handle paths

### Acknowledgments:

This work was funded by the Austrian Science Fund (FWF), grant P 25507- B24.

### References:

- [1] U. Arnet, S. Drongelen, a Scheel-Sailer,, "Shoulder load during synchronous handcycling and handrim wheelchair propulsion in persons with paraplegia," *J. Rehabil. Med.*, vol. 44, no. 3, pp. 222-228, 2012.
- [2] W. M. Richter, R. Rodriguez, "Stroke pattern and handrim biomechanics for level and uphill wheelchair propulsion at self-selected speeds.," *Arch. Phys. Med. Rehabil.*, vol. 88, no. 1, pp. 81-7, Jan. 2007

## INVESTIGATION OF THE BIOMECHANICAL BEHAVIOR OF THE URETHRA DUCT IN RELATION WITH LUMEN OCCLUSION

**Arturo Natali<sup>1</sup>, Emanuele Luigi Carniel<sup>2</sup>, Piero Pavan<sup>3</sup>, Chiara Giulia Fontanella<sup>3</sup>, Silvia Todros<sup>3</sup>, Alessandro Frigo<sup>3</sup>, Paola Pachera<sup>3</sup>, Walter Artibani<sup>3</sup>, Maria Angela Cerruto<sup>3</sup>, Raffaele De Caro<sup>3</sup>, Veronica Macchi<sup>3</sup>, Andrea Porzionato<sup>3</sup>, Alessandro Rubini<sup>3</sup>, Laura Cavicchioli<sup>3</sup>, Gulia Maria De Benedictis<sup>3</sup>**

<sup>1</sup> University of Padova, Department of Industrial Engineering, Centre for Mechanics of Biological Materials, Padova, Italy,

<sup>2</sup> University of Padova, Department of Industrial Engineering, Centre for Mechanics of Biological Materials, Padova, Italy,

<sup>3</sup> Centre for Mechanics of Biological Materials, Department of Industrial Engineering, University of Padova, Padova, Italy

Urinary incontinence represents a pathology with a relevant social and economic impact. Different prostheses are currently adopted for incontinence surgical therapy, among which the artificial urinary sphincter is considered the most effective solution at present [1]. This prosthesis exerts a variable pressure field on the urethra, occluding the duct. However, several complications, as tissue atrophy and erosion, were observed after medium-long term implantation, leading to surgical recurrence. The artificial sphincter conformation and mechanical action are mostly based on surgical practice. Prosthesis should be also evaluated by mean of a biomechanical investigation of urethral tissues and structure response, in particular with regard to the occlusion of the duct.

At this purpose, an integrated experimental and computational approach is exploited [2,3]. A computational framework of urethra mechanics is here proposed, based on experimental investigation of the mechanical properties of urethral tissues and structure. Histological analyses are performed aiming at characterizing tissues conformation and are processed to make virtual solid and finite element models of urethral duct. A specific hyperelastic formulation is developed to characterize the non-linear mechanical behavior of urethral tissues. The inverse analysis of tests on a urethra samples enables to define preliminary constitutive parameters. Additional tests are developed on the overall urethra, as inflation tests, in order to evaluate additional data from the structural response and to assess parameters reliability. The computational model of a urethra is exploited to evaluate the mechanical response aiming at the interpretation of the conditions for urethral lumen occlusion.

The present integrated experimental and computational protocol allows evaluating the mechanical behavior of urethral duct during lumen occlusion, representing the mechanical action of an artificial urinary sphincters and slings and offering a valid reference for surgical activity.

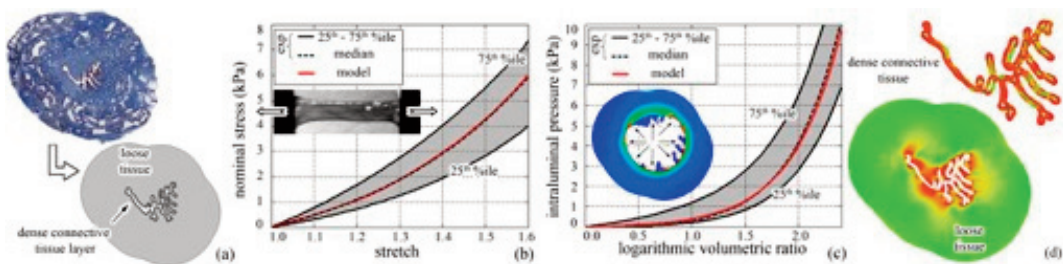


Figure Caption: Analysis of the morphology and histology of urethral tissues (a); constitutive identification of urethral tissues by the inverse analysis of tensile tests (b); reliability assessment of urethral model by the analysis of inflation tests (c); evaluation of urethral tissues response during lumen occlusion, contours and compressive strains (d).

### References:

- [1] E. Chung. (2014, August). A state-of-the-art review on the evolution of urinary sphincter devices for the treatment of post-prostatectomy urinary incontinence: past, present and future innovations. *J. Med. Eng. Technol.* 38(6). pp. 328-332.
- [2] A. N. Natali, E. L. Carniel, A. Frigo, P. G. Pavan, S. Todros, P. Pachera, C. G. Fontanella, A. Rubini, L. Cavicchioli, Y. Avital, G. M. De Benedictis. (2016, February). Experimental investigation of the biomechanics of urethral tissues and structures. *Exp. Physiol.* DOI: 10.1113/EP085476
- [3] A. N. Natali, E. L. Carniel, C. G. Fontanella, A. Frigo, S. Todros, A. Rubini, G. M. De Benedictis, *Mechanics of the urethral duct: tissue constitutive formulation and structural modeling for the investigation of lumen occlusion*, *Journal of Biomechanics*, submitted 2016

## 3D FE HEAD MODELLING: TECHNIQUES AND SOLUTIONS FOR IMPACT ANALYSIS

**Philippe Young<sup>1</sup>, Ross Cotton<sup>2</sup>, Siddiq Qidwai<sup>3</sup>, Amit Bagchi<sup>3</sup>, Nithyanand Kota<sup>3</sup>**

<sup>1</sup> University of Exeter, Simpleware Ltd, Exeter, United Kingdom,

<sup>2</sup> Simpleware Ltd, Exeter, United Kingdom,

<sup>3</sup> US Naval Research Laboratory, Washington, United States

A high-quality head model has been generated from Magnetic Resonance Imaging that can be used for studying impact. Developed by Simpleware Ltd. and the U.S. Naval Research Laboratory, the head model is unique in terms of representing pre-segmented image data, rather than a 'fixed' computational model, that can be easily adapted to different Finite Element (FE) meshing requirements [1]. The model is also novel in terms of being able to incorporate CAD and image-based structures. The Simpleware/NRL head model addresses several recurring limitations of head impact modelling in terms of mesh adaptability, and to date has been successfully tailored for military [2], and sports simulations [3].



Figure Caption: "Simpleware-NRL head model with helmet"

### References:

- [1] Young, P.G., Beresford-West, T.B.H., Coward, S.R.L., Notarberardino, B., Walker, B., Abdul-Aziz, A., 2008. An efficient approach to converting 3D image data into highly accurate computational models. *Philosophical Transactions of the Royal Society A*, 366, 3155-3173
- [2] Cotton, R.T., Pearce, C.W., Young, P.G., Kota, N., Leung, A.C., Bagchi, A., Qidwai, S., 2016. Development of a geometrically accurate and adaptable finite element head model for impact simulation: the Naval Research Laboratory-Simpleware Head Model. *Computer Methods in Biomechanics and Biomedical Engineering*, Vol 19(1), 2016.
- [3] Gerber, B., 2016. Eliminate football concussion with shocking simulation. *ANSYS Blog*, Feb 3 2016. <http://www.ansys-blog.com/reducing-concussions-in-football-with-simulation/>.

# THEORETICAL ANALYSIS OF THE POTENTIAL ULTRASONIC NEUROMODULATION MECHANISMS

**Michael Plaksin<sup>1</sup>, Yoni Weissler<sup>1</sup>, Shy Shoham<sup>1</sup>, Eitan Kimmel<sup>1</sup>**

*<sup>1</sup> Technion - Israel Institute of Technology, Haifa, Israel*

Low intensity ultrasound (US) can noninvasively suppress or excite Central Nervous System (CNS) activity. While applications are already emerging, the underlying biophysics remains under debate. Two leading mechanisms that may excite neurons through plasma membrane capacitance changes are suggested: the intramembrane cavitation (the bilayer sonophore or BLS model) and the acoustic radiation pressure (1-2). Here, we use detailed predictive modeling to show that only intramembrane cavitation can explain all the observed aspects of ultrasonic neuromodulation.

The BLS biomechanics and the acoustic Radiation Pressure Gradients (RPG) - induced membrane dynamics were coupled with biophysical membrane models to predict dynamical biophysical responses of artificial bilayer membranes, and of common neocortical Hodgkin-Huxley type models.

Only the Neuronal Intramembrane Cavitation Excitation (NICE) models were able to explain US-induced action potential generation through BLS-type pulsating nano-bubbles inside the bilayer plasma membrane: the leaflets' periodic vibrations induce US-frequency membrane capacitance and potential oscillations, leading to slow charge accumulation across the membrane, until action potentials are generated. In contrast, the analysis of RPG-induced membrane capacitance variations associated with membrane area changes explain artificial membrane results, but were found to be highly unlikely sources for neural excitation. This model-based prediction was found to explain the results of a significant body of experimental studies, through neural cell-type-selective acoustic control mechanisms.

The current study's theoretical framework has the potential to pave the way towards new CNS therapeutic protocols, using the US as the only method that currently allows targeted noninvasive neuromodulation with millimeter spatial resolution essentially anywhere in the brain.

## References:

1. Plaksin M, Shoham S, Kimmel E (2014) Intramembrane cavitation as a predictive bio-piezoelectric mechanism for ultrasonic brain stimulation. *Phys. Rev. X* 4:011004.
2. Prieto ML, Oralkan Ö, Khuri-Yakub BT, Maduke MC (2013) Dynamic response of model lipid membranes to ultrasonic radiation force *PLoS ONE* 8:e77115.

# TRANSITIONAL HEMODYNAMICS AND GAS EXCHANGE IN PREMATURE POSTPARTUM ADAPTATION: DELAYED VS. IMMEDIATE CORD CLAMPING

**Berk Yigit<sup>1</sup>, Ece Tutsak<sup>2</sup>, David J. R. Hutchon<sup>3</sup>, Kerem Pekkan<sup>4</sup>**

<sup>1</sup> Carnegie Mellon University, Pittsburgh, United States,

<sup>2</sup> Koç University, Istanbul, Turkey,

<sup>3</sup> Memorial Hospital, Darlington, United Kingdom,

<sup>4</sup> Department of Mechanical Engineering, Koc University, Istanbul, Turkey

Hemodynamics of the fetal to neonatal transition is orchestrated through complex physiological changes and result in cardiovascular adaptation to the adult biventricular circulation. Clinical practice during this critical period can influence vital organ physiology of term and preterm babies. Recent studies suggest that physiological transition with delayed cord clamping (DCC) is advantageous for achieving hemodynamic stability and improving oxygenation compared to the traditional immediate cord clamping (ICC) [1]. Here, we investigate the cardio-respiratory dynamics at birth and during the neonate's postpartum adaptation period for gestational ages (GA) from 20 weeks (immature preterms) through 40 weeks (term) using our computational framework and clinically motivated scaling laws for the gestational development of human fetus [2]. Our results show that transitional hemodynamics is smoother in DCC compared to ICC for all GAs. Blood volume of the neonate increases by 12% for moderately preterm and term infants (32-40 wks) and by 16% for very and extremely preterm infants (22-30 wks) with DCC compared to ICC. Placental transfusion significantly improves the cardiac output and the arterial blood pressure by 21% in term (36-40 wks), by 24% in moderately preterm (32-36 wks), by 27% in very preterm (28-32 wks) and by 32% in extremely preterm (22-28 wks) births compared to infants who received ICC (Figure A). Arterial blood oxygen saturations are significantly higher in DCC, whereas infants who had ICC suffered a decline in oxygenation where saturations as low as 10% were observed during the first minutes of transition (Figure B). Results presented in this study suggest that DCC provides superior hemodynamics and ventilation at birth compared to ICC, which will help preventing the complications associated with poor oxygenation arising in premature births.

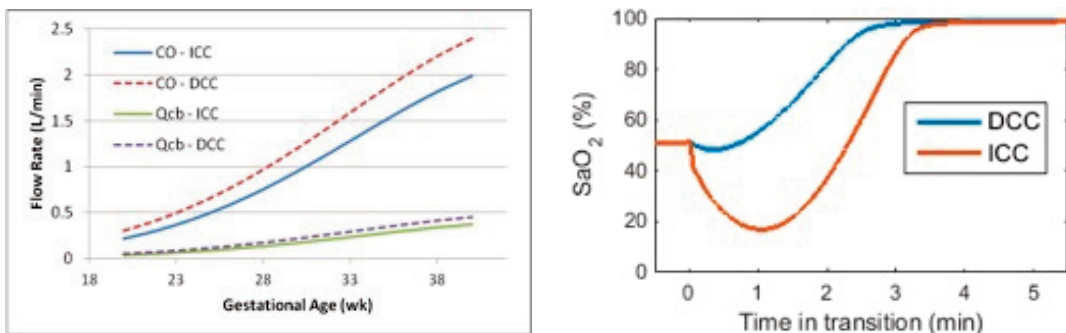


Figure: A: Postnatal cardiac output (CO) and cerebral blood flow (Qcb) levels in DCC and ICC. B: Time course of changes in arterial oxygen saturation (SaO<sub>2</sub>) with DCC and ICC after birth (32 weeks).

## Acknowledgments:

ERC Grant 307460 and Marie Curie FP7 293931

## References:

- [1] B. Yigit, W.J. Kowalski, D.J. Hutchon, and K. Pekkan, *Journal of Biomechanics* 48, 1662 (2015).  
[2] B. Yigit and K. Pekkan, *Journal of The Royal Society Interface* 13, 20151019 (2016).

# PATIENT-SPECIFIC BIOMECHANICAL SIMULATIONS OF PREGNANCY

**Andrea Westervelt<sup>1</sup>, Michael Fernandez<sup>1</sup>, Joy Vink<sup>1</sup>, Chia-Ling Nhan-Chang<sup>1</sup>, Kristin Myers<sup>1</sup>**

<sup>1</sup> Columbia University, New York, United States

## Introduction:

Excessive mechanical loading, tissue stretch, and premature remodeling of the uterine cervix are thought to play a role in preterm birth (PTB). In this study, we built a parameterized, patient-specific, finite element (FE) model of the pregnant uterus and cervix to understand how anatomical and tissue mechanical factors influence cervical tissue stretch.

## Methods:

Geometric properties of the uterus, cervix, and their positions relative to bony reference landmarks were measured via ultrasound (GE Voluson E8) of a 25-week pregnant patient. Based on these parameters, a computer model of pregnancy was generated by Boolean operations (Fig 1A, Trelis Pro). The uterus was built by creating two ellipsoids to represent the outer and inner uterine walls. The shells were scaled, translated, and rotated to depict uterine wall thickness. The cervix was built as a hollow cylinder rounded at both ends to eliminate non-anatomical corners. The fetal membrane (FM) was generated with uniform thickness in a similar manner to the uterus.

For FE analysis (FEBio), the uterus and cervix were modeled as composite materials meshed using linear tetrahedral elements [1, 2]. The FM was modeled as an Ogden material meshed with hexahedral elements [3]. The FM was prescribed a tied contact to the inner uterine wall and top cervix region and a sliding contact to the cervical internal os region (Fig. 1A). For FE simulation, intrauterine pressure was applied at 8.67 kPa [4]. Cervical length (CL), utero-cervical angle (UCA), posterior cervical offset (PCO), and gestational cervical stiffness were varied individually. Stiffness variations were ranged from nonpregnant (NP) to pregnant term properties [2]. For model comparisons, we calculated the volume percentage above a 1.1 stretch threshold of the internal cervical os.

**Results:** Stretch at the internal cervical os increases with: a decrease in cervical stiffness or decrease in CL, or an increase in UCA or increase in PCO (Fig.1B).

**Conclusions:** Cervical stiffness has the largest impact on tissue stretch compared to geometric factors.

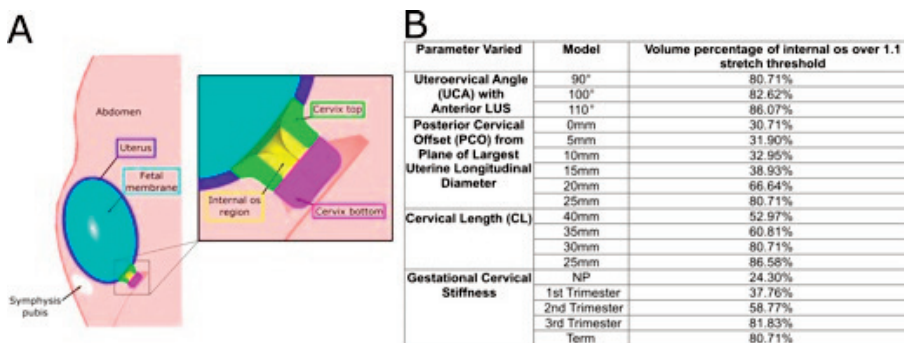


Figure Caption: (A) 3D computer model of pregnancy. (B) Cervical parameter influence on tissue stretch.

## Acknowledgments:

This study was supported by the NSF GRF.

## References:

- [1] J. Conrad et al., *Dynamics*, 1966.
- [2] K. M. Myers et al., *J. Biomech.*, vol. 48, no. 9, pp. 1533–1540, 2015.
- [3] W. Buerzle et al., *Biomech. Model. Mechanobiol.*, vol. 12, no. 4, pp. 747–62, Aug. 2013.
- [4] C. S. Buhimschi et al., *Fetal Matern. Med. Rev.*, vol. 14, no. 4, pp. 273–307, Nov. 2003.

# STATISTICAL SHAPE MODELS TO RECONSTRUCT WHOLE FEMUR SURFACE FROM PELVIC RADIOGRAPHS

John O'Connor<sup>1</sup>, Janet Hill<sup>2</sup>, David Beverland<sup>2</sup>, Nicholas Dunne<sup>3</sup>, Alex Lennon<sup>4</sup>

<sup>1</sup> School of Mechanical and Aerospace Engineering, Queen's University Belfast, Ashby Building, Belfast, United Kingdom,

<sup>2</sup> Primary Joint Unit, Musgrave Park Hospital, Belfast, United Kingdom,

<sup>3</sup> School of Mechanical & Manufacturing Engineering, Dublin City University, Dublin, Ireland,

<sup>4</sup> School of Mechanical and Aerospace Engineering, Queen's University Belfast, Belfast, United Kingdom

## Introduction:

Computational modelling studies of total hip replacement (THR) often use generic femur geometries as three-dimensional (3D) imaging is not standard for THR [1]. Statistical shape modelling (SSM) has been used previously to reconstruct 3D geometry of the proximal femur from X-ray projections and measure morphometric parameters [2]. The aim of this study is to reconstruct whole femur geometry using only proximal femur imaging.

## Methods:

A sample of 47 3D femora was segmented from the Virtual Skeleton Database [3]. Scalismo was used to create a Gaussian process model that was deformed to each training example and principal component analysis was performed to identify modes of variation and their associated variance [4] [5]. To test reconstruction, two-dimensional (2D) AP projections of four femur models with known 3D geometry (ground truth shape) were generated. Landmarks (Fig. 1) were manually selected on the projection of ground truth shape and rigidly aligned to corresponding points on an AP projection of the shape model. Shape parameters for each mode were then calculated by iteratively minimizing the sum of the squared distance between the landmark sets.

## Results and discussion:

Reconstructed models predicted overall length, intertrochanteric distance and femoral head diameter with a mean error of  $25.75 \pm 20.17$  mm,  $3.63 \pm 2.32$  mm and  $3.92 \pm 1.69$  mm respectively. The method is currently being improved using additional landmarks, training shapes and lateral radiographic images. Ongoing work will incorporate the reconstruction algorithm into musculoskeletal modelling and finite element analysis to investigate positioning of implants in THR.

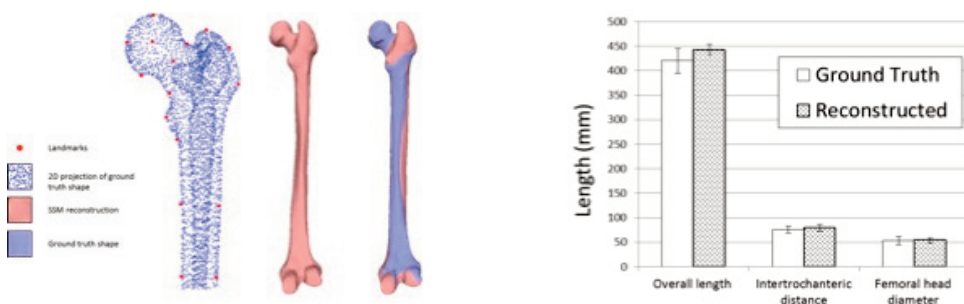


Figure Caption: (Left) 2D projection of landmarks, reconstructed femur and ground truth femur; (Right) mean overall length, intertrochanteric distance and femoral head diameter recorded on four ground truth femora and their associated reconstructions (+/- 1SD)

## References:

- [1] Dopico-González, C., et al. *J. Biomech.*, 43(3):512-20, 2010.
- [2] Schumann, S., et al. *Med. Eng. Phys.*, 32(6): 638-44, 2010
- [3] Kistler, M., et al. *J. Med. Internet Res.*, 15 (11): e245, 2013
- [4] Lüthi, M., et al. *Int. Work. Mach. Learn. Med. Imaging.*, (1): 66-73, 2013
- [5] Clogenson, M., et al. *Int. J. Comput. Assist. Radiol. Surg.*, 10(7):1097-107, 2014

## IMAGE-BASED TRANSPORT MODELING IN HUMAN PLACENTAL TERMINAL VILLI

**Romina Plitman Mayo<sup>1</sup>, D. Steve Charnock-Jones<sup>2</sup>, Graham J. Burton<sup>3</sup>, Michelle L. Oyen<sup>4</sup>**

*1 Centre for Trophoblast Research, Department of Physiology, Development and Neuroscience, University of Cambridge, UK, Nanoscience Centre, Department of Engineering, University of Cambridge, UK, 11 Jj Thomson Avenue, Cambridge, United Kingdom,*

*2 Centre for Trophoblast Research, Department of Physiology, Development and Neuroscience, University of Cambridge, UK,, Department of Obstetrics and Gynaecology, Addenbrooke's Hospital, University of Cambridge, UK, Cambridge, United Kingdom,*

*3 Centre for Trophoblast Research, Department of Physiology, Development and Neuroscience, University of Cambridge, UK,, Cambridge, United Kingdom,*

*4 Nanoscience Centre, Department of Engineering, University of Cambridge, UK, Centre for Trophoblast Research, Department of Physiology, Development and Neuroscience, University of Cambridge, UK, Cambridge, United Kingdom*

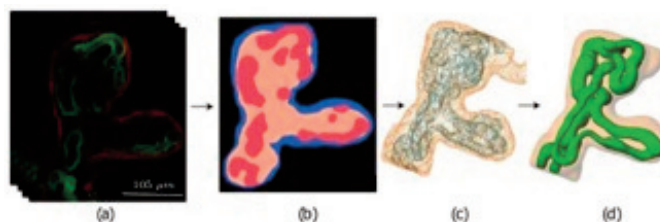
The placenta is the organ that interfaces between the mother and the developing fetus, allowing for the exchange of gases, nutrients and waste. Due to ethical limitations and the complicated acquisition and manipulation of the ex-vivo organ, placental research has been very challenging. Computational modeling of biological systems is becoming increasingly popular, and has the potential to become an invaluable tool in detecting pathologies and health risks for newborns.

Immunofluorescence microscopy was combined with computational simulations to investigate oxygen transport in the human placenta [2]. Image stacks of placental villi were obtained from samples of a perfusion-fixed healthy term placenta. The three-dimensional architecture of the villi was reconstructed from the segmented images, and converted to a finite element model. The diffusion of oxygen through the trophoblastic membrane and fetal plasma was modeled, including the villous membrane oxygen consumption. Parametric studies were performed to assess the villous efficiency and sensitivity to model parameters.

The results suggest that capillary variations lead to significant changes in blood velocity, and that the combination of capillary bending and dilatation can decelerate the flow by 80%, allowing for better oxygenation. Additionally, it was demonstrated that vortical flow does not develop in the fetal capillaries. Interestingly, a small increase of the inlet volumetric flow rate resulted in a significant increase of oxygen flux. The parametric studies revealed that the capacity of a villus to transport oxygen efficiently depends mostly on its geometry rather than on the material properties.

Placental research is in need of new research techniques. Image-based modeling could provide insights into the functioning of the human placenta, since aspects like the structure-function relation in the terminal villi, can be investigated in detail. Computational modeling could serve in the future to simulate complicated in-vivo scenarios.

*Figure Caption: " (a) Immunofluorescent microscopic image where the trophoblastic membrane (red) and the fetal capillaries (green) are visible, (b) Segmented slide,*



*(c) Point cloud of the geometries and (d) Resulting volumes [2]"*

### References

[2] R. Plitman Mayo. *Three-Dimensional Modeling of Human Placental Villi*, revised manuscript in review, *Placenta* (2016).

# HIGH-FIDELITY NUMERICAL SIMULATIONS OF VORTICAL STRUCTURES AND CARDIOVASCULAR DISEASE

**Steven Frankel**<sup>1</sup>

*<sup>1</sup> Technion - Israel Institute of Technology, Haifa, Israel*

Cardiovascular disease (CVD) is the leading cause of death in the US. With the rise of 4D imaging techniques, advanced numerical simulation capabilities, and ever increasing computing power, the role of vortical structures in CVD is becoming more widely studied. What are vortical structures? How might they contribute to CVD? How can they be imaged in vivo, captured in numerical simulations, and measured in laboratory experiments? In this talk, some of these questions will be discussed in the context of using an in-house high-fidelity numerical simulation tool called WenoHemo to study extra-cardiac vs. intra-atrial powered Fontan hemodynamics for univentricular heart disease patients and thoracic aortic aneurysms among other applications.

# PATIENT-SPECIFIC NUMERICAL MODEL OF CALCIFIC AORTIC STENOSIS AND ITS TREATMENT BY BALLOON-EXPANDABLE TRANSCATHETER AORTIC VALVE: EFFECT OF POSITIONING ON THE ANCHORAGE

**Gil Marom<sup>1</sup>, Matteo Bianchi<sup>1</sup>, Ram P. Ghosh<sup>1</sup>, Danny Bluestein<sup>2</sup>**

<sup>1</sup> Stony Brook University, Stony Brook, United States,

<sup>2</sup> Stony Brook University, Department of Biomedical Engineering, Stony Brook, United States

Calcific aortic stenosis is a degenerative process in which the aortic valve (AV) narrows due to the formation and growth of calcium deposits on its leaflets. Transcatheter aortic valve replacement (TAVR) has become the only lifesaving solution for patients that cannot undergo the standard surgical valve replacement. Despite its promising outcomes, adverse events such prosthesis migration may occur as a result of suboptimal placement, leading to poor device performance and procedural failure. The aim of this study is to evaluate the effect of various TAVR deployment positions on the procedural outcome by assessing the risk for migration. First, a finite element analysis of balloon-expandable Edwards SAPIEN valve crimping was performed. Then, the crimped TAVR stent was deployed by balloon-inflation in a patient-specific calcified aortic root (AR), reconstructed from CT scans of a retrospective case of valve migration into the left ventricle. The deployment location was parametrized in three configurations and the anchorage was quantitatively assessed based on the contact between the stent and the AR during the deployment and the recoil phases. The proximal deployment resulted in higher risk for valve migration, higher stress level in the native tissue, and lower contact area between the native leaflets and the stent. The distal and midway positioning resulted in comparable outcomes, even though the distal deployment provided slightly better anchorage. The models accurately mimic the pathophysiological features of the patient's anatomy and simulate different procedural scenarios. As a next step, we plan to model the flow through the paravalvular gaps to better understand how the position influence them. The proposed approach might be used as a predictive tool for procedural planning in order to ultimately achieve better clinical outcomes.

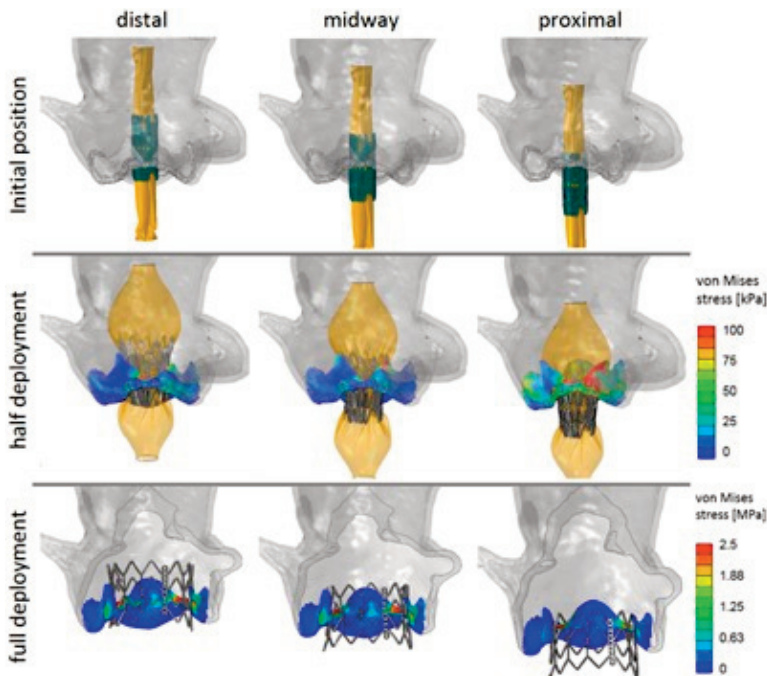


Figure: Various stages of the stent deployment in the three deployment locations with von Mises contours plots.

## PULMONARY ARTERIAL BIAXIAL TISSUE MECHANICS IN PAH

**Daniela Valdez-Jasso**<sup>1</sup>

<sup>1</sup> University of Illinois at Chicago, Chicago, United States

Pulmonary arterial hypertension (PAH) is characterized by a rise in blood pressure in the pulmonary circulatory system. To quantify the arterial properties as PAH progresses, we used a rat animal model of PAH and determined the stress-strain relations of the left- and right-PA. 24 male Sprague-Dawley rats were included in this study. 12 rats were treated with a subcutaneous monocrotaline (MCT) injection to induce PAH and were paired with a control group that was injected with a placebo solution. Every week, 3 placebo and 3 MCT-treated rats underwent hemodynamic measurements to determine stage of the disease. PA segments were then harvested, cannulated, and assembled in a tubular biaxial testing chamber. The vessels were tested at the in vivo and  $\pm 5\%$  axial stretch. Pressure and flow were prescribed to simulate values measured in vivo. Outer diameter, axial tension and stretch were recorded and used for the calculation of axial and circumferential stress-strain curves. Our results confirmed a steady increase in pulmonary pressures. The stress-strain curves in both axial and circumferential directions increased significantly. However, in the placebo group they remained overall constant, indicating that the vessels remain unaffected by the 4 weeks time lapse. Our results are consistent with the work done in mice [1,2]. To further understand the changes in the tissue-level mechanical response, the vessels were immediately imaged using a multi-photon microscope (MPM). As shown in Figure 1, the fiber organization went from being random (no preferred direction) and wavy in the placebo vessel to being highly aligned and mostly straighten in the MCT. Our future goal is to identify the causes for this remodeling process, and directly connect the cellular-level structure to the tissue-level function.

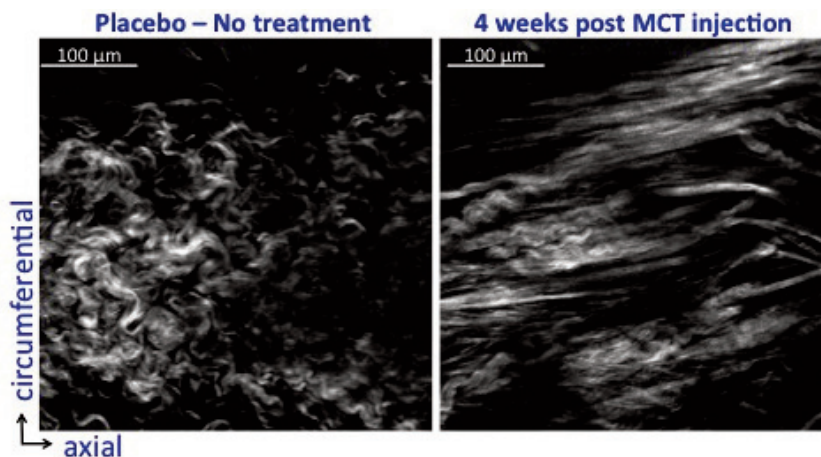


Figure Caption: MPM images of left pulmonary artery fiber structure in the normotensive (left) and PAH state (right) at their respective mean pulmonary arterial pressures.

### Acknowledgments:

University of Illinois at Chicago College of Engineering Seed Fund, Graduate College Abraham Lincoln Fellowship, and the Honors College Undergraduate Research Award.

### References:

- [1] Tabina DM and Chesler NC., *J Biomechanics* 43(10): 1864-1869, 2010.
- [2] Chesler NC., *J Biomechanical Engineering* 126, 2004.

# MODELING AND COMPUTATIONAL SIMULATION OF HEMODYNAMICALLY-INDUCED ATHEROSCLEROSIS

**Pinhas Bar-Yoseph<sup>1</sup>, Michal Markowitz<sup>2</sup>**

*1 Technion - Israel Institute of Technology, Haifa, Israel,*

*2 Biomechanics Center of Excellence, Mechanical Engineering, Technion, Tel Aviv, Israel*

Atherosclerotic plaque rupture is the main cause of myocardial infarction, coronary thrombosis and stroke. Hence, a better understanding of this pathology is needed to develop effective approaches for prediction, treatment and intervention.

The material and structural characteristics of atherosclerotic plaque are important factors in the natural progression of atherosclerosis-related diseases and may have important clinical predictive value. Increased stresses on vulnerable plaque may lead to plaque rupture, while plaque rupture with superimposed thrombosis is the cause of acute coronary syndromes such as unstable angina and myocardial infarction, as well as non-coronary syndromes such as stroke, which may lead to sudden death. Therefore, coupled hemodynamic and structural stress analyses are pivotal to understanding plaque stability and vulnerability to rupture. In particular, investigating the correlation between different stages of plaque progression and patterns of mechanical stress may help to detect vulnerable stenosis in patients and may save lives.

This lecture is divided into two parts. In the first part of this lecture, a novel approach to the modeling of hemodynamically induced blood coagulation is introduced. We demonstrate that our mathematically simple, mesoscopic model can achieve remarkable, qualitative and quantitative agreement with in-vitro, in-vivo experiments, including the relatively new mechanism of platelet tethering induced aggregation, first introduced in Nature Medicine, 2009. The complexity of the blood cascade has prompted current modeling techniques to use complex multi-scale methods or continuum methods modeling the coagulation cascade in high detail. We propose a simple mesoscopic model, applied on a highly simplified cascade, which models the coagulation constituents as non-continues density populations, with reactions based on particle interactions. The proposed model is the first to incorporate the mechanism of platelet tethering and fibrin polymerization into one model, matching the results described in and allowing the model to provide insight into complex coagulation cases which employ both. Our model does not only capture the described phenomena of the coagulation process; it also provides insight into the conditions driving coagulation growth and the relations between the microscopic and macroscopic properties.

In the second part of this lecture, we critically review various mathematical models which were developed by researches to describe different aspects of the initiation and the progression of the plaque envelope up to the point of rupture, and then we propose a novel simplified approach and present preliminary results.

# MODELING OF MICROSTRUCTURE AND MECHANICS OF HEALTHY AND ANEURYSMATIC ABDOMINAL AORTAS

**Justyna Niestrawska<sup>1</sup>, Gerhard A. Holzapfel<sup>1</sup>**

*<sup>1</sup> Institute of Biomechanics, Graz University of Technology, Graz, Austria*

Arterial walls act similarly to fiber reinforced composite materials. Changes in the ground matrix and the embedded collagen fibers were shown to play a significant role in the pathogenesis of, e.g., aneurysms.

In recent experiments [1] healthy human abdominal aortas (AA) and abdominal aortic aneurysm (AAA) tissues were systematically compared regarding both their structure (utilizing second-harmonic generation, SHG) and related mechanics (utilizing biaxial tensile tests). The experiments revealed significant differences in both structure and mechanics between AA and AAA. AA tissues showed three distinct layers with a significantly lower out-of-plane orientation of collagen fibers compared to the in-plane dispersion. Imaging of AAA tissues revealed mostly strong straight and thick collagen fibers in the adventitia, a high distribution of collagen fibers out-of-plane (Figure) and calcification and lipid droplets at the luminal side. Additionally the layered structure was lost in almost all samples. The mechanical parameters for AAA tissues were very heterogeneous and significantly different to AA tissue.

To account for these findings an existing constitutive model [2] was modified to consider in-plane and out-of-plane dispersions separately [3]. A bivariate von Mises distribution was used to derive two dispersion parameters from the obtained structural images. Two structure tensors were constructed to incorporate the distribution parameters into a free-energy function, including both the mechanical and structural features of the material. The structural parameters were obtained from the SHG images and the model was fitted to the mechanical data, providing good fitting results ( $R^2 \geq 0.94$ ).

The proposed model was implemented into FEAP. Simulations of biaxial tension tests were performed, showing that the different stress-strain responses of healthy and diseased tissues can be modeled within the experimentally predicted range of stresses.

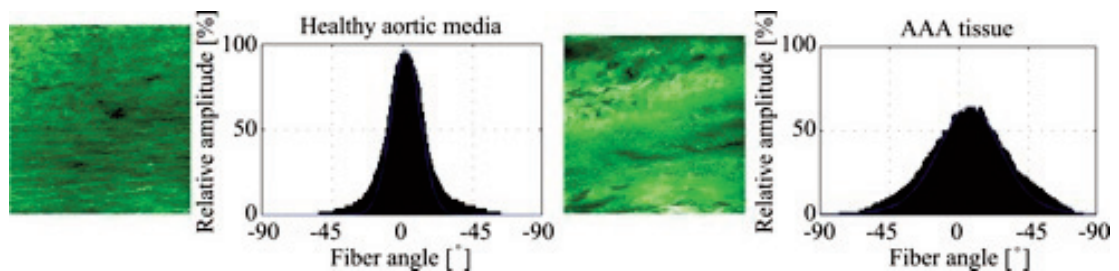


Figure Caption: SHG images of the different collagen structure in the media of AA and AAA tissues. The graphs show the angular dispersion of collagen fiber orientation [1].

## References:

- [1] J.A. Niestrawska et al., submitted.
- [2] T.C. Gasser et al., *J. R. Soc. Interface*. 3:15-35 2006.
- [3] G.A. Holzapfel et al., *J. R. Soc. Interface*. 12:20150188, 2015.

## RESULTS OF IN-VITRO TESTS ON A 2:1 PROTOTYPE OF A PERCUTANEOUS VENTRICULAR ASSIST DEVICE

**Alen Karabegovic<sup>1</sup>, Christoph Janeczek<sup>1</sup>, Markus Hinteregger<sup>1</sup>, Margit Gföhler<sup>1</sup>**

<sup>1</sup> Technische Universität Wien, Vienna, Austria

A miniature, Helium operated percutaneous ventricular assist device (pVAD) has been developed for usage as a bridge-to-recovery in combination with the intra-aortic balloon pump. Its limited dimensions of less than 50 mm in length and 6 mm in diameter enable positioning of the device between the left ventricle and the aorta, where it may assist the damaged heart by delivering flow up to 2.5 l/min.

In order to test the pVAD prior to animal trials, a pulsatile mock circulatory loop has been constructed that can replicate various acute changes of haemodynamic parameters.

Construction of the circulatory loop started by simulating circulatory diseases in a lumped parameter model. Mechanical assembly was actuated by manipulating pressure in an evacuated reservoir representing the left ventricle. Behavior of the aortic pressure was defined using an aortic compliance and a pair of resistances, while an open reservoir replicated the mitral side.

The 2:1 pVAD prototype was tested in the mock circulation at various circulatory parameters. Results from tests at 81 bpm and ejection fraction of 50% are shown in Figure below. The area enclosed by the PV loops represents the ventricular work [1] that shrinks with increasing speeds. This indicates an unloading effect on the left ventricle - at 15000 rpm the pVAD decreases the work performed by heart by 41%.

At speeds above 13000 rpm the aortic valve remains closed during systole. This implies that no pulse would be measured from the patient. Further increase of speed may result in an onset of suction that can lead to additional complications such as the collapse of ventricular walls [2]. The development of suction detection and prevention algorithms will be possible after first in-vivo studies on the 1:1 heart pump prototype.

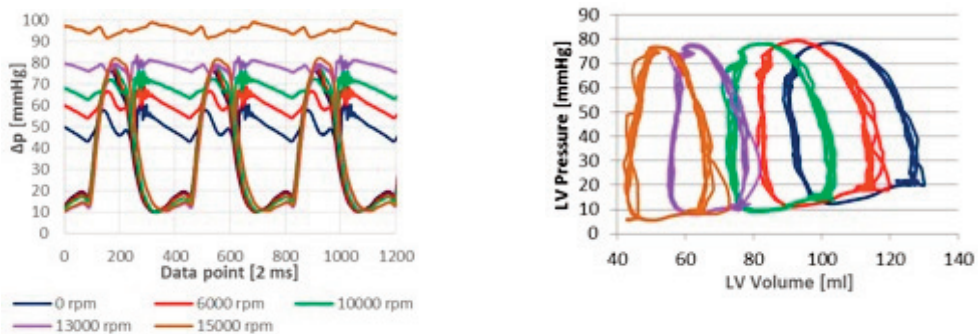


Figure Caption: Left ventricular and aortic pressures (a) and the recorded left ventricular PV loops (b).

### Acknowledgments:

This work was done within the Research Studio 'Assistocor', funded by the Austrian Federal Ministry for Economy, Family and Youth (BMWFJ) and operated by the Austrian Research Promotion Agency (FFG).

### References:

- [1] P. A. Iaizzo, Ed., *Handbook of Cardiac Anatomy, Physiology, and Devices*. Totowa, NJ: Humana Press, 2009.
- [2] A. Drummond, *Biomedical Surgical Planning for Pediatric Ventricular Assist Device (PVAD)*. ProQuest, 2008.

## COMPUTER SIMULATION OF ELECTROPORATION AND DRUG TRANSPORT THROUGH MEMBRANES

**Nenad Filipovic<sup>1</sup>, Igor Saveljic<sup>2</sup>, Irena Tanaskovic<sup>2</sup>**

<sup>1</sup> University of Kragujevac, Faculty of Engineering, Bioirc Doo Kragujevac, Kragujevac, Serbia,

<sup>2</sup> University of Kragujevac, Kragujevac, Serbia

We analyzed computational and experimental electroporation model with human aorta tissue. The segments in native state of the aorta are treated by electroporation method through a series of electrical impulses from 50 V/cm to 3000V/cm. For each patient we analyzed one sample with and one sample without electroporation as a control. Electrical field distribution is solved by the Laplace equation. The convection-diffusion equation is used to solve heat transfer problems. Experimental histology has shown a smaller number of vascular smooth muscle cells (VSMC) nuclei at the tunica media, while the elastic fibers morphology is maintained 24 h after electroporation. In the computational model the fitting procedure is applied for conductivity values in order to make material properties of the aorta tissue. The fitting procedure gives tissue conductivity of 0.45 [S/m] for applied electrical field of 2500 V/cm. We also examined with computational model a non-invasive drug delivery system and effects of electrical potential on the drug diffusion in the aorta tissue. The initial numerical results are in good comparison with experimental observation. We demonstrate that the application of an applied voltage can greatly improve the efficacy of localized drug delivery as compared to diffusion alone.

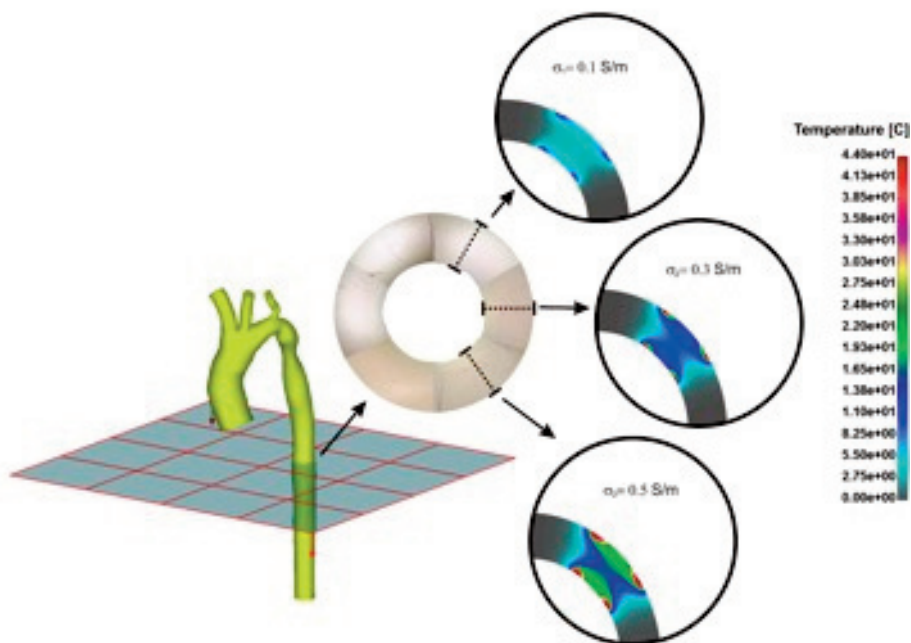


Figure 1. Temperature distribution during electroporation with prescribed 2500 V/cm for three different tissue conductivities -  $\sigma = 0.1 \text{ S/m}$ ,  $0.3 \text{ S/m}$  and  $0.5 \text{ S/m}$

### Acknowledgments:

This study was funded by grants from the Serbian Ministry of Education, Science and Technological Development III41007 and ON174028.

# TARGETED DELIVERY IN UPPER AIRWAYS USING INHALED MAGNETIC PARTICLES

**Yan Ostrovski**<sup>1</sup>, **Pantelis Koullapis**<sup>2</sup>, **Stavros Kassinos**<sup>3</sup>, **Josue Sznitman**<sup>4</sup>

*1 Technion - Israel Institute of Technology, Haifa, Israel,*

*2 Computational Sciences Laboratory (Ucy-CompSci), Nicosia, Cyprus,*

*3 Computational Sciences Laboratory (Ucy-CompSci), Department of Mechanical and Manufacturing Engineering, University of Cyprus, Nicosia, Cyprus,*

*4 Technion - Israel Institute of Technology, Dept. of Biomedical Engineering, Haifa, Israel*

The lungs constitute an attractive delivery pathway for treating lung diseases topically, e.g. lung cancer. In the last decades, substantial progress has been made in understanding flow phenomena and particle transport mechanisms in the pulmonary tree. Nevertheless, drug targeting abilities to specific diseased location remain poor. To tackle this problem, there has been a growing interest in the last years in implementing magnetic particles (MPs), to externally divert aerosol deposition to desired regions. In particular, CFD simulations have been sought to improve our understanding of the transport characteristics of MPs in the pulmonary environment.

Although the literature on such topic is not abundant, few isolated studies have attempted to shed light on MPs' dynamics, individually in each lung region. For example, Pourmhran et al (2015) simulated MP deposition in a reconstructed tracheobronchial geometry retrieved from CT scans. Martinez et al (2013) studied deposition of ellipsoid MPs in a simplified terminal bronchiole dichotomous bifurcation. In the most distal regions of the lungs, i.e. the acinar region, Krafcik et al (2015) simulated a single MP motion, whereby a single hemisphere was used to model the alveolar geometry. Most recently, Ostrovski et al (in revision) simulated the deposition of such particles in an asymmetric acinar tree, with 6 branching generations and 277 alveolar cavities. In all the mentioned work, the authors found a considerable increase in deposition due to the magnetic force exerted on the particles. Nevertheless, non-had managed to achieve a highly localized deposition.

Up until today, it remains to be shown whether the use of MPs can be leveraged for site-specific targeting of inhaled therapeutics to upper airways. Here, we utilize CFD to investigate the feasibility of a new targeting technique geared at highly-localized upper airway deposition. This inhalation technique combines MPs with specific particle sizing, and a carefully tuned breathing maneuver.

## Acknowledgments:

This work was supported by the Israel Science Foundation (grant nr. 990/12). P. Koullapis was supported by a Short Term Scientific Mission (STSM) fellowship within COST Action 1404 "SimInhale" (Horizon 2020).

## MULTIFUNCTIONAL NANOCONSTRUCTS FOR CANCER THERANOSIS: FROM IN SILICO TO PRECLINICAL MODELS

**Paolo Decuzzi<sup>1</sup>**

*<sup>1</sup> Italian Institute of Technology , Genova, Italy*

Most nanoparticles for biomedical applications originate from the self-assembling of individual constituents through molecular interactions and possess limited geometry control and stability. Here, discoidal polymeric nanoconstructs (DPNs) are demonstrated by mixing hydrophobic and hydrophilic polymers with lipid chains and curing the resulting paste directly within silicon templates. The size, shape, surface properties and mechanical stiffness of DPNs can be precisely, and independently, tailored during the synthesis process. Specifically, by changing the paste composition, soft- and rigid-DPNs (s- and r-DPNs) are synthesized exhibiting the same geometry, a moderately negative surface electrostatic charge (-14 mV), and different mechanical stiffness ( $\sim 1.3$  and  $15$  kPa, respectively). These multifunctional nanoconstructs are used as carriers of imaging and therapeutic agents for cancer theranostics. Upon injection in mice bearing brain or skin cancers, s-DPNs exhibit  $\sim 24$ h circulation half-life and accumulate up to  $\sim 20\%$  of the injected dose per gram tumor, detecting malignant masses as small as  $\sim 0.1\%$  the animal weight via PET imaging. In silico simulations and in vitro microfluidic testing are used to elucidate the mechanisms regulating the in vivo vascular behavior of DPNs and their biomedical performance. The unprecedented behavior of DPNs is ascribed to the unique combination of geometry, surface properties, and mechanical stiffness which minimizes s-DPN sequestration by the mononuclear phagocyte system. Our results could boost the interest in using less conventional delivery systems for cancer theranosis.

# DESIGNING SHEAR RESPONSIVE NANO-MEDICINE FOR TARGETED DRUG DELIVERY

## **Netanel Korin**<sup>1</sup>

*<sup>1</sup> Faculty of Biomedical Engineering, Technion- Israel Institute of Technology, Haifa, Israel*

The interplay between vascular physiology, hemodynamics, and transport phenomena plays a dominant role in cardiovascular diseases. These factors are also pivotal to the development of efficient targeted nano-medicine for cardiovascular diseases. This talk we will focus on the development of mechano-responsive nanomedicine for targeted drug delivery to sites of vascular narrowing. Inspired by the phenomenon of platelet shear activation, we developed a drug delivery approach that is activated by high shear stress in regions of artery stenosis as a means to selectively deliver target drugs to these disease sites (Korin et al., *Science*, 2012). To implement this new targeting strategy, we designed poly(lactic-co-glycolic acid) nano-particles aggregates which are cued to break when subjected to pathologically high local shear stress while staying intact under normal physiological flow. Using this drug delivery strategy we have shown in a variety of in vitro microfluidic based models and in several in vivo models that we can efficiently deliver a thrombolytic drug to dissolve clots at sites of stenosis. Altogether, our work illustrates how computational biomechanics can be used to design and develop novel cardiovascular therapeutic strategies.

## DRUG-ELUTING IMPLANTS: RELEASE MECHANISMS AND MODELS

### **Meital Zilberman**<sup>1</sup>

*<sup>1</sup> Department of Biomedical Engineering, Faculty of Engineering, Tel Aviv University, Tel-Aviv, Israel*

Drug-eluting implants can provide life-giving help to many systems in the body. When made of a bioresorbable polymer, such devices degrade with time and the end products are nontoxic. These devices can remain intact in the body for a predicted period of time and then degrade without the need for surgical removal. A novel class of bioresorbable, composite fiber structures loaded with bioactive agents has been developed and studied by us. These unique polymeric structures are designed to combine good mechanical properties with a desired controlled release profile, in order to serve as basic elements of broad range of medical implants and scaffolds for tissue regeneration. All types of bioactive agents, water soluble and water insoluble agents, can be incorporated in these structures. Examples for applications of such fibers: drug-eluting stents, meshes with controlled release of antibiotics, wound dressings with controlled release of pain killers, scaffolds with controlled release of growth factors etc.

Mathematical models for predicting bioactive agent release profiles from the fibers are beneficial as a preliminary step, especially in the case of releasing expensive bioactive agents from the implants. Such models were developed by us and will be presented. A good example presents antiproliferative drug release from the fibers for both applications, drug-eluting stents and local cancer treatment. These drugs are highly hydrophobic, and therefore their release from porous biodegradable structures is advantageous. Our models and studies indicated that the chemical structure of the polymer chain directly affects the drug release profile through water uptake in the early stages or degradation and erosion in later stages. It also affects the release profile indirectly, through the polymer's 3D porous structure. The drug volume and molecular area also dominantly affect its diffusion rate from the 3D porous structure. Additional examples will be presented during the talk.

# SIMULATION OF PROTEIN FOLDING BASED ON STATISTICAL KNOWLEDGE

**Simcha Srebnik**<sup>1</sup>

*<sup>1</sup> Technion - Israel Institute of Technology, Haifa, Israel*

Predicting the folded state of proteins from their primary sequence remains one of the greatest challenges in molecular biology today. Folding of proteins to their unique native state occurs over a relatively narrow timespan of the order of milliseconds. The presence of a single or few low entropy folded structures, out of essentially an infinite number of conformations, known as Levinthal's paradox, suggests the existence of phenomenological and universal behavior that directs folding. Two main approaches exist today to tackle the protein folding problem. In homology-based modeling a protein is folded according to a priori knowledge of similar polypeptides with already known fold. This method fails for unknown sequences or mutations. Free modeling of protein folding is a force-field based approach that predicts the final tertiary fold without a priori folding knowledge. This second approach usually requires massive computing and financial resources. As a consequence, laboratory experiments that require computerized simulations of proteins suffer from investment of enormous computing resources and time.

We developed a computational algorithm based on internal protein coordinates combined with statistical analysis of transition probabilities extracted from the vastly growing protein data bank. Our preliminary model allows us to predict secondary structures from the amino acid sequence to within 3Å rmsd (root mean squared deviation) from the crystal structure without a priori knowledge of the final structure, within a fraction of a second on a desktop computer (compared with several months on superclusters using atomistic models). The method relies on energy mapping of the conformational space of pairs of aa's, using a Monte Carlo algorithm to sample the restricted conformational space. Thus, this algorithm allows for a rapid convergence to low-energy folded states, as well as the investigation of protein misfolding.

# MOLECULAR MODELING OF BIOMATERIALS USED IN DRUG DELIVERY SYSTEMS

**Dafna Knani**<sup>1</sup>

<sup>1</sup> Department of Biotechnology Engineering, Braude College, Karmiel, Israel

Drug delivery systems are often made of porous polymer matrices. One method used to prepare a foamed polymer matrix is the Controlled Expansion of Saturated Polymers process (CESP) in which amorphous polymer is exposed to CO<sub>2</sub> at high pressure with a significant lowering of glass transition temperature. This plasticizing effect allows to process temperature-sensitive polymers at relatively low temperatures.

In the present study computational tools were applied to estimate plasticizing effect of CO<sub>2</sub> and calculate CO<sub>2</sub> and H<sub>2</sub>O loading capacities for three absorbable polyesters: polycaprolactone (PCL) and two copolymers of (Poly-D,L-Lactid-co-Glycolid)-co-Polyethylenglycol. Plasticization caused by CO<sub>2</sub> was estimated by solubility parameter and radial distribution function at several CO<sub>2</sub> concentrations and by enlargement of free volume detected by mean square displacement of helium atoms, calculated after dynamic simulation. It was found that the maximal value of the solubility parameter and density can serve as a tool to predict saturation concentration.

The loading capacity of the biopolymers that were preloaded with CO<sub>2</sub> molecules was significantly higher than the non-treated polymers. Similar results were obtained for H<sub>2</sub>O molecules loading.

## References:

D. Knani, D. Alperstein, Th. Kauth, D. Kaltbeitzel, and Ch. Hopmann., *Molecular modeling study of CO<sub>2</sub> plasticization and sorption onto absorbable polyesters*, *Polymer Bulletin*, 72 (6), 1467-1486 (2015).

# COMPUTATIONAL MODELLING OF CELLULAR BODIES IN HIGH ELASTIC DEFORMATION

Hayley Wyatt<sup>1</sup>, Muhammad Rahman<sup>2</sup>, Sam Evans<sup>2</sup>, Angela Mihai<sup>1</sup>

<sup>1</sup> School of Mathematics, Cardiff University, Cardiff, United Kingdom, <sup>2</sup> School of Engineering, Cardiff University, Cardiff, United Kingdom

Cellular bodies are strong, flexible structures, capable of large deformations from which they recover completely. In many modern applications (e.g. biomedical tissue scaffolds) and biological structures (e.g. plant stems), large stresses and strains also occur due to the interplay between the structural architecture and the material properties of the constituents [1]. For these complex materials, reliable computer models supported by mathematical and mechanical analyses are needed. In this study, finite element models (FEM) were developed to explore the mechanical behaviour of cellular structures of nonlinear elastic material with varying geometric features and the computed results were compared with experimental data. The models consisted of periodic cellular structures with square and diamond-shaped cells created in SolidWorks and imported into the FEBio software suite, where the cell wall material was characterised by a Neo-Hookean or Mooney-Rivlin hyperelastic model. These structures were subjected to uniaxial tensile loading. Numerically, it was found that the overall stiffness of the cell walls increased with the increasing wall thickness, and that for a constant material volume, the stiffness of the walls also increased with the increasing number of cells (Fig. 1). Experimentally, analogous structures were tested and analysed using the digital image correlation (DIC) technique [2]. It was found that the experimental data produced by DIC compared well with the FEM results, both in terms of force-displacement curves and strain distributions. The results from this study provide valuable information in understanding the behaviour of cellular structures and can be used to optimise their design.

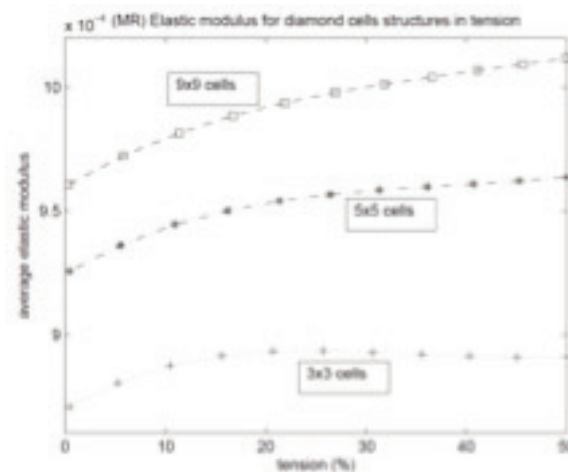


Figure 1. The mean elastic modulus for the diamond structures (for the Mooney-Rivlin material) with varying number of cells

## Acknowledgments:

The support for L.A.M. and H.W. by the Engineering and Physical Sciences Research Council of Great Britain under research grant EP/M011992/1 is gratefully acknowledged.

## References:

- [1] Mihai L.A., et al, *Nonlinear Poisson effects in soft honeycombs*, Proc. R. Soc. A, 471:20140363
- [2] Evans S.L. et al, *Measuring the mechanical properties of human skin in vivo using digital image correlation and finite element modelling*. J. Strain Anal. Eng. 44, 337-345, 2009.

# MECHANICAL FLEXURE BEHAVIOR OF BIO-INSPIRED COLLAGEN-REINFORCED THIN SHEET COMPOSITES

**Mirit Sharabi**<sup>1</sup>, **David Varssano**<sup>2</sup>, **Yehuda Benayahu**<sup>3</sup>, **Dafna Benayahu**<sup>4</sup>, **Rami Haj-Ali**<sup>1</sup>

<sup>1</sup> The Fleischman Faculty of Engineering, Tel Aviv University, Tel Aviv, Israel, <sup>2</sup> Sackler Faculty of Medicine, Tel Aviv University, Department of Ophthalmology, Tel Aviv Medical Center, Tel Aviv, Israel, <sup>3</sup> George S. Wise Faculty of Life Sciences, Tel Aviv University, Tel Aviv, Israel, <sup>4</sup> Tel Aviv University; Dept. Cell and Developmental Biology, Tel Aviv, Israel

Soft tissue can be viewed as a multi-layered composite structure reinforced with multidirectional collagen fiber systems used to control the overall mechanical properties. The structural complexity is manifested in the presence of several hierarchical levels; from the natural material structure to its arrangement as composite laminates and up to its macro-arrangement as a tissue construct. In this work, we fabricated, performed mechanical testing, and proposed a nonlinear computational model for the mechanical behavior of a composite construct. The latter was made of multidirectional collagen fibers reinforced hydrogel mat [1]. Three dimensional finite element (FE) models with multidirectional fiber alignments were generated and tested under flexure; the constructs were clamped in their circumference and centrally loaded by a rigid spherical indenter. The models were hyperelastic and were built with continuum and beam elements representing the matrix and fibers, respectively. Following the numerical results, novel bio-composite constructs, inspired by the native corneal structure, were fabricated from long collagen fibers reinforced poly alginate-based matrix [2,3]. The constructs were also tested to flexure using a special testing apparatus (Figure 1). The hyperelastic behavior predicted by the calibrated FE models was similar to the experimental results. The integration of the new bio-inspired construct with compatible and hyperelastic FE model enables tailoring the mechanical behavior to this of native tissues under varied loading modes. This combination is advantageous in engineering and design of complex constructs for soft tissue substitutes.

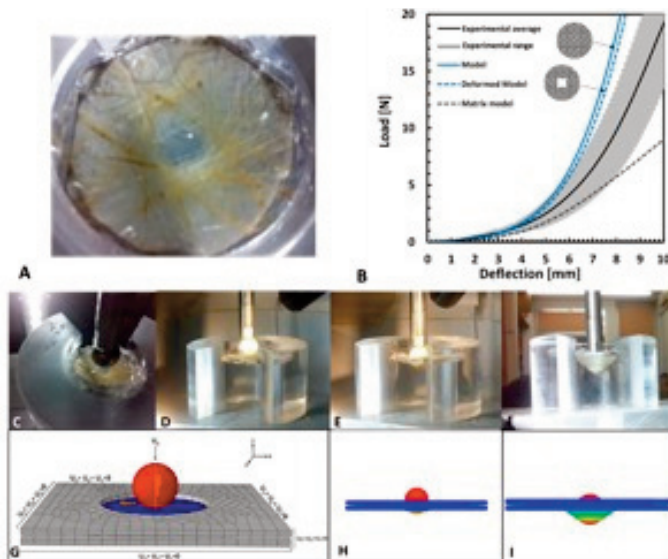


Figure 1: Bio-composite constructs: (a) Bio-inspired cornea composite (b) Flexure behavior of experimental construct vs. the compatible FE model (c-f) Mechanical testing apparatus for flexure behavior of the bio-composite construct. (g-i) FE model: geometry, boundary conditions and flexural test.

## References

- [1] Sharabi et al. (2016), submitted.
- [2] Sharabi et al. *Composites Science and Technology* (2015), 117, 268-276.
- [3] Sharabi et al. *Journal of the mechanical behavior of biomedical materials* (2014), 36, 71-81.

# DEVELOPMENT OF AN ADAPTIVE BONE REMODELING MODEL DRIVEN BY MECHANICAL AND BIOLOGICAL STIMULI FOR IMPLANT ANALYSIS

**Vee San Cheong<sup>1</sup>, Melaine J Coathup<sup>1</sup>, Gordon Blunn<sup>1</sup>, Paul Fromme<sup>2</sup>**

<sup>1</sup> John Scales Centre for Biomedical Engineering, Institute of Orthopaedics and Musculoskeletal Science, University College London, Middlesex, United Kingdom,

<sup>2</sup> Department of Mechanical Engineering, University College London, London, United Kingdom

Existing bone remodeling algorithms adapt the elastic modulus of the bone by comparing the current stimulus level to the equilibrium value. This is a mechanically-driven model and only a few studies have included the influence of mechanosensing cells that result in bone growth [1]. Moreover, X-ray and histology results for massive segmental prostheses show that bone growth initiates from the bone interface but does not fully osseointegrate with the implant [2], even though the strains should induce bone formation from a mechanical point of view. Hence, while current models have successfully modelled bone adaption, they have failed to accurately predict the course of adventitious bone formation. We show here that the inclusion of biological processes of osteoconduction and osteoinduction are required to augment existing processes of bone adaptation. Strain energy density (SED) was used as the criteria for bone remodeling, where the rate of bone growth is controlled by the difference in the current SED against the reference value [3]. This was extended to include the influence of overload for bone resorption. Thereafter, the above-mentioned biological features were achieved by building an osteoconnectivity matrix starting from the bone interface to account for neighbouring elements (cells). The current level of remodeling and the matrix then controls the rate of bone formation of adjoining elements. Physiological loading was applied to finite element (FE) bone prosthesis to predict extra-cortical bone growth. The FE results show good correspondence to experimental and clinical results (Figure 1). This algorithm shows potential for further use in prosthesis design and where prediction of bone growth in addition to bone adaption is important.

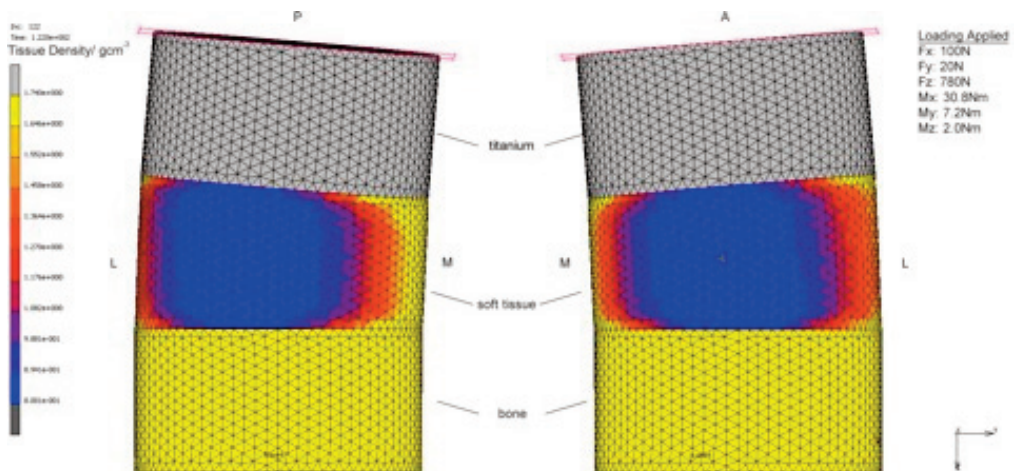


Figure 1: Physiological loading applied to a cylindrical model shows a differential in the extent of bone remodeling, in line with histological results that the medial-posterior aspect has higher level of bone adaptation. (Left): Posterior view. (Right): Anterior view.

## Acknowledgments:

This work is funded by a grant from the Orthopaedic Research UK

## References:

- [1] Kameo, Y., et. al. *Acta Mechanica*. 2014; 225(10), 2833-2840
- [2] Coathup, M, et. al. *Clin Orthop Relat Res*. 2015;473(4):1505-14
- [3] Huiskes, R., et. al. *J Biomech*. 1987;20(11-12):1135-50

# NEOTISSUE GROWTH IN A PERFUSION BIOREACTOR SYSTEM: A MULTISCALE MULTIPHYSICS MODEL

**Hans van Oosterwyck**<sup>1</sup>

<sup>1</sup> KU Leuven, Mechanical Engineering Dept. - Biomechanics Section, Leuven, Belgium

The creation of man-made living implants is the holy grail of tissue engineering (TE). As basic science advances, one of the major challenges in TE is the translation of the increasing biological knowledge on complex cell and tissue behavior into a predictive and robust engineering process. Mastering this complexity is an essential step towards clinical applications of TE. Computational modeling allows to study the biological complexity in a more integrative and quantitative way. In this talk I will show how multiscale multiphysics computational tools can help in quantifying and optimizing the TE product and process. For the culture of tissue engineering constructs composed of cells and carriers, bioreactors are used. We have developed a model capable of simulating neotissue (cells + extracellular matrix) growth in perfusion bioreactors [1], including the influence of scaffold geometry, fluid flow induced shear stress [2,3], oxygen and lactate on the speed of growth (figure 1). This model is capable of answering questions regarding the optimal placement of the scaffold inside the bioreactor, the optimal culture strategy (e.g. refreshment regime, fluid flow velocity) and the optimal scaffold geometry.

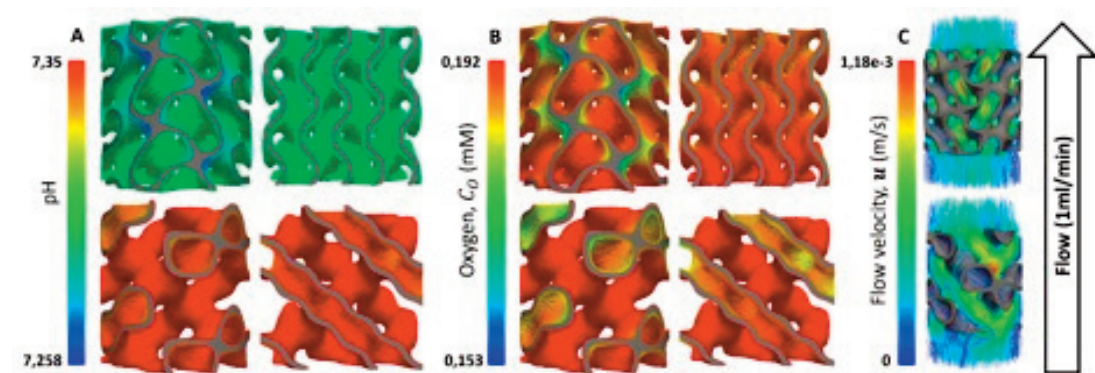


Figure Caption: Spatial distribution within neotissue of pH (A) and  $C_o$  (oxygen) (B) at 28 days of culture in a perfusion bioreactor for two different scaffold geometries (gyroid (top), Dcup (bottom)). For each geometry a side view (left) as well as a axial cross section (right) are shown. Perfusion flow streamlines are shown, colored by velocity (C).

## Acknowledgments:

Y.G. is funded by Belgian National Fund for Scientific Research (FNRS) grant FRFC 2.4564.12. I.P. is funded by the Research Foundation Flanders (FWO Vlaanderen). The research leading to these results has received funding from the European Research Council under the European Union's Seventh Framework Program (FP/2007-2013)/ERC Grant Agreement No. 279100. This work is part of Prometheus, the Leuven R&D division of Skeletal Tissue Engineering.

## References:

- [1] Guyot Y, Papantoniou I, Chai YC, Van Bael S, Schrooten J, Geris L. A computational model for cell/ECM growth on 3D surfaces using the level set method: a bone tissue engineering case study. *Biomech Model Mechanobiol.* 2014 Nov;13(6):1361-71.
- [2] Guyot Y, Luyten FP, Schrooten J, Papantoniou I, Geris L. A three-dimensional computational fluid dynamics model of shear stress distribution during neotissue growth in a perfusion bioreactor. *Biotechnol Bioeng.* 2015 Dec;112(12):2591-600.
- [3] Guyot Y, Papantoniou I, Luyten FP, Geris L. Coupling curvature-dependent and shear stress-stimulated neotissue growth in dynamic bioreactor cultures: a 3D computational model of a complete scaffold. *Biomech Model Mechanobiol.* 2016 Feb;15(1):169-80.

## COMBINING AN IN SILICO MODEL WITH IN VITRO EXPERIMENTS TO CREATE A FRAMEWORK FOR PROCESS OPTIMIZATION. CASE STUDY: OPTIMIZING THE PRODUCTION OF AGGREGATES IN A MICRO-WELL

**Maxim Cuvelier**<sup>1</sup>, **Bart Smeets**<sup>2</sup>, **Gabriella Nilsson Hall**<sup>3</sup>, **Ioannis Papantoniou**<sup>3</sup>, **Herman Ramon**<sup>2</sup>

1 Ku Leuven, Dept. of Mechatronics, Biostatistics and Sensors (Mebios), Ku Leuven, Prometheus, DIV. of Skeletal Tissue Engineering, Heverlee, Belgium, 2 Ku Leuven, Dept. of Mechatronics, Biostatistics and Sensors (Mebios), Heverlee, Belgium, 3 Ku Leuven, Prometheus, DIV. of Skeletal Tissue Engineering, Ku Leuven, Skeletal Biology and Engineering Research Center, Leuven, Belgium

Researchers have been investigating the use of 3D culturing techniques to enhance cell culture quality for regenerative medicine and drug delivery applications [1]. For example, microaggregates have been shown to affect cell fate due to increased auto- and paracrine signaling and a stimulating mechanical micro-environment. As 3D scaffold free cell culturing techniques are gaining in popularity, traditional in vitro trial-and-error optimizations are becoming time consuming and expensive. This is why we are developing a standardized framework, based on the combination of in silico modeling and in vitro experiments to optimize the production process leading to high quality products for therapeutic applications. As a case study for the framework, we investigated the optimization of high-throughput hPDC micro-aggregate production. Micro-well culturing systems were found to be suitable for the high-throughput generation of micro-aggregates which can be used to produce chondrogenic tissue for cell therapy applications [2].

A mechanistic model was developed to capture the dynamics of micro-aggregate formation in the micro-wells and used to perform an in silico parameter study. Cell aggregation was modelled using an adhesion model based on Maugis-Dugdale contact theory. By increasing the adhesion energy of connected cells over time, the formation of smooth aggregates is made possible in simulations. Cell migration was also modelled by introducing traction forces and polarized cells, as this has a profound influence on the process. With this polarization, different biological phenomena such as haptotaxis, persistent randomwalks etc. can be implemented.

From simulations, the dynamics, shape and mechanical environment of microaggregates were estimated as a function of the cells' mechanical properties and the initial cell seeding density – see Figure 1. By using an in silico model in parallel with in vitro experiments, the foundation was provided for a tool that can be used to optimize cell culture systems in more systematic manner.

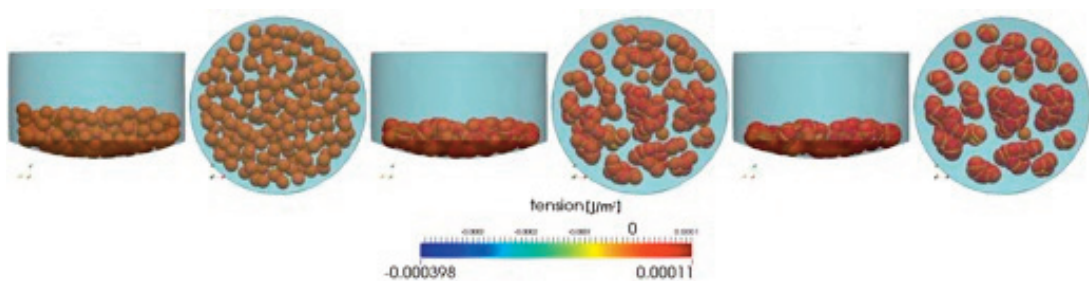


Figure Caption: Dynamic simulation of the aggregation process. From left to right: 0h, 3h and 6h after cell seeding. As time progresses, cells condensate into tight clusters. The balance of cell-cell adhesion and cell motility determines the final shape and amount of aggregates.

### References:

- [1] Rehfeldt, Florian, et al. "Cell responses to the mechanochemical microenvironment—implications for regenerative medicine and drug delivery." *Advanced drug delivery reviews* 59.13 (2007): 1329-1339.
- [2] Moreira Teixeira, L. S., et al. "High throughput generated micro-aggregates of chondrocytes stimulate cartilage formation in vitro and in vivo." *European cells & materials* 23 (2012): 387-399.

# COMPUTATIONAL ANALYSIS OF FLOW AND BIOMECHANICAL TRANSPORT IN A MULTICHAMBER BIOREACTOR

**Laura Iannetti<sup>1</sup>**

<sup>1</sup> Beta Cae Italy Srl, Torino, Italy

Next generations of bioreactors are being developed to generate multiple human cell-based tissue analogs within the same fluidic system to better recapitulate the complexity and interconnection of human physiology. The effective development of these devices requires a solid understanding of their interconnected fluidics, to predict the transport of nutrients and waste through the constructs and improve the design accordingly. In this work we focus on a specific model bioreactor aimed at generating osteochondral constructs, i.e., a biphasic constructs in which one side is cartilaginous in nature, while the other is osseous. Then, we have developed a general computational approach to model the microfluidics of a multi-chamber, interconnected system that could be applied to human-on-chip devices. This objective requires overcoming several challenges at the level of computational modeling. The main one consists in addressing the multi-physics nature of the problem that combines free flow in channels with hindered flow in porous media (scaffold). In particular we analyzed the fluid behavior within two different scaffold made of gelatin methacrylate (gelMA) and poly-L-lactate (PLLA) respectively.

Fluid dynamics is also coupled with advection-diffusion-reaction equations that model the transport of biomolecules throughout the system and their interaction with living tissue. In order to guarantee a healthy environment for cellular development we numerically determinate the distribution of nourishments' concentration within the bioreactor (figures 1, 2) and successfully compared these results with the experimental ones (figure 3). Ultimately, we aim at providing a predictive approach useful for the general organ-on-chip community. To this purpose, we have developed a lumped parameter approach that allows us to analyze the behavior of multi-unit bioreactor systems with a modest computational effort, provided that the behavior of a single unit can be fully characterized.



Figure 1: BSA advection, with gelMA scaffold, Q 1-2 [ml/day].

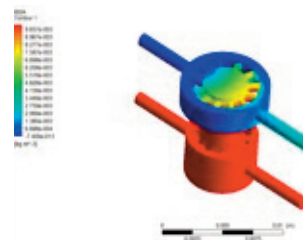


Figure 2: BSA advection, with PLLA scaffold, Q 1-2 [ml/day].

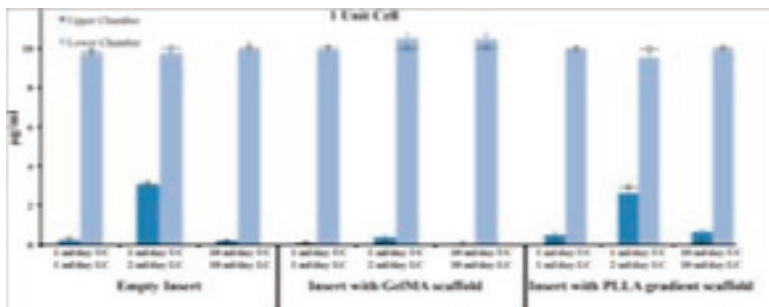


Figure 3: BSA concentration within bioreactor, numerical results (bar graph) vs experimental one (star).

## References:

- [1] L.Iannetti, G.D'Urso, "Computational model of flow and biochemical transport in a multichamber bioreactor", 2015. [2] T. P. Lozito, P. G. Alexander, H. Lin, R. Gottardi, A. W.-M. Cheng, and R. S. Tuan, "Three-dimensional osteochondral microtissue to model pathogenesis of osteoarthritis." *Stem Cell Res. Ther.*, vol. 4 Suppl 1, no. Suppl 1, p. S6, 2013.

# AN ISOGEOMETRIC FINITE ELEMENT MODEL FOR THE MECHANICS OF LIPID BILAYER MEMBRANES

**Roger Sauer**<sup>1</sup>

<sup>1</sup> RWTH Aachen University, Graduate School Aices, Aachen, Germany

This work presents a new computational finite element (FE) model for lipid bilayer membranes. The formulation is based on geometrically non-linear Kirchhoff-Love shell theory [1], and is thus able to describe general 3D surface deformations. The numerical discretization is based on isogeometric finite elements that provide a C1-continuous surface description, even during deformation [2]. Due to the in-plane fluidity of lipid bilayers, numerical stabilization is required for quasi-static computations. Three different classes of stabilization schemes [3], based on added stiffness, added viscosity or nodal projection, are adapted to the formulation. Due to the area-incompressibility, mixed FE formulations are considered as an alternative to pure displacement-based formulations. Several numerical examples are considered in order to illustrate the accuracy and the capabilities of the proposed formulation, and to compare the different stabilization schemes. The presented formulation is capable of simulating non-trivial surface shapes associated with tube formation and protein induced budding of lipid bilayers [4]. In the latter case, the presented formulation yields non-axisymmetric solutions, which have not been observed in previous simulations. It is shown that those non-axisymmetric shapes are preferred over axisymmetric ones.

## Acknowledgments:

The author is grateful to the German Research Foundation (DFG) for supporting this research under grants GSC 111 and SA1822/5-1.

## References:

- [1] Sauer, R. A. and Duong, T. X. (2015). On the theoretical foundations of thin solid and liquid shells. *Math. Mech. Solids*, published online, DOI: 10.1177/1081286515594656.
- [2] Duong, T. X., Roohbakhshan, F., and Sauer, R. A. (2016). A new rotation-free isogeometric thin shell formulation and a corresponding continuity constraint for patch boundaries. *submitted*
- [3] Sauer, R. A. (2014). Stabilized finite element formulations for liquid membranes and their application to droplet contact. *Int. J. Numer. Meth. Fluids*, 75(7):519(545).
- [4] Sauer, R.A., Duong, T.X., Mandadapu, K.K., Steigmann, D.J. (2016), A stabilized finite element formulation for liquid shells and its application to lipid bilayers. *submitted*

# MULTISCALE MOVING CONTACT LINE THEORY AND SIMULATION OF CELL MOTILITY

**Shaofan Li**<sup>1</sup>

<sup>1</sup> Institution Department of Civil and Environmental Engineering, University of California at Berkeley, Berkeley, United States

In this talk, we first present a novel Multiscale Moving Contact Line (MMCL) theory, which offers a powerful numerical tool for simulation of dynamic wetting, liquid droplet spreading on solid substrates, and various capillary actions. In the proposed multiscale moving contact line theory, we couple molecular scale adhesive interaction i.e. the van der Waals type force with the macroscale flow – that is: we combine a coarse-grained adhesive contact model with a modified Gurtin-Murdoch surface hydroelasto-dynamics theory to formulate a multiscale moving contact line hydrodynamics theory in order to simulate dynamic wetting, droplet spreading, and a broader class of colloidal phenomena and their chemomechanical mechanisms.

The advantage of adopting the coarse grain adhesive contact model in the moving contact line theory is that it can levitate and separate the liquid droplet with the solid substrate, so that the proposed multiscale moving contact line theory avoids imposing the non-slip condition, and then it removes the subsequent singularity problem, which allows the surface energy difference and surface stress propelling droplet spreading naturally.

Second, we shall introduce a soft matter computational formulation for modeling actin filament aggregates, which is essentially an active soft gel model that can capture the main thermodynamic characteristics of Actin filaments.

By employing the proposed methods, we have successfully simulated droplet spreading over various elastic substrates, and cell durotaxi over the substrates with non-uniform elastic stiffness. The obtained numerical simulation results compare well with the experimental and molecular dynamics results reported in the literature.

## References:

Fan, H. and S. Li [2015] ``Modeling universal dynamics of cell spreading on elastic substrates," *Biomechanics and Modeling in Mechanobiology (BMMB)*, 14, 1265-1280,

Li, S. and H. Fan [2015] ``On multiscale moving contact line theory," *Proceedings of Royal Society of London A*, 471, No. 20150224.

## SIMULATING CONTACT PHENOMENA IN DENTAL BIOMECHANICS

**Christoph Bourauel<sup>1</sup>, Ludger Keilig<sup>2</sup>, Istabrak Hasan<sup>2</sup>, Meike Eschbach<sup>3</sup>, Susanne Reimann<sup>4</sup>**

*1 Endowed Chair of Oral Technology, Dental School, Rheinische Friedrich-Wilhelms University Bonn, Bonn, Germany,*

*2 Endowed Chair of Oral Technology and Department of Prosthetic Dentistry, Preclinical Education and Materials Science, Dental School, Rheinische Friedrich-Wilhelms University Bonn, Bonn, Germany,*

*3 Endowed Chair of Oral Technology, Dental, University of Bonn, Bonn, Germany,*

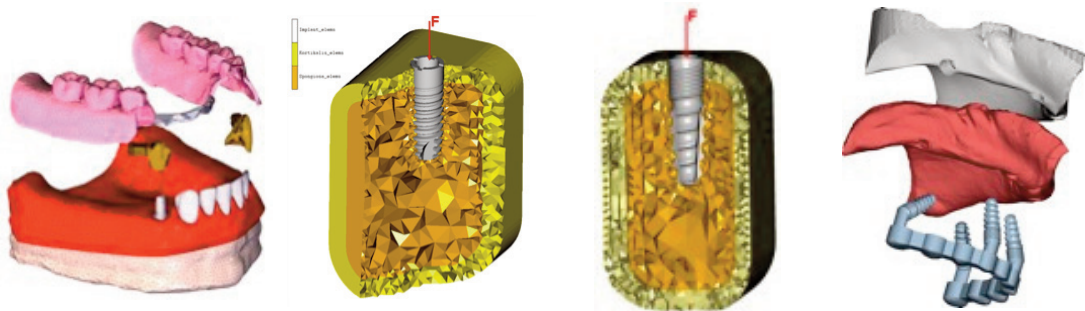
*4 Endowed Chair of Oral Technology, Department of Orthodontics, Bonn, Germany*

### Introduction:

Dental restorations and materials have to cover a wide range of biomechanical characteristics to comply with the intraoral loading situations. A variety of treatment concepts have been developed in the past, comprising metallic materials, ceramics and polymers for construction of prosthetic elements, implants and superstructures. Contact situations between the different dental structures and restorations have a significant influence on the load transfer of masticatory forces to teeth, periodontal ligament and the alveolar bone. This paper presents an overview of different contact phenomena in dental biomechanics.

### Methods:

The following finite element models were generated to simulate different intraoral situations (Figures below): (1) Idealised model of the lower dental arch with reduced dentition and partial denture, with different retentive elements at the anterior teeth. Different clasps with friction contact condition were investigated. (2) Idealised bone segment with Straumann® or tioLogic® implants with and without fine threading of the neck. Immediate loading and osseointegrated situations were simulated. (3) Patient individualised FE model of the maxilla. A fixed full bridge, supported by 4 implants ('All-on-Four' concept) was analysed in immediate loading and osseointegrated situation. Additionally, contact conditions between implants and suprastructure were investigated.



*Left: Idealised lower dental arch with prosthesis. Middle: Idealised bone segments with different dental implants. Right: Patient specific FE model of the maxilla with 4 implants and fixed bridge.*

### Results and Discussion:

(1) Denture movability was drastically influenced by the type of retentive element and ranged from 0.3 to 0.7 mm. This resulted in strains in the underlying mucosa of up to 70 %. (2) Depending on implant type and status of osseointegration, implant displacements as well as stresses and strains in the bone covered an enormous range from physiologic loading up to extreme overload. (3) In the immediate loading situation, the All-on-Four concept may result in extreme overloading of the spongy bone with strains up to 10,000  $\mu$ strain. Contact phenomena critically influence the biomechanical loading of the alveolar bone and should be considered in every simulation of intraoral situations.

## MANUFACTURABILITY OF CUSTOM ENDOSTEAL DENTAL IMPLANTS BY SELECTIVE LASER MELTING

Jérôme Lafrenière<sup>1</sup>, Vladimir Brailovski<sup>2</sup>, Anatolie Timercan<sup>2</sup>, Michel Poirier<sup>1</sup>, Eric Wagnac<sup>3</sup>

<sup>1</sup> V2r Biomedical, Montreal, Canada,

<sup>2</sup> Ecole de Technologie Supérieure, Montreal, Canada,

<sup>3</sup> Ecole de Technologie Supérieure, V2r Biomédical, Montreal, Canada

The intricate geometry of custom endosteal dental implants (CEIs) has exposed the limitations of CNC milling in their manufacturing process. The poor dimensional accuracy of the milled implants in critical regions requires design trade-offs and post-manufacturing reworks detrimental to the fit with prosthetic parts and at the bone-implant interface (Fig 1). This study aims to determine if selective laser melting (SLM) can be used to manufacture CEIs with increased dimensional accuracy in critical regions and to assess inherent limitations of the method related to design and finishing processes. Three-dimensional modeling of a CEI was performed according to realistic clinical requirements and from anatomical structures reconstructed from computed tomography data (Fig 2). SLM system (EOSINT M 280, EOS) and material (Ti-6Al-4V ELI) requirements included achievable mechanical properties, accuracy, surface roughness and biocompatibility. Given the parts' geometrical complexity and the support-adding building method, the effect of the model orientation relatively to the manufacturing platform had to be studied. As such, parts were analysed to find orientations minimizing support structures (quantity, position and volume) and exempting functional surfaces. Pilot parts were SLM-built in two orientations using Al-Si-10Mg, preferred to Ti-6Al-4V ELI for economical reasons and to enhance the authors' understanding of the effects of thermal and mechanical property variation. The parts were then heat treated to relieve internal stresses and separated from the support plate. Aligning the CEI posts longitudinal axis with the vertical axis of the buildplate, and placing the CEI downward resulted in optimal reproduction of the bone-implant interface, but also in unsatisfactory preservation of the CEI posts. While the addition of part-specific combinations of polar and azimuthal rotations has reduced this effect, design modifications are deemed necessary. The parallelism deviations observed between the posts ( $0.72^\circ \pm 0.30^\circ$ ) were commensurate to the values observed on CNC-milled implants. The dimension variations observed ( $110\mu\text{m} \pm 44\mu\text{m}$ ) were in line with the achievable accuracy ( $\pm 100\mu\text{m}$ ) and within the clinically-acceptable tolerance ( $\pm 200\mu\text{m}$ ). The results give confidence in the manufacturability of CEIs by SLM. The next steps, using the material intended for the application, will include design optimisation, surface roughness analysis and fatigue testing of finished parts.

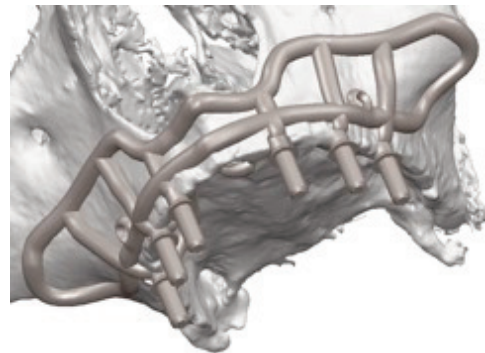
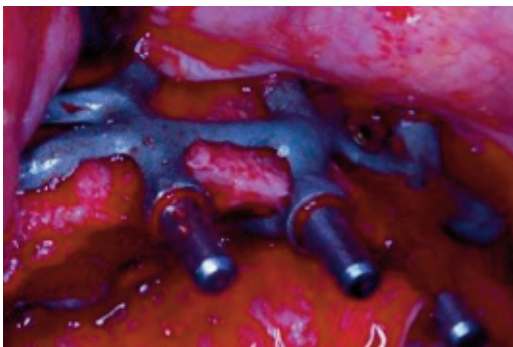


Figure 1 - Milled, surgically placed CEI, showing poorly reproduced post and screw fixation site features, adversely affecting fit and function

Figure 2 - CEI CAD model on CT-reconstructed atrophic maxilla, featuring anatomically contoured posts and countersunk screw fixation sites

# PRECLINICAL ANALYSIS TO ASSESS ASEPTIC LOOSENING OF ORTHOPAEDIC IMPLANTS

Heidi-Lynn Ploeg<sup>1</sup>

<sup>1</sup> University of Wisconsin-Madison, Madison, United States

As the rate of total joint arthroplasty (TJA) increases, aseptic loosening remains the primary reason for revision [1,2,3]. Although it is well-known that aseptic loosening is the main challenge in TJA survival rates, the approach to preclinical analysis to reduce revision rates due to aseptic loosening is not well understood. Reasons for aseptic loosening are multifactorial including the patient, surgical approach, biological reactions, micromotion at the implant-bone interface, load transfer from the joint to the host bone, and bone adaptation. The objective of this study was to highlight different pre-clinical methods to investigate orthopaedic implant fixation relative to the transfer of loads and displacements at the implant-bone interface, and bone adaptation.

The last generation of metal-on-metal hip prostheses used a high precision low clearance bearing to provide a low friction ball and socket joint. During implantation the acetabular component deforms due to the pressfit; however, excessive deformation of the acetabular component can lead to premature failure of the joint. It was therefore important to establish an accurate method of quantifying cup deformation and develop finite element (FE) models to study what factors affect the press-fit condition. Methods to measure press-fit deformation of monoblock acetabular cups for metal-on-metal total hip arthroplasty and resurfacing were investigated. The present study compared, cup deformation patterns from two experiments simulating press-fit of an acetabular cup into the pelvis: the pinch and press-fit tests.

Strain-displacement relationships were unique to the pinch and press-fit tests, even for the same acetabular cup, since the boundary conditions for each test were different. For the pinch test, strains shared a strong linear relationship with rim displacements and therefore could be used as a surrogate when it is inconvenient to use transducers. Cup deformation in the press-fit test was more complex mainly because of fixation from the equatorial fins. Before the fins engaged the bone surrogate, rim displacements could be predicted from cup strain but, after fin engagement, strain could not accurately predict rim displacement. Multiple approaches are necessary to assess cup deformation due to press-fitting.

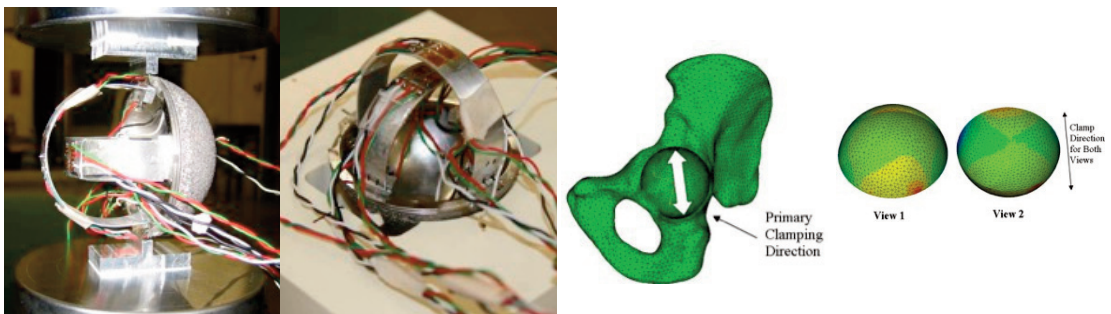


Figure Caption: Preclinical testing and finite element analysis to assess aseptic loosening in an acetabular component.

## Acknowledgments:

The author acknowledges contributions of collaborators and former UW Bone and Joint Biomechanics Laboratory members, including but limited to: Ameet Aiyangar, Kristopher Biegler, and Anthony Au.

## References:

1. Garellick G, Kärrholm J, Lindahl H, Malchau H, Rogmark C, Rolfson O, Swedish Hip Arthroplasty Register, Annual Report 2013, [http://www.shpr.se/Libraries/Documents/AnnualReport\\_2013-04-1\\_1.sflb.aspx](http://www.shpr.se/Libraries/Documents/AnnualReport_2013-04-1_1.sflb.aspx)
2. Hip and Knee Arthroplasty, Annual Report 2015, Australian Orthopaedic Association National Joint Replacement Registry, Adelaide:OAO, 2105, <https://aoanjrr.sahmri.com/documents/10180/217745/Hip%20and%20Knee%20Arthroplasty>
3. Sadoghi P, Liebensteiner M, Agreiter M, Leithner A, Böhrer N, Labek G, Revision surgery after total joint arthroplasty: a complication-based analysis using worldwide arthroplasty registers, *The Journal of Arthroplasty* 28:1329-1332, 2013.

# MEASURING THE BIOMECHANICAL PROPERTIES OF THE BONE-IMPLANT INTERFACE: A MULTIPHYSICAL APPROACH

Romain Vayron<sup>1</sup>, Romain Bosc<sup>2</sup>, Guillaume Haiat<sup>3</sup>

<sup>1</sup> Université Paris-Est - Cnrs, Laboratoire Modélisation et Simulation Multi Echelle, Créteil, France,

<sup>2</sup> Cnrs, Laboratoire Modélisation et Simulation Multiéchelle, Creteil, France,

<sup>3</sup> Cnrs, Laboratoire Modélisation et Simulation Multiéchelle, Fac des Sciences, Upec, Creteil, France

Endosseous cementless implants are widely used in orthopaedic, maxillofacial and oral surgery. However, failures are still observed and the assessment of the biomechanical strength of the bone-implant interface may improve the understanding of osseointegration phenomena.

A multiphysical approach was carried out using a dedicated animal model consisting in coin-shaped titanium implants implanted in vivo on the proximal part of the tibia of rabbits (see Fig. 1).

The first objective of this study was to investigate the evolution of elastic properties of newly formed bone tissue as a function of healing time. Nanoindentation and micro-Brillouin scattering techniques are coupled with histological analysis.

The second aim was to investigate the effect of bone healing on the ultrasonic response of coin-shaped titanium implants inserted in rabbit tibiae.

The third objective was to retrieve the different quantities related to the bone-implant interface such as the stress intensity factor. Mode III cleavage experiments were performed.

The bone mechanical properties were measured in mature and newly formed bone tissue. A significant effect of healing time was obtained on the indentation modulus and ultrasonic velocities of bone tissue. The significant decrease of the echo of the interface as a function of healing time (from  $r=0.53$  to  $r=0.49$ ) can be explained by the increase of the BIC. The approach allows to estimate mode III fracture energy (around  $77.5 \text{ N.m}^{-1}$ ) and stress intensity factor ( $0.27 \text{ MPa m}^{1/2}$ ).

Advanced modeling and simulation is needed to better understand the evolution of the biomechanical properties of the bone-implant interface, which will be the aim of the project BoneImplant funded by the European Research Council."

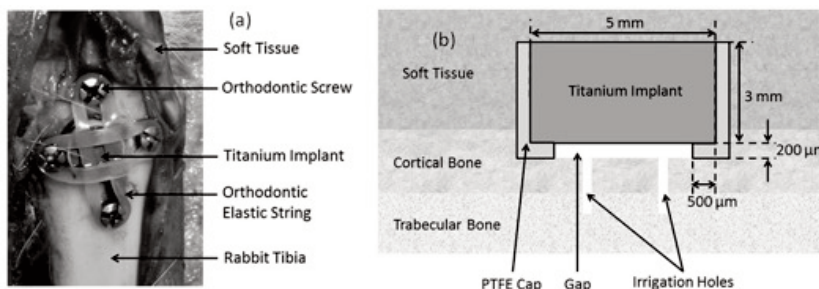


Figure Caption: "Fig 1: (a): Image of the coin-shaped implant model during a surgical intervention on a rabbit tibia. (b) Cross-sectional schematic representation of the coin-shaped implant model."

## Acknowledgments:

"This work has been supported by French National Research Agency (ANR) through the PRTS program (project OsseoWave n°ANR-13-PRTS-0015-02)."

# MECHANOBIOLOGY OF BONE-IMPLANT INTERFACE; A MIXED THEORETICAL AND EXPERIMENTAL APPROACH.

**Pascal Swider**<sup>1</sup>, **Kjeld Søballe**<sup>2</sup>, **Bechtold Joan Elisabeth**<sup>3</sup>

<sup>1</sup> Imfit Umr Cnrs 5502, University of Toulouse, Toulouse, France,

<sup>2</sup> Aarhus University Hospital, Department of Orthopaedic Surgery, Aarhus, Denmark,

<sup>3</sup> Departments of Orthopaedic Surgery, Mechanical and Biomedical Engineering, University of Minnesota, Minneapolis, United States

The long-term survival of arthroplasty is strongly related to the quality of the immediate post-operative healing of periprosthetic tissue. The central hypothesis was that modeling of mechanobiological interactions and neo-vascularization of periprosthetic zone might help to investigate the multifactorial events in tissue healing. The methodology of reactive transports in deformable porous media has been associated to computational cell biology (cellular migration and proliferation in presence of anabolic growth factors). The populations of osteoblasts and endothelial cells, the phases of bone growth factors, angiogenic factors and fibronectin have taken into account to propose a set of governing equations describing the process of intramembranous healing.

We investigated the influence of daily mechanical stimuli on the response of our canine experimental model. The model provided results in good agreement with in-vivo studies. The shear micro motion tended to decrease the bone formation at the implant surface. Radial micro motions due to ligaments and muscles modified the radial stimuli but showed a limited influence on the distribution pattern of mineralized tissue. Initial concentrations of endothelial cells in the host bone and transforming angiogenic factors at the implant surface had predominant and favorable effects on the final endothelial cells concentration at the implant surface and into the post-operative gap. Chemotaxis played a favorable role on the concentration of endothelial cells at the implant surface and the tissue neo-vascularization.

The theoretical models allowed modelling the mechanobiological response of periprosthetic tissue in space and time. In-silico models will be reliable enough to be used as predictive models for clinical cases, after implementation of targeted comparative studies involving more in-vivo data.

## Acknowledgments:

The French Minister of Education and Research is acknowledged for its assistance. Related experimental studies were conducted with the support of NIH AR4205 USA (PI. J.E. Bechtold).

## References:

*Soballe et al. 1992. Orthop. 10, 2: 285-299.*

*Bechtold et al. 2001. Acta Orthop Scand 72, 6: 650-656.*

*Ambard D, Swider P. 2006. European Journal of Mechanics, 25, 6: : 927-937.*

*Khalil G et al. 2011. J Biomech. 44(10):1980-6. 2011.*

# WAVE PROPAGATION IN GENERALIZED CONTINUA IN PRESENCE OF INTERFACES

**Giuseppe Rosi<sup>1</sup>, Luca Placidi<sup>2</sup>, Vu Hieu Nguyen<sup>3</sup>, Salah Naili<sup>3</sup>**

*1 Université Paris-Est - Cnrs, Laboratoire Modélisation et Simulation Multi Echelle, Laboratoire Msme, Fac des Sciences, Upec, Créteil, France,*

*2 International Telematic University Uninettuno, Rome, Italy,*

*3 Université Paris-Est - Cnrs, Laboratoire Modélisation et Simulation Multi Echelle, Créteil, France*

Studying wave propagation in presence of complex interfaces, or more properly interphases, between biological tissues or artificial materials (e.g. those at the interface between bone and implant) is a challenging task. In the frequency regime of ultrasound (of the order of MHz), the wavelength becomes comparable to the characteristic size of tissue microstructure, so that a classic continuum description (Cauchy model in which the well known Cauchy tetrahedron argument is used) is no longer reliable. Moreover, complexity of microstructure geometry at small scales and high contrast between material properties of constituents (e.g. bone, water, marrow, titanium) make the full microstructure numerical simulations (based on Finite Element Method or Finite Difference Time Domain) very challenging.

In a first approach, one can choose to represent the behavior of this system in an average sense. This can be done by enriching the classical continuum description by Cauchy with some additional fields, i.e. by using a generalized continuum model. In this sense two main modelling choices are possible: adding higher order derivatives of the strain or adding additional degrees of freedom. Each of these choices has its advantages and drawbacks, depending on the desired features.

The thick interface itself can be modeled as a surface with concentrated material properties (mass, inertia, stiffness). The interaction of generalized continua and interfaces with material properties allow to impose richer boundary conditions, useful for describing, with a simplified model, complex interface/interphase conditions, as those for instance occurring at the interphase separating implant from bone.

In elementary configurations, the solution of this continuum model can be calculated in the frequency domain for computing reflection and transmission coefficients, or by using a numerical Laplace transform for the time domain.

In this presentation, we show some numerical results (in frequency or time domain) concerning wave propagation in generalized continua in presence of interfaces.

## Acknowledgments:

The authors wish to thank the Laboratoire International Associé Coss&Vita (CNRS) for the financial support and the Université Paris-Est through the PEPS program (15R03051A- METCARMAT).

# TUNABLE POROUS BIOMATERIAL TO REDUCE STRESS-SHIELDING IN TOTAL HIP ARTHROPLASTY

**Damiano Pasini**<sup>1</sup>

*<sup>1</sup> McGill University, Mechanical Engineering, Montreal, Canada*

"316L stainless steel, cobalt chromium alloys, and titanium-based alloys are commonly used for hip replacement implants. Although successful with respect to implant fixation, their use in hip replacement results in implants much stiffer than the surrounding bone tissue. The stiffness mismatch causes stress shielding, with consequent reduction of femoral bone stock, a serious problem leading to clinical complications and increased risk of revision surgery.

We present a hip implant made of a microarchitected porous biomaterial with mechanical properties locally tuned to those of the host bone. Ti-6Al-4V graded microlattice prototypes with minimally invasive geometry are built via Selective Laser Melting and in-vitro experiments are conducted on six composite femurs implanted with either an optimal porous implants or a fully solid control stem. The surface strain on the medial calcar is recorded via Digital Image Correlation. The change of strain between intact and implanted femur is used as a proxy for stress shielding. The femurs with fully solid implant showed a larger region of reduced strain post implantation as compared to the porous implant. The latter shows 27% decrease of surface strain change which serves as an indication of stress shielding reduction. On the other hand, the computational work on a fully physiological implanted femur accounts for bone remodeling and compares a five year stress shielding projection for both the optimized porous implant and the fully solid control. The computational results show a 6% bone loss in the optimum implant down from 29% of a fully solid implant after five years. The reduction of surface strain experimentally measured, and the reduction in projected stress shielding via physiological simulations, seemingly indicate that the tuned fully porous implant can significantly reduce stress shielding in Total Hip Arthroplasty."

# IMPROVING ACETABULAR REAMING QUALITY FOR TOTAL HIP ARTHROPLASTY USING A SERRATED BLADE REAMER

**Yvan Petit**<sup>1</sup>, **Ménard Jérémie**<sup>2</sup>, **Levasseur Annie**<sup>1</sup>, **Fernandes Julio**<sup>3</sup>

1 Ecole de Technologie Supérieure, Montreal, Canada, 2 Hôpital du Sacre-Coeur, Montreal, Canada, 3 Hôpital du Sacré-Coeur, Montreal, Canada

## Introduction:

Hip arthroplasty is a common surgery for the treatment of osteoarthritis, improving the function and quality of life of patients [1-3]. It requires careful preparation of the acetabular cavity, which consists in extracting a sufficient quantity of bone to prepare the acetabular cavity for receiving the implant. Generally, the implant must be press-fitted [4, 5] with proper contact between the bone and the implant to allow osseointegration and long-term stability [4-7]. The goal of this work was to reduce surface irregularities and deviations from the required cavity with a new cutting edge design.

## Methods:

A reamer prototype composed of four serrated blades (SB) was designed and manufactured to produce a uniform hemispherical cavity. Forty-two testing samples made of polyurethane foam were used to simulate the cortical bone. A conventional reamer (CR) and the SB were tested 7 times at penetration speeds of 0.20 mm/s, 0.55 mm/s and 0.90 mm/s. The reamed surfaces were digitized with high-resolution laser scanner to calculate surface irregularities and the diameter of the cavity.

## Results:

The type of cutting edge (CR versus SB) influenced the quality of the reamed surface ( $p < 0.01$ ), ranging between 0.19 mm to 0.21 mm for the CR and between 0.07 mm and 0.12 mm for the SB. The CR leaves more surface irregularities at 0.55 mm/s than at 0.20 mm/s ( $p = 0.001$ ). Similarly, surface irregularities increased from low speed to 0.55 mm/s ( $p = 0.007$ ) and 0.9 mm/s ( $p = 0.005$ ) with the SB. The difference between the cavity and the nominal diameter was 0.13 mm ( $\pm 0.05$ mm) larger for the CR and 0.06 mm ( $\pm 0.03$ mm) smaller for the SB ( $p < 0.01$ ).

## Conclusion:

The serrated blade reamer improves the quality of the surface and produces a more accurate hemispheric cavity. Such tool may influence the stability of the acetabular implant and reduce the risks of revision surgery.

## Acknowledgments:

This research was funded by NSERC and FCI.

## References:

- [1] Bourne RB et al., 2010, *Clin Orthop Relat Res*, 468(2), 542-6.
- [2] Daras M et al., 2009, *Am J*, 38(3), 125-9.
- [3] *Canadian Joint Replacement Registry 2008-2009 Annual Report*, pp. 88.
- [4] Kim YS et al., 1995, *J Arthroplasty*, S14-21.
- [5] Mackenzie JR, et al., 1994, *Clin Orthop Relat Res*, 298, 127-36.
- [6] Baad-Hansen T et al., 2006, *Clin Orthop Relat Res*, 448, 173-9.
- [7] Macdonald W et al., 1999, *J Arthroplasty*, 14(6), pp. 730-7.

## COMPUTER MODELLING OF THE SPINE TO SUPPORT NEXT GENERATION OF PREVENTION AND INTERVENTION INJURIES AND PATHOLOGIES

**Pierre-Jean Arnoux**<sup>1</sup>, **Yvan Petit**<sup>2</sup>, **Virginie Gallot**<sup>3</sup>, **Carl-Eric Aubin**<sup>4</sup>

<sup>1</sup> Ifsttar, Marseille, France,

<sup>2</sup> Ecole de Technologie Supérieure, Montreal, Canada,

<sup>3</sup> Cnrs, Marseille, France, <sup>4</sup> Ecole Polytechnique, Montreal, Canada

"The spine is a complex and central component of the body, involved in posture equilibrium, movements, and protection of the spinal cord. Spine and spinal cord pathologies, trauma, and degenerative conditions affect a significant portion of the population, which require costly treatments and have a significant impact on the quality of life. Understanding the spine biomechanics is a very important research field to better prevent injuries or pathologies, and planning medical or surgical interventions. New generation of "Virtual humans" through computer models supported by recent advances in medical imaging have opened important perspectives, enabling to support injury prevention, the design of enhanced medical devices, and surgical intervention planning.

The iLab-Spine (International Laboratory on Spine Imaging and Biomechanics) is an international group of researchers from Marseille-France (IFSTTAR / Aix-Marseille University / CNRS / AP-HM), and Montréal-Canada (Polytechnique Montréal, Ecole de Technologie Supérieure, Sainte-Justine University Hospital Center and Sacré-Coeur Hospital). It was established in 2015 after a decade of intense collaboration and student exchange between the involved centres. The overall goal is to develop state-of-the-art tools and computer models aiming at improving the understanding of spine and spinal cord injury and pathologies, biomechanically analysing protective and surgical devices, and designing and validating improved injury prevention and surgical technologies.

The challenges are to develop relevant tools to address current and future needs of the medical technology, transport safety and personal equipment industries. For instance, the level of modelling sophistication, especially tissues interactions, mechanical behaviour, ..., has to be adapted to tackle a variety of research questions at the micro- and macro-levels, types of disorders, as well as physiological, multi-physic and loading conditions.

# DESIGN AND FABRICATION OF A SITE SPECIFIC BIORESORBABLE CAGE FOR TIBIAL TUBEROSITY ADVANCEMENT IN DOGS

Miguel Castilho<sup>1</sup>, João Folgado<sup>2</sup>, Jorge Rodrigues<sup>3</sup>, Paulo Fernandes<sup>2</sup>

<sup>1</sup> Department of Orthopedics, University Medical Center Utrecht, Utrecht, Netherlands,

<sup>2</sup> Idmec, Instituto Superior Técnico, Universidade de Lisboa, Lisbon, Portugal,

<sup>3</sup> Idmec, Instituto Superior Técnico, Universidade de Lisboa, Lisboa, Portugal

Tibial tuberosity advancement (TTA) in dogs implies the implantation of a cage to space the two bone pieces and promote the bone fusion after surgery. This cage is usually made of titanium, thus non-biodegradable and it does not provide an adequate implant-bone tissue integration. The objective of this work is to design and fabricate an alternative cage that fulfill the requirement of biodegradability and promote bone ingrowth, taking in account the site specific characteristics both geometry and mechanical properties.

To achieve this goal the cage is design using a suitable topology optimization method (Dias et al. 2014) in order to optimize the microstructure for the mechanical environment of the implant site. Thus, a three-dimensional finite element model (3D FEM) of the TTA system was first created to evaluate the mechanical stresses and strains at cage domain during different stages of the dog walk. Since the cage is assumed periodic, obtained by the repetition in space of a representative volume element (RVE), the microstructure was computed by the optimization of a RVE addressing the accessed local mechanical requirements, and at same time ensuring the maximum permeability essential for the bone ingrowth inside the implant. The designed cage was fabricated by 3D powder printing of a tricalcium phosphate cement (Castilho et al 2014). The figure shows the computational model, the optimized RVE and the printed cage. This work demonstrates that this integrated CAD/Optimization approach enabled the design and fabrication of a cage with tailored permeability and mechanical properties for TTA application. These results support the potential of the design optimization strategy used to the development of customized implants for different clinical scenarios.

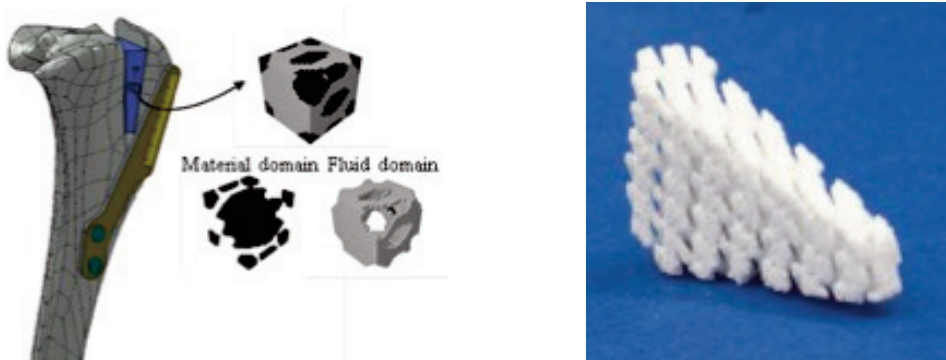


Figure Caption: Computational model of the dog knee, and designed RVE (left). Printed cage (right)

## Acknowledgments:

This work was supported by FCT through IDMEC, under LAETA, project UID/EMS/50022/2013 and project PTDC /BBB-BMC/5655/2014. We are very thankful to Prof. Elke Vorndran and Prof. Uwe Gbureck from University of Wurzburg for the fabrication facilities and discussions on this matter.

## References:

Dias, M., Guedes, J., Flanagan, C., Hollister, J., Fernandes, P., 2014. Optimization of scaffold design for bone tissue engineering: A computational and experimental study. *Medical Engineering & Physics* 36, 448–457.

Castilho, M., Dias, M., Vorndran, E., Gbureck, U., Fernandes, P., Pires, I., Gouveia, B., Armés, H., Pires, E., Rodrigues, J., 2014. Application of a 3D printed customized implant for canine cruciate ligament treatment by tibial tuberosity advancement. *Biofabrication* 6, 025005.

# BIOMANUFACTURING AS AN EFFECTIVE ROUTE FOR SKELETAL TISSUE REGENERATION

**Marco Domingos<sup>1</sup>, Bruna Frydman<sup>2</sup>**

*1 School of Mechanical, Aerospace and Civil Engineering, University of Manchester, Manchester, United Kingdom,*

*2 School of Mechanical, Aerospace and Civil Engineering, University of Manchester, Manchester, United Kingdom*

The most common strategy in bone Tissue Engineering (TE) comprises the use of 3D scaffolds in combination with human cells and biological molecules to promote guided bone regeneration. The success of this strategy is strongly dependent on the ability of the 3D engineered scaffolds to mimic the native biomechanical environment enabling cells to adhere, proliferate and differentiate. The essential requirements for these 3D structures have evolved during the years, and nowadays they are no longer expected to act only as passive structural matrices capable of supporting cell adhesion/proliferation but also to act as 3D carriers for the delivery of bioactive molecules to enhance tissue regeneration. In this context, the introduction of Biomanufacturing techniques have allowed for the automated production of highly reproducible 3D matrices with well designed internal/external geometries and spatial definition of functional gradients. Despite the great success and increasing importance of these techniques in the field of TE, there are still some issues that need to be properly addressed. This work aims to provide a clear overview of the manufacturing techniques, strategies and biomaterials currently used in bone tissue engineering as well as to discuss innovative routes for the design of bioactive scaffolds capable of augmenting cell-matrix interactions and ultimately lead to neo tissue formation.

# A NEW MULTISCALE MICROMECHANICAL MODEL OF VERTEBRAL TRABECULAR BONES

**Eyass Massarwa**<sup>1</sup>, **Rami Haj-Ali**<sup>2</sup>, **Jacob Aboudi**<sup>1</sup>, **Hans-Joachim Wilke**<sup>3</sup>, **Fabio Galbusera**<sup>4</sup>

<sup>1</sup> The Fleischman Faculty of Engineering, Tel Aviv University, Tel-Aviv, Israel,

<sup>2</sup> The Fleischman Faculty of Engineering, Tel Aviv University, Tel Aviv, Israel,

<sup>3</sup> Institute of Orthopaedic Research and Biomechanics, Ulm University, Ulm, Germany,

<sup>4</sup> Ircs Istituto Ortopedico Galeazzi, Milan, Italy

Please use any of the following sections that are relevant for your abstract structure.

A new three-dimensional (3D) multiscale micromechanical framework is proposed to predict the effective mechanical properties of a vertebral trabecular bone (VTB) porous material. A nested 3D modeling analysis framework spanning the multiscale levels of the VTB is introduced. This hierarchical framework employs the 3D parametric high fidelity generalized method of cells (HFGMC) micromechanical method as well as a sublaminate-model for the repeating multi-layered medium using 3D lamination theory. At the lower nano-scale, the 3D HFGMC method is applied to generate the effective elastic properties of a repeating unit cell (RUC) representing the mineralized collagen fibrils (MCFs) assembly. Next at the sub-micron-scale, the 3D sublaminate model is applied to compute the effective continuum elastic properties of a repeated stack of multilayered lamellae demonstrating the nature of a single trabeculae. The third micron-scale level employs, again, the 3D HFGMC method using a RUCs representing the VTB porous microstructure. The latter RUC geometry is taken from  $\mu$ CT scans of VTB samples harvested from different vertebrae of human cadavers ( $n=10$ ). The predicted anisotropic effective elastic properties for native VTBs are investigated for the scanned samples as a function of age and sex. Predicted VTB properties are compared to reported values found in the literature showing a very good agreement.

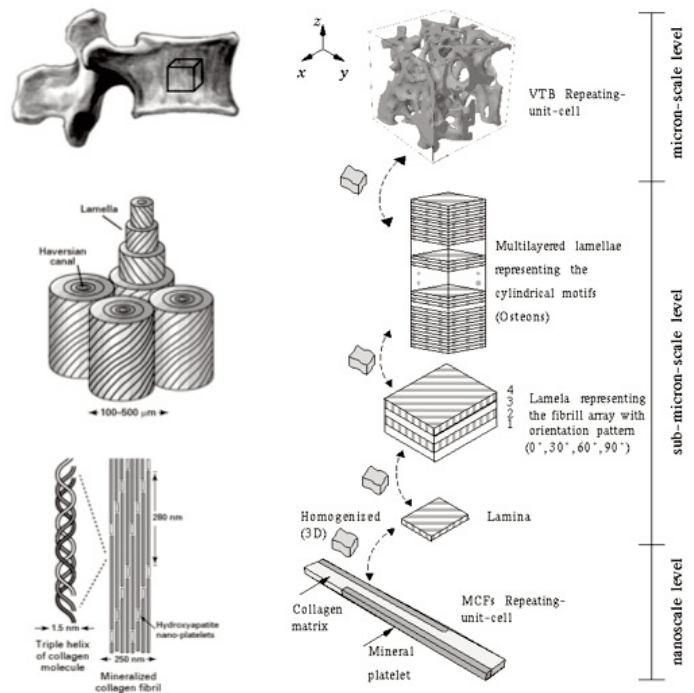


Fig.1 (a) The hierarchical structure of lumbar vertebral bone (Lorna J. Gibson et al., 2010) .

(b) A schematic representation of the proposed nano-to-micron multi-scale modeling of vertebral trabecular bone (VTB) using the HFGMC approach.

## References:

[1] Haj-Ali, R. and J. Aboudi (2013). "A new and general formulation of the parametric HFGMC micromechanical method for two and three-dimensional multi-phase composites." *International Journal of Solids and Structures* 50(6): 907-919.

[2] Kopperdahl, D.L., Keaveny, T.M., 1998. Yield strain behavior of trabecular bone. *Journal of Biomechanics* 31, 601-608.

# GRAPH BASED OVER-SEGMENTATION OF BONE POROUS MICRO-STRUCTURE

**Yizhak Ben-Shabat<sup>1</sup>, Gil Elbaz<sup>1</sup>, Anath Fischer<sup>1</sup>**

*<sup>1</sup> Technion - Israel Institute of Technology, Haifa, Israel*

3D reconstruction of bone micro-structures from scanned data has been recently investigated in bio-engineering. One of the main challenges when handling micro-structure models is the large amount of data with high levels of detail that requires long processing time and massive computer resources. Functional region segmentation which include irregularities is considered a difficult problem.

An extended approach is to perform over-segmentation, where the number of segments can be greater than the number of functional regions, yet significantly smaller than the number of points. This 3D approach was inspired by the extensive research of 2D over-segmentation. Creating super-pixels (2D sub-segments) is a common pre-processing stage for many computer vision tasks. However, super-points over-segmentation, for reconstructed 3D data from micro-CT is not yet available.

In previous work curvature analysis was applied on an adaptive volumetric representation of bone micro structure [1]. Furthermore, geometric analysis of pores was applied by using computer vision algorithms [2] for computing a parametric representation. In this work we propose a new generic approach for over-segmentation of 3D point cloud data and specifically adjust it for bone porous micro-structures. The proposed approach is based on computing a connectivity graph between neighboring points by applying K nearest neighbors, neighbors within a set radius R or Delaunay triangulation neighbors. Next, a similarity metric is assigned to the graph edges. This weight is computed using a local descriptor of the point. The basic descriptors include Euclidian distance and angles between estimated normal vectors. Based on this similarity quantity, the points are unified to form point clusters termed "super-points". The approach is based on the Local Variation [3] and probabilistic Local Variation [4] merge criteria. These super-points may be used for applications such as local surface approximation, registration and shape matching. The main contribution of this research is a novel over-segmentation method for bone porous micro-structures which are represented by 3D point clouds. The feasibility of the method is demonstrated on bone micro-structures.

## References:

- [1] Ben-Shabat, Y., and Fischer, A., 2014, "Design of Adaptive Porous Micro-structures for Additive Manufacturing," *24th CIRP Des. Conf.*, 21(0), pp. 133-137.
- [2] Elbaz, G., Ben-Shabat, Y., and Fischer, A., 2016, "Geometric Analysis of Porous Structures based on Hough Transform and Genetic Algorithms for Additive Manufacturing," *Virtual Phys. Prototyp.*
- [3] Felzenszwalb, P. F., and Huttenlocher, D. P., 2004, "Efficient Graph-Based Image Segmentation," *Int. J. Comput. Vis.*, 59(2), pp. 167-181.
- [4] Baltaxe, M., Meer, P., and Lindenbaum, M., 2015, "Local Variation as a Statistical Hypothesis Test," *Int. J. Comput. Vis.*, 117(2), pp. 131-141.

# COMPUTER-AIDED TISSUE ENGINEERING OF A NOVEL BONE-LIGAMENT-BONE MULTISTRUCTURED CONSTRUCT

**Cedric Laurent<sup>1</sup>, Damien Durville<sup>2</sup>, Xiong Wang<sup>3</sup>, Rachid Rahouadj<sup>1</sup>**

<sup>1</sup> Cnrs, Lemta, Umr 7563, Université de Lorraine, Vandoeuvre-Lès-Nancy, France,

<sup>2</sup> Cnrs, Mssmat, Umr 8579, Ecole Centrale Paris, Chatenay-Malabry, France,

<sup>3</sup> Cnrs, Imopa, Umr 7365, Biopôle, Université de Lorraine, Vandoeuvre-Lès-Nancy, France

The question of anchoring tissue-engineered ligament within the joint is still unresolved and constitutes a real clinical challenge. Recent studies proposed anchorage strategies together with a tissue-engineered ligament<sup>4</sup>: however, they are based on a trial-and-error approach, and may not result in a Bone-Ligament-Bone (BLB) construct with required properties compared to rationally-designed scaffolds. Recently, we have proposed and validated a computational approach to design a braided ligament scaffold with suited properties<sup>1,3</sup>. In the present work, this approach is extended to the case of a BLB scaffold, using the versatility of 3D printing to design both the microstructure of the bone scaffold (based on recent published geometries<sup>5</sup>) and its external shape enabling anchorage within bony tunnels. A new BLB construct with suited properties for both ligament and bone parts is thus proposed, as well as a solution for scaffold anchorage based on the deformation of an intermediate part (Fig.1). This anchorage is then characterized both numerically and experimentally, starting from homogenized properties for both ligament and bone parts, and the local cellular microenvironment due to physiological loading is predicted within the whole BLB scaffold. Such a computer-based approach also enables to characterize local cellular micro-environment, and therefore to understand the biological process leading to a progressive bone-ligament transition. Based on the computed mechanical stimuli at the surface of the multi-structured scaffold, mechanoregulation models are used in order to predict and optimize the regeneration of bone-ligament transition. These models will be confronted in the future to biological observations, obtained from dynamic culture in our dedicated bioreactor<sup>2</sup>

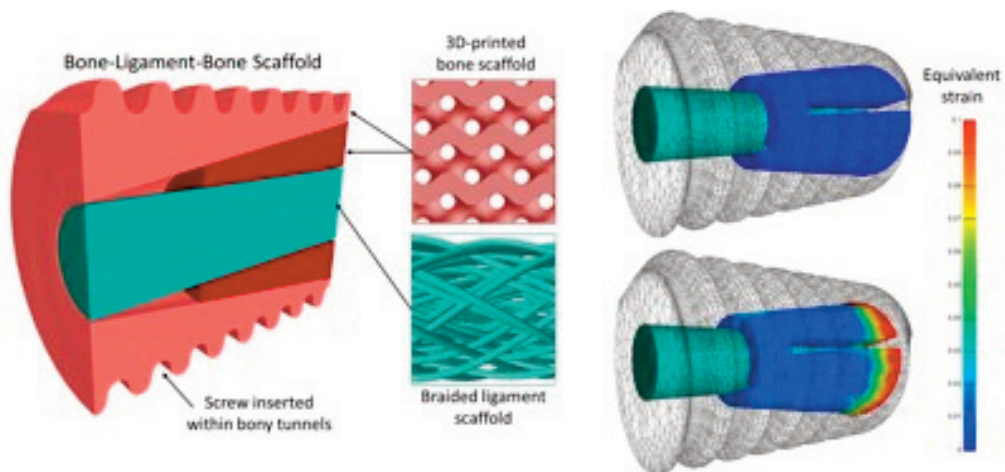


Figure Caption: Bone-Ligament-Bone multi-structured scaffold including anchorage within bony tunnels.

## References:

1. Laurent, C.P. et al. *J. Mech. Behav. Biomed. Mater.* 40:222–233, 2014.
2. Laurent, C.P. et al. *Processes* 2:167–179, 2014.
3. Laurent, C.P. et al. *J. Mech. Behav. Biomed. Mater.* 12:184–196, 2012.
4. Ma, J. et al. *Tissue Eng. Part A* 18:103–116, 2012.
5. Yoo, D. *Med. Eng. Phys.* 34:625–639, 2012.

# ADHESIVE, CONTRACTILE, AND RESISTIVE FORCES DURING CANCER CELL INVASION IN CONNECTIVE TISSUE

*Lena Lautscham*<sup>1</sup>, *Nadine Lang*<sup>1</sup>, ***Ben Fabry***<sup>1</sup>

*<sup>1</sup> Department of Physics, University of Erlangen-Nuremberg, Erlangen, Germany*

In cancer metastasis and other physiological processes, cells that migrate through the 3-dimensional (3D) extracellular matrix of the connective tissue must overcome the steric hindrance posed by small pores. It is currently assumed that low cell stiffness promotes cell migration through confined spaces, but other factors such as adhesion and traction forces may be equally important.

To study 3D migration under confinement in a stiff (1.77 MPa) environment, we use soft lithography to fabricate polydimethylsiloxane (PDMS) devices consisting of linear channel segments with 20  $\mu\text{m}$  length, 3.7  $\mu\text{m}$  height, and a decreasing width from 11.2 to 1.7  $\mu\text{m}$ . To study 3D migration in a soft (550 Pa) environment, we use self-assembled collagen networks with an average pore size of 3  $\mu\text{m}$ . We then measure the ability of four different cancer cell lines to migrate through these 3D matrices, and correlate the results with cell physical properties including contractility, adhesiveness, cell stiffness, and nuclear volume. Furthermore, we alter cell adhesion by coating the channel walls with different amounts of adhesion proteins, and we increase cell stiffness by overexpression of the nuclear envelope protein laminA.

Although all cell lines are able to migrate through the smallest 1.7  $\mu\text{m}$  channels, we find significant differences in the migration velocity. Cell migration is impeded in cell lines with larger nuclei, lower adhesiveness, and to a lesser degree also in cells with lower contractility and higher stiffness. Our data show that the ability to overcome the steric hindrance of the matrix cannot be attributed to a single cell property but instead arises from a combination of adhesiveness, nuclear volume, contractility, and cell stiffness. Furthermore, 3-D cell migration is enhanced by a higher network stiffness, opposite to cell behavior in 2-D, as long as the pore size does not fall below a critical value where it causes excessive steric hindrance. These findings reveal fundamental differences in the migration behavior of cells in a 2-D versus a 3-D environment, as well as large differences in the migration strategies between common tumor cell types.

# ARTIFICIAL HYDROGELS TO STUDY CELL-MATRIX-MECHANICS

**Florian Rehfeldt<sup>1</sup>**

<sup>1</sup> Georg-August-University, 3rd Institute of Physics - Biophysics, Göttingen, Germany

The mechanical properties of microenvironments in our body vary over a broad range and are as important to cells as traditional biochemical cues [1]. An especially striking experiment of this mechano-sensitivity demonstrated that systematic variation of the Young's elastic modulus  $E$  of the substrate can direct the lineage differentiation of human mesenchymal stem cells (hMSCs)[2].

To elucidate the complex interplay of physical and biochemical mechanisms of cellular mechano-sensing, well-defined extracellular matrix (ECM) models are essential. While elastic substrates made of poly-acrylamide (PA) are widely in use, they have the potential drawback that the precursors are cytotoxic and therefore do not allow for 3D culture systems. Here, a novel biomimetic ECM model based on hyaluronic acid (HA) was successfully established that exhibits a widely tuneable and well-defined elasticity  $E$ , enables 2D and 3D cell culture and enables us to mimic a variety of distinct in vivo microenvironments [3]. Quantitative analysis of the structure of acto-myosin fibers of hMSCs on elastic substrates with an order parameter  $S$ , reveals that the stress fiber morphology is an early morphological marker of mechano-guided differentiation and can be understood using a classical mechanics model [4,5,6]. Furthermore, the cytoskeleton also dictates the shape of the nucleus and lends support to a direct mechanical matrix-myosin-nucleus pathway [5].

## Acknowledgments:

This work was funded in part by Deutsche Forschungsgemeinschaft (DFG) within the collaborative research center SFB 755, project B8 and the Volkswagen Stiftung for funding within the Niedersachsen Israel framework (MWK-VWZN2722)

## References:

1. Rehfeldt, F., A. J. Engler, A. Eckhardt, F. Ahmed, and D. E. Discher. 2007. Cell responses to the mechanochemical microenvironment - Implications for regenerative medicine and drug delivery. *Adv Drug Deliver Rev* 59.
2. Engler, A. J., S. Sen, H. L. Sweeney, and D. E. Discher. 2006. Matrix Elasticity Directs Stem Cell Lineage Specification. *Cell* 126.
3. Rehfeldt, F., A. E. X. Brown, M. Raab, S. Cai, A. L. Zajac, A. Zemel, and D. E. Discher. 2012. Hyaluronic acid matrices show matrix stiffness in 2D and 3D dictates cytoskeletal order and myosin-II phosphorylation within stem cells. *Integrative Biology* 4:422-430.
4. Eltzner, B., C. Wollnik, C. Gottschlich, S. Huckemann, and F. Rehfeldt. 2015. The Filament Sensor for Near Real-Time Detection of Cytoskeletal Fiber Structures. *PLoS one* 10:e0126346.
5. Zemel, A., F. Rehfeldt, A. E. X. Brown, D. E. Discher, and S. A. Safran. 2010. Optimal matrix rigidity for stress-fibre polarization in stem cells. *Nature Physics* 6:468-473.
6. Zemel, A., F. Rehfeldt, A. E. X. Brown, D. E. Discher, and S. A. Safran. 2010. Cell shape, spreading symmetry, and the polarization of stress-fibers in cells. *Journal of Physics-Condensed Matter* 22.
7. Swift, J., I. L. Ivanovska, A. Buxboim, T. Harada, P. C. D. P. Dingal, J. Pinter, J. D. Pajeroski, K. R. Spinler, J.-W. Shin, M. Tewari, F. Rehfeldt, D. W. Speicher, and D. E. Discher. 2013. Nuclear Lamin-A Scales with Tissue Stiffness and Enhances Matrix-Directed Differentiation. *Science* 341.

# MECHANICAL AND MOLECULAR MECHANISMS DRIVING INTERCELLULAR COMMUNICATION DURING COLLECTIVE CELL MIGRATION

**Assaf Zaritsky<sup>1</sup>, Yun-Yu Tseng<sup>2</sup>, M. Angeles Rabadán<sup>2</sup>, Xavier Trepas<sup>3</sup>, Michael Overholtzer<sup>2</sup>, Alan Hall<sup>2</sup>, Gaudenz Danuser<sup>1</sup>**

*1 Ut Southwestern Medical Center, Dallas, TX, United States,*

*2 Memorial Sloan-Kettering Cancer Center, New York, Ny, United States,*

*3 Institute for Bioengineering of Catalonia, Icrea and University of Barcelona, Barcelona, Spain*

Collective cell migration of cohesive groups involves intercellular mechanical communication transmitted between adjacent cells through cell-cell contacts to eventually drive long-range communication. We discovered how local mechanical fluctuations induce long-range communication and identified some potential molecular players driving this mechanism.

By designing and applying new analytical methods to migrating monolayers of epithelial cells, we find that cells at the front transmit mechanical cues by inducing normal and shear strains on neighboring follower cells. Accumulation and propagation of these mechanical cues over time and space create groups of cells that migrate and exert forces in a coordinated manner. Such motion patterns direct cells from within the monolayer toward the sites of shear-strain-induced motion at the monolayer front. These results provide a model of long-range mechanical communication between cells, in which local alignment of velocity and stress translates local mechanical fluctuations into globally collective migration.

Effective cell-cell mechanical communication is likely induced by active cytoskeletal rearrangements, controlled by the small GTPase proteins of the RHO family (Rho GTPases). Spatiotemporal analysis revealed a surprising role of the Rho GTPase RHOA in regulating long-range communication: partial depletion simultaneously shifts cells at the front and back of the monolayer from a non-motile to a motile state. A comprehensive targeted screen discovered a group of RHOA activators that differentially alter intercellular communication: either by enhancing local or long-range communication. Reduced actomyosin contractility resembled the former elevation in local communication, presumably by passive cell-cell force transmission.

Altogether, our results are a first step towards explaining how Rho family signaling pathways are spatially and temporally controlled to promote mechanically induced intercellular communication.

## TWO DISTINCT ACTIN NETWORKS MEDIATE TRACTION OSCILLATIONS TO CONFER MECHANOSENSITIVITY OF FOCAL ADHESIONS

**Jian Liu**<sup>1</sup>

Please use any of the following sections that are relevant for your abstract structure.

Cells sense the mechanical stiffness of their extracellular matrix (ECM) by exerting traction force through focal adhesions (FAs), which are integrin-based protein assemblies. Strikingly, FA-mediated traction forces oscillate in time and space and govern durotaxis – the tendency of most cell types to migrate toward stiffer ECM. The underlying mechanism of this intriguing oscillation of FA traction force is unknown. Combining theory and experiment, we develop a model of FA growth, which integrates coordinated contributions of a branched actin network and stress fibers in the process. We show that retrograde flux of branched actin network contributes to a traction peak near the FA distal tip and that stress fiber-mediated actomyosin contractility generates a second traction peak near the FA center. Formin-mediated stress fiber elongation negatively feeds back with actomyosin contractility, resulting in the central traction peak oscillation. This underpins observed spatio-temporal patterns of the FA traction, and broadens the ECM stiffness range, over which FAs could accurately adapt with traction force generation. Our findings shed light on the fundamental mechanism of FA mechanosensing and hence durotaxis.

# PHYSICS OF ADHESION REGULATION: THE CASE OF CADHERIN

**Ana Suncana Smith**<sup>1</sup>

<sup>1</sup> *Eam, Erlangen, Germany*

In embryogenesis, vertebrate cells assemble into organized tissues. In cancer, metastasis tumor cells spreading in the circulatory system use mechanisms of adhesion to establish new tumors. At the root of these life-forming or life-threatening biological phenomena is cell adhesion, the binding of a biological cell to other cells or to a material substrate or scaffold. The most obvious fundamental question to ask is then as follows: What factors control or govern cell adhesion? For a long time, the paradigmatic answer to this question was that specific protein molecules embedded in the cell wall (or membrane) were responsible for cell adhesion, in either a key-lock fashion (in cell-cell adhesion) or a suction-cup fashion (in cell-substrate adhesion). But, a new realization has emerged during the past two decades that physical mechanisms, promoted by the cell membrane, play an unavoidable, yet not fully understood role. Although these physical elements, namely membrane fluctuations and ability to change shape, do not at all depend on any specific proteins, they can have a major impact on the protein-mediated adhesion, and can be viewed as mechanism that control the binding affinity to the cell-adhesion molecules. In my talk I will show how these mechanisms can be studied in mimetic models both experimentally and theoretically, the result of which can be discussed in the cellular context.

## Acknowledgments:

This work was funded by the European Research Council (StG MembranesAct 2013-337283), the Research Training Group 1962 at the FAU Erlangen-Nürnberg, and the Excellence Cluster: Engineering of Advanced Materials

## References:

1. T. Bihl, U. Seifert and A.-S. Smith: *Nucleation of Ligand-Receptor Domains in Membrane Adhesion*. *Phys. Rev. Lett.* 109, 258101 (2012)
2. C. Monzel, D. Schmidt, R. Merkel, U. Seifert, K. Sengupta, A.-S. Smith: *Signature of a Non-harmonic Potential as Revealed from a Consistent Shape and Fluctuation Analysis of an Adherent Membrane*. *Phys. Rev. X* 4, 021023 (2014).
3. T. Bihl, S. Fenz, R. Merkel, E. Sackmann, U. Seifert, K. Sengupta, A.-S. Smith. *Association rates of membrane-coupled cell adhesion molecules*. *Biophys. J.* 107, L33 (2014).
4. T. Bihl, U. Seifert, A.-S. Smith. *Multiscale approaches to protein-mediated interactions between membranes - Relating microscopic and macroscopic dynamics in radially growing adhesions*. *New J. Phys.* 18, 083016 (2015).
5. C. Monzel, C. Kleusch, D. Kirchenbüchler, D. Schmidt, U. Seifert, A.-S. Smith, K. Sengupta, R. Merkel. *Dynamic Optical Displacement Spectroscopy*, *Nature Comm.* 6, 8162 (2015).

# FORCE APPLICATION MODEL FOR DEFINING MECHANICAL MECHANISM OF METASTATIC INVASION

**Martha Alvarez<sup>1</sup>, Ronen Nissim<sup>2</sup>, Yaniv Ben-David<sup>2</sup>**

<sup>1</sup> Technion, Faculty of Biomedical Engineering, Haifa, Israel,

<sup>2</sup> Faculty of Biomedical Engineering at Technion, Israel Institute of Technology, Haifa, Israel

Metastatic invasion through tissue is a critical step in formation of metastases, the typically lethal spread of cancer in the body. During invasion, a single cancer cell can move through the extracellular matrix and between cells in tissue or lining blood vessels. During this process the cancer cells change morphology and apply forces to their surroundings. We have recently shown that metastatic breast-cancer cells attempt to penetrate a gel by indenting it if its stiffness is suitable, even when the gel is non-degradable and impenetrable, with small pores. Specifically, when a 2D gel is soft enough for the cells to push, yet stiff enough for them to grip and develop force on, the cells will indent it. Here, we show a possible mechanism for how a metastatic cancer cell generates normal forces to invade, our model is based on a measurements of the deformation to an elastic substrate caused by the cells when attempting invasion. We evaluated invasion-related force application mechanisms by identifying specific cell elements affecting the mechanical interactions of cancer cells with their substrate. High and low metastatic breast cancer cells (MDA-MB-231 and MDA-MB-468) were used to determine the mechanical role of myosin II (inhibited by blebbistatin treatment) and microtubules (disrupted by nocodazole) in force application, as defined through quantifiable invasive parameters (e.g. indentation depth and cell area) on cells indenting an impenetrable gel. The role of binding proteins was tested by small molecule inhibitor of Formin Homology 2 domains (SMFH2) which induces remodeling of actin filaments, on the cytoskeleton and inside the nucleus and also on microtubules. We found that the inhibition of myosin II and the disruption of microtubules cause morphology changes (cell area of indentation and at gel's surface) but do not affect indentation depth. Instead, the inhibition of formins through on the cytoskeleton and nucleus reduces the indentation depth revealing that binding molecules play a role during invasion. Quantifying cells mechanics behind indentation will reveal possible therapeutic targets to prevent metastasis and deliver a potential in vitro diagnostic method for cancer.

## References:

Krista-Muscal, R., L. Dvir, and D. Weihs, *Metastatic cancer cells tenaciously indent impenetrable, soft substrates. New Journal of Physics*, 2013. 15: p. bra.

Liron. Dvir, Ronen Nissim, Martha Alvarez-Elizondo, Daphne Weihs, *Quantitative measures to reveal coordinated cytoskeleton-nucleus reorganization during in vitro invasion of cancer cells, New Journal of Physics*, 2015. 17.

# THEORETICAL ANALYSIS OF STRESS DISTRIBUTION AND CELL POLARIZATION SURROUNDING A MODEL WOUND

**Yonit Maroudas-Sacks<sup>1</sup>, Assaf Zemel<sup>2</sup>**

*<sup>1</sup> Hebrew University of Jerusalem, Jerusalem, Israel,*

*<sup>2</sup> Institute of Dental Sciences and Fritz Haber Research Center for Molecular Dynamics, Jerusalem, Israel*

It is widely accepted that the spatial organization of cells and their cytoskeleton polarity is affected by the local elastic field acting upon them. In the process of wound healing, acto-myosin filaments align to form a supracellular contractile ring on the margin of closing wounds. To theoretically investigate this process we have calculated the elastic field actively generated in a round monolayer of contractile cells adhered to a thin elastic substrate surrounding a model wound. The cells are modelled as a radial distribution of point force dipoles that may alter in magnitude and orientation in response to the local elastic stress. We demonstrate that the presence of a hole in the center of the cell monolayer induces tangential acto-myosin polarization around the hole, suggesting that ring formation is a consequence of the contractile activity of cells in the bulk, and is affected by factors such as substrate rigidity, cell adhesion, and wound radius. We further show how the interplay between cellular contractility and tractions imposed by migrating “leader cells” affects the physical deformation of individual cells and the relative contribution of these factors to wound closure.

## MECHANOTRANSDUCTION DURING CELL ADHESION: NUMERICAL ANALYSIS OF THE INFLUENCE OF SUBSTRATE TOPOLOGY

**Maxime Vassaux**<sup>1</sup>

<sup>1</sup> Aix-Marseille Université, Marseille, France

The shape that stem cells reach at the end of adhesion process influences their differentiation. Rearrangement of cytoskeleton and modification of intracellular tension may activate mechanotransduction pathways controlling cell commitment. In the present study, the mechanical signals involved in cell adhesion were computed in in vitro stem cells of different shapes using a single cell model, the so-called Cytoskeleton Divided Medium (CDM) model based on the Non-Smooth Contact Dynamics [1] code LMGC90.

In the CDM model, the filamentous cytoskeleton and nucleoskeleton networks were represented as a mechanical system of multiple tensile and compressive interactions between the nodes of a divided medium, namely a tensegrity structure. Discrete modelling of cytoskeleton mechanical structures (stress fibres, microtubules, microfilaments and intermediate filaments) allows introducing in the cell computational model additional geometrical and material details, which are available in the literature [2]. Realistic forces at the focal adhesion complexes (FACs) have been observed considering physical cytoskeleton (CSK) microstructures properties as well as anisotropic densities using probabilistic distributions to account for variability of the microstructures geometry.

On the basis of such cell computational model, the influence of the substrate topology has been investigated. Three topologies are tested: flat, convex and concave (see figure 1). The influence of the topology is analysed observing intracellular mechanical state, and more specifically the nucleoskeleton's state.

Experimental results obtained at IS2M in Mulhouse have shown that cells tend to migrate and adhere preferably on concave surfaces. First numerical results show that, for identical cell models, concave surfaces lead to lower vertical strain of the core of the cell as well as lower total forces in the stress fibres than convex surfaces. Such result, since cell's CSK can be considered as a tensegrity structure, imply that the cell does not migrate and adhere preferably on surface topologies maximizing its global stiffness.

Further numerical analysis of the mechanical behaviour of adherent cells is to be implemented in order to figure out mechanical criteria influencing topology preference, which could include general stability of the cell.



Figure Caption: Half-cut view of a three-dimensional of a spread cell on a convex (left), a flat (center) and a concave (right) substrate.

### References:

[1] Jean, M. (1999). The non-smooth contact dynamics method. *Computer methods in applied mechanics and engineering*, 177(3), 235-257

[2] Milan, J. L., Lavenus, S., Pilet, P., Louarn, G., Wendling, S., Heymann, D. & Chabrand, P. (2013). Computational model combined with in vitro experiments to analyse mechanotransduction during mesenchymal stem cell adhesion. *Eur. Cells Mater.*, 25, 97-113.

# MICROMECHANICS, WRINKLING FORMATION, AND WAVE PROPAGATION IN SOFT MATRIX-FIBER AND LAYERED BIOLOGICAL TISSUES

**Stephan Rudykh**<sup>1</sup>

<sup>1</sup> Technion - Israel Institute of Technology, Haifa, Israel

Soft biological tissues frequently comprise soft matrix with stiffer fibers or layers. These microstructures are sophisticatedly tailored to enable various physiological functions and to provide required mechanical properties. In this study, we specifically focus on the role of microstructures in the overall response of fiber-matrix tissues. In particular, we analyze the mechanical behavior of 2D layered materials [1-3] and 3D fiber composites [4]. We derive micromechanical models for stiff-soft laminates, and estimates for 3D fiber-matrix materials. The proposed model stress-strain relations are compared with finite element simulations, showing an excellent agreement [1, 4]. Moreover, we analyze wrinkling formation and fiber buckling frequently observed in soft natural materials. We derive explicit estimates for critical strain and critical wave length of the buckled wavy shapes. We experimentally demonstrate the existence of these macro- and micro-modes of instabilities in periodic layered structures. The results for the critical strain and wavelength are found to be in good agreement with the theoretical and numerical predictions [2]. Finally, we show the influence of deformation on elastic waves in soft microstructured materials [5-7]

## References:

- [1] Rudykh and Boyce, *Analysis of elasmoid fish imbricated layered scale-tissue systems and their bio-inspired analogues at finite strains and bending*. *IMA J Appl Math*, 2014
- [2] Li, Kaynia, Rudykh and Boyce, *Wrinkling of Interfacial Layers in Stratified Composites*. *Adv Eng Mater*, 2013
- [3] Rudykh and Boyce, *Transforming Small Localized Loading into Large Rotational Motion in Soft Anisotropically-Structured Materials*. *Adv Eng Mater*, 2014
- [4] Rudykh and deBotton, *Instabilities of Hyperelastic Fiber Composites: Micromechanical Versus Numerical Analyses*. *J Elasticity*, 2012
- [5] Rudykh and Boyce, *Transforming Wave Propagation in Layered Media via instability-induced Wrinkling Interfacial Layer*. *Phys Rev Lett*, 2014
- [6] Galich and Rudykh, *Influence of stiffening on elastic wave propagation in extremely deformed soft matter: from nearly incompressible to auxetic materials*. *Extreme Mech Lett*, 2015
- [7] Galich and Rudykh, *Comment on "Disentangling longitudinal and shear elastic waves by neo-Hookean soft devices"*. *Appl Phys Lett*, 2015

# MATHEMATICAL MODELING OF BURNS

## **Fred Vermolen**<sup>1</sup>

*<sup>1</sup> Delft Institute of Applied Mathematics / Delft University of Technology, Delft, Netherlands*

In this talk, we consider cell-based and continuum-based models for the development of contractures and hypertrophic scars. The models are based on partial differential equations for the chemicals that play a role as well as on stochastic differential equations and stochastic processes if it comes to the behavior of cellular entities such as fibroblasts, myo-fibroblasts and macrophages. We will see the interplay between the immune system response and the occurrence of contractures and hypertrophy. Next to the cell-based models, we will also present our work in the full continuum scale where cells are represented in terms of densities and where we consider neo-Hookean elastic behavior. The results will be evaluated under variation of several parameters such as the apoptosis rate of myo-fibroblasts.

## **Acknowledgments:**

We like to thank the Dutch Burns Foundation (Nederlandse Brandwondenstichting) for their financial support under project WO/12.03.

## AGENT-BASED MULTI-LEVEL SIMULATIONS OF DRUG-INDUCED LIVER DAMAGE AND REGENERATION: FROM DATA TO MODELS AND BACK

**Dirk Drasdo**<sup>1</sup>, **Celliere Geraldine**<sup>2</sup>, **Boissier Noemie**<sup>2</sup>, **Hoehme Stefan**<sup>3</sup>, **Hengstler Jan G.**<sup>4</sup>

<sup>1</sup> Inria Paris, Izbi Leipzig, Paris, France, <sup>2</sup> Inria Paris, Paris, France, <sup>3</sup> Izbi, University of Leipzig, Leipzig, Germany, <sup>4</sup> Ifado, Dortmund, Germany

We will show how the iterative application of a pipeline consisting of confocal scanning microscopy, image analysis and modeling can be used to establish a multi-level model spanning molecular, cell, tissue and whole body scale to drug-induced liver damage and subsequent regeneration. By a model-guided experimental strategy (J. Hepat. 2014) simulated predictions successfully guided the experiments towards a previously unrecognized and subsequently validated order mechanism during liver regeneration of pericentral liver lobule damage, reminiscent of wound healing (PNAS 2010). A liver lobule is the smallest repetitive anatomical and functional unit of liver.

Within an integrative model we showed that the consensus detoxification scheme of the blood from ammonia in healthy liver fails to explain in vivo detoxification experiments, and proposed the existence of an ammonia sink (Hepatology 2014) that subsequently could experimentally be found (J. Hepat. 2016). High doses of ammonia is toxic for the body leading to encephalopathy and death; paracetamol (APAP) overdose is the main reason for acute liver failure in UK and USA. The found mechanism has a great potential of improving treatment of APAP overdose.

Spatial temporal simulations are either performed directly in the reconstructed 3D confocal micrographs, or in representative tissue samples obtained by sampling information from the analyzed images (Arch. Toxicol 2014) using our new tool TiQuant (Bioinformatics, 2015). Our simulations display lobule micro architecture, simulate each hepatocyte as individual agent parameterized by measurable biophysical and bio-kinetic quantities, represent the capillary network including blood flow (by Poiseuille flow) and transport of metabolites by PDEs, and intracellular metabolic pathways by ODEs. Simulations of ammonia detoxification have been performed both, in compartment models representing functional hepatocyte compartments and in the spatial temporal multilevel model to identify possible critical differences between the model types.

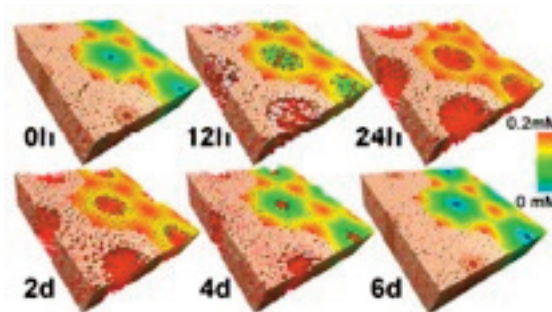


Figure Caption: Regenerating liver lobules and ammonia concentration

### Acknowledgments:

Funding by EU Notox, BMBF VLN, ANR IFLOW.

# MODELING FIBROBLAST POPULATED COLLAGEN LATTICE CONTRACTION

**John Dallon**<sup>1</sup>, **Emily Evans**<sup>2</sup>

<sup>1</sup> Brigham Young University, 275 Tmcb, Department of Mathematics, Provo, United States,

<sup>2</sup> Brigham Young University, Provo, United States

In order to better understand wound contraction fibroblast populated collagen lattices have been studied for many years. In this talk I will discuss mathematical models for lattice contraction. The models are force based and formulated with components at the cellular and subcellular level with the goal of understanding the macroscopic behavior of the lattice. Two lattice models will be presented, one where the collagen is modeled as a triangulated grid of springs and one where the collagen is modeled as a collection of entangled fibers. The model will be used to simulate contraction and cut disks experiments.

# A ROBUST AND EFFICIENT ADAPTIVE MULTIGRID SOLVER FOR THE OPTIMAL CONTROL OF PHASE FIELD FORMULATIONS OF GEOMETRIC EVOLUTION LAWS

**Anotida Madzvamuse<sup>1</sup>, Feng W. Yang<sup>1</sup>, Chandrasekhar Venkataraman<sup>2</sup>, Vanessa Styles<sup>1</sup>**

*1 University Of Sussex, School Of Mathematical AND Physical Sciences, Department Of Mathematics, Brighton, United Kingdom,*

*2 School of Mathematics and Statistics, Mathematical Institute, North Haugh, St Andrews, United Kingdom*

We propose and investigate a novel solution strategy to efficiently and accurately compute approximate solutions to semilinear optimal control problems, focusing on the optimal control of phase field formulations of geometric evolution laws. The optimal control of geometric evolution laws arises in a number of applications in fields including material science, image processing, tumour growth and cell motility. The main focus of this work is to propose, derive, implement and test an efficient solution method for such problems. The solver for the discretised PDEs is based upon a geometric multigrid method incorporating advanced techniques to deal with the nonlinearities in the problem and utilising adaptive mesh refinement. An in-house two-grid solution strategy for the forward and adjoint problems, that significantly reduces memory requirements and CPU time, is proposed and investigated computationally. Furthermore, parallelisation and an adaptive-step gradient update for the control are employed to further improve efficiency. We present a number of computational results that demonstrate and evaluate our algorithms with respect to accuracy and efficiency. A highlight of the present work is simulation results on the optimal control of phase field formulations of geometric evolution laws in 3-D which would be computationally infeasible without the solution strategies proposed in the present work.

## Acknowledgments:

All authors acknowledge support from the Leverhulme Trust Research Project Grant (RPG-2014-149). The work of CV, VS and AM was partially supported by the EPSRC UK Grant (EP/J016780/1). AM received funding from the EU Horizon 2020 MSCA-ITN grant No 642866. CV is partially supported by an EPSRC Impact Accelerator Account award. This research was finalised whilst all authors were participants in the Isaac Newton Institute Program, Coupling Geometric PDEs with Physics for Cell Morphology, Motility and Pattern Formation.

# IMPLICATIONS OF ANOMALOUS KINETICS ON THE COURSE OF WOUND CONTRACTION AND CLOSURE

**Etelvina Javierre**<sup>1</sup>

*<sup>1</sup> Centro Universitario de la Defensa, Academia General Militar, Zaragoza, Spain*

Wound healing evolves by an intricate activation and inhibition of cell migration and proliferation, through sensing and transduction mechanisms of chemical and mechanical cues. Moreover, this activity takes place on the extracellular matrix, whose composition is highly heterogeneous and changes dynamically during the healing process.

Fibroblasts migration has been observed to depart from the classical random walk, which is characterized by a mean square displacement proportional to time. Instead, migrating fibroblasts have shown a sub-diffusive or super-diffusive migration behavior depending on the matrix properties or on chemical stimuli [1]. Similarly, soft tissues have been shown to behave accordingly to a constitutive equation that is not elastic nor viscoelastic. These variations to classical models arise from the fact that cellular and tissular behavior show memory effects which can be modeled through partial differential equations of fractional order.

This work extends well-established wound contraction models [2,3] to include anomalous transport kinetics of the cellular and chemical species and fractional viscoelasticity for the extracellular matrix. These generalizations produce alterations on the cellular densities, with notable effects on the temporal apparition of myofibroblasts and on the wound level of contraction. Hence, this general framework brings the effects of anomalous kinetics to the discussion of physiological and pathological healing.

## Acknowledgments:

This research was supported by the Spanish Ministry of Economy and Competitiveness (Grant MTM2013-40842-P)

## References:

- [1] Weihs, D, Mason, TG, Teitell, MA. Effects of cytoskeletal disruption on transport, structure, and rheology within mammalian cells. *Phys Fluids* 2007; 19:103102.
- [2] Murphy, KE, Hall, CL, Maini, PK, McCue, SW, McElwain, DLS. A Fibrocontractive Mechanochemical Model of Dermal Wound Closure Incorporating Realistic Growth Factor Kinetics. *Bull Math Biol* 2012; 74:1143-1170.
- [3] Valero, C, Javierre, E, García-Aznar, JM, Gómez-Benito, MJ. A Cell-Regulatory Mechanism Involving Feedback between Contraction and Tissue Formation Guides Wound Healing Progression. *PLoS ONE* 2014; 9(3):e92774.

# THE EFFECT OF NON-SURGICAL REALIGNMENT THERAPIES UPON KNEE CONTACT MECHANICS

*Howard J Hillstrom, Jim Tse, Darryl D. D'Lima, Glenn Garrison, Benjamin J. Fregly*

Knee osteoarthritis (OA) has been biomechanically associated with high body mass index, soft tissue injuries, and malalignment. Patients with knee OA most typically suffer from varus malalignment which overloads the medial compartment. The effect of knee brace alignment upon compressive loading within the joint for treating OA is unknown. This study was facilitated by recruiting a test subject who was fit with an instrumented knee replacement (e-tibia) that can measure knee contact force in vivo.<sup>1,2</sup> Purpose: to measure contact force on an individual wearing (1) five different knee brace constructs, (2) one knee brace adjusted to several alignments to determine the 'biomechanical dosage' effect, and (3) while wearing medial or lateral foot wedges. A single-subject study was conducted on a female (69 years old, 81 kg) who had an e-tibia TKR. Composed of a polyethylene insert, tibial tray, and telemetry system, the e-tibia measured three forces ( $F_x$ ,  $F_y$ ,  $F_z$ ) and three moments ( $M_x$ ,  $M_y$ ,  $M_z$ ) using 12 load cell strain gages that were integrated within the prosthesis. The subject walked at her self-selected speed on a level walkway while simultaneously measuring e-tibia contact loading and 3D inverse dynamics. All brace conditions reduced the 1st and 2nd peaks of the joint contact force and moments in general and the medial compartment force in specific (Figure 1). Increasing valgus brace alignment decreased medial forces and increasing varus brace alignment decreased lateral forces. Medial and lateral wedged insoles preferentially reduced the 1st or 2nd peak of the contact force. The addition of a brace provided contact forces that were comparable to the brace only condition. The data supports the concept that knee braces share load with the knee.<sup>3</sup>

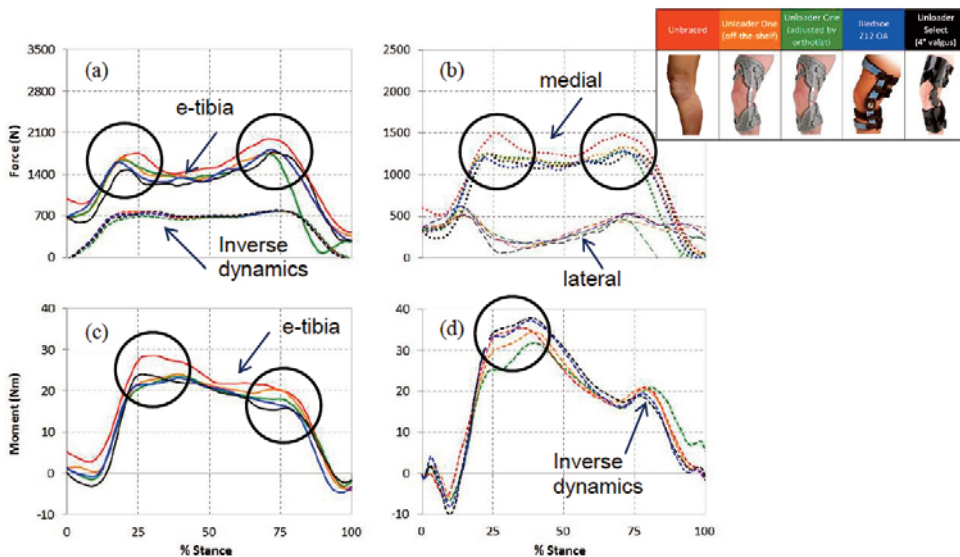


Figure 1: e-tibia contact and inverse loading while walking level – knee braces reduced the 1st and 2nd peak of the (a) total knee contact force compared to unbraced (upper left), (b) medial compartment contact forces, (upper right), (c) contact moments, where (d) inverse dynamics were of little discriminatory value in net joint force (a) and moment (d)

## Acknowledgments:

The test subject and S.Backus, L. Tran, A. Kraszewski, A. Kontaxis, M. Lenhoff

## References:

1. Kutzner et al. J Biomech. 2011; Apr 29;44(7):1354-60.
2. Fregly BJ. Int J Comput Vis Biomech. 2009; 2: 145-155., 3. 3. Pollo, F. E. et al. Am J Sports Med. 30; 3 (2002): 414-21.

# APPLICATION OF A VALIDATED COMPUTATIONAL KNEE MODEL TO PREDICT IMPROVED JOINT RECONSTRUCTION

*Mootanah R., Carpanen D., Reisse F., Rozbruch S.R., Hillstrom H.J.*

Knee osteoarthritis (OA) is a degenerative joint disease, often caused by increased joint contact stress due to lower limb malalignment [1] or meniscal tear [2]. Surgical procedures, such as high tibial osteotomy and partial meniscectomy, are performed to correct lower limb malalignment, and resect torn meniscal tissues, respectively. However, surgical outcomes are not always unpredictable due to unknowns, such as the alignment correction that would minimize peak joint stress values or the percent volume and location of meniscal tissue that can be removed without causing a substantial increase in peak stress within the knee joint. The aim of this study was to use a cadaveric-specific validated finite element (FE) knee model [3] to investigate surgical techniques that would lead to improved outcomes.

Simulations of knee joints with different degrees of varus and valgus malalignment, as well as different percent volume and location of meniscectomies, were created. The relationship between Mechanical Axis Deviation (MAD) and peak knee joint stress show that, for this particular knee, the malalignment correction that minimized knee joint contact stress did not correspond to the commonly-accepted mechanical axis deviation of zero mm, nor the Fujisawa Point. At the end of weight acceptance during walking, a partial meniscectomy of 30% in the anterior, central and posterior locations resulted in an increase in peak stress by 28%, 39% and 32%, respectively, in the medial compartment and 10%, 17% and 12%, respectively, in the lateral compartment. However, corresponding results for running showed higher increase in peak stress values in the lateral compartment (21%, 33% and 37%, respectively) than in the medial compartment (11%, 12% and 10%, respectively). This is because the knee experiences a valgus thrust during running and a varus thrust during walking.

This study is the first to demonstrate the relationship between knee joint stress and malalignment correction, as well as the safe percent volume of meniscal tissue that can be removed at different locations. The validated knee model is a first step towards developing a surgical planning tool.

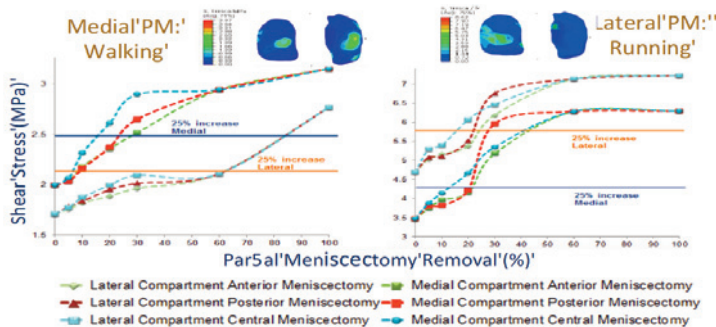


Figure Caption: Effect of volume and location of partial meniscectomy on shear stress in the knee joint during (left) walking and (right) running. PM = Partial Meniscectomy.

## Acknowledgments:

The Chelmsford Medical Education and Research Trust and the Higher Education Funding Council for England for funding this research. Special thanks to Carl Imhauser, Mark Lenhoff, Matthew F Koff, Austin Fragomen for their valuable assistance.

## References:

1. Petersson IF, Jacobsson LT, 2002. *Best Pract Res Clin Rheumatol*, 16(5):741-760
2. Ronger C. et al., 1995. *The American Journal of Sports Medicine*, 23(2): 240
3. Mootanah R. et al., 2014. *Computer Methods in Biomechanics and Biomedical Engineering*, 17(13):1502-1517

# SIMULATION OF COUPLED NEUROMUSCULAR COORDINATION AND KNEE JOINT MECHANICS DURING MOVEMENT

Colin R Smith<sup>1</sup>, Darryl G Thelen<sup>1,2,3</sup>

<sup>1</sup> Department of Mechanical Engineering,

<sup>2</sup> Department of Biomedical Engineering, <sup>3</sup>Department of Orthopedics and Rehabilitation

Knee joint behavior during locomotion results from interactions of neuromuscular coordination, passive joint structures, and articular contact mechanics. Because of the complexity of this dynamic system, these variables are often studied in isolation. Musculoskeletal models with simplified knee joint representations are used to investigate neuromuscular coordination during movement. Detailed finite element models predict the interaction of muscle, ligament and cartilage tissue loads at the joint level, without considering coordination and whole body movement dynamics. A mechanistic model that incorporates the functional interaction between neuromuscular coordination, knee joint structure and whole body movement is important to understand the causes of knee pathologies and to improve surgical treatments.

We recently introduced a novel multibody knee model that includes six degree of freedom tibiofemoral and patellofemoral joints. Cartilage surfaces and ligament attachments were segmented from MR images of a healthy adult female. Fourteen ligaments were represented by bundles of nonlinear elastic springs. Cartilage contact pressures are calculated using an elastic foundation model. The knee model was integrated into a generic musculoskeletal model and validated by comparing simulated knee kinematics with in vivo kinematics measured by dynamic MRI [1]. We also introduced a novel simulation routine, termed COMAK (concurrent optimization of muscle activations and kinematics), that predicts internal knee tissue loads from kinematic and kinetic measurements of movement. At each time step, COMAK calculates the muscle forces, secondary knee kinematics, ligament forces and cartilage contact pressures that minimize the weighted sum of squared muscle activations while satisfying overall dynamic constraints. The constraints require that the muscle forces and internal knee loads generate the measured hip, knee (flexion) and ankle accelerations [2]. The model and simulation routine are being implemented in OpenSim and will be made publically available through simtk.org.

To investigate the influence of neuromuscular coordination and structural joint properties on knee behavior during walking, we used a high throughput computing cluster to perform probabilistic analyses. By treating model and simulation parameters as stochastic variables, we have assessed the sensitivity of predicted knee mechanics to neuromuscular coordination strategies and model geometric and constitutive properties. Recently, we have begun evaluating the use of statistical shape modeling to rapidly generate subject-specific knee models, as well as to study the influence of articular surface geometry and ligament attachment location on knee mechanics during movement. We envision our novel approach will enable the next generation of motion analysis tools, in which subject-specific joint behavior can be simulated, and the effects of interventions can be predicted and considered for clinical treatment planning.

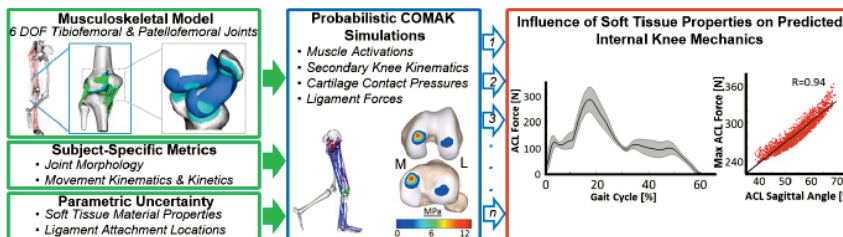


Figure Caption: Probabilistic analyses of model and simulation parameters allow for sensitivity studies of knee mechanics to neuromuscular coordination strategies, model geometries and material properties.

## Acknowledgments:

NIH EB015410 and HD084213, NCSRR Visiting Scholars Program

## References:

[1] Lenhart RL, et al. (2015) "Prediction and Validation of Load Dependent Behavior of the Tibiofemoral and Patellofemoral Joints during Movement." *Annals of Biomedical Engineering*, 43(11): 2675-85.

[2] Smith, CR, et al (2016). "Influence of Ligament Properties on Tibiofemoral Mechanics in Walking". *J Knee Surg* 29(2): 99-106

## UKA COMPONENT FATIGUE TEST DEVELOPMENT USING DOE AND FEA

**Danny Levine<sup>1</sup>, Jeffrey Bischoff<sup>1</sup>, Yang Son<sup>1</sup>, Jeremy Phillips<sup>1</sup>**

<sup>1</sup> Zimmer Biomet, Warsaw, United States

Unicompartmental knee arthroplasty (UKA) is a clinical option for knee osteoarthritis continuum of care, providing soft tissue sparing and a less invasive approach compared to total knee arthroplasty. Fatigue fracture of implant components (Figure 1) [1], led to a proposed new pre-clinical test method from ASTM [2]. While the proposed 3-point bend test (Figure 2) can produce fractures at clinically relevant locations, it does not guide comparison of worst-case scenarios for a new design to that of a clinically available predicate; thus, does not provide an accurate basis for comparative evaluation. This study combines design of experiments (DOE) tools with finite element analysis (FEA) to identify worst-case loading for UKA tibial baseplates.

Load position significantly influences stress, as baseplates typically have fixation features on the inferior surface that may create stress risers. An FEA/DOE tool (ANSYS DesignXplorer) was used to vary load at A/P and M/L positions through ranges estimated from implant retrieval data and in-vivo kinematics [3]. Peak stress in the tibial baseplate was obtained (Figure 3) for each set of load coordinates. Results were mapped and used to locate the worst-case load position (Figure 4). Additionally, fatigue testing of two designs with worst-case loads confirmed the predicted fracture initiation site and relative ranking.

Per the proposed ASTM test method [2], load placement is defined by a fixed point based upon the articular surface geometry and makes no allowance for joint kinematics. Results here indicate that the difference in stress between an articular surface center load and a worst-case load is small (<10%). However, since peak stress location can shift, predicted ranking of designs may be incorrect without an improved tool to predict worst-case load position.

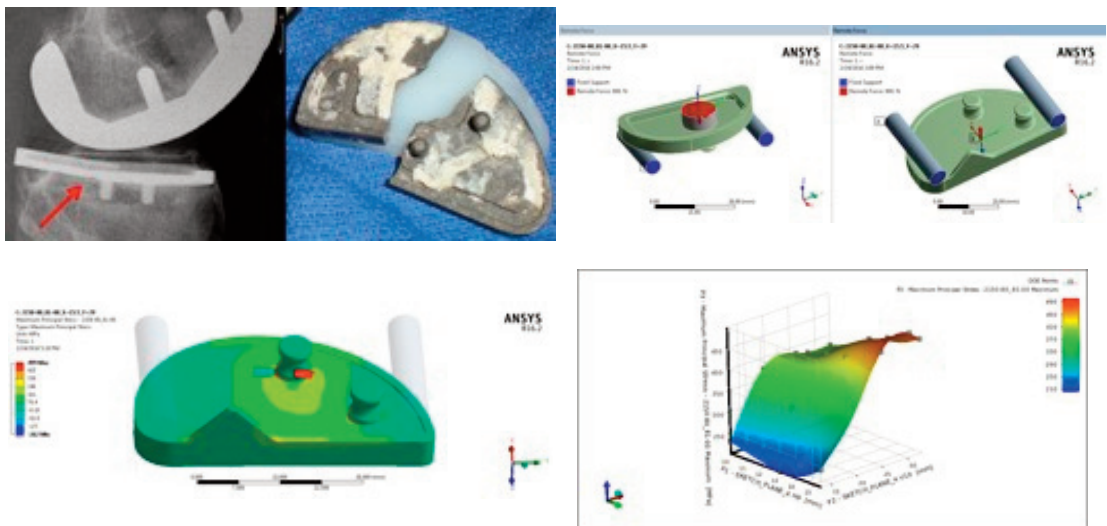


Figure Captions: [1] Fractured tibial baseplate; [2] Three-point bend model; [3] Maximum principal stress in baseplate; [4] Response surface

### References:

- [1] Palumbo, BT, et al, *The Journal of Arthroplasty*, pp 40-45 Vol. 26 No. 6 Suppl 1 2011
- [2] WK45235, ASTM, 2015
- [3] Akizuki, S, et al, *The Journal of Arthroplasty*, pp 963-971, Vol. 24 No. 6, 2009

# SOFT TISSUES LOADINGS ON HEALTHY KNEE AT DIFFERENT PHYSIOLOGICAL FLEXIONS: A COUPLED EXPERIMENTAL-NUMERICAL APPROACH

*Boris Dousteysier*<sup>1</sup>, *Woo Suck Han*<sup>2</sup>, *Chafiaa Hamitouche*<sup>3</sup>, *Eric Stindel*<sup>3</sup>, *Jérôme Molimard*<sup>2</sup>

<sup>1</sup> Ecole Nationale Supérieure des Mines de Saint-Etienne, Cis-Emse, F-42023 Saint Etienne, France, Inserm U1059, Sainbiose, F-42023 Saint Etienne, France, Laboratoire de Traitement de L'information Médicale, Inserm Umr 1101, 29609 Brest, France, Saint Etienne, France,

<sup>2</sup> Ecole Nationale Supérieure des Mines de Saint-Etienne, Cis-Emse, F-42023 Saint Etienne, France, Inserm U1059, Sainbiose, F-42023 Saint Etienne, France, Université de Lyon, F-69000 Lyon, France, Saint Etienne, France,

<sup>3</sup> Laboratoire de Traitement de L'information Médicale, Inserm Umr 1101, 29609 Brest, France, Brest, France

## Introduction

Knee degradation and pain when developing osteoarthritis are strongly related not only to the pressure on the cartilage, but also to the knee stability and to the subsequent loadings on the ligaments. Authors proposed the knee models without any flexion [1][2]. Knee flexion had been introduced by controlling actively muscular groups [3] or by using a full displacement-controlled model [4]. But in both cases, the pressure applied on the articulation has been questioned, the forces used to achieve the flexion being far from the physiology in the former and the bone positioning uncertainties leading to high variations in the cartilage pressure and ligament loads in the latter. Here, we propose a mixed approach, both using medical imaging (MRI, EOS X-ray system [5]) and force platform in conjunction with a finite element model.

## Method

A healthy volunteer underwent a MRI and an EOS imaging of the knee. EOS images gave the exact position of the bones for five flexion angles of the knee, ranging from 0° to 85°. The subject's knee was loaded with a specific force on his foot during all acquisitions to keep consistent boundary conditions on the knee. A 3D geometrical model of the bones and cartilages was segmented from the MRI stacks; this model was meshed and smoothed for Finite Element Analysis (FEA). The bones of the model were fitted to those of the EOS images to have the physiological positions of the knee. The ligaments were then added as truss elements (under tensile forces only). The FEA was carried out according to the experimental boundary conditions (force and flexion angle), so as to ensure the global knee mechanical equilibrium.

## Results

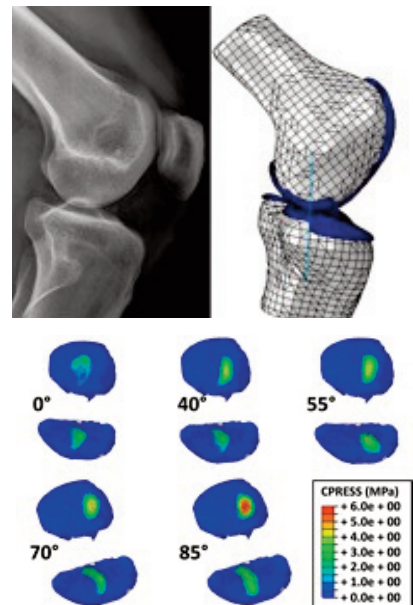
To validate this patient-specific model, its bony structure was confronted with the EOS images once the mechanical equilibrium reached. The difference of position was within the error range of the image registration, showing a satisfying equilibrium state. Last, this model gave us an estimation of the tension in the ligaments for every flexion as well as a pressure map on the cartilages.

## Discussion

This healthy model of the knee will be completed with the menisci to have a more precise pressure map on the cartilages. It will then be used as a reference in studying arthritic knee joints for clinical cases.

Figure1: FEA (right) of the EOS imaging (left)

Figure2: Pressure map on tibial cartilage at several flexion angles



## References:

[1] Peña, et al. *Journal of biomechanics* 39.9: 1686-1701, 2006.

[2] Donahue, et al. *Journal of biomechanical engineering* 124.3: 273-280, 2002.

# EFFECT OF WEIGHT LOSS ON CARTILAGE STRESSES IN OBESE SUBJECTS: DATA FROM THE OSTEOARTHRITIS INITIATIVE (OAI)

*Olesya Klefs<sup>1</sup>, Mika Mononen<sup>2</sup>, Miika Nieminen<sup>1</sup>, Simo Saarakkala<sup>1</sup>, Rami Korhonen<sup>3</sup>*

*1 Research Unit of Medical Imaging, Physics and Technology, Faculty of Medicine, University of Oulu, Medical Research Center, University of Oulu and Oulu University Hospital, Oulu, Finland,*

*2 Department of Applied Physics, University of Eastern Finland, Kuopio, Finland,*

*3 Department of Applied Physics, University of Eastern Finland, Diagnostic Imaging Center, Kuopio University Hospital, Kuopio, Finland*

## Introduction:

It is known that obesity is strongly related to the onset and progression of knee osteoarthritis (OA)<sup>1-2</sup>. Messier et al.<sup>1</sup> detected a significant relationship between weight loss and reduction in compressive knee joint forces. Cumulatively accumulated stresses have been suggested to show locations leading to OA<sup>2</sup>. Therefore, the aim of this study was to find the relationship between the change in body mass index (BMI) and cumulative stresses within articulate cartilage during gait in obese subjects, and compare these results with normal weight controls.

## Methods:

FE models of the knee of three obese subjects (BMI=37±2) and three healthy controls (BMI= 23±1) were created based on 3D-DESS MRI data from the OAI database. Cartilage was considered as a transversely isotropic poroelastic material and meniscus as a transversely isotropic elastic. For each model, generic input of walking was implemented<sup>2</sup>. Weight loss to BMI=24 in obese subjects was simulated. Normalized (to increment sizes during simulation) cumulative maximum principal stresses were calculated during the stance phase of one gait cycle and compared with healthy controls.

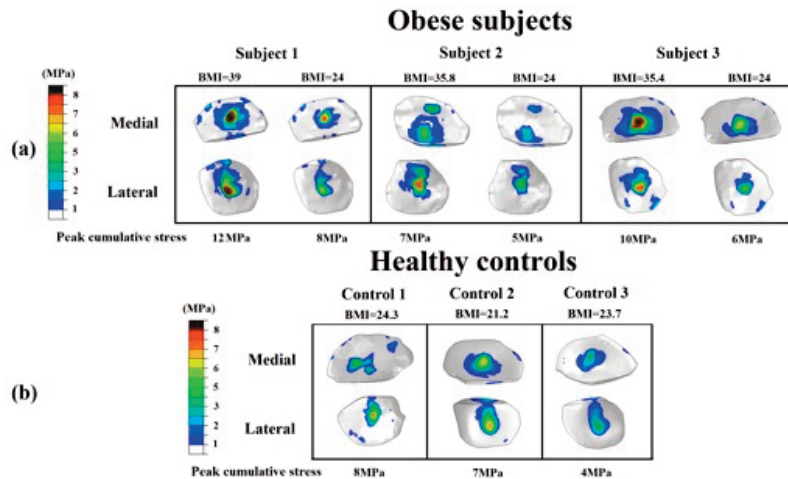
## Results:

Peak cumulative stresses within articular cartilage in obese subjects were 10±2 MPa (Figure 1-a), and after the simulated weight loss, they were 6±1 MPa, which was within similar range as in healthy control subjects (6±2 MPa) (Figure 1-b). Weight loss by 35±3% decreased the peak values of cumulative stresses by 30±6%. Furthermore, areas of high cumulative stresses were also decreased due to simulated weight loss in obese subjects.

## Conclusions:

Substantial reduction in cumulative stresses within articular cartilage was shown in obese subjects after simulated weight loss, being in the same range as in healthy controls. Increased levels of cumulative stresses have been suggested to be an indicator for the onset of knee OA<sup>3</sup>, and this kind of simulation approach presented here may be clinically useful in evaluating subject specific effects of weight loss or surgical operations on knee OA.

*Figure 1: Cumulative maximum principal stresses during the stance phase of gait in (a) three obese subjects with simulated weight loss and (b) three healthy controls.*



## References:

- 1Messier et al. Arthritis Rheum., 52(7), 2Mononen et al. Sci. Rep., 2016, 3Miller et al. Med Sci Sports, 46(3).

# NONLINEAR ELASTICITY IN THE INTERACTION OF LIVING CELLS WITH THEIR MECHANICAL ENVIRONMENT

**Yair Shokef**<sup>1</sup>

<sup>1</sup> Tel-Aviv University, School of Mechanical Engineering and Sackler Center for Computational Molecular and Materials Science, Tel-Aviv, Israel

The elastic cytoskeleton contains molecular motors that produce mechanical forces by which cells attach to and pull on their surroundings. This mechanical interaction is responsible for many aspects of cellular function, from cell spreading and proliferation to stem-cell differentiation and tissue development. Both the cytoskeleton and the extracellular matrix comprise cross-linked, semi-flexible polymeric filaments, and as such they exhibit very nonlinear viscoelastic behavior that includes a power-law stiffening of the elastic moduli with increasing stress. We theoretically consider active force-dipoles embedded in a nonlinear elastic medium, with constitutive relations inspired by fracture mechanics, which obey the strain-stiffening scaling laws of biopolymers. For strong nonlinearity, the differential shear modulus diverges at finite strain, and we may employ a small strain (but strongly nonlinear) expansion. We find that for a single spherical force-dipole, strains change sign with distance, indicating that even around a contractile cell or single molecular motor complex there is radial compression; it is only at long distance that one recovers the linear response in which the medium is radially stretched. The renormalization of the far-field strain field implies that the material's nonlinearity causes the active force dipole to be equivalent to one which is dramatically larger and stronger. To investigate the mechanical interaction between several such cells in a nonlinear medium, we consider an array of active cells. Assuming the deformation around each cell is spherically symmetric, we connect the far-field strain field to the boundary condition of vanishing displacement on the plane of symmetry between neighboring cells. Our results explain experimental measurements of long-distance inter-cellular interactions on fibrin coated substrates, and suggest novel interpretations of the important question of whether cells regulate the stress that they exert or the deformation around them.

## References:

- [1] Y. Shokef, S. A. Safran, *Phys. Rev. Lett.* 108, 178103 (2012).
- [2] Y. Shokef, S. A. Safran, *Phys. Rev. Lett.* 109, 169901 (2012).
- [3] D. Ben-Yaakov, R. Golkov, Y. Shokef, S. A. Safran, *Soft Matter* 11, 1412 (2015).
- [4] D. Ben-Yaakov, Y. Shokef, S. A. Safran, *in preparation*.

# MECHANICS OF CELL ADHESION: PRINCIPLES OF SYMMETRY BREAKING AND SELF-POLARIZATION

**Assaf Zemel**<sup>1</sup>

*<sup>1</sup> Institute of Dental Sciences and Fritz Haber Research Center for Molecular Dynamics, Jerusalem, Israel*

Living cells are round in suspension but once they adhere to a solid matrix their shape spontaneously evolves to the cells' native and functional form. Research in recent years has highlighted the role of the matrix rigidity in governing this process; including the acquisition of cell shape and regulation of cytoskeleton structure and polarity. When spreading on soft substrates cells typically remain round and small while on substrates of intermediate rigidity they often optimally elongate. Matrix rigidity has also been shown to regulate the polarization of the cytoskeleton in parallel to the long axis of the cell. These observations indicate that cell morphology, internal structure (and fate) are regulated by means of a force balance between the cell and the environment. Theoretical work will be presented describing few generic principles of force balance that may play a role in the symmetry breaking and acquisition of cell morphology and internal structure. This includes the effects of matrix rigidity on the spreading area and shape anisotropy (elongation) of stationary and migrating cells, the effects of matrix rigidity on the spontaneous alignment of actomyosin forces in the cytoskeleton, as well as the possible elastic effects that the cell nucleus may have in the determination of cytoskeleton organization in its vicinity.

# SHAPE REGULATION GENERATES ELASTIC INTERACTION BETWEEN ACTIVE FORCE DIPOLES

Roman Golkov<sup>1</sup>, Yair Shokef<sup>2</sup>

<sup>1</sup> Tel-Aviv University, Tel-Aviv, Israel,

<sup>2</sup> Tel-Aviv University, School of Mechanical Engineering and Sackler Center for Computational Molecular and Materials Science, Tel-Aviv, Israel

Experiments show that the rigidity of the extracellular matrix influences the interactions between living cells [1]. On soft gels cells tend to touch and remain in contact, while on stiff gels cells contact and migrate away from each other. In our coarse-grained model we represent cells by spherical force dipoles applying contractile forces or displacements on their surrounding linearly-elastic infinite medium [2,3,4]. The elastic interaction energy vanishes for dipoles of any shape that apply isotropic forces or displacements [5,6].

To identify an interaction mechanism we distinguish between "passive" and "active" force dipoles. "Passive" dipoles apply constant isotropic forces or displacements on their surface, while in our model "active" dipoles alter the applied forces and displacements in accordance to the changes in their mechanical environment, and in order to preserve their spherical shape [7].

In our general solution for two "active" cells, we may include or exclude each of the terms that regulate the volume and position and thus consider four scenarios of mechanical regulation. Regulation of the cell volume sets the sign of the interaction energy and regulation of cell position determines the exponent in the algebraic decay of the interaction energy with the cell-cell separation. Namely when motion is actively regulated the exponent is  $-4$ , and when it is not, the exponent is  $-6$ . The latter case is similar to van der Waals interactions between induced electric dipoles.

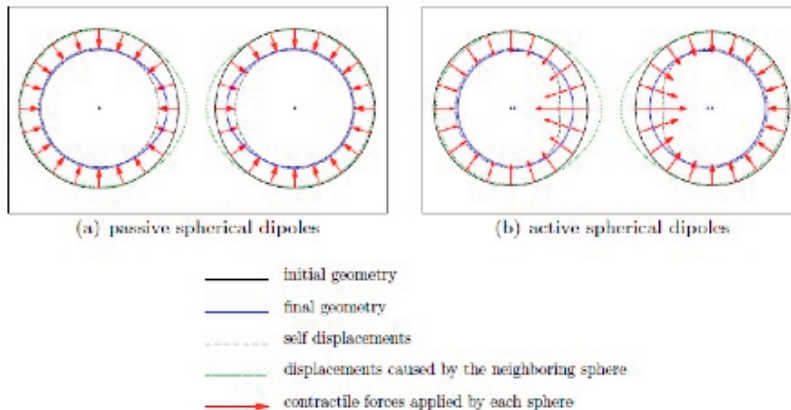


Figure 1: Two contracting cells in an infinite elastic medium: (a) passive cells apply isotropic force (b) active cells regulate the force they apply in order to remain spherical even in the presence of other cells.

## References:

- [1] C. A. Reinhart-King, M. Dembo, D. A. Hammer, *Biophys. J* 95 (12) (2008) 6044.
- [2] Y. Shokef, S. A. Safran, *Phys. Rev. Lett.* 108 (2012) 178103.
- [3] Y. Shokef, S. A. Safran, *Phys. Rev. Lett.* 109 (2012) 169901.
- [4] D. Ben-Yaakov, R. Golkov, Y. Shokef, S. A. Safran, *Soft Matter* 11 (2015) 1412.
- [5] G.Sines, R.Kikuchi, *Acta Metallurgica* 6 (1958) 500-508.
- [6] U.S.Schwarz, S.A.Safran, *Phys. Rev. Lett.* 88 (2002) 048102.
- [7] R.Golkov, Y.Shokef, *arXiv:1601.03655*

# CELLULAR MECHANOSENSITIVITY: CELL REORIENTATION UNDER CYCLIC STRETCHING

**Eran Bouchbinder**<sup>1</sup>

<sup>1</sup> Weizmann Institute of Science, Rehovot, Israel

Mechanical cues from the extracellular microenvironment play a central role in regulating the structure, function and fate of living cells. Nevertheless, the precise nature of the mechanisms and processes underlying this cellular mechanosensitivity remains a basic open problem. In this talk we focus on one of the most striking manifestations cellular mechanosensitivity – cell reorientation in response to cyclic stretching. We first show that existing approaches are incompatible with our extensive measurements of cell reorientation. We then propose a new theory which focusses on the cell's stored elastic energy, corresponding to a 2D anisotropic linear elastic material, whose variation with the cell's orientation drives the dissipative cell reorientation dynamics. Our theory is in excellent quantitative agreement with the complete temporal reorientation dynamics of individual cells, measured over a wide range of experimental conditions, thus elucidating a basic aspect of mechanosensitivity.

## References:

Ariel Livne, Eran Bouchbinder and Benjamin Geiger,

“Cell reorientation under cyclic stretching”, *Nature Communications* 5, 3938 (2014).

# MODEL OF CELL-CELL MECHANOSENSING IN NON-LINEAR FIBROUS MATRIX

**Ayelet Lesman**<sup>1</sup>, **Jacob Notbohm**<sup>2</sup>, **Phoebus Rosakis**<sup>3</sup>, **David Tirrell**<sup>4</sup>, **Guruswami Ravichandran**<sup>5</sup>

<sup>1</sup> Tel Aviv University, School of Mechanical Engineering, Tel Aviv, Israel,

<sup>2</sup> University of Wisconsin–madison, Department of Engineering Physics, Madison, Wisconsin, United States,

<sup>3</sup> University of Crete, Department of Theoretical and Applied Mathematics, Crete, Greece,

<sup>4</sup> California Institute of Technology, Division of Chemistry and Chemical Engineering, Pasadena, California, United States,

<sup>5</sup> California Institute of Technology, Division of Engineering and Applied Science, Pasadena, California, United States

Biological cells sense and respond to mechanical forces, but how such a mechanosensing process takes place in a nonlinear inhomogeneous fibrous matrix remains unknown. We show that cells in a fibrous matrix induce deformation fields that propagate over a longer range than predicted by linear elasticity. Synthetic, linear elastic hydrogels used in many mechanotransduction studies fail to capture this effect. We develop a nonlinear microstructural finite-element model for a fibre network to simulate localized deformations induced by cells. The model captures measured cell-induced matrix displacements from experiments and identifies an important mechanism for long-range cell mechanosensing: loss of compression stiffness owing to microbuckling of individual fibres. We show evidence that cells sense each other through the formation of localized intercellular bands of tensile deformations caused by this mechanism.

## ACTIVE CONTRACTION OF BIOLOGICAL FIBER NETWORKS

**Pierre Ronceray<sup>1</sup>, Chase Broedersz<sup>2</sup>, Martin Lenz<sup>3</sup>**

*1 Laboratoire de Physique Théorique et Modèles Statistiques (Lptms), Cnrs, Univ. Paris-Sud, Université Paris-Saclay, Orsay, France,*

*2 Arnold-Sommerfeld-Center for Theoretical Physics and Center for Nanoscience, Ludwig-Maximilians-Universität München, München, Germany,*

*3 Lptms, Cnrs, Univ. Paris-Sud, Université Paris-Saclay, Orsay, France*

Large-scale force generation is essential for biological functions such as cell motility, embryonic development, and muscle contraction. In these processes, forces generated at the molecular level by motor proteins are transmitted by disordered fiber networks, resulting in large-scale active stresses. While fiber networks are well characterized macroscopically, this stress generation by microscopic active units is not well understood. I will present a comprehensive theoretical study of force transmission in these networks. I will show that the linear, small-force response of the networks is remarkably simple, as the macroscopic active stress depends only on the geometry of the force-exerting unit. In contrast, as non-linear buckling occurs around these units, local active forces are rectified towards isotropic contraction and strongly amplified. This stress amplification is reinforced by the networks' disordered nature, but saturates for high densities of active units. I will show that our predictions are quantitatively consistent with experiments on reconstituted tissues and actomyosin networks, and that they shed light on the role of the network microstructure in shaping active stresses in cells and tissue.

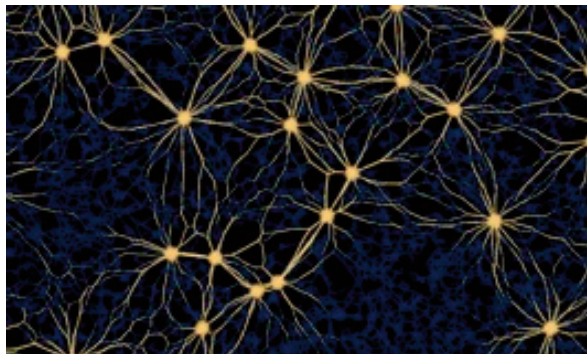


*Figure Caption: Numerical simulation of a lattice model for actively contracting biological fiber networks. Strong “active units” (yellow circles) pull on the surrounding elastic network, remodeling it into star-shaped patterns of tensed fibers that indicate stress amplification.*

### References:

Pierre Ronceray, Chase P. Broedersz and Martin Lenz, Fiber networks amplify active stress, Proc. Nat. Acad. Sci. USA, 2016. doi: 10.1073/pnas.1514208113

# BROKEN DETAILED BALANCE AT MESOSCOPIC SCALES IN ACTIVE BIOLOGICAL SYSTEMS

**Chase Broedersz**<sup>1</sup>

*<sup>1</sup> Arnold-Sommerfeld-Center for Theoretical Physics and Center for Nanoscience, Ludwig-Maximilians-Universität München, München, Germany*

Systems in thermodynamic equilibrium are not only characterized by time-independent macroscopic properties, but also satisfy the principle of detailed balance in the transitions between microscopic configurations. Living systems function out of equilibrium and are characterized by directed fluxes through chemical states, which violate detailed balance at the molecular scale. It is unclear, however, to what extent the dynamics of cellular assemblies at mesoscopic scales violate detailed balance, even if the system is out of equilibrium. We will introduce a method to probe for broken detailed balance and demonstrate how such non-equilibrium dynamics is manifest at the mesoscopic scale. The periodic beating of an isolated flagellum from *Chlamydomonas reinhardtii* exhibits probability flux in the phase space of shapes. With a model, we show how the breaking of detailed balance can also be quantified in stationary, non-equilibrium stochastic systems in the absence of periodic motion. We further demonstrate such broken detailed balance in the non-periodic fluctuations of primary cilia of epithelial cells and actin-myosin networks. Our analysis provides a general tool to identify non-equilibrium dynamics in cells and tissues.

# A CHEMO-MECHANICAL FREE-ENERGY-BASED APPROACH TO MODEL DUROTAXIS AND EXTRACELLULAR STIFFNESS-DEPENDENT CONTRACTION AND POLARIZATION OF CELLS

Vivek Shenoy<sup>1</sup>, Hailong Wang<sup>1</sup>, Xiao Wang<sup>1</sup>

<sup>1</sup> University of Pennsylvania, Philadelphia, United States

We propose a chemo-mechanical model based on stress-dependent recruitment of myosin motors to describe how the contractility, polarization and strain in cells vary with the stiffness of their surroundings and their shape. A contractility tensor, which depends on the distribution of myosin motors, is introduced to describe the chemical free energy of the cell due to myosin recruitment. We explicitly include the contributions to the free energy that arise from mechanosensitive signaling pathways (such as the SFX, Rho-Rock and MLCK pathways) through chemo-mechanical coupling parameters. Taking the variations of the total free energy, which consists of the chemical and mechanical components, in accordance with the second law of thermodynamics provides equations for the temporal evolution of the active stress and the contractility tensor. We have numerically implemented our free energy based approach to model spatial distribution of strain and contractility in (a) cells supported by flexible microposts, (b) cells on 2D substrates and (c) in 3D matrices. We demonstrate how the polarization of the cells and the orientation of stress fibers can be deduced from the eigenvalues and eigenvectors of the contractility tensor. Our calculations suggest that the chemical free energy of the cell decreases with the stiffness of the extracellular environment as the cytoskeleton polarizes in response to stress-dependent recruitment of molecular motors. The mechanical energy, which includes the strain energy and motor potential energy, however increases with stiffness, but the overall energy is lower for cells in stiffer environments. This provides a thermodynamic basis for durotaxis, whereby cells preferentially migrate towards stiffer regions of the extracellular environment. Our models also explain, from an energetic perspective, why the shape of the cells can change in response to stiffness of the surroundings. Along with making testable predictions, we have estimated the magnitudes of the chemo-mechanical coupling parameters for myfibroblasts based on data reported in literature.

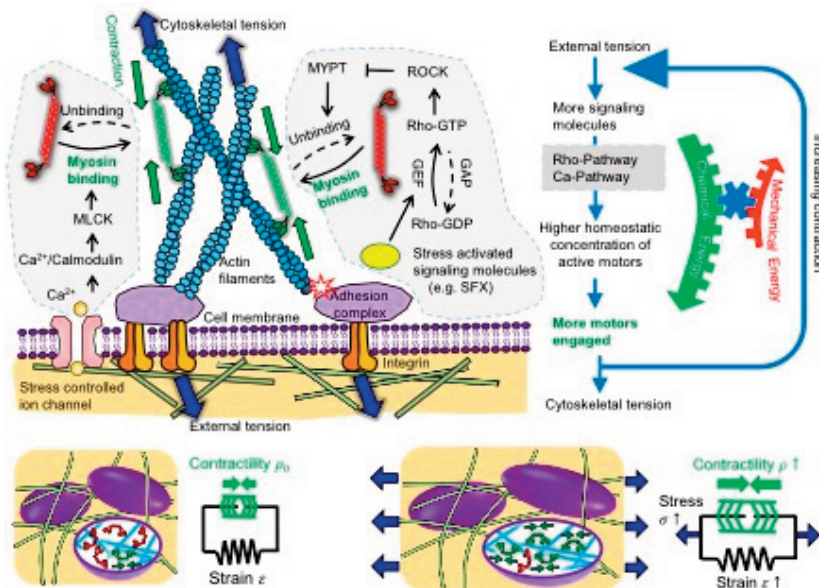


Figure 1: Schematic depiction of the chemo-mechanical coupling and stress-dependent feedback mechanisms in our model.

## FLUCTUATIONS SPECTRUM IN ACTIVE GELS

Adar Sonn-Segev<sup>1</sup>, Anne Bernheim-Groswasser<sup>2</sup>, Yael Roichman<sup>3</sup>

<sup>1</sup> University of Oxford, Oxford, United Kingdom,

<sup>2</sup> Department of Chemical Engineering, Ilse Kats Institute for Nanoscale Science and Technology, Beer Sheva, Israel,

<sup>3</sup> Tel Aviv University, Tel Aviv, Israel

Active gels inspired from the cell's skeleton are a paradigmatic model to understand the complex mechanisms governing key cellular operations/processes such as motion and mechanics<sup>1</sup>. These active gels are also attractive soft matter systems with which to study the physics and statistical mechanics of non-equilibrium materials. Well-studied examples of such materials are networks constructed by the structural protein actin and its associated molecular motors myosin II. These active gels undergo structural evolution together with stochastic behavior characterized by non-equilibrium fluctuations, due the presence of the active motors. The simultaneous investigation of motor-induced mechanics and stochastic effects is challenging due to the continuous evolvement of these gels. Here, we present long-lived active gels which reach steady-state active dynamics, allowing us to decouple the effect of motor proteins on the mechanical properties of the gels from the random stochastic events induced by the same motor proteins. We find that the mechanical properties and the reorganization dynamics of active cytoskeleton gels exhibit the same dependence on motor protein concentration regardless of the scale of their features. However, the statistics and type of motor induced active events depends significantly on their feature size. We model the fluctuation spectrum as a series of active discrete events coupled with thermal motion (see figure).

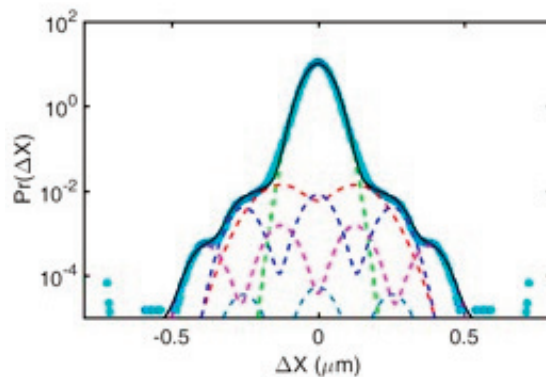


Figure Caption: Fluctuation spectrum of a tracer bead in an active acto-myosin network at steady state. The measured fluctuation spectrum (cyan circles) is modeled (solid black line) as a series of consecutive discrete active events (series components in dashed lines)

### Acknowledgments:

We thank Nir Gov, Haim Diamant, Sam Safran, and especially Yair Shokef for useful discussion.

### References:

1) Yaron ideses, Adar Sonn-Segev, Yael Roichman, and Anne bernheim-Groswasser, *Soft matter*, 9, 7127-7137 (2013).

# QUANTITATIVE CHARACTERIZATION OF THE NUCLEAR REFRACTIVE INDEX

**Mirjam Schürmann**<sup>1</sup>, **Paul Müller**<sup>1</sup>, **Jana Scholze**<sup>1</sup>, **Chii J. Chan**<sup>2</sup>, **Jochen Guck**<sup>2</sup>

<sup>1</sup> Biotechnology Center TU-Dresden, Dresden, Germany,

<sup>2</sup> Biotechnology Center TU-Dresden, Cavendish Laboratory, University of Cambridge, Dresden, Germany

Material properties of individual cells are established intrinsic markers to characterize and distinguish cell populations. This includes mechanical properties of single cells that are analysed in our research group with novel techniques; but also the refractive index (RI) of individual suspended cells to distinguish for example cell differentiation, infection or cancerous stages. The RI of inner cellular compartments, however, has not been comprehensively studied yet. Regarding the nuclear RI, there are contradictory trends reported in the literature. An early study of the nuclear RI found higher values compared to the cytoplasm, however recent tomographic approaches point towards a lower nuclear RI [1,2,3]. Here, we used digital holographic microscopy to show that the RI of isolated nuclei of four different cell lines is lower compared to the RI of the complete cells [4]. We furthermore found an inverse linear relationship between the volume and the RI of the nuclei by treatments with drugs interfering with the chromatin conformation and by exposing them to different osmotic and electrostatic conditions. This suggests, that the RI of the nucleus is mostly governed by the material density. To further investigate the RI of inner cellular compartments in their natural environment we performed phase imaging tomography of single cells in suspension. For this, the cells were rotated in an opto-fluidic cell rotator by a combination of a dual-beam laser trap and a microfluidic flow. During this rotation quantitative phase images were taken at different orientations and subsequently analysed to yield the 3D RI map by a backpropagation algorithm employing the Rytov-approximation [5]. Taken together, the results give an insight into the RI distribution within cells with obvious implications for biological questions, but also for technological advances of optical manipulation of cells or for adaptive optics where the RI distribution of individual cells plays a crucial role.

## References:

- [1] A. Brunsting and P. F. Mullaney, *Biophysical Journal*, 14(6), 439–53 (1974).
- [2] W. Choi, C. Fang-Yen, K. Badizadegan, S. Oh, N. Lue, R. R. Dasari, and M. S. Feld, *Nature Methods*, 4(9), 717–719 (2007).
- [3] N. Lue, W. Choi, G. Popescu, K. Badizadegan, R. R. Dasari, and M. S. Feld, *Optics Express*, 16(20), 16240–16246 (2008).
- [4] M. Schürmann, J. Scholze, P. Müller, J. Guck and C.J. Chan, *Journal of Biophotonics*, (2016)
- [5] P. Müller, M. Schürmann and J. Guck, *BMC Bioinformatics*, 16, 1-9, (2015)

# MIGRATION, FORCE GENERATION AND MECHANOSENSING OF TUMOUR CELLS IN 3-DIMENSIONAL ENVIRONMENTS

**Ben Fabry**<sup>1</sup>

*<sup>1</sup> Department of Physics, University of Erlangen-Nuremberg, Erlangen, Germany*

The migration of cells through the fibrous network of the extracellular matrix is an integral part of many biological processes, including tissue morphogenesis, wound healing and cancer metastasis. To migrate through the pores of the dense meshwork of the extracellular matrix, cells must generate considerable forces that are exerted on the matrix. Accurate measurement of these traction forces is crucial for understanding the invasion of cancer cells or the migration of immune cells in tissue.

Traction forces can be estimated by culturing cells in a three-dimensional (3D) substrates with known stiffness and measuring the substrate deformations as the cells adhere and migrate. Present methods for traction-force reconstruction rely on the linear force-displacement response of the substrate. However, the connective tissues of most organs are highly nonlinear, as are reconstituted tissue equivalents such as collagen and fibrin gels, both of which stiffen strongly under shear and collapse with an abnormal apparent Poisson's ratio greater than 1 when stretched.

We developed a method for measuring cell traction forces in physiologically relevant 3D biopolymer networks with highly nonlinear mechanical properties. This method is based on a finite-element approach and a constitutive equation that captures the complex mechanical properties of diverse biopolymers such as collagen gels, fibrin gels and Matrigel. With this method, we studied the contractility, migration and shape changes of breast carcinoma cells in collagen gels with differing concentrations and matrix stiffness. Our measurements show that breast carcinoma cells generated nearly constant forces regardless of the collagen concentration and matrix stiffness. Furthermore, time-lapse force measurements showed that these cells migrated in a gliding motion with alternating phases of high and low contractility, elongation, migratory speed and persistence.

# PROXIMITY OF METASTATIC CELLS STRENGTHENS THE MECHANICAL INTERACTION WITH THEIR ENVIRONMENT

**Yulia Merkher**<sup>1</sup>, **Daphne Weihs**<sup>2</sup>

<sup>1</sup> Technion – Israel Institute of Technology, Biorheology and Cell Mechanics Lab, Haifa, Israel,

<sup>2</sup> Technion – Israel Institute of Technology, Haifa, Israel

The main cause of cancer-related deaths is metastasis - spreading of cancer cells to different sites in the body. A critical step in metastasis formation is invasion of cells through the surrounding tissue. During invasion, cancer cells change their shape and apply forces. We have previously identified that about 30% of single, metastatic, breast cancer cells will indent impenetrable synthetic, non-degradable, polyacrylamide gels, when gel stiffness is in the range 1-10 kPa. By measuring the depth of indentation of an initially flat gel and monitoring time-dependent microscopic changes in cell morphology we were able to distinguish between benign and metastatic cells, also identifying their metastatic potential (MP) [1,2]; benign cells do not indent the gels. Recent works have indicated that metastases from solid tumors occur predominantly by collective cell invasion. Hence, in the current study we evaluate the mechanical interactions of cell clusters with the impenetrable gel. We observe that indenting subpopulations of metastatic cells are doubled in clusters, and cells are also indent more deeply; this increases likelihood to successfully form metastasis in the body. Concurrently, double the fraction of high MP cells indent gels as compared to low MP cells, while benign cells do not indent even in clusters. We also show that the gel-platform can be used to determine the time-dependent impact of chemotherapeutics on the cells ability to apply forces and indent gels. Our approach can provide a rapid, mechanical prediction of the likelihood for invasiveness of cancer cells and can further be applied in a patient-specific approach, thus providing a personalized prognosis that may improve treatment of cancer patients and increase their life expectancy.

## References:

1. Revital Kristal-Muscal, Liron Dvir, and Daphne Weihs, "Metastatic cancer cells tenaciously indent impenetrable, soft substrates", *New Journal of Physics* 15, 035022 (2013).
2. Liron Dvir, Ronen Nissim, Martha Alvarez, and Daphne Weihs, "Quantitative measures to reveal coordinated cytoskeleton-nucleus reorganization during in vitro invasion of cancer cells", *New Journal of Physics* 17, 043010 (2015).

## ISOTHERMAL LANGEVIN DYNAMICS IN SYSTEMS WITH POWER-LAW SPATIALLY-DEPENDENT FRICTION

**Shaked Regev**<sup>1</sup>, **Niels Grønbech-Jensen**<sup>2</sup>, **Oded Farago**<sup>3</sup>

<sup>1</sup> Ben Gurion University, Be'er Sheva, Israel,

<sup>2</sup> Department of Mathematics, Department of Mechanical and Aerospace Engineering, University of California, Davis, United States,

<sup>3</sup> Ben Gurion University of the Negev, Beer Sheva, Israel

We study the dynamics of Brownian particles in a heterogeneous one-dimensional medium with a spatially-dependent diffusion coefficient of the form  $D(x) \sim |x|^c$ , at constant temperature. The particle's probability distribution function (PDF) is calculated both analytically, by solving Fick's diffusion equation, and from numerical simulations of the underdamped Langevin equation. At large times, the PDFs calculated by both approaches yield identical results, corresponding to subdiffusion for  $c < 0$ , and superdiffusion for  $0 < c < 1$ . For  $c > 1$ , the diffusion equation predicts that the particles accelerate. Here, we show that this phenomenon, previously considered in several works as an illustration for the possible dramatic effects of spatially-dependent thermal noise, is unphysical.

We argue that in an isothermal medium, the motion cannot exceed the ballistic limit ( $\langle x^2 \rangle \sim t^2$ ). The ballistic limit is reached when the friction coefficient drops sufficiently fast at large distances from the origin, and is correctly captured by Langevin's equation.

# INTEGRATING CARDIAC BIOMECHANICS AND MR ELASTOGRAPHY

**David Nordsletten**<sup>1</sup>

<sup>1</sup> King's College London, London, United Kingdom

Personalised models of cardiac mechanics have evolved into a powerful tool for studying the human heart in health and disease [1]. Combining detailed information on the heart kinematics extracted from medical images, with mathematical models of cardiac function, patient-specific models provide a mathematical representation of individual hearts. As model parameters are linked to intrinsic tissue properties such as stiffness and contractility, unique and accurate parameter estimates are a prerequisite for the potential translation of personalised models to the clinic.

In parallel, magnetic resonance elastography (MRE) has evolved into a powerful tool for interrogating material stiffness [2]. MRE has been exploited in the liver, breast, and brain using measured periodic waves to extract material stiffness properties. Transducing waves via external vibrations, MRE provides a more direct measure of the characteristics of tissues and their potential diseases. Integrating this work into the heart is complicated by a myriad of challenges including the inherent cardiac motion of the heart, evolving material properties due to the contractile state of the muscle, and the nonlinear effects of deformation on the apparent stiffness of the material.

In this talk, we discuss the merger of these two worlds, bridging between the nearly quasi-static model-based assessment of heart function and the high frequency wave-based assessment. In particular, we discuss the simple influence of deformation on apparent stiffness, explaining both from the realm of traditional wave mechanics and biomechanical theory. Illustrating this relationship, we present data in phantom materials that confirm our theoretical understanding of nonlinear biomechanics and its impact on MRE measures. We conclude with future outlook and the potential of integrated biomechanical modeling and MRE for assessment of the heart.

## Acknowledgments:

Authors acknowledge funding from the Engineering and Physical Sciences Research Council (EP/N011554/1).

## References:

[1] Asner et al. Estimation of passive and active properties in the human heart using 3D tagged MRI, *BMMB*. 10.1007/s10237-015-0748-z

[2] Sinkus, R., et al. High-resolution tensor MR elastography for breast tumour detection. *Physics in medicine and biology* 45.6 (2000): 1649.

# MAGNETIC RESONANCE ELASTOGRAPHY OF THE BRAIN

**Katharina Schregel<sup>1</sup>, Eva Wuerfel<sup>1</sup>, Dirk Petersen<sup>2</sup>, Jens Wuerfel<sup>3</sup>, Ralph Sinkus<sup>4</sup>**

<sup>1</sup> University Medicine Goettingen, Goettingen, Germany,

<sup>2</sup> Institut für Neuroradiologie, Lübeck, Germany,

<sup>3</sup> Medical Image Analysis Center (Miac Ag), Basel, Switzerland,

<sup>4</sup> Kings College London, Imaging Sciences & Biomedical Engineering Division Kings College, London, United Kingdom

## Introduction

Palpation is a valuable diagnostic tool to detect tissue pathologies. The skull however limits brain palpation. Magnetic Resonance Elastography (MRE) allows for objective quantification of brain biomechanics in vivo and non-invasively<sup>1</sup>. Many neurodegenerative diseases like multiple sclerosis (MS) for example lead to changes of normal tissue structure and influence the biomechanical properties. This should render them detectable with MRE.

## Methods

To test this, we introduced an animal model of MS. Toxic demyelination was evoked in a group of C57BL/6 mice<sup>2</sup>. These animals were compared to healthy controls. T2w MRI- and full 3D-MRE-exams were performed three-weekly on a 7T animal scanner. For MRE, mechanical shear waves with a frequency of 1 kHz are sent into the brain. Wave propagation leads to shear deformation of brain tissue. This is measured using a spin echo sequence with a motion-encoding gradient of the same frequency as the excitation and in the direction of wave propagation. Viscoelastic properties are reconstructed from the displacement field. After each scanning period, three animals of each group were sacrificed for histopathology.

## Results

Reconstructed MRE-maps depict the underlying brain anatomy well. The corpus callosum appeared rather stiff, while the liquid-filled ventricles exhibited low shear properties (Fig.). Control animals showed an initial increase of viscoelasticity. In treated animals, a significant decrease of viscoelasticity was observable. Histopathology depicted progressive demyelination and degradation of the extracellular matrix structure.

## Conclusion

Brain MRE is feasible and offers a virtual brain palpation. Viscoelasticity decreases with demyelination and extracellular matrix degradation. Hence, MRE is a promising tool for diagnosis and monitoring of neurodegenerative diseases.

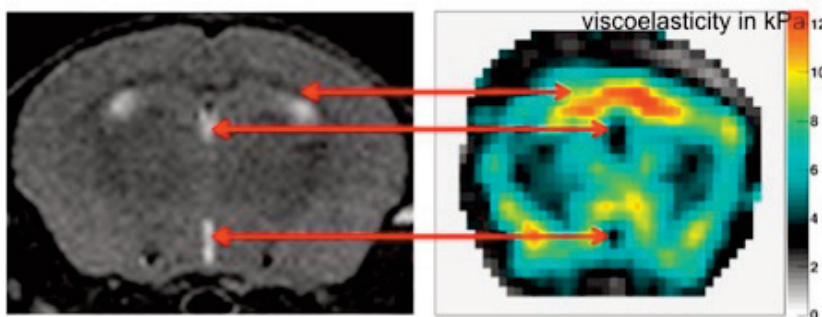


Figure Caption: T2w-MRI image and corresponding MRE-map. These maps graphically visualize brain anatomy

## References:

<sup>1</sup> Green MA et al. (2008) NMR Biomed

<sup>2</sup> Schregel K et al. (2012) PNAS

# PAEDIATRIC LIVER VISCOELASTIC PROPERTIES DIFFER FROM ADULTS: A MULTIFREQUENCY MR ELASTOGRAPHY STUDY

Emily Etchell<sup>1</sup>, Lauriane Juge<sup>1</sup>, Alice Hatt<sup>2</sup>, Ralph Sinkus<sup>3</sup>, Lynne Bilston<sup>1</sup>

<sup>1</sup> Neura & Unsw, Sydney, Australia,

<sup>2</sup> Neura, Sydney, Australia,

<sup>3</sup> Kings College London, Imaging Sciences & Biomedical Engineering Division Kings College, London, United Kingdom

Mechanical properties of the liver are important for a diverse range of real world biomechanics applications – from predicting liver injuries to assessing stiffness changes due to fibrotic liver disease. Data for children, however, has been scarce. The aim of this study was to determine how the shear modulus of the healthy human liver varied with age during childhood, and compare to adults.

Magnetic resonance elastography was used to measure the shear modulus in the liver of 13 healthy children (aged 5-14 years), 11 healthy adolescents (aged 14-18 years) and 10 young healthy adults (aged 22-36 years). Measurements were made at three frequencies (28, 56, and 84Hz) on a 3T MRI scanner, using a fast-field-echo based elastography sequence<sup>1</sup>, using a 32 element torso coil and custom vibration transducer synchronized to the imaging sequence. Shear moduli ( $G^*$ ) for each frequency were calculated using in-house inversion software<sup>2</sup>.

At 56Hz and 85Hz, the liver shear modulus increased with age (Spearman,  $r = 0.38$ ,  $P = 0.03$ , and  $r = 0.54$ ,  $P = 0.001$ , respectively). At 56Hz & 84Hz, the shear modulus in children and adolescents was lower than in adults (56 Hz:  $G^*$ children =  $2.2 \pm 0.3$  kPa,  $G^*$ adolescents =  $2.2 \pm 0.2$  kPa,  $G^*$ adults =  $2.6 \pm 0.3$  kPa, ANOVA,  $P = 0.009$ ; 84Hz:  $G^*$ children =  $5.6 \pm 0.8$  kPa,  $G^*$ adolescents =  $6.5 \pm 1.2$  kPa,  $G^*$ adults =  $7.8 \pm 1.2$  kPa, ANOVA,  $P = 0.0003$ ). As in adults, liver shear modulus in children increased with frequency, but it varied less with frequency in children and adolescents than adults (ANOVA,  $P = 0.0009$ ).

We conclude that liver stiffness in children and adolescents is lower and varies less with frequency than in adults. Stiffness increases with age during normal development, approaching adult values during adolescence.

## Acknowledgments:

LB is supported by an NHMRC Fellowship and this research was supported the Australian Research Council.

## References:

1. Garteiser P et al. *NMR Biomed* 2013;26(10):1326-1335.
2. Sinkus R et al. *Magn Reson Med* 2007;58(6):1135-1144.

# FUNCTIONAL CHANGES IN THE SHEAR MODULUS OF THE MOUSE BRAIN CORTEX OBSERVED WITH ELECTRICAL STIMULATION OF THE HIND LIMB USING MAGNETIC RESONANCE ELASTOGRAPHY (MRE)

**Samuel Patz**<sup>1</sup>, **Navid Nazari**<sup>2</sup>, **Paul Barbone**<sup>2</sup>, **Ralph Sinkus**<sup>3</sup>

<sup>1</sup> Harvard Medical School, Brigham & Women's Hospital, Boston, United States,

<sup>2</sup> Boston University, Boston, United States,

<sup>3</sup> Kings College London, Imaging Sciences & Biomedical Engineering Division Kings College, London, United Kingdom

## Purpose:

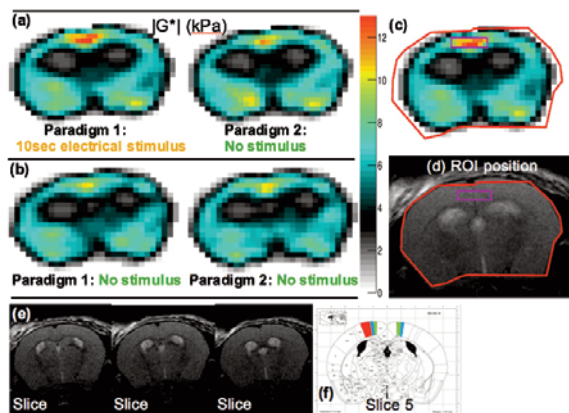
Using MRE, evaluate a new contrast mechanism associated with changes in the brain's shear modulus due to functional stimuli.

## MRI:

A spin-echo MRE sequence [1] was modified to allow two interleaved functional paradigms: P1/P2 for stimulation/no stimulation, respectively. Each paradigm is active 10s to avoid neuronal habituation. The k-space data acquisition was segmented into 10s blocks to be compatible with this approach. For each k-space segment, P1 and P2 are applied sequentially before advancing to the next k-space segment. A period of 1.8s was allowed for hemodynamic equilibrium between paradigms. 8 wave phases in x, y, and z, 2 paradigms, and 9 slices account for 432 images, acq. time= 58 min.

## Animal:

5 healthy black mice were studied. Each was anesthetized with isoflurane with the level adjusted for a respiratory rate of ~40/min. For electrical stimulation, two 30 gauge needles were inserted in a hind limb and during P1, a constant current was supplied: ~1mA, 3Hz, pulse width ~250@.s. A control scan was also performed where no stimulus was applied for either paradigm. The MRE apparatus was modified from an earlier version [1]. The modification uses a cage assembly that clamps the mouse head and is mounted on pivots. Vibration frequency=1kHz.



## Results:

The Figure shows an example of mouse brain data. A 20% increase in  $|G^*|$  was observed for stimulation (a) in the somatosensory and motor cortex areas, whereas no difference was observed in the control (b). (c) & (d) show ROI placement; (e) shows the corresponding anatomical scans for the MRE maps, which are averaged over slices 4-6. (f) shows a corresponding cross section from a mouse atlas [2] with the contralateral somatosensory cortex shown in red and the bilateral primary (M1) and secondary (M2) motor cortex shown in blue and green, respectively. Similar results were seen in 3 of the 5 mice studied. Note  $|G^*|$  is 10% lower in (b) than the “no stimulus” (a) scan, possibly due to incomplete hemodynamic relaxation in (a).

## Conclusion:

A 20% change in  $|G^*|$  was observed. This is ~10x larger than what is observed with fMRI.

## Acknowledgments:

We thank K Shregel, T Johnson, M Viapiano, M Nowicki, S Mukundan, for their assistance.

## References:

1. Shregel et al., Proc Natl Acad Sci USA, 2012.
2. Paxinos and Franklin. The Mouse Brain in Stereotaxic Coordinates. 2001: Academic Press.

# INVESTIGATING THE PERFORMANCE OF A NEW ULTRASONIC ELASTOGRAPHY TECHNIQUE FOR CARDIAC STIFFNESS ASSESSMENT THROUGH FINITE ELEMENT SIMULATIONS

Annette Caenen<sup>1</sup>, Mathieu Pernot<sup>2</sup>, Darya Shcherbakova<sup>1</sup>, **Pascal Verdonck**<sup>3</sup>, Patrick Segers<sup>1</sup>, Abigail Swillens<sup>1</sup>

<sup>1</sup> Ibitech - Biommeda, Department of Electronics and Information Systems, Ghent University, Ghent, Belgium,

<sup>2</sup> Institut Langevin, Ecole Supérieure de Physique et de Chimie Industrielles, Cnrs Umr 7587, Inserm U979, Paris, France,

<sup>3</sup> Ibitech - Biommeda, Department of Electronics and Information Systems, Ghent University, Ghent University, Ghent, Belgium

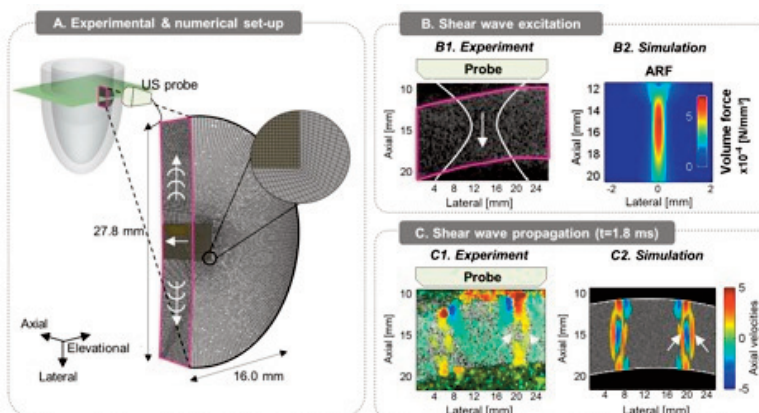
Shear Wave Elastography is a non-invasive ultrasound technique for stiffness quantification, clinically proven successful for breast cancer and liver fibrosis diagnosis. It induces a vibration source inside the tissue by appropriate focusing of acoustic energy. This generates shear waves (SW's) with their propagation speed linked to the tissue stiffness. However, cardiac application of this technique is challenging, as the ventricular geometry and anisotropic tissue generate complex wave phenomena, causing issues for current tissue characterization algorithms. To study these complex SW phenomena in the heart, we used a combined experimental and numerical approach in a left ventricular model.

For the experiments, a ventricular phantom was created using a 10% polyvinyl alcohol solution (fig. A). SW's were excited in this phantom using a focused high-intensity ultrasonic beam, creating an acoustic radiation force, cfr. fig. B1. The phantom's stiffness was determined via uniaxial tensile tests.

For the simulations, fig. A illustrates the corresponding numerical model created in the finite element software Abaqus. The acoustic force from the experiment was computed in an ultrasound simulator (Field II) and imposed as a volume force in Abaqus (cfr. fig. B2). An elastic material law was derived from the mechanical testing.

The modeled SW propagation (fig. C2) corresponds qualitatively well with the experiment (fig. C1), especially when modeling following features: (i) the water surrounding the phantom and (ii) the surface radiation force at the phantom-water transition present when exciting SW's. Both model and experiment show SW dispersion, i.e. the wave front arising from the downward push (red zone in B2) has split in two (cfr. arrows in fig.C1-2).

When assessing tissue stiffness with algorithms for non-dispersive wave regimes, the shear modulus was 16.5 kPa, i.e. 32.1% lower than the mechanically tested value of 24.3 kPa. This can be improved using an algorithm taking into account dispersion: 26.2 kPa (+ 7.8%). However, as both methods show a significant deviation from the ground truth stiffness, we will look for additional insights into the complex SW physics via modeling to ultimately improve these tissue characterization techniques.



# IMPACTING CANCER CELLS VIA MECHANICAL WAVES: CAN WE CHANGE CELLULAR BEHAVIOR?

**Marlies Hoelzl<sup>1</sup>**

<sup>1</sup> Department of Biomedical Engineering, London, United Kingdom

## Purpose:

Developing a non-invasive treatment to alter cancer cell motility by inducing focused shear waves at specific frequencies and amplitudes.

## Introduction:

The main cause of cancer mortality is metastasis. Work has shown that mechanical forces can translate into biochemical signals affecting cancer cell survival. [1] We study a novel system to non-invasively impact metastasis, which we validate in vitro with the aim of observing changes in metastatic potential in vivo. The system gets refined for clinical translation and waves get focused by magnetic resonance elastography (MRE).

## Methods:

Metastatic human breast cancer cells MDA-MB231 were used to form tumor spheroids. After 4 days, spheroids were embedded into a bovine collagen type 1 layer at the position of highest shear stress (Fig.A, B). 14 h afterwards, cells got treated for 3h (Frequency: 10Hz; Displacement: 200 $\mu$ m). Spheroids were monitored over 3 days by microscopy pictures. MRE was used to characterize the stiffness of bovine collagen type 1 and allowed us to calculate the intensity and area of maximum shear stress. (Simulations via COMSOL 5.1)

## Results:

Fig.C,D (56h) show the impact on the metastatic spread of the spheroid after exposure to a shear strain over 3h. Spheroids exposed to the oscillatory shear strain showed reduced cell spread behavior (i.e. fewer cells) in comparison to the control spheroids 56h after the insult. Detailed analysis showed that the shear stress also influences cell spread regarding the distance to the spheroid itself (E). Control cells move further away from the shaken spheroid cells at the same timepoint.

## Discussion:

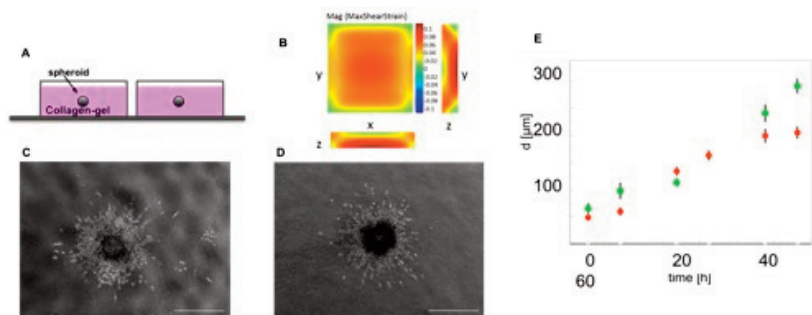
Shear stress over 3h impacts the behavior of tumor cell spheroids in their ability of cancer cell spread. Shaken spheroid starts with a reduced number of invading cells. After 24 and 32h the shaken spheroid appears to have a higher or same amount of cells; this is due to the fact that shaking not only causes inhibitory effects on the metastatic behavior, but also a delay of progress of the spheroid growth itself. In conclusion we show that altering the environment of the spheroid by inducing shear stress causes an inhibitory effect on the cell spread of tumor spheroid.

## Acknowledgements:

This research was funded/supported by Cancer Research UK, Cancer Imaging Centre, Medical Engineering Initiative, EPSRC Pioneering research and skills, Medical Research Council and Department of Health and National Institute for Health Research (NIHR) Biomedical Research Centre based at Guy's and St Thomas' NHS Foundation Trust and King's College London. The views expressed are those of the author(s) and not necessarily those of the NHS, the NIHR or the Department of Health.

## References:

[1] Cheng, *PlosOne*2009



# BREAST BIOMECHANICAL MODELING FOR COMPRESSION OPTIMIZATION IN DIGITAL BREAST TOMOSYNTHESIS

**Anna Mira**<sup>1</sup>, **Ann-Katherine Carton**<sup>2</sup>, **Serge Muller**<sup>2</sup>, **Yohan Payan**<sup>3</sup>

<sup>1</sup> Univ. Grenoble Alpes, Chrs, Ge-Healthcare, La Tronche, France,

<sup>2</sup> Ge-Healthcare, Buc, France,

<sup>3</sup> Univ. Grenoble Alpes, Chrs, La Tronche, France

Mammography is a specific type of breast imaging that uses low-dose X-rays to detect cancer in early stage. During the exam, the women breast is compressed between two plates until a nearly uniform breast thickness is obtained. This technique improves image quality and reduces dose but can also be the source of discomfort and sometime pain for the patient. Therefore, alternative techniques allowing reduced breast compression is of potential interest.

The aim of this work is to develop a 3D biomechanical Finite Element (FE) breast model in order to analyze various breast compression strategies and their impact on image quality and radiation dose.

Previously developed biomechanical breast models use a simplified breast anatomy by modeling adipose and fibro-glandular tissues only [1]. However, breast reconstruction surgery has proven the importance of suspensory ligaments and breast fasciae on breast mechanics [2]. We are therefore considering using a more realistic breast anatomy by including skin, muscles and suspensory ligaments. A particular attention is granted also to the computation of the residual stress in the model due to gravity and to boundary conditions (thorax anatomy, patient position inside MRI machine).

A physical correct modeling of the breast requires the knowledge of the stress-free breast configuration. Here, this undeformed shape is computed using the prediction-correction iterative scheme proposed by [3]. The unloading procedure uses the breast configuration in prone and supine position in order to find a unique displacement vector field induced by gravitational forces. .

Finally, the model is evaluated by comparing the estimated breast deformations under gravity load with the experimental ones measured in three body positions: prone, supine and oblique supine.

## References:

1. *Rajagopal, V. et al. (2010). Modeling breast biomechanics for multi - modal image analysis—successes and challenges. Wiley Interdisciplinary Reviews: Systems Biology and Medicine, 2(3), 293-304.*
2. *Lockwood, T. (1999). Reduction mammoplasty and mastopexy with superficial fascial system suspension. Plastic and reconstructive surgery, 103(5), 1411-1420.*
3. *Eiben, B. et al (2016). Symmetric Biomechanically Guided Prone-to-Supine Breast Image Registration. Annals of biomedical engineering, 44(1), 154-173.*

# CORONARY ATHEROSCLEROTIC PLAQUE ELASTICITY RECONSTRUCTION METHODS BASED ON IN VIVO INTRAVASCULAR ULTRASOUND STRAIN MEASUREMENTS

**Jacques Ohayon**<sup>1</sup>, **Simon Le Floc'h**<sup>2</sup>, **G rard Finet**<sup>3</sup>, **Guy Cloutier**<sup>4, 5</sup>, **Roderic I. Pettigrew**<sup>5</sup>

<sup>1</sup> Laboratory TIMC-DyCTIM2, UJF, CNRS UMR 5525, In3S, Grenoble, France.

<sup>2</sup> Engineering School Polytech Annecy-Chamb ry, USMB, Chamb ry, France.

<sup>3</sup> Laboratory LMGC, CNRS UMR 5508, University of Montpellier II, Montpellier, France.

<sup>4</sup> Hospices Civils of Lyon, UCBL and INSERM Unit 886, Lyon, France.

<sup>5</sup> Laboratory of Biorheology and Medical Ultrasonics, CHUM, Montr al, Qu bec, Canada.

<sup>6</sup> Laboratory of Integrative Cardiovascular Imaging Science, NIDDK, NIH, Bethesda, MD, USA.

The clinical success of a surgical intervention depends on knowledge of whether an coronary atherosclerotic plaque is at risk for rupture and can be responsible for the development of neurological or cardiovascular events, respectively. The medical history and paraclinical tests are sometimes insufficient to resolve this uncertainty. Therefore our group innovated with the development of new imaging techniques allowing computing IVUS palpograms [1] and modulograms [2, 3] from in vitro phantom experiments and in vivo data acquired in patients referred for a coronary atherectomy. The robustness and performance of the palpography and modulography methods were investigated with regard to various factors which may affect the prediction of plaque vulnerability. The in vivo study showed that the high values of the stress amplitude correspond to those VP identified from histology as lipid rich lesions. The morphologies of VP with large soft cores estimated from the modulograms also correspond to those identified from histology as lipid rich lesions. The proposed imaging method appears promising for the evaluation of VP rupture. Furthermore, the performance for the stabilization of VP using new treatment strategies could be investigated by using such imaging technique.

## References:

1. Le Floc'h S et al. *Ultrasound in Medicine and Biology*, 38(12):2084-97, 2012.
2. Deleaval F et al. *Ultrasound in Medicine and Biology*, 39(8):1469-81, 2013.
3. Tacheau A et al. *Ultrasound in Medicine and Biology*, 42(3):727-41, 2016.

# AN INTEGRATED AND NON-INTRUSIVE COMPUTATIONAL APPROACH TO UNCERTAINTY QUANTIFICATION AND STATISTICAL INVERSE PROBLEMS FOR SOFT TISSUE BIOMECHANICS: TOWARDS MODEL SELECTION

**Paul Hauseux<sup>1</sup>, Jack Hale<sup>1</sup>, Alexandre Bilger<sup>1</sup>, Lars Beex<sup>1</sup>, Stéphane Bordas<sup>2</sup>**

<sup>1</sup> University of Luxembourg, Luxembourg, Luxembourg,

<sup>2</sup> University of Luxembourg, Cardiff University, University of Strasbourg, Luxembourg, Luxembourg

Soft tissue properties and models are variable, patient-dependent, age, lifestyle and gender-dependent. There is also no consensus about the importance of the choice of constitutive models in biomechanics, which appears to be strongly case dependent.

The problem of identifying the most adequate model (and its parameters) describing the deformation of an organ given boundary conditions, quantifying uncertainties on the associated parameters and evaluating bounds for quantities of interest are all critical to giving confidence in the results to the user.

We present in this paper a few contributions towards this goal:

- An image to mesh pipeline based on 3D Slicer and CGAL
- A mesh to solution pipeline based on FEniCS [1] which enables to investigate different constitutive models by changing one single line of Python code, including an adaptive model order reduction approach based on the proper orthogonal decomposition (POD)
- A non-intrusive forward uncertainty quantification approach based on advanced Monte-Carlo methods relying on (1) derivative information (2) multi-level Polynomial-Chaos Monte-Carlo approach
- A large-scale non-intrusive pipeline for Bayesian inverse problems and uncertainty quantification able to identify material properties in heterogeneous soft hyper-elastic tissues based on Dolfin adjoint [2]

We demonstrate preliminary results showing the accuracy and efficiency of the methods on a selection of problems in large strain hyper-elasticity and conclude with some perspectives for future work.

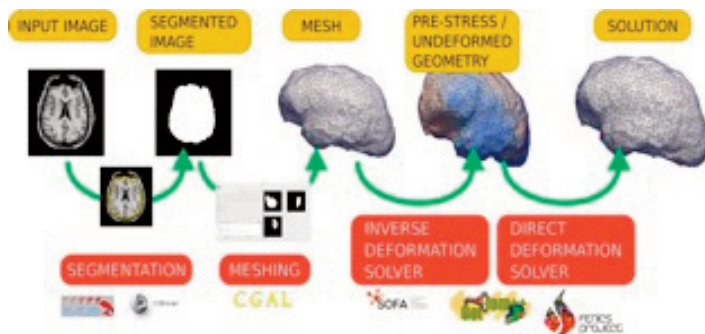


Figure Caption: Computational framework: from image to solution

## Acknowledgments:

Funding from the European Research Council for Stéphane Bordas (ERC StG RealCut) is gratefully acknowledged.

## References:

[1] Logg, A., Mardal, K. & Wells, G. *Automated solution of differential equations by the finite element method: The FEniCS book.* (2012).

[2] Farrell, Patrick E., et al. "Automated derivation of the adjoint of high-level transient finite element programs." *SIAM Journal on Scientific Computing* 35.4 (2013): C369-C393.

# IMPROVING PATIENT SAFETY THROUGH REAL-TIME NUMERICAL SIMULATION

**Stephane Cotin**<sup>1</sup>

*<sup>1</sup> Inria, Strasbourg, France*

The variety, complexity and societal impact of modern medicine have been a strong motivation for many recent scientific developments. While medical imaging has become an integral part of today's medicine, new fields are emerging, such as robotics, simulation, augmented reality, or workflow analysis. In this talk I will highlight the increasingly important role of (real-time) numerical simulation in the context of training, as a mean to improve or maintain surgical skills.

But the role of numerical simulations in medicine can also extend to the field of assistance in the operating room. One particularly important area is augmented reality, which consists in combining, in real time, a virtual model with a live image of the patient or operative field. This allows for instance to visualize internal structures of an organ, which are normally invisible to the surgeon, onto the organ during surgery. As a result, it can significantly improve the outcome of the surgical procedure and facilitate decision making. However, many challenges must be addressed in order to achieve these goals. In particular, patient-specific anatomical and biomechanical models must be developed, and robust non-rigid registration methods need to be investigated, while remaining compatible with the constraints of real-time calculation.

In this talk, I will highlight our results in the field of training and per-operative guidance with two examples, and discuss some of the remaining challenges that still hinder the use of computational anatomy and simulation in medicine.

# PERI-PROSTHETIC FRACTURES SIMULATION FOR MINIMAL INVASIVE SURGERY

**Daniel Baumgartner**<sup>1</sup>, **Courtecuisse Hadrien**<sup>2</sup>, **Ehlinger Matthieu**<sup>3</sup>

<sup>1</sup> Strasbourg University, Icube, Strasbourg, France,

<sup>2</sup> Icube, Strasbourg, France,

<sup>3</sup> Strasbourg University Hospital, Icube, Strasbourg, France

In the context of population aging, the number of femoral fractures is increasing roughly. In France, in 2015, 33 % of people over 65 fall at least once per year. These falls result in femoral fracture for 5 % of them. To treat surgically these fractures, the setting up of a prosthesis is often revealing unavoidable even if it changes the mechanical behavior of the bone structure. In fact, weak areas appear due to the prosthesis itself. Consecutively, new peri-prosthetic fractures can occur and figure out new surgical challenges. The main objective of this study is to simulate fracture of femoral bone coupled with prosthesis. The final goal and global context of that approach is to propose some guidelines for optimal distance between hip and knee prosthesis as well as type of prosthesis to minimize the risk of peri-prosthetic fracture. To reach that objective, the methodology used consists in five steps: 1 - classification of fracture types and scenarios, 2 - CT-scan acquisition before and after the fracture, 3 - segmentation of data, 4 - mesh generation and boundary condition identification, 5 - fracture simulation and validation against experimental cases. Three fall scenarios were considered: 1 - fall on the knee (collision with concrete where the impact occurs on the condyles at 2.8 m/s initial velocity), 2 - torsion (rotation around proximo-distal axis at 0.1 rad/ms initial angular velocity), 3 - lateral impact (collision with concrete where the impact occurs on the shaft at 4.4 m/s initial velocity). Moreover, the CT-scan acquisition and the data segmentation are pretty sensitive because of the image artefact due to the prosthesis existence. The fracture simulation relies on a triangular FE mesh in which the prosthesis is considered as rigid with tied contact interfaces with the bone. Besides, the shaft is divided in five heterogeneous parts where cortical layers as well as cancellous bone are distinguished. Cortical and cancellous bone are also able to break, thus reproducing fracture, thanks to a Tsai-Wu criterion. The complete FE modeling and simulation is achieved using the Altair Hyperworks 11.0 software suite. A special attention is carried out to the hourglass energy that must remain lower than 10 % of the total energy. So, three different fracture schemes were predicted. These schemes correspond to the three fall scenarios and are validated against medical routine observations. As a first perspective of that pilot study, a parametric study will be undertaken to explore the influence of distance between hip and knee prosthesis as well as type of prosthesis on the fracture scheme for each fall scenario.

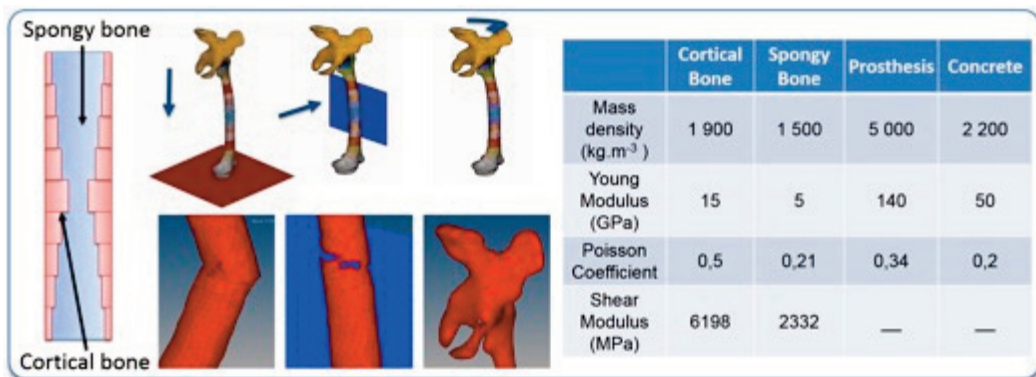


Figure Caption: FE modelling of peri-prosthetic femoral fractures in three fall scenarios

## NOVEL MODEL FOR LOAD CARRIAGE ERGONOMICS OPTIMIZATION

161

**Amir Hadid<sup>1</sup>, Yoram Epstein<sup>2</sup>, Nogah Shabshin<sup>3</sup>, Gal Gozes<sup>4</sup>, Avihai Atoon<sup>5</sup>, Amit Gefen<sup>6</sup>**

<sup>1</sup> Tel Aviv University; Dept. of Biomedical Engineering, Binyamina, Israel,

<sup>2</sup> Tel Aviv University; Dept. of Physiology, F. of Medicine, Tel Aviv, Sheba Hospital; Heller Inst. of Medical Research, Ramat Gan, Israel,

<sup>3</sup> Haemek Medical Center, Afula, Israel,

<sup>4</sup> Tel Aviv University; Dept. of Biomedical Engineering, Tel-Aviv, Israel,

<sup>5</sup> Tel Aviv University; Dept. of Biomedical Engineering, Tel Aviv, Israel,

<sup>6</sup> Tel Aviv University, Dept. of Biomedical Engineering, Tel Aviv, Israel

Soldiers and recreational backpackers are often required to carry heavy loads. Shoulder strain is one of the limiting factors of load carriage, due to higher susceptibility to short-term injuries such as soft tissue damage and trapped nerves or obstruction of blood vessels. The aim of the current study was to develop a model for various loads and strap materials and structures in order to simulate real life loading scenarios and to help in optimizing load carriage systems design.

Open-MRI scans were used for reconstructing a 3D geometrical model of an unloaded shoulder and for measuring the soft tissue deformations caused by a 25 kg backpack; subsequently, a subject-specific finite element (FE) stress-strain analyses was developed. Loads were applied at the strap-shoulder contact surfaces of the model by pulling the strap towards the shoulder until the desired load was attained. Strain at the subclavian artery served as the outcome measure for comparisons. The following material properties were evaluated: Homogeneous straight strap with varied material properties:  $E=0.5, 1.2$  and  $5$  MPa. Dual layer straight strap with  $E=20$  MPa for the inner layer and  $0.5$  MPa for the outer layer. Based on the results of the first simulations, a new anatomical strap was designed to maximize bone contact and avoid deformation on the soft tissues of the shoulder. It was compared to the straight strap (both with homogeneous single layer).

A stiffer strap material ( $E=5$  MPa) resulted in 4 fold reduction in brachial plexus strains compared to the softer strap ( $E=0.5$  MPa). The dual strap structure resulted in brachial plexus strains, which were lower compared to the single layer  $E=0.5$  MPa strap. The anatomical strap design resulted in additional 4 fold decrease in brachial plexus strains compared to the lowest strains obtained for the straight strap (see figure).

The newly developed model successfully enabled predictions of soft tissue deformations in the brachial plexus for different backpack strap materials and geometries. Anatomical strap and appropriate strap materials can potentially minimize brachial plexus strains and the associated medical complications.

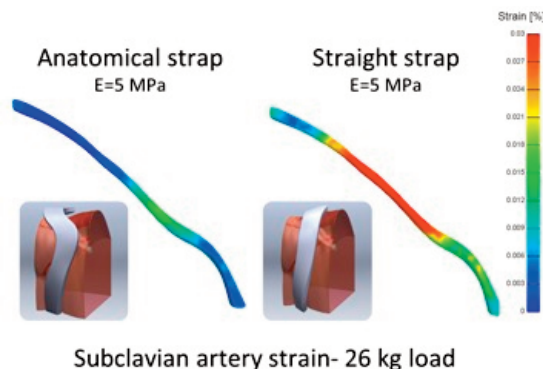


Figure Caption: Effective strains on the subclavian artery during 26 kg simulated load.; Left: Newly designed anatomical strap. Right: straight strap

# A PREDICTIVE MULTISCALE MODEL FOR SIMULATING PLATELETS ACTIVATION IN SHEAR FLOWS

Peng Zhang<sup>1</sup>, Chao Gao<sup>1</sup>, Na Zhang<sup>1</sup>, Marvin J. Slepian<sup>2</sup>, Yuefan Deng<sup>1</sup>, **Danny Bluestein**<sup>1</sup>

<sup>1</sup>Stony Brook University, Stony Brook, NY,

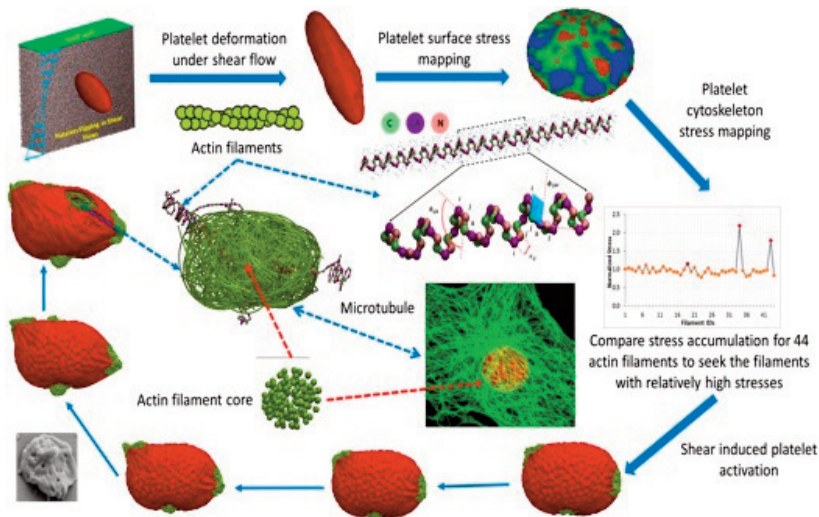
<sup>2</sup>University of Arizona, Tucson, AZ

Flow-induced platelet activation may prompt clot formation in cardiovascular devices and in arterial diseases. Upon activation, platelets undergo complex filopodial formation. Continuum methods fail to capture such molecular-scale mechanism. We developed a multiscale model which interfaces nanoscale microstructures of platelets and mesoscale transport of blood flows [1-4].

We consider: (i) top/mesoscale using dissipative particle dynamics (DPD) to describe viscous blood flows; (ii) bottom/nanoscale using coarse-grained MD (CGMD) to describe the platelet membrane, cytoplasm and the cytoskeleton [4]. In this fully interactive model, spatial interface between DPD and CGMD is established. Alpha-helix structure is used for constructing helically-arranged actin filaments (Fig. 1). A novel multiple time-stepping algorithm [2] was developed for handling the disparity in time-stepping sizes between DPD (ms) and CGMD (ns).

Fig.1 shows the multiscale fluid-platelet system with shear stress at 85.76 dyne/cm<sup>2</sup>, platelet membrane (Young's modulus-31.2  $\mu$ N/m), cytoplasm, and the platelet internal structure. The hemodynamic stresses are mapped on the membrane and transferred to the cytoskeleton while the platelets are flowing and flipping. Filopodial formation is stimulated for up to 44 actin filaments. The resultant filopodia formation compared favorably with in vitro measurements (Fig. 1).

Our multiscale methodology can be applied for solving similar complex clinical problems at the juncture of biology and engineering.



## Acknowledgements:

This project was funded by NIH (NHLBI R21 HL096930-01, NIBIB Quantum U01EB012487, DB) and used the XSEDE computer resource award on TACC Stampede (TG-DMS140019, PZ).

## References:

- [1] Zhang, P., et al, *Cell Mol Bioeng*, 7:552-574, 2014.
- [2] Zhang, P., et al, *J Comput Phys*, 284:668-686, 2015.
- [3] Pothapragada, S., et al, *Int J Numer Meth Biomed Engng*, 31:1-16, 2015.
- [4] Zhang, N. et al, *J Comput Phys*, 257:726-736, 2014.

## COMPUTATIONAL MODELING OF EMBOLUS TRANSPORT IN THE INFERIOR VENA CAVA

Ken Aycock<sup>1</sup>, Robert Campbell<sup>1</sup>, Brent Craven<sup>2</sup>, Keefe Manning<sup>1</sup>

<sup>1</sup> The Pennsylvania State University, University Park, United States,

<sup>2</sup> U.S. Food and Drug Administration, Silver Spring, United States

Pulmonary embolism (PE) occurs when an embolus travels into the pulmonary circulation and obstructs blood flow to the lungs. Inferior vena cava (IVC) filters have been used for nearly half a century to mitigate the risk for PE in at-risk patients by providing a mechanical barrier to embolus transport. However, despite years of development, IVC filter complications remain common, including recurrence of PE.

We present our computational approach for simulating embolus transport and for predicting the embolus-trapping efficiency of an IVC filter. Blood emboli are modeled as rigid spheres with diameters ranging from 3mm to 7mm and embolus-to-blood density ratios of 0.98, 1.00, and 1.02. The coupled fluid-structure interactions between the blood and the emboli are modeled using a coupled fictitious domain/discrete element method. Collisions between the emboli and the IVC filter and between the emboli and the IVC wall are considered using Hertzian contact theory. Simulations are performed with the gravitational body force oriented opposite to the direction of the flow (i.e., representative of a patient sitting or standing upright; see Figure 1).

The simulations predict that the embolus trapping efficiency increases with increasing embolus diameter and increasing embolus-to-blood density ratio. The predicted embolus pathlines, embolus-trapping positions, and the embolus-trapping efficiency of the IVC filter are presented and are compared with data from in vitro experiments.

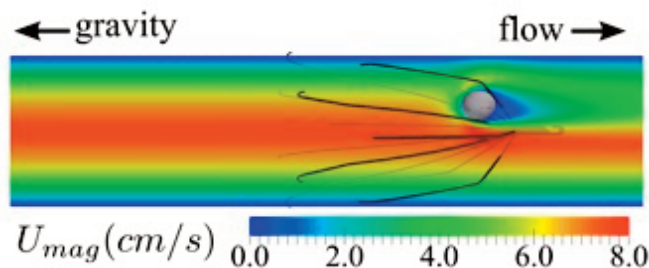


Figure 1: Velocity magnitude contours on a plane bisecting the idealized IVC following the capture of a 5mm embolus in an off-center embolus-trapping position.

### Acknowledgments:

This research was supported by the Walker Assistantship program at the Penn State Applied Research Laboratory.

# HIGH RESOLUTION PRESSURE DROP FOR COMBINED FUNCTIONAL AND BIOMECHANICAL ASSESSMENT OF CORONARY STENOSES – A VALIDATED NUMERICAL STUDY

**Oren Rotman**<sup>1</sup>, **Uri Zaretsky**<sup>2</sup>, **Avraham Shitzer**<sup>3</sup>, **Shmuel Einav**<sup>4</sup>

<sup>1</sup> Department of Biomedical Engineering, Stony Brook University, Ny, USA, <sup>2</sup> Department of Biomedical Engineering, Tel-Aviv University, Tel-Aviv, Israel, <sup>3</sup> Stony Brook, Ny, United States,

<sup>2</sup> Department of Biomedical Engineering, Tel-Aviv University, Tel-Aviv, Israel, Tel-Aviv, Israel,

<sup>3</sup> School of Mechanical Engineering, Technion Iit, Haifa, Israel, Haifa, Israel, <sup>4</sup> Department of Biomedical Engineering, Stony Brook University, Ny, USA, <sup>4</sup> Department of Biomedical Engineering, Tel-Aviv University, Tel-Aviv, Israel, Tel-Aviv, Israel

Blood pressure drop and arterial distensibility are important, allegedly independent, parameters that are indicative of the coronary arteries patency and atherosclerosis severity. In the present study we show that these two parameters are dependent, allowing to obtain both parameters from a single measurement, and to do so a high resolution differential pressure measurement system is required. The objective of the study was to unveil the relationship between local fluid pressure drops and tube distensibility, through various scenarios of stenosis severity, tube diameter, and flow rate (for coronary hemodynamic conditions). The investigation was performed using validated Fluid-Structure Interaction (FSI) analysis on silicone mock arteries with intermediate size stenosis (0-65%). Highly accurate pressure drop measurements ( $\pm 0.05$  mmHg) were performed with our in-house fluid-filled double-lumen catheter measurement system.<sup>1, 2</sup> The results indicated that our accurate pressure drop measurement method facilitated the differentiation among several levels of the mock arteries' stiffness, with distensibilities ranging from 1 to 7% (Figure 1). Local pressure drops were markedly affected by the mock arteries' stiffness, and could be best described using a second order polynomial function. These changes in pressure drop could be detected even when there was no stenosis present, and FFR values remained insensitive at 1.00. The results indicated the clinical potential of a high accuracy pressure drop-based parameter to be superior to FFR. Such a parameter would provide cardiovascular interventionalists with lesion specific bio-mechanical and functional data, for improved real time decision making in the cath-lab.

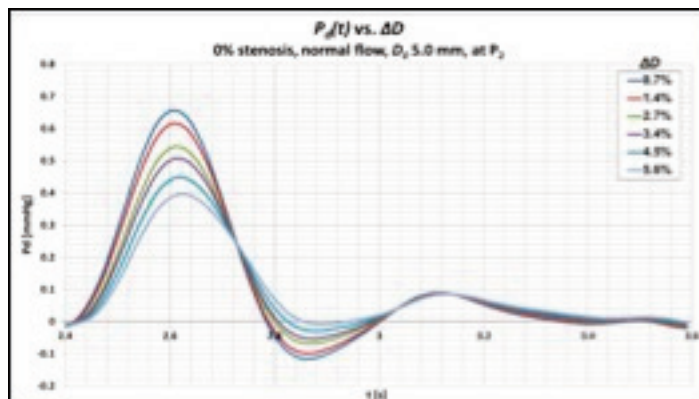


Figure 1: Example for The effect of the compliant tube distensibility on the local pressure drop, which is detectable only with high precision measurement.

## References:

1. Rotman, O.M., Zaretsky, U. Shitzer, A. Einav, S. "Method for High Accuracy Differential Pressure Measurements using Fluid-Filled Catheters". *Ann Biomed Eng*, 42 (8), 1705-1716 (2014).
2. Rotman, O.M., Weiss, D., Zaretsky, U., Shitzer, A., Einav, S. "High Accuracy Differential Pressure Measurements using Fluid-Filled Catheters – A Feasibility Study in Compliant Tubes", *J. of Biomechanics*, 48 (12), 3543-3548 (2015)

# SENSITIVITY OF PULMONARY OUTFLOW PATCH RECONSTRUCTION WITH RESPECT TO THE NATIVE AND ARTIFICIAL TISSUE PROPERTIES

Seyedehsamaneh Lashkarinia<sup>1</sup>, Samir Donmazov<sup>1</sup>, Tijen Alkan Bozkaya<sup>2</sup>, Senol Piskin<sup>1</sup>, Kerem Pekkan<sup>1</sup>

<sup>1</sup> Department of Mechanical Engineering, Koc University, Istanbul, Turkey, <sup>2</sup> Koc University Medical School, Istanbul, Turkey

Palliative repair of pediatric congenital vascular defects involve complex surgical reconstructions that should incorporate native vessel growth, hemodynamics and post-surgery pressure. Here the sensitivity of a new computational patient-specific pre-surgical patch planning procedure for the palliative repair of main pulmonary artery (MPA) stenosis in Tetralogy of Fallot [1] is investigated. Effects of geometric parameters such as stenosis size, surgical incision shape and material properties of patch are studied through an idealized unloaded de-pressurized MPA model. The release of residual stresses after surgical incision are simulated by applying an equivalent intramural pressure [2]. The extra pull produced by the surgeon is represented by traction boundary conditions in the circumferential direction of the cut. Cubic-wrapped patch having the same curvature as the surrounding native tissue is implanted in the computer. Time-dependent finite shell elements having 1mm thickness (Ansys Inc) are employed. Stress-strain data obtained in-house, through the biaxial tensile tests (Bose Inc) for the mechanical properties of common patch materials like Dacron, PTFE, porcine pericardium and human pericardium. Each specimen is stretched up to 10-20% of its original length in orthogonal directions by applying sinusoidal force. Both linear elastic and hyper elastic material properties are computed by performing least squares fitting. The computed von Mises stress distributions demonstrate that the maximum stress occurs in the artery for all materials except for the porcine pericardium (Figure). Difference between stresses in the patch and artery results a discontinuous stress distribution at the loaded post-operative state, which may lead to early shunt failure of the arterial reconstruction.

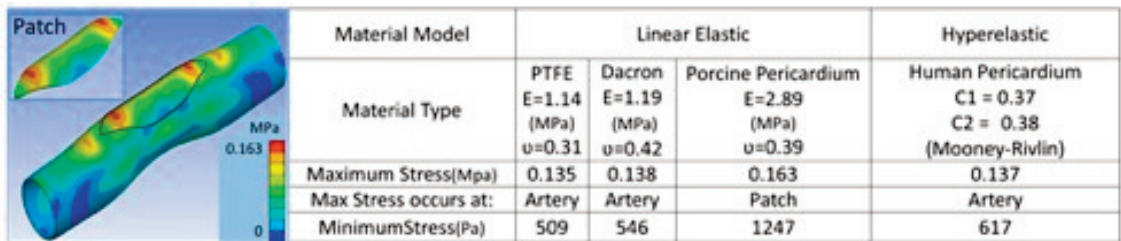


Figure: Von Mises stress distribution for idealized MPA with 50% stenosis repaired by a porcine pericardium patch considering post-surgery blood pressure of 20mm-Hg. Table summarizes the different patch materials studied for this surgical scenario.

## Acknowledgments:

Funding is through the ERC Proof-of-Concept KidsSurgPlan (PI: Kerem Pekkan) and TUBITAK 1003.

## References:

- [1] Yoshida, M., et al. *Eur J Cardiothorac Surg* 44:e46-52.2013
- [2] Donmazov, S., et al. *J Biomech Eng* 137:061011.2015

# PHYSIOLOGIC MODELING AND SURGICAL OPTIMIZATION IN SINGLE VENTRICLE CONGENITAL HEART DEFECTS

**Alison Marsden**<sup>1</sup>, **Jeffrey Feinstein**<sup>1</sup>, **Vijay Vedula**<sup>1</sup>, **Daniele Schiavazzi**<sup>1</sup>, **Tain Yen Hsia**<sup>2</sup>

<sup>1</sup> Stanford University, Stanford, United States, <sup>2</sup> Great Ormond Street Hospital, London, United Kingdom

Single ventricle heart patients typically undergo a three-staged surgical repair to route the venous return directly to the pulmonary arteries, separating the systemic and pulmonary circulations. We will present our recent work combining shape optimization and multiscale modeling to perform virtual surgery and physiologic simulations in the three stages of the single ventricle repair. First, multiscale modeling and optimization will be applied to propose, test, and optimize a novel design called the Assisted Bidirectional Glenn to replace the stage one Blalock Taussig shunt surgery. A surrogate pattern search method is coupled to the finite element flow solver in an automated loop for efficient shape optimization. Multiscale modeling couples the 3D Navier-Stokes solution with a 0D lumped parameter network to model the systemic and pulmonary circulations, capturing changes in global circulatory response resulting from changes in local anatomy. Second, we will present a novel Bayesian algorithm to automatically tune lumped parameter models to match patient specific data for single ventricle patients. We will discuss the extension of these methods for propagation of uncertainties in clinical data to model predictions. Finally, we will discuss new directions in modeling ventricular flow in single ventricle patients using an Arbitrary Lagrangian Eulerian (ALE) method for moving domain simulations.

## Acknowledgments:

This work was supported by a Leducq Foundation Transatlantic Network of Excellence Grant, a Burroughs Wellcome Fund Career Award at the Scientific Interface, and an NSF CAREER award.

## References:

1. Schiavazzi, D. E., Arbia, G., Baker, C., Hlavacek, A.M., Hsia, T.Y., Marsden, A.L., Vignon-Clementel, I.E., "Uncertainty quantification in virtual surgery hemodynamics predictions for single ventricle palliation," *International Journal of Numerical Methods in Biomedical Engineering*.
2. Esmaily-Moghadam, M., Hsia, T-Y, Marsden, A.L., "The Assisted Bidirectional Glenn: a novel surgical approach for first stage single ventricle heart palliation," *Journal of Thoracic and Cardiovascular Surgery*, 149(3), pp. 699-705, (2015).
3. Marsden, A.L., "Optimization in cardiovascular modeling," *Annual Review of Fluid Mechanics*, Vol. 46 pp. 519-546, (2014).

# THE EFFECT OF KNEE OSTEOARTHRITIS ON GAIT VARIABILITY AND EQUILIBRIUM ABILITY

**Rita Kiss<sup>1</sup>**

*<sup>1</sup> Brne, Mechatronika, Optika És Gépészeti Informatika Tanszék, Budapest, Hungary*

Please use any of the following sections that are relevant for your abstract structure

.The effect of knee osteoarthritis on gait variability and equilibrium ability

Author: Rita M Kiss\*, Ákos Pethes\*\*, Zoltán Bejek\*\*\*, Gergely Nagymáté\*

\* Budapest University of Technology and Economics, Dept. of Mechatronics

\*\* Szent János Hospital, Dept of Orthopedics and Traumatology

\*\*\* Semmelweis University, Dept. of Orthopedics:

Knee osteoarthritis (OA) is one of the most common joint diseases in elderly patients, which results in mobility limitation in equilibrium limitation. The patients group of patients was made up of 45 patients with severe OA. The control group consisted of 20 healthy elderly. Gait analysis during treadmill walking was performed using Zebris CMS-HS ultrasound-based motion analysis system, which recorded the spatial coordinates of the designated anatomical points and calculates the variability of spatial-temporal and angular parameters represented by coefficient variables.

Our data suggest that the variability of gait depend significantly on speed and on gender. The CV of spatial-temporal parameters increased significantly, and the CV of motion of affected knee decreased. The joints of the non-affected side and pelvis play an important role in the compensation and adaptation, as confirmed by the increased variability of the angular parameters of those joints.

Balancing capacity after sudden perturbation was modelled using a PosturoMed©. The motions of the rigid plate were recorded by Zebris motion analysis system, and calculated the Lehr's damping ratio (D).Results indicate that the non-affected limb always becomes the dominant one, playing a decisive role in balancing capacity. Balancing ability significantly reduced not only while standing on the affected limb but also while standing on both limbs and on the healthy limb; it was not affected by age or gender.

The increased variability of gait, and the decreased equilibrium ability of patients with knee osteoarthritis may also indicate an increased risk of falling.

## Acknowledgments:

This project is supported by the Hungarian Scientific Fund K083650. The author wishes to express her thanks to radiologist Katalin Köllő for her assistance in the evaluation of the radiographic images.

## A KEY DATASET FOR THE COMPREHENSIVE ASSESSMENT OF THE MUSCULOSKELETAL SYSTEM: THE CAMS-KNEE PROJECT

**William R. Taylor<sup>1</sup>, Pascal Schütz<sup>1</sup>, Barbara Postolka<sup>1</sup>, Jörn Dymke<sup>2</sup>, Verena Schwachmeyer<sup>2</sup>, Marco Hitz<sup>1</sup>, Renate List<sup>1</sup>, Ines Kutzner<sup>2</sup>**

<sup>1</sup> Institute for Biomechanics, ETH Zürich, Switzerland

<sup>2</sup> Julius Wolff Institute, Charité – Universitätsmedizin Berlin, Germany

Many aspects of modelling and understanding biomechanical interactions in the human musculoskeletal system, including e.g. the development of implants for joint replacement, joint and implant stability, wear mechanisms, and loading of the soft tissue structures, are limited by the lack of availability of complete and synchronous kinematic and kinetic datasets.

The CAMS-Knee (Comprehensive Assessment of the Musculoskeletal System) project directly targets this deficit and envisions moving the worldwide field of musculoskeletal biomechanics forward by making unique datasets of human kinematics and kinetics freely available on the internet to provide researchers in the field of orthopaedics a reliable and highly accurate resource for model validation and investigation of the knee joint. Here, teams from ETH Zürich, Switzerland and the Charité – Universitätsmedizin Berlin, Germany have joined forces and measured 6 subjects (5m, 1f, aged 68±5 years, mass 88±12 kg, height 173±4 cm) while each performing multiple repetitions of walking, stair decent, ramp descent and deep knee bend exercises. Each subject possessed an INNEX knee implant (Zimmer, Switzerland; type FIXUC), in which the tibial component was instrumented with a 9-channel telemetry transmitter (90-100 Hz) that allowed six-component load measurements of the 3 contact forces and 3 joint moments acting on the tibial component to be recorded (Heinlein et al., 2007) (Figure 1). To analyse the motion of the body, 74 skin markers were attached mainly to the lower extremities and an opto-electronic system (Vicon, UK) with 22 cameras captured the kinematics at a sampling frequency of 100 Hz. The ground reaction forces were measured using up to 7 force plates (Kistler, Switzerland), at a frequency of 2kHz, and 16 channel EMG recorded the activity of the lower limb musculature. In addition, the skeletal kinematics of the knee were captured throughout the movement using the ETH moving (max horizontal acceleration: 8ms<sup>-2</sup>) fluoroscopy system (field of view: 30.5cm, Pulsed image acquisition rate: 25Hz, Shutter time: 1ms, Image resolution: 1000x1000 pixels), which allowed 3D reconstruction of the tibial and femoral components (Accuracy: rotations: <1°; translations in-plane: <1mm, out-of-plane: <3mm). All measurement systems recorded simultaneously and were temporally synchronised.



Figure 1: The moving fluoroscope (left) allows the capture of skeletal kinematics throughout complete cycles of daily activities including walking, ramp descent and stair descent. Internal joint contact forces were captured using telemetric prostheses (right), implanted in 6 subjects.

As a result, the CAMS-Knee project provides unique datasets on the internal and external loading conditions as well as the whole body and skeletal kinematics. Public release of the data is planned for early 2018.

### Acknowledgments:

We would like to acknowledge the financial support of the Robert Mathys Foundation (RMS). Additional funding was also provided by the German Federal Ministry of Education and Research (OVERLOAD-PrevOP, 01EC1408A).

### References:

Heinlein, B., Graichen, F., Bender, A., Rohlmann, A., Bergmann, G., 2007. Design, calibration and pre-clinical testing of an instrumented tibial tray. *Journal of biomechanics* 40, S4-S10

## A COMPUTE BIOMECHANICAL GAIT ANALYSIS COMPARISON USING WALKING STICKS AND WALKER IN ADULT SCOLIOSIS PATIENTS

**Ram Haddas<sup>1</sup>, Isador Lieberman<sup>2</sup>**

<sup>1</sup> Texas Back Institute Research Foundation, Plano, United States,

<sup>2</sup> Texas Back Institute, Plano, United States

Patients with degenerative adult scoliosis demonstrate an altered gait pattern. Walkers are frequently prescribed in an effort to improve balance, mobility, and reduce lower back pain, but the literature demonstrates conflicting evidence regarding their effectiveness. As an alternative to walkers, walking sticks have been prescribed to assist with mobility, promote a more balanced upright posture and trigger activation of the spine stabilizer muscles during the gait cycle.

Ten subjects with symptomatic degenerative scoliosis performed gait analysis under 3 testing conditions; 1. with walking sticks (Fig. 1), 2. with walker, and 3. without any device. Reflective markers were incorporated to collect full body three-dimensional kinematics using 10 cameras at a sampling rate of 100Hz. All raw data were exported from the Vicon Nexus system and imported into a custom Matlab program for processing. Three-dimensional joint rotation angle at the spine and lower extremity were analyzed using the custom algorithm.

The use of walking sticks resulted in significant slower cadence (22.8 step/min  $p<0.00$  compared to no device and 6.8 step/min  $p<0.02$ ). Stride and step times were longer compared to the walker (0.36 s  $p<0.00$  and 0.52 s  $p<0.01$ , respectively) and with no device (0.68 s  $p<0.00$  and 0.39 s  $p<0.01$ , respectively). Walking sticks significantly resulted in more dorsiflexion angle at initial contact (Right 6.9°  $p<0.02$ ; Left 6.4°  $p<0.03$ ) in comparison to the walker. Head orientation presented more extension position using the walking sticks (6.7°  $p<0.05$ ) and the walker (8.6°  $p<0.04$ ). The use of the walking sticks significantly increase ankle (21.6°  $p<0.00$ ), knee (24.6°  $p<0.01$ ), and hip (15.0°  $p<0.00$ ) flexion range of motions in comparison to the walker. Moreover, the walking sticks promoted more knee (15.6°  $p<0.00$ ), hip (3.9°  $p<0.00$ ), and head (4.0°  $p<0.00$ ) range of motion in the frontal plane in comparison to a walker.

Walking sticks did improve the biomechanics and did facilitate positioning of the trunk and lower extremity during walking in adult degenerative scoliosis patients. Formal gait and motion analysis can provide a method to assess the impact of severe spinal deformity on function and changes after treatment.

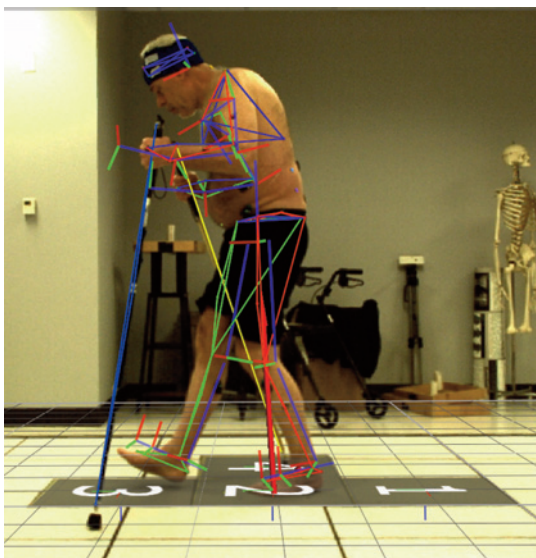


Figure Caption: Full body and Walking Sticks Compute Biomechanical models

## DAMAGE OF SOFT BIOLOGICAL TISSUES: CONTINUUM MODEL AND FE IMPLEMENTATION

Amirhossein Hamedzadeh<sup>1</sup>, T.Christian Gasser<sup>2</sup>, Salvatore Federico<sup>1</sup>

<sup>1</sup> University of Calgary, Calgary, Canada,

<sup>2</sup> Kth Royal Institute of Technology, Royal Institute of Technology (Kth), Stockholm, Sweden

For many applications soft biological tissues can be described as a matrix permeated by water and reinforced by collagen fibers. Specifically, collagen fiber properties and their spatial organization/orientation are key parameters influencing damage and failure properties of the tissue at the macroscale. In order to further understand such mechanisms, the present work aims at combining irreversible phenomena of collagen fibers with Lanir's [1,2] microstructural tissue representation. Specifically, we assumed that collagen fibrils are interlinked by proteoglycan (PG) cross-bridges, which in turn forms a collagen fiber. An individual collagen fibril starts carrying tensile load as soon as it reached its engagement stretch  $\lambda_s$ , i.e. the fibril is straight. Following [3], engagement stretch of the fibrils was governed by a triangular probability density function (PDF) and their mechanical properties were described by a linear relation between nominal stress and logarithmic strain. The collagen fiber stress was calculated both, with and without enforcing incompressibility at the fiber level. Next, a brittle failure mechanism was incorporated by assuming that collagen fibrils rupture at the failure stretch  $\lambda_f$  with respect to their straightened configuration. Finally, the outlined collagen fibers were embedded in a matrix with neo-Hookean properties and the macroscopic model response was tested. Specifically, the computational results from simple tension (see Figure 1) exhibited stress-stretch properties that were consistent with in-vitro experimental results of collagenous soft biological tissues. Most interestingly, despite only a brittle failure mechanism (fibril rupture) has been integrated, at the macroscale the model predicted plastic-like phenomena like remaining tissue elongation, see Figure 1. In conclusion, based on simple (but plausible) load-carrying concepts at fibril, fiber and continuum levels, the proposed model showed promising results.

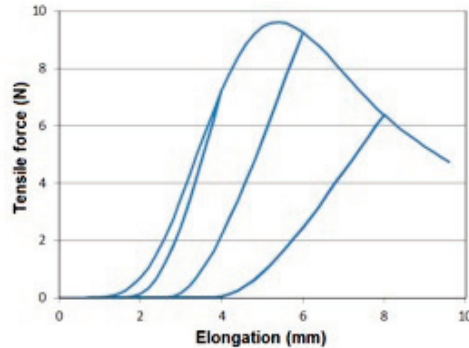


Figure 1: Computed force versus elongation response for cyclic simple tension.

### References:

[1] Lanir, Y., 1983, *J. Biomech.* 16, 1-12

[2] Federico, S., Grillo, A., 2012, *Mech. Mat.* 44, 58-71

[3] Martufi G., Gasser, T.C., 2011, *J. Biomech.*, 44, 2544-2550

# FINITE ELEMENT RECONSTRUCTION OF ACUTE SUBDURAL HAEMATOMA CADAVER EXPERIMENTS

**Zhao Ying Cui<sup>1</sup>, Nele Famaey<sup>2</sup>, Bart Depreitere<sup>3</sup>, Svein Kleiven<sup>4</sup>, Jos Vander Sloten<sup>5</sup>**

<sup>1</sup> Ku Leuven, Mechanical Engineering, Biomechanics Section, Leuven, Belgium,

<sup>2</sup> Ku Leuven, Mechanical Engineering, Biomechanics Section, Leuven, Belgium,

<sup>3</sup> Ku Leuven, Department of Neurosurgery, University Hospital Gasthuisberg, Leuven, Belgium,

<sup>4</sup> Kth, Neuronic Engineering, Stockholm, Sweden,

<sup>5</sup> Ku Leuven, Mechanical Engineering, Biomechanics Section, Vat Be0419.052.173, Heverlee, Belgium

## Introduction:

Acute subdural haematoma (ASDH) is a type of intracranial haemorrhage following head impact. Bridging vein (BV) rupture is considered a major cause of ASDH, which is why a biofidelic representation of BVs in finite element (FE) head models is essential for the successful prediction of ASDH.

## Materials and methods:

We investigated the mechanical behavior of the BVs in the KTH FE head model [2].

First, a sensitivity study was performed, quantifying the effect of varying loading conditions (pulse duration (PD), rotational (RA) and linear acceleration (LA) and peak rotational velocity (RV)) and mechanical properties (Young's modulus (E) and outer diameter (OD)) on the BV strains using a multiple linear regression model.

Secondly, previously performed cadaver head impact experiments [1] were simulated with varying sets of mechanical properties. For each set of 12 simulations the prediction result of the simulations is cross checked with its corresponding experimental case and the number of successful prediction is tracked.

## Results:

The correlation analysis showed that RV had a significant correlation with the maximum value of the RA and PD. These three parameters showed a pronounced positive correlation with the BV strains. RV had the biggest effect. In contrast, LA had no effect on the BV strains. For the mechanical properties it was found that both E and OD were negatively correlated with the BV strains. A multiple linear regression model using E, OD and AREA as independent variables to predict the BV strain yielded an adjusted R<sup>2</sup>-value of 0.81.

The second part of this study showed that depending on the choice of mechanical parameters, the success rate of the simulations fluctuated between 67% and 75%.

## Discussion & Conclusion:

An adjusted R<sup>2</sup>-value of 0.81 indicates that a big part of the BV behavior can be predicted with the E, OD and RV. It is also found that the prediction rates of the cadaver experiments are fairly good, which could be improved by either finding a higher number of relevant predictors or a more biofidelic representation of the BVs. Given the limited data available, it would also be very interesting to acquire a bigger database with accident or impact cases where BV rupture occurred. This would greatly benefit the improvement and validation of the BV representation in the FE head model.

**Acknowledgments:** This work was supported the Institute for the Promotion of Innovation through Science and Technology in Flanders (I.W.T.) and the Research Foundation – Flanders (FWO).

## References:

[1] B. Depreitere, et al., *Journal of neurosurgery* 104 (6) (2006) 950-956

[2] S. Kleiven, *International Journal of Crashworthiness* 11 (1) (2006) 65-79.

# THE EFFECT OF STRAINS AND STRESSES ON COLLAGEN REORIENTATION IN INTACT AND INJURED CARTILAGE

Petri Tanska<sup>1</sup>, Petro Julkunen<sup>2</sup>, Rami Korhonen<sup>3</sup>

<sup>1</sup> Department of Applied Physics, University of Eastern Finland, Kuopio, Finland,

<sup>2</sup> Diagnostic Imaging Center, Kuopio University Hospital, Department of Applied Physics, University of Eastern Finland, Kuopio, Finland,

<sup>3</sup> Department of Applied Physics, University of Eastern Finland, Diagnostic Imaging Center, Kuopio University Hospital, Kuopio, Finland

Cartilage injury may disrupt normal collagen architecture of cartilage which may lead to the onset of osteoarthritis (OA). Our aim was to investigate the ability of a fibril reorientation algorithm [4] to predict adaptation of the collagen network in the presence of injury.

FE models representing osteochondral explants were constructed with fibril-reinforced poroviscoelastic swelling properties (Fig. 1) [3]. One was kept intact while the other one included a 20 $\mu$ m wide and 750 $\mu$ m deep crack throughout the explant. Models included similar depth-dependent structure and composition for cartilage [1,3]. Bone-cartilage interface was fixed. Fluid flow was allowed through free surfaces. Following an initial free-swelling step, a ramp load of 2MPa for 0.1s was applied in unconfined compression using a rigid platen with a frictional contact [2]. Reorientation algorithm assumed that collagen fibrils align according to tensile principal strain directions. The fibrils were slowly rotated towards these preferred directions and a new simulation followed. The architecture was evaluated after 50 consecutive iterations assuming convergence of the fibril directions. We also investigated the alternative possibility that the fibrils could align based on positive stress directions and whether shear forces affect to the reorientation by introducing a sliding of 40mm/s for 0.1s after the compression.

The presence of the crack led to more disorganized collagen architecture near the crack, particularly at the crack end. With sliding, the strain based algorithm predicted slightly more disorganized architecture in the superficial zone near the crack when compared to the both intact and injured cartilages experiencing only compression. Stress based algorithm predicted more homogenous architecture at the superficial and middle zones.

The collagen disorganization in injured cartilage was concentrated at the crack end rather than the superficial zone. However, the predicted architecture in intact cartilage did not correspond the one typically present in cartilage, probably due to unconfined geometry not resembling anatomically correct confinement of the tissue boundaries. Furthermore, shear modulated the architecture near the damaged area suggesting a potential pathway to the progression of cartilage degeneration in OA.

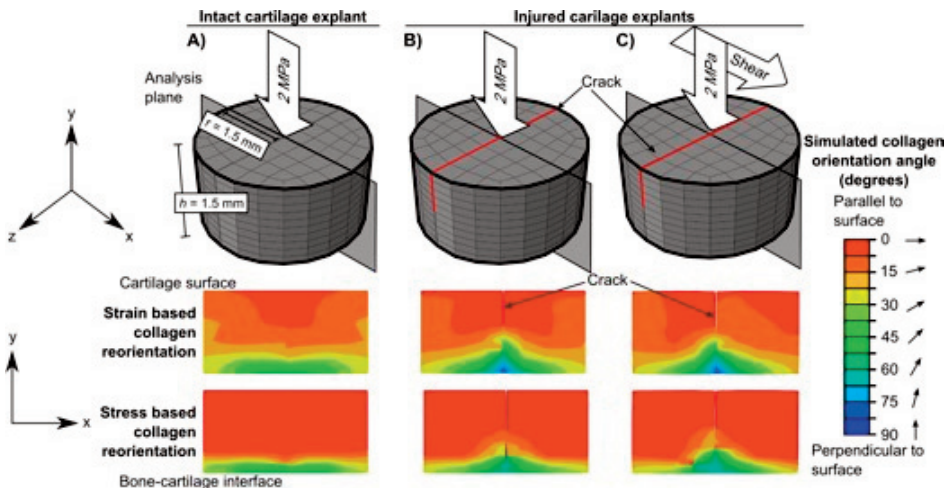


**Figure 1:** Influence of the strain and stress based collagen reorientation algorithms on mechanically loaded intact and injured cartilage explants in unconfined compression.

[1] Julkunen P. J Biomech 2007. [2] Teepie E. J Orthop Res 2008. [3] Wilson W. J Biomech 2005. [4] Wilson W. Osteoarthritis Cartilage 2006.

# BIOMECHANICAL EVALUATION OF THE (UN)REINFORCED ROSS PROCEDURE

Heleen Fehervary<sup>1</sup>, Julie Vastmans<sup>1</sup>, Tine Dijkmans<sup>1</sup>, Jos Vander Sloten<sup>2</sup>, Nele Famaey<sup>3</sup>

<sup>1</sup> Ku Leuven, Mechanical Engineering, Biomechanics Section, Heverlee, Belgium,

<sup>2</sup> Ku Leuven, Mechanical Engineering, , Biomechanics Section, Vat Be0419.052.173, Heverlee, Belgium,

<sup>3</sup> Ku Leuven, Mechanical Engineering, , Biomechanics Section, Leuven, Belgium

## Introduction:

Young adults suffering from aortic valve disease can be treated with the Ross procedure in which the aortic root is replaced by a pulmonary root autograft. This implies the pulmonary autograft being subjected to higher systemic pressures, which results in long term dilation for approximately 20% of the cases [1]. A promising solution to overcome this problem is an exostent which is wrapped around the artery and provides external support. This study investigates the biomechanical properties of the Ross procedure with and without this reinforcement.

## Materials & Methods:

9 Lovenaar sheep were treated with a simplified Ross procedure: a section of thoracic aorta descendens was replaced by a section of pulmonary artery. In 6 sheep, this section was then reinforced with a Personalized External Aortic Root Support (PEARS, [2]) textile and in 3 sheep the section remained unreinforced. 6 months after the procedure, the animals were sacrificed and the tissue was harvested. This resulted in 5 different tissue types: unreinforced aorta in native position (UAA), unreinforced pulmonary in native position (UPP), unreinforced pulmonary artery placed in aorta position (UPA), reinforced aorta in native position (RAA) and reinforced pulmonary artery placed in aorta position (RPA). These tissues were tested mechanically on a planar biaxial and a uniaxial tensile set-up. From this experimental data stress-strain curves were calculated on which the GOH-model [3] was fitted. The results of the parameter fitting were used in a finite element analysis of the Ross procedure.

## Results & Discussion:

The adaptation of the mechanical behavior of unreinforced pulmonary artery (UPP, yellow) when placed in aorta position (UPA, green) is shown in the stress-strain curves of Figure 1. The altered pressure to which the pulmonary artery is subjected in aorta position, causes changes in the arterial wall stress. This in turn, can cause growth and remodeling phenomena, of which the result is visualized in Figure 1: 6 months after the unreinforced pulmonary tissue is placed in aortic position it approximates unreinforced aorta (UAA, red).

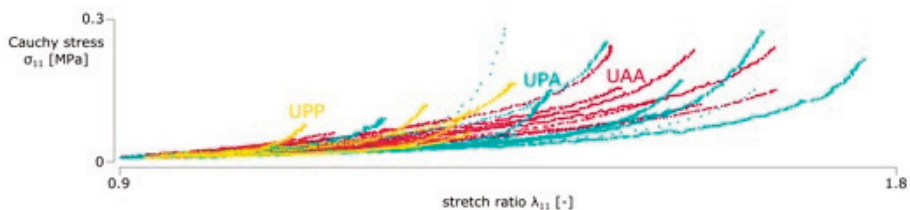


Figure Caption: " The stress-strain curves show the adaptation of the mechanical behavior of unreinforced pulmonary artery (UPP) when placed in aorta position (UPA): after 6 months it approximates unreinforced aorta (UAA)"

## Acknowledgments:

The authors would like to thank prof. dr. Filip Rega, dr. Peter Verbrugghe and dr. Tom Verbelen for their help in the experiments. This work was supported by a postdoctoral fellowship of the Research Foundation-Flanders and the Materialise chair for patient-specific, image-based biomechanics.

## References:

[1] J. W. Brown et al, *Eur J Cardiothorac Surg.*, 37(5):1002-7, 2010.

[2] J. Pepper et al, *Interact. Cardiovasc. Thorac. Surg.*, 10(3):360-365, 2010.

[3] T.C. Gasser et al, *J. R. Soc. Interface.*, 3(6):15-35, 2006."

# MICROSTRUCTURAL MODELS OF LIGAMENT AND TENDON ELASTICITY AND VISCOELASTICITY

**Tom Shearer<sup>1</sup>, William Parnell<sup>1</sup>**

*<sup>1</sup> University of Manchester, Manchester, United Kingdom*

Ligaments and tendons are fundamental structures in the musculoskeletal systems of vertebrates that consist of collagenous fibres organised in a hierarchical structure. Their main subunit is the fascicle which is made of fibrils arranged in a crimped pattern. In this talk, I will discuss two models that describe the mechanical behaviour of ligaments and tendons and are based on the microstructure described above.

The first model is a non-linear elastic model, which is expected to be valid in the low strain-rate limit. I will derive a new strain energy function for modelling ligaments and tendons based on the geometrical arrangement of their fibrils, and will compare the ability of the new model [2] to reproduce experimental data with that of the commonly-used Holzapfel-Gasser-Ogden (HGO) model [1]. I will show that the new model gives a better fit to stress-strain data for human patellar tendon than the HGO model, with the average relative error when using the new model being 0.053 (compared with 0.57 when using the HGO model).

The second model is a viscoelastic model. By assuming that each fibril is now linearly viscoelastic, I will show that several complex, non-linear viscoelastic effects can be explained solely by the distribution of the fibril crimp lengths. The viscoelastic model also shows excellent agreement with experimental data, and can reproduce different data sets with the same set of constitutive parameters simply by changing the distribution of the crimp lengths.

## References:

1. G.A. Holzapfel, T.C. Gasser and R.W. Ogden, A new constitutive framework for arterial wall mechanics and a comparative study of material models. *J. Elast.* 61, 1-48, 2000.
2. T. Shearer, A new strain energy function for the hyperelastic modelling of ligaments and tendons based on fascicle microstructure. *J. Biomech.* 48, 290-297, 2015.

## INVESTIGATION OF THE STATE OF STRESS GENERATED BY HIGH LOADS IN THE OVINE LUMBAR INTERVERTEBRAL DISC USING A NEW ANISOTROPIC HYPERELASTIC MODEL.

**Gloria Casaroli**<sup>1</sup>, **Fabio Galbusera**<sup>2</sup>, **Tomaso Villa**<sup>3</sup>

<sup>1</sup> Politecnico DI Milano, Milano, Italy,

<sup>2</sup> Ircs Istituto Ortopedico Galeazzi, Milan, Italy,

<sup>3</sup> Politecnico DI Milano, Dept. of Chemistry, Material and Chemical Engineering "G. Natta", Milano, Italy

Many finite element models of the intervertebral disc have been developed, and the most of them consider the annulus fibrosus a fiber reinforced material. We believe that an anisotropic hyperelastic material is a good alternative for the representation of both the fibers and the matrix. The aim of this study was to generate a finite element model of the intervertebral disc characterized by anisotropic hyperelastic material and to define which load is the most unsafe. We generated a finite element model of the ovine lumbar disc and we assigned to the annulus the law suggested by Holzapfel. Two families of fibers were defined. We assigned the mechanical parameters performing a full factorial optimization method: for the ground matrix we simulated some compression tests on samples with Neo-Hookean material neglecting the presence of the fibers [1]; for the fibers, we simulated traction tests assuming for the matrix the parameters found previously. We assigned to the nucleus Neo-Hookean properties and to the endplates elastic properties taken from literature [2]. We performed some numerical analysis based on a parallel in vitro study in which flexion, lateral bending and axial rotation with magnitude double of the physiological one have been applied. The simulations showed that flexion generates the highest state of stress in the posterior region in circumferential and axial direction. According to in vitro test, axial compression and axial rotation do not induce high stress in the annulus; however, axial compression is the condition that most increases the intradiscal pressure and the stress in the endplates. This model permits to perform many other investigations and renders it a valid tool for biomechanical investigations on spinal instrumentation and on the mechanisms of herniation.

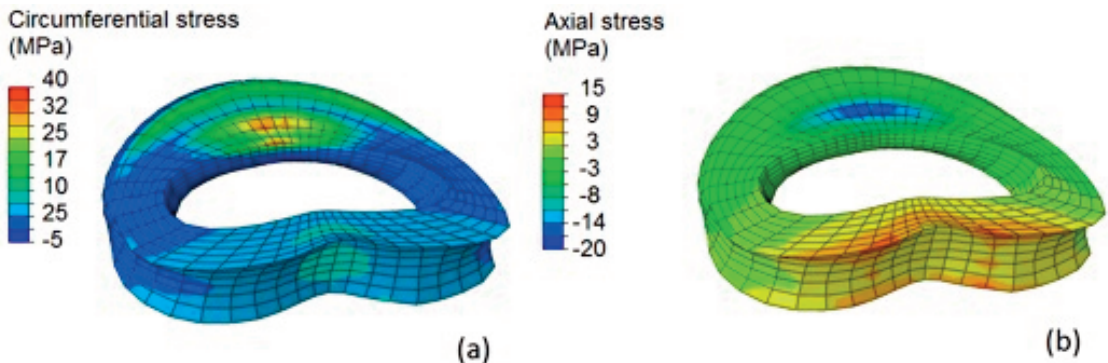


Figure Caption: State of stress in circumferential (a) and axial (b) direction generated by a flexion of 13°.

### References:

[1] Little, J. P. et al. 2010. "The Mechanical Response of the Ovine Lumbar Anulus Fibrosus to Uniaxial, Biaxial and Shear Loads." *Journal of the Mechanical Behavior of Biomedical Materials* 3: 146-57.

[2] Ayturk, Ugur M et al. 2012. "Modeling Degenerative Disk Disease in the Lumbar Spine: A Combined Experimental, Constitutive, and Computational Approach." *Journal of biomechanical engineering* 134(10).

# EFFECT OF NATURAL HONEY TREATMENT AND EXTERNAL STRETCHING ON KINEMATICS OF CELL MIGRATION DURING GAP CLOSURE

Yulia Berkovitch<sup>1</sup>, Amit Gefen<sup>2</sup>, Daphne Weihs<sup>3</sup>, Samer Toume<sup>4</sup>

<sup>1</sup> Technion-Israel Institute of Technology, Biorheology and Cell Mechanics Lab., Haifa, Israel,

<sup>2</sup> Tel Aviv University, Dept. of Biomedical Engineering, Tel Aviv, Israel,

<sup>3</sup> Technion - Israel Institute of Technology, Haifa, Israel, <sup>4</sup> Technion-Israel Institute of Technology, Faculty of Biomedical Engineering, Haifa, Israel

Wound healing is a complex natural response to tissue injury intended to restore the integrity and function of the tissue at the wounded site. The wound healing process occurs naturally under physical/mechanical forces, e.g. local stretching, and in many cases, benefits from application of applied remedies. Identification of potentially effective compounds requires specialized approaches to determine their effects on different cell types [1], [2]. However, working in vivo has quantification limits and ethical concerns arise. This is especially true for natural origin compounds, such as plant extracts, honey, and larvae, which have a complex composition and determining their clinical efficacy is challenging [3]. Thus, in vitro gap closure assays can be used to evaluate the effects of natural treatments and external strains on migration associated with gap closure.

Here, we evaluate the changes in cell migration during gap closure in vitro, following treatment with honey and/or under applied external strains. We generated monolayers of NIH3T3 mouse fibroblasts and induced a small gap (wound) at their center. Using custom image processing modules [4], we measured the kinematics of the gap closure, focusing on times of initiation and rates of migration. We evaluated the effects of different concentrations of a well-known natural wound-care agent, i.e. honey. Honey has been used in skin wound care for many years due to its anti-inflammatory, antimicrobial, and cell-stimulating properties. Using our assay we are able to show the direct effects of honey on the migratory capabilities of the cells and the kinematics of gap closure. In addition, we evaluate the effects of externally applied stretching, with and without addition of natural remedies, on the gap closure process. For this, we grow the cell monolayer on an elastic, stretchable membrane, which is then stretched in varying levels using a 3-D printed cell stretching apparatus [5]. We evaluated the effects on gap closure kinematics of different levels of externally applied strains, showing that low (3%) strains may accelerate gap closure, while higher (6%) strain may not be as efficient, relative to unstretched control. Thus, combining external deformation with various treatments can enhance the rate of migration and thus shorten the time required for wound healing.

## Acknowledgments:

The work was partially supported by the Israeli Ministry of Science and Technology 3rd Age Program.

## References:

- [1] M. A. Boink, L. J. van den Broek, S. Roffel, K. Nazmi, J. G. M. Bolscher, A. Gefen, E. C. I. Veerman, and S. Gibbs, "Different wound healing properties of dermis, adipose, and gingiva mesenchymal stromal cells," *Wound Repair Regen.*, vol. 24, no. 1, pp. 100–109, Jan. 2016.
- [2] A. Gefen and D. Weihs, "Mechanical cytoprotection: A review of cytoskeleton-protection approaches for cells," *J. Biomech.*, vol. 49, no. 8, pp. 1321–1329, May 2016.
- [3] G. Topman, F.-H. Lin, and A. Gefen, "The natural medications for wound healing - Curcumin, Aloe-Vera and Ginger - do not induce a significant effect on the migration kinematics of cultured fibroblasts," *J. Biomech.*, vol. 46, no. 1, pp. 170–174, Jan. 2013.
- [4] G. Topman, O. Sharabani-Yosef, and A. Gefen, "A standardized objective method for continuously measuring the kinematics of cultures covering a mechanically damaged site," *Med. Eng. Phys.*, vol. 34, no. 2, pp. 225–232, Mar. 2012.
- [5] S. Toume, A. Gefen, and D. Weihs, "Printable low-cost, sustained and dynamic cell stretching apparatus," *J. Biomech.*, vol. 49, no. 8, pp. 1336–1339, May 2016.

## FOOT TYPE BIOMECHANICS: A MATTER OF STRUCTURE, FUNCTION, AND FLEXIBILITY

The foot is comprised of 28 bones, 33 joints and 112 ligaments controlled by 13 extrinsic and 21 intrinsic muscles and therefore one of the most mechanically complex parts of the human body. As a result there is no one 'normal' foot. Different structures such as planus (low), rectus (moderate), and cavus (high) arches that may exhibit over-pronatory, normal, or over-supinatory function (Figure 1), and have low, normal, or high degrees of flexibility can all occur in an asymptomatic individual devoid of foot disorders or injury. Based upon epidemiology, when a foot disorder or injury is present, it is more often associated with planus or cavus foot types as opposed to rectus. Structural alignment appears to be an important factor.

Cross-sectional and longitudinal data from epidemiological and controlled biomechanical experiments as well as computational models will be presented to illustrate these concepts. When structure is modified, either surgically (e.g. Evans calcaneal osteotomy) or non-surgically (e.g. custom foot orthoses), in general an improved foot function results. In a longitudinal study of recently diagnosed patients with Rheumatoid arthritis there was a 73% less likelihood of developing hallux valgus (bunion deformity) in those randomly assigned to custom foot orthoses compared to those with a sham placebo orthosis (Budiman-Mak et al) which suggests that foot deformity could be prevented. Using a measure of foot function (i.e. center of pressure excursion index (CPEI)) in the Framingham cohort an analysis by quintiles of CPEI linked hallux valgus to pes planus feet while an analysis by foot type linked pes planus to hallux valgus and hallux rigidus (1st metatarsal phalangeal joint osteoarthritis). A study of Navy Seals found that planus and rectus foot types were associated with twice the odds ratio of receiving a stress fracture than those with rectus feet (Kaufman et al, 1999). Research on both older (Hannan et al, ) and younger cohorts (Zifchock et al, 20016) is finding differences in foot types across racial/ethnic groups as well as genders. A recent genome wide association study (GWAS) has found that hallux valgus may be heritable (Hannan et al).

When modeling the 1st metatarsophalangeal joint, contact pressure is affected by foot type (Figure 2). Once again, the planus and cavus foot structures have a higher magnitude of stress. With appropriate boundary and loading conditions it is possible to assess how a 'virtual' surgery (e.g. Cheilectomy, Moberg, etc) is likely to change the mechanics of a joint. Several clinical examples will be provided to illustrate how the data from epidemiological studies, controlled biomechanical experiments, and computational models may be utilized to inform clinicians of the pathomechanics of foot disorders and injury as well as the effect of surgical and non-surgical treatment.

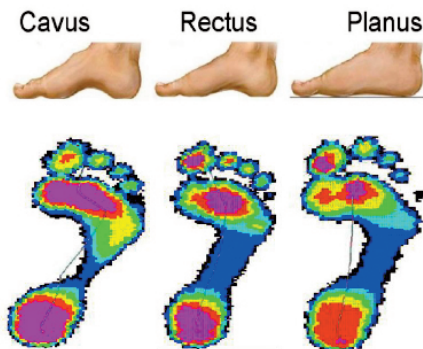


Figure 1: Cavus foot structures typically exhibit over-supination (excessively concave center of pressure (COP)) while planus foot structures often exhibit over-pronation (insufficiently concave COP)

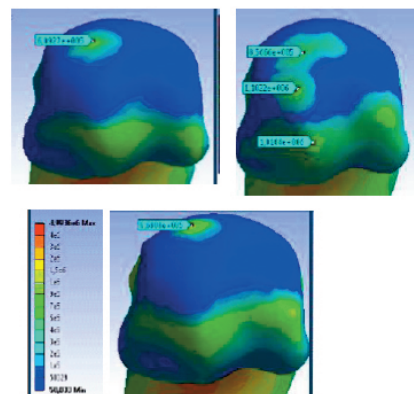


Figure 2: Stress distribution in the distal 1st Metatarsal (head) for the (a) Rectus (0.61 MPa), (b) Pes planus (1.10 MPa), (c) Pes cavus (0.97 MPa) foot types

### Acknowledgments:

NIH 1R03HD053135-01, Stride Rite, NICHD-NCMRR, NIA, NIAMS, NSF, Foot and Ankle Research Fund

# BIOMECHANICS OF FOOT WITH TOTAL ANKLE ARTHROPLASTY

**Yan Wang<sup>1</sup>, Duo Wai-Chi Wong<sup>1</sup>, Ming Zhang<sup>1</sup>**

*<sup>1</sup> Interdisciplinary Division of Biomedical Engineering, The Hong Kong Polytechnic University, Kowloon, Hong Kong*

Total ankle arthroplasty is one of the most common surgeries for ankle reconstruction. Biomechanical exploration of rationale information is of critical importance in clinic. This study aims to investigate the biomechanics of total ankle arthroplasty using finite element analyses.

Finite element models of a normal foot and foot with total ankle arthroplasty (Figure 1) were developed [1, 2], involving most of the anatomical characteristics. Three characteristic instants during gait, named the first peak, mid-stance, and the second peak, were simulated. Boundary and loading conditions were obtained from gait analysis. The model was validated through comparison of plantar pressure and joint contact pressure between computational predictions and experimental measurements.

The results of simulation in total ankle arthroplasty model were compared to that in the normal foot model. It was found that total ankle arthroplasty did not induce notable variation of plantar pressure. But joint contact pressure was apparently affected, increased by 20%, 67% and 44% correspondingly at the talonavicular, medial cuneonavicular and the first tarsometatarsal joints. von Mises stress in the second metatarsal bone increased by 31% at the second peak instants. Joint motion of the prosthetic ankle in the sagittal plane could not achieve the full range as in normal foot, and it was compensated by larger deformation of the forefoot. The prosthetic joint borne asymmetric loading, especially at the second peak instant (Figure 2).

Total ankle arthroplasty induced a series of biomechanical variations to the entire foot, especially at the second peak instant including joint contact pressure, bone stress and joint motion. These deviations might result in risk of negative outcomes postoperatively.



Figure 1 Finite element model of total ankle arthroplasty foot.

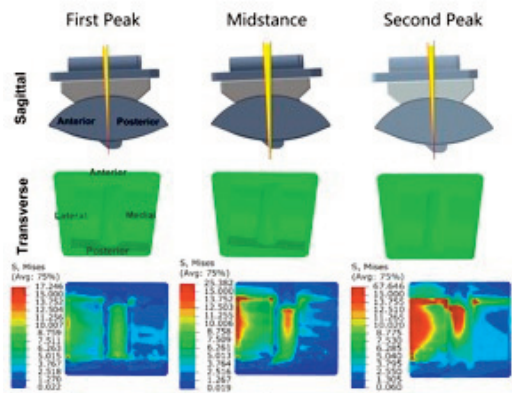


Figure 2 Joint motion of ankle prostheses and stress distribution in the prosthetic component

## Acknowledgments:

This project was supported by Hong Kong Research Grant Council GRF (PolyU152216/14E,152002/15E) and NSFC (11272273, 11120101001)

## References:

1. Wang, Y., et al., *Effects of Ankle Arthrodesis on Biomechanical Performance of the Entire Foot. PloS one*, 2015. 10(7): p. e0134340.
2. Wang, Y., D.W.-C. Wong, and M. Zhang, *Computational models of the foot and ankle for pathomechanics and clinical applications: a review. Annals of biomedical engineering*, 2016. 44(1): p. 213-221.

# THE EFFECT OF THE GROUND REACTION FORCE MANIPULATION ON THE COP WITH EMPHASIS ON THE SHEAR FORCES

**Hadar Shaulian<sup>1</sup>, Alon Wolf<sup>2</sup>**

<sup>1</sup> Technion- Israel Institute of Technology, Haifa, Israel,

<sup>2</sup> Technion-Israel Institute of Technology, Haifa, Israel

## Introduction:

The foot Center of Pressure (COP) is a locus about the foot which can be defined as the average location of all external forces acting between the foot and the ground during the stance phase of gait. This is also the origin of the Ground Reaction Force (GRF) vector. [1,2]

The GRF vector can be split into the vertical direction (V) which relates to tensile strength and the Anterior-Posterior (AP) and the Lateral-Medial (LM) directions which relate to the shear forces acting on the foot during gait.

In this study we have examined the effect of shifting the GRF (hence the COP), on the shear forces change.

## Methods:

Twelve healthy male subjects walked a ten-meter distance whilst wearing a biomechanical shoe device which allowed for controlled manipulation of the COP location [3]. The device was set to convey three different para-sagittal locations of the COP: the neutral sagittal, medial and lateral axes. The medial and lateral axes were placed 0.8 cm and 1.5 cm from the neutral position, respectively.

COP trajectory was collected using a Vicon motion analysis system while the GRF was recorded using two three-dimensional force plates.

Each of the components of the GRF vector was divided into the four sections of stance defined by Parry and Davids [4].

## Results:

As the result of the offset of the biomechanical elements, throughout the stance The GRF was shifted. The largest relative shift of the force occurred along the LM direction, while in majority of the cases, in all GRF directions the most significant change is at the begging of the stance phase. In addition, the most significant asymmetry between right foot and left foot was observed at the same LM direction (fig. 1). This may suggest that controlling the COP LM direction can support in improving the left to right gait asymmetry.

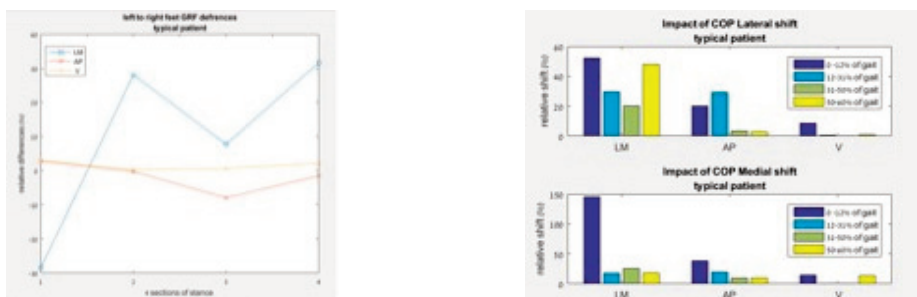


Figure 1: (a) The relative change of GRF as a result of COP change relative to its natural position (b) GRF differences between left and right foot at natural COP position

## References:

- [1] K.J. Chesnin, L. Selby-Silverstein, M.P. Besser, *Gait & Posture*, 2000, 12, 128.
- [2] P.R. Cavanagh, *Journal of Biomechanics*, 1978, 11, 487.
- [3] A. Haim et al., *Journal of Biomechanics*, 2008, 41, 3010.
- [4] J. Perry, J. Davids, *Journal of Pediatric Orthopaedics*, 1992, 12, 815.

# INFLUENCE OF MUSCLE STRENGTH ON HIP CONTACT FORCES FOLLOWING TOTAL HIP ARTHROPLASTY WITH A MINIMAL DIRECT ANTERIOR APPROACH

Xuan Zhang<sup>1</sup>, **Enrico De Pieri**<sup>2</sup>, Bernd Friesenbichler<sup>3</sup>, Nicola Maffiuletti<sup>3</sup>, Stephen J. Ferguson<sup>2</sup>

<sup>1</sup> Eth Zurich; Institute for Biomechanics, Zurich, Switzerland, Xi'an Jiaotong University, Xi'an, P.R. China, Zurich, Switzerland,

<sup>2</sup> Eth Zurich, Institute for Biomechanics, Zurich, Switzerland,

<sup>3</sup> Schulthess Klinik, Zurich, Switzerland

## Introduction:

Musculoskeletal modelling provides a valuable and versatile tool to predict hip contact forces (HCF): they allow evaluation of pre- and post-operative joint forces and can be used to analyze the influence of different surgical techniques. In this study, the difference between pre- and post-operative HCF was investigated for simulated gait, using pre- and post-operative gait and muscle strength data from 21 patients with unilateral THA, operated with a minimal direct anterior (MDA) approach.

## Methods:

Pre- and post-operative (28 weeks) gait parameters (step time and length, stride time, single and double support time) were compared in 21 hip arthroplasty patients to evaluate differences in the kinematics. When the differences were <10%, a generic motion capture marker dataset was used as the kinematic input for both sets of gait simulations (AnyBody Modeling System). Pre- and post-operative maximum voluntary contraction torques was measured on the operated and non-operated side in each patient to provide reference values for the modification of the muscle strength of the affected muscle groups in the musculoskeletal model. HCF were calculated for a whole gait cycle, for the pre- and post-operative condition.

## Results and Discussion:

The comparison of gait parameters between pre- and post-THA did not reveal any major difference (>10%), allowing the use of an unaltered kinematic input for both models. With MDA surgery, the difference in muscle strength between the operated and non-operated leg was reduced at 28 weeks post-op (Figure 1). Reduction in muscle strength had a small influence on HCF on only the operated side. The post-operative HCF better approximated the normal values (Figure 2). However, the influence of patient-specific kinematics on HCF should still be evaluated.

We conclude that variations in muscle strength, within a realistic pre- and post-operative range, result in only small differences in joint forces. Nevertheless, with an MDA approach, a return towards muscle symmetry is observed, which results in hip contact forces more closely resembling normal values.

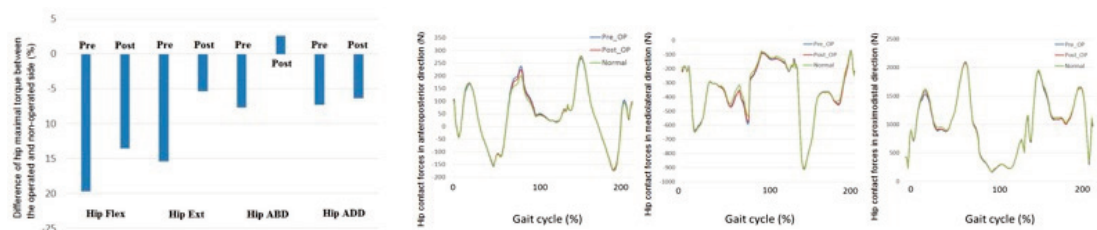


Figure 1: Difference of hip maximum torque between the operated and non-operated side, before and after THA.

Figure 2: Hip contact forces on operated side before and after THA.

# FORCE TRANSMISSION THROUGH THE WRIST DURING PERFORMANCE OF PUSHUPS ON A HYPEREXTENDED AND A NEUTRAL WRIST

**Olga Polovinets<sup>1</sup>, Alon Wolf<sup>2</sup>, Ronit Wollstein<sup>3</sup>**

<sup>1</sup> Technion Israel Institute of Technology,

<sup>2</sup> Technion,

<sup>3</sup> Technion Israel Institute of Technology, School of Medicine; Department of Plastic Surgery, University of Pittsburgh, Pittsburgh, Pa

## Introduction:

Push-ups are a basic sport activity used for multiple purposes, such as military physical training [1], [2] rehabilitation after injury, and martial arts [3]. The wrist is an important joint in this activity, transferring the force to the upper limbs. The biomechanics of the wrist are not yet completely understood. The purpose of this study was to compare the forces in the wrist during push-ups on a hyperextended wrist and during push-ups performed on a straight wrist. We hypothesized that force transmission in the wrist differs between these two push-ups methods.

## Methods:

Fourteen healthy right-handed male volunteers performed 2 sets of push-ups on a straight wrist and 2 sets on a hyperextended wrist. The push-ups were performed in a gait analysis laboratory using a Vicon motion capture system and 26 reflector markers to follow the kinematics of the exercise. The force vectors were measured using two AMTI force plates and computed using Matlab software. An ultrasound machine was used to determine the capitate bone location. Statistical analysis using IBM SPSS software on the forces, the force angle and marker position was performed.

## Results:

In both methods, the force was not uniform throughout the push-up task. The force patterns did not change while the dominant hand was loaded with a higher force, regardless of the type of push-up. Knuckle push-ups had a more uniform force, the angle of force distribution was smaller and a capitate marker had smaller location distribution. In hyperextended push-ups the horizontal distance between the capitate bone location and force origin was smaller, the force origin was closer to the ulna marker and force passed more dorsally to the joint (fig. 1).

## Conclusions:

Forces through the wrist are distributed differently during the different types of push-ups. In hyperextension the forces are more: dorsal, ulnar and have a wider distribution.

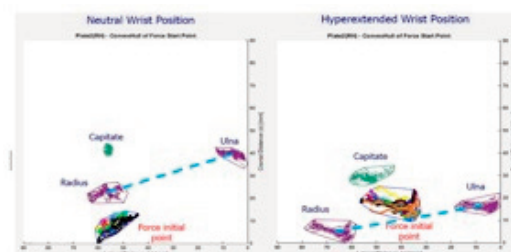


Figure 1: Projection of measured anatomical markers on the force plate and the correspondent convex-hull of the location points, hyperextended vs. neutral push-ups.

## References:

- [1] S.B. Jones et al., *Military medicine*, 2007, 172, 115.
- [2] M.J. Armentano et al., *Military medicine*, 2007, 172, 312.
- [3] M. Brudnak, D. Dundero, F. Van Hecke, *Medical Hypotheses*, 2002, 59, 485.

## PATIENT-SPECIFIC SIMULATION OF SPINE DEFORMITY CORRECTION BASED ON BIPLANAR RADIOGRAPHIC IMAGES

**Fabio Galbusera<sup>1</sup>, Tito Bassani<sup>1</sup>, Benedikt Schlager<sup>2</sup>, Hans-Joachim Wilke<sup>2</sup>, Marco Brayda-Bruno<sup>3</sup>**

<sup>1</sup> Irccs Istituto Ortopedico Galeazzi, Milan, Italy,

<sup>2</sup> Institute of Orthopaedic Research and Biomechanics, Ulm University, Ulm, Germany,

<sup>3</sup> Spine Surgery III, Irccs Istituto Ortopedico Galeazzi, Milan, Italy

Spine deformities, including adolescent and degenerative scoliosis and fixed sagittal imbalance are frequently surgically corrected with high success rates and patient satisfaction. Nowadays many implantable devices, techniques and tools are available as surgical options, and the choice of the optimal one for a specific clinical case has been shown not to be trivial [1]. Besides, the selection of the fusion levels and the degree of tolerable correction are a matter of debate.

Recently, we presented a user-friendly method to perform patient-specific simulations of surgical correction of spine deformities, based on three-dimensional reconstruction of the patient anatomy conducted on biplanar full-body radiographs [2]. The method can predict the stresses acting in the instrumentation after performing corrective maneuvers and under physiological loads. The approach has been extended to allow simulating, in addition to fixation with pedicle screws, also sublaminar hooks and osteotomies. As a proof of concept, the simulation of the surgical correction of three clinical cases has been performed: (1) a patient suffering from degenerative lumbar spondylolisthesis at L4-L5; (2) a case of adolescent scoliosis corrected with a hybrid approach (pedicle screws and hooks); (3) a case of sagittal imbalance corrected by means of pedicle subtraction osteotomy and posterior fixation. For each case, several possible variations of the approach (e.g. by changing the fusion length) have been performed. A comparative analysis of the loads and stresses in the instrumentation as well as of the stresses at the bone-implant interface has been conducted. Taking into account the several assumptions (e.g. about the lack of patient-specific material properties), the modeling approach proved to be able to highlight biomechanical differences among the various surgical options, which may have a relevance in the choice of the optimal solution.

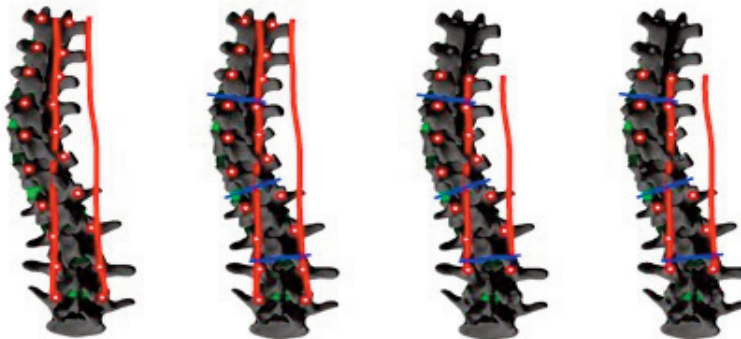


Figure Caption. Various plausible options for the surgical correction of a case of adolescent idiopathic scoliosis, which were simulated by means of the novel method.

### Acknowledgments

The work was funded by the Italian Ministry of Health (GR-2011-02351464).

### References

[1] Aubin et al., *Eur Spine J.* 2007 Jan;16(1):57-64.

[2] Galbusera et al., *Front Bioeng Biotechnol.* 2015; 3:178.

# ULTRASPINE: MINIMALLY INVASIVE FRACTIONATION OF DEGENERATE INTERVERTEBRAL DISC NUCLEUS PULPOSUS BY ULTRASOUND AND ITS REPLACEMENT BY AN INJECTABLE HYDROGEL

*Shan Quiao*<sup>1</sup>, *Delphine Elbes*<sup>1</sup>, *Olga Boubriak*<sup>1</sup>, *Jill Urban*<sup>2</sup>, *Robin Cleveland*<sup>1</sup>, ***Constantin Coussios***<sup>1</sup>

*1 University of Oxford, Institute of Biomedical Engineering, Old Road Campus Research Building, Oxford, United Kingdom,*

*2 University of Oxford, Department of Anatomy, Physiology & Genetics, Oxford, United Kingdom*

We present a novel method for image-guided minimally invasive removal of degenerated nucleus pulposus (NP) in the intervertebral disc (IVD) using High Intensity Focussed Ultrasound, potentially enabling its replacement using injectable hydrogels. The feasibility of therapeutic ultrasound delivery to the intervertebral disc is first investigated computationally, using patient-specific reconstruction from MR and CT data and a full acoustic propagation model to predict the ultrasound field delivered using an array of therapeutic ultrasound transducers. We demonstrate that ultrasound-mediated fractionation of the NP is therefore possible in patients with a broad range of body-mass-indices (BMI) in the range 15-35 in all segments of the lumbar spine other than L5-S1. Following injection of ultrasound-sensitive nanoparticles through a fine-gauge needle into the centre of the NP, successful fractionation of bovine tail discs is subsequently demonstrated experimentally under real-time ultrasound guidance. Lastly, we demonstrate successful injection of a model nucleus replacement material only in IVDs that have been successfully fractionated by ultrasound, confirming the need for disc fractionation prior to IVD replacement. Future work will focus on biomechanical testing of both ultrasound-fractionated and hydrogel replaced discs, in order to demonstrate the functional viability of this novel IVD replacement strategy.

## Acknowledgments:

The authors gratefully acknowledge the financial support of the UK's Engineering and Physical Sciences Research Council (EPSRC) under award EP/K021729/1. The authors would also like to thank collaborators at the University of Leeds (Prof. Ruth Wilcox, Dr Danielle Miles, Dr Marlene Mengoni and Dr Sebastien Sikora) and at the Ort Braude College of Engineering (Prof. Sarit Savan) for their advice and experimental contributions to the Ultraspine project.

# UNDERSTANDING CEREBROSPINAL FLUID FLOW IN THE SPINAL SUBARACHNOID SPACE AND PERIVASCULAR FLUID TRANSPORT INTO THE SPINAL CORD: THE ROLE OF CSF PRESSURE PULSE SHAPE

Elizabeth Clarke<sup>1</sup>, David Fletcher<sup>2</sup>, Lynne Bilston<sup>3</sup>

1 Murray Maxwell Biomechanics Laboratory, Institute for Bone and Joint Research, Kolling Institute of Medical Research, University of Sydney, Sydney, Australia, 2 School of Chemical and Biomolecular Engineering, University of Sydney, Sydney, Australia, 3 Neura & Unsw, Sydney, Australia

Syringomyelia is an enigmatic neurological disorder in which high pressure fluid-filled cysts form in the spinal cord. It is associated with obstructions in the spinal subarachnoid space (SSAS). Fluid enters the cord from the SSAS via peri-arterial spaces, driven, at least in part, by arterial pulsations. The aim of this study was to determine how the features of the pressure pulses associated with spinal CSF flow might influence perivascular flow into the spinal cord.

Exploratory CFD simulations of three human volunteers (1 healthy control, 2 Chiari malformation patients with/without a syrinx) were conducted to determine the features of the spinal CSF pressure pulses. SSAS geometries and input flows were determined from MRI as previously described (Clarke et al 2013). The SSAS pressure pulses were then used as input to a CFD model of a 'typical' perivascular space surrounding a penetrating spinal artery, that includes simulated arterial pulsations (Bilston et al, 2010), to estimate the influence on fluid transport into the spinal cord. A parametric analysis systematically varied temporal offsets between arterial and CSF pressure pulses, timing and magnitude of the peak CSF pressure, timing of reversal from high to low CSF pressure, and the area under the pressure-time curve.

Our model predicted that the patient with syringomyelia had higher flow into the spinal cord than those without syringomyelia. Peak CSF pressure, timing of the high and low pressure peaks in the SSAS pressure and heart rate had minimal effect on inflow. Increased area under the high pressure region of the SSAS pulse substantially increased flow into the spinal cord, for specific time offsets between arterial and SSAS pulses. These results indicate that a period of sustained high SAS pressure while arterial diameter is low may enhance CSF flow into the spinal cord.

## Acknowledgments:

LB is supported by an NHMRC Fellowship and this research was supported by the Column of Hope Foundation and the NHMRC.

## References:

- Bilston LE, Stoodley M & Fletcher DF, 2010. *J Neurosurg.* 112, 808-813.  
Clarke E, Fletcher D, Stoodley M & Bilston L, 2013. *J Biomech.* 46, 1801-1809.

## FINITE ELEMENT ANALYSIS OF PRE AND POST LUMBAR FUSION FOR SCOLIOSIS PATIENTS

Ram Haddas<sup>1</sup>, Ming Xu<sup>2</sup>, Isador Lieberman<sup>3</sup>, James Yang<sup>2</sup>

<sup>1</sup> Texas Back Institute Research Foundation, Plano, United States,

<sup>2</sup> Texas Tech University, Lubbock, United States, <sup>3</sup> Texas Back Institute, Plano, United States

Degenerative adult scoliosis results from age related changes leading to segmental instability, deformity and stenosis. Spinal fusion is a standard surgical treatment for deformity. In comparison to in vitro or in vivo approaches, finite element (FE) model studies eliminate the issues with cadaver use in addition to being cost efficient, time efficient, and an accurate surrogate. The purpose of this study was to investigate the effect of adjacent load transfer before and after fusion surgery for scoliosis patients.

Ten three-dimensional nonlinear FE models of the lumbosacral spine were created based on pre- and post-scoliosis surgery CT scans (Fig. 1). Pedicle screws and rods were implanted at L5-S1, L2-L4, L2-S1, T12-L5, L1-S1, for the 30, 39, 57, 64 and 81-year old subjects, respectively. For the analysis the S1 level in each model was fixed. A 500N compressive follower load and each of the following six loads were applied to the top level of each model: (1) flexion; (2) extension; (3) right lateral; (4) left lateral bending moments along with (5) right axial; and (6) left axial rotation moments. Intradiscal pressure (IDP), intersegmental rotation range of motion (ROM) and facet joint forces (FJF) at the adjacent level of the fusion and the top fused level were compared.

The application of the six different follower loads had only a minor to moderate effect at the adjacent level and large effect at the fused levels on the intersegmental rotation ROM, IDP, and FJF. Compared to the pre-surgery, the post-surgery intersegmental rotation ROM increased (2.80 %) at the adjacent level and decreased (86.69 %) at the fused level; the IDP increased (10.43 %) at the adjacent level and decreased (26.86 %) at the fused level; and the FJF increased (12.64 %) at the adjacent level and decreased (71.26%) at the fused level.

With this study we were able to investigate the effect adjacent load transfer before and after fusion surgery in scoliosis patients. The results will help define the variables contributing to adjacent level deterioration in the clinical environment.

*Figure Caption: Figure 1. Pre and post FE models: 30-year old (top), 39-year old, 57-year old (middle), 64-year old and 81-year old (bottom).*



# NOVEL INJECTABLE BIOMIMETIC GLYCOSAMINOGLYCAN ANALOGUES FOR INTERVERTEBRAL DISC REGENERATION: REPLACING LIKE WITH LIKE

**Sarit Sivan**<sup>1</sup>

<sup>1</sup> Ort Braude College, Karmiel, Israel

Intervertebral disc (IVD) degeneration and accompanying lower back pain (LBP) impose a major medical and societal challenge, costing around 1.5% of the GNP in industrialized countries [1]. The load-bearing biomechanical role of IVD is governed by the composition and organization of its major macromolecular constituents, the large aggregating proteoglycan (PG)- aggrecan embedded within collagen fibrills [2]. The primary role of aggrecan is to withstand high compressive stress. Key to this role is the negatively fixed charge density of its sulphated glycosaminoglycan (GAG) chains, which imparts a high osmotic pressure to the tissue, thus regulating and maintaining tissue hydration under load [3]. With the onset of disc degeneration, aggrecan is lost from the disc's inner regions [4], resulting in water loss and concomitant loss of disc height. Increased innervation and vascularization, which are related to the development of 'discogenic' LBP have also been reported [5]. A number of biomaterials, especially hydrogels, were suggested as replacement for disc tissue. However, none of the materials studied was found suitable enough to withstand the highly applied loads of the native disc tissue. We have developed biomimetic GAG analogues based on sulphonate-containing polymers. These GAG analogues have physico-chemical properties similar to those of the GAG on aggrecan molecules within the native disc nucleus. They are deliverable via injection into the disc where they polymerize in situ, forming a non-degradable, nuclear 'implant'. In vitro, these GAG analogues possess appropriate fixed charge density, hydration and osmotic responsiveness, thereby displaying the capacity to restore disc height and function. Preliminary biomechanical tests using a degenerate explant model [6] showed that the implant is stable and adapts to the space into which it is injected. These hydrogels mimic the role taken by GAGs in vivo and unlike other hydrogels, provide an intrinsic swelling pressure which can maintain disc hydration and stiffness under the high and variable compressive loads encountered in vivo.

## Acknowledgments:

This study was supported by the Engineering and Physical Science Research Council (GR/S41197/01) and by the Marie-Curie Intra European Fellowship (MEIF-CT-2005-025147, NovoDisc).

## References:

- [1]. Maetzel, A. et al. *Best Pract Res Clin Rheumatol* 2002;16:23-30. [2]. Pearce RH, et al. *J Orthop Res* 1987;5:198-205. [3]. Urban J, et al. *Clin Rheum Dis* 1980;6:51-76. [4]. Roberts S, et al. *Ann Rheum Dis* 1982;41:78-85.  
[5]. Freemont, A.J. et al. *Lancet* 1997;350:178-181. [6]. Roberts, S. et al. *BMC Musculoskeletal Disorders* 2008;9(1):24.

# VERTEBRAL LOADING DURING DAILY LIVING ACTIVITIES ESTIMATED FROM MEASURED SPINAL KINEMATICS: ELDERLY VS. YOUNG SUBJECTS

**Dominika Ignasiak<sup>1</sup>, Stephen J. Ferguson<sup>1</sup>**

*<sup>1</sup> Eth Zurich, Institute for Biomechanics, Zurich, Switzerland*

Excessive mechanical loading of spinal structures plays an important role in the development of vertebral fractures. Spinal loading patterns may depend greatly on the vertebral kinematics<sup>1</sup>, which differ between elderly and young individuals<sup>2</sup>. Therefore, the aim of this study was to investigate whether the age-related changes in spine kinematics lead to overloading of spinal segments.

A validated musculoskeletal model of the thoracolumbar spine<sup>3</sup>, developed in AnyBody, was used to estimate spinal segmental loading (at levels T1T2-L5Sacrum) during daily living tasks. Inverse dynamics simulations were performed of subject-specific spinal segmental motion patterns previously measured in healthy young (N=21, age=27.0±4.0) and elderly volunteers (N=21, age=70.1±3.9) during a flexion task<sup>2</sup>, sitting down and standing up from a chair.

The maximum compressive loads predicted for the elderly subjects performing the flexion task were significantly lower at T4T5 and lumbar levels (Fig). A trend of higher loading was found at segments T7T8-T11T12, but a significant difference was found only at T9T10. During sitting down and standing up from a chair, the maximum compressive loads were significantly lower in the upper thoracic levels (T1T2-T7T8 and T1T2-T6T7, respectively) and similar to the young at other levels. Maximum shear forces were also found to be lower (T2T3-T10T11 for flexion, T5T6-T6T7 for sitting tasks) or similar to those for the young, with the only exception being elevated shear forces at L5S1 during flexion.

The estimation of loads during daily living tasks indicates that the loading at several spinal segments is similar for elderly and young subjects, despite differences in motion patterns between the two groups. Nevertheless, as bone quality deteriorates with advancing age, this load level may eventually exceed vertebral strength and contribute to risk of fractures, but further analysis of more complex tasks is needed.

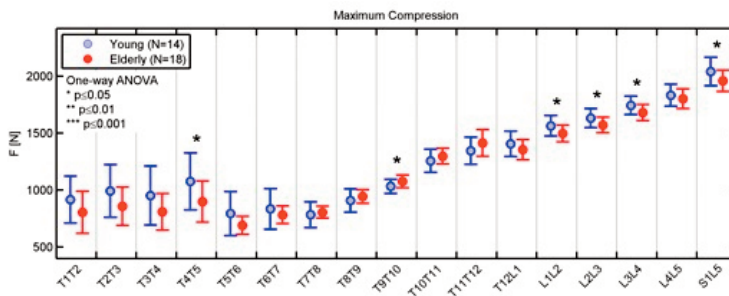


Figure Caption: Maximum segmental compression forces during simulated flexion task (analysed for successfully completed simulations).

## Acknowledgments:

This study was supported by a research Grant from AOSpine International, Switzerland.

## References:

1. Davis & Marras, *Clin Biomech*, 2000.
2. Ignasiak et al., *Proc. ESB2015, Prague 2015*.
3. Ignasiak et al., *J Biomech*, 2016.

## BIOMECHANICS OF IMPLANT FAILURE AFTER PSO: INFLUENCE OF THE HARDWARE CONFIGURATION THROUGH A FINITE ELEMENT ANALYSIS

**Tomaso Villa<sup>1</sup>, Claudia Ottardi<sup>1</sup>, Luigi La Barbera<sup>1</sup>, Andrea Luca<sup>2</sup>**

*1 Politecnico DI Milano, Dept. of Chemistry, Material and Chemical Engineering "G. Natta", Milano, Italy,*

*2 Irocs Istituto Ortopedico Galeazzi, Milano, Italy*

PSO is a technique usually performed at L3 or L4 levels that achieves corrections up to 35° for restoring the correct sagittal balance. The procedure still shows a high rate of complications (10-25%, usually rod breakage at the osteotomy level). In literature few studies investigate the biomechanics of PSO: the goal of this work is to fill this gap through a computational comparative analysis that investigates the effects of a set of variables in the instrumentation in order to decrease its rate of failure.

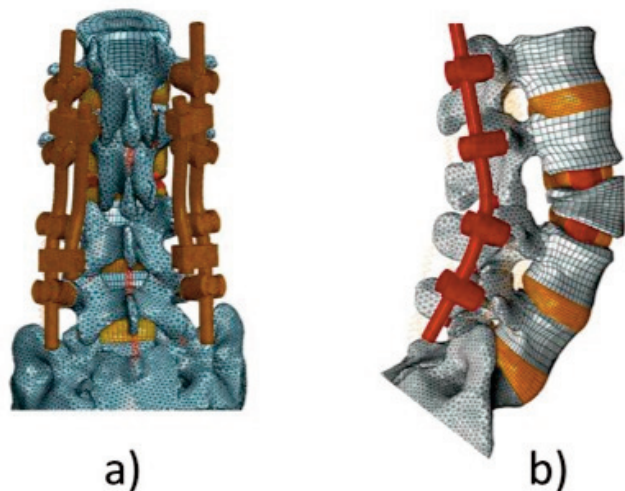
The influence of the following parameters on the stress arising in the rods has been investigated: (i) number of rods (one or two, Fig.1a) (ii) material of the rods (Ti or CoCr alloy) (iii) diameter of the rods (5 or 6 mm) (iv) anterior support (TLIF or XLIF and their position, Fig. 1b). A FE model of L1-S1 lumbar spine was built. PSO was simulated at L3 and spinal fixators were designed simulating a fixation two levels above and below the osteotomy. When the anterior support was simulated, the cages were inserted above, below and both above and below the osteotomy.

All the devices were modelled with the CAD software PTC Creo and the finite elements analyses were conducted using the software Abaqus 6.12-3.

The condition of standing was simulated using a follower load of 500 N and pure moments of  $\pm 7.5$  Nm in flexion, extension, lateral bending and axial rotation evaluating the load sharing between the anterior part of the spine and the rods and the stress in the rods.

Results show that the main stress concentration on the rods is at the osteotomy level. A stiffer material increases the load and the stress on the rods, a smaller diameter decreases the load on the rod but increases stress at the osteotomy level and a configuration with two rods increases the load on the instrumentation with a decrease of stress on the principal rods. Co-Cr double parallel rods produces the higher stress reduction on the implants near the treated level. When two cages are used an important reduction of the stresses is noted, marginal differences were found comparing the position of the cage above or below the osteotomy and different materials and finally a larger cage causes a 10% decrease of the stresses on the rods compared with the TLIF.

*Figure Caption: Figure 1: PSO at L3 level: a) double rod simulation, b) double cage simulation*



# FINITE ELEMENT ANALYSIS BASED LUMBOSACRAL REVISION SURGERY USING AN INDIVIDUAL NAVIGATION TEMPLATE

**Peter E. Eltes<sup>1</sup>, Marton Bartos<sup>2</sup>, Damien Lacroix<sup>3</sup>, Peter Pal Varga<sup>4</sup>, Aron Lazary<sup>4</sup>**

*1 National Center for Spinal Disorders, School of Ph.D Studies, Semmelweis University, Budapest, Hungary,*

*2 Do3d Innovations Ltd., Budapest, Hungary,*

*3 Department of Mechanical Engineering, Insigneo Institute for in Silico Medicine, The University of Sheffield, Sheffield, United Kingdom,*

*4 National Center for Spinal Disorders, Budapest, Hungary*

## Background:

A revision surgery in case of a lumbosacral non-union can be challenging especially if an implant related failure is complicating the clinical situation. In the S1 segment the proper insertion of the new screws in a revision surgery can be impossible without surgical navigation. In this paper, we present a case who has been surgically managed by the application of a CT based 3D reconstruction method combined with finite element analysis (FEA) and computer assisted design (CAD).

## Method:

A step-by-step approach was developed to manage the clinical problem. (1) Quantitative CT based patient-specific FE model of the sacrum was created. (2) CAD model of the pedicle screw was inserted in the sacrum model in a bicortical convergent and a monocortical divergent position. (3) Static FEAs (Abaqus, Dassault Systemes) were performed using 500 N tensile load applied to the screw head. (4) A template with the two screw guiding structures designed and created for the sacrum using 3D design and 3D printing technologies. (5) The surgery was performed using the patient- and condition-specific template.

## Results:

Based on the FEA results the modified bicortical convergent screw had better stability resulting in optimal von Mises stress distribution and less displacement compared to the monocortical divergent placement. The template design concept (Fig 1.) was shown to be accurate based on the CT scan and virtual model comparison. Intraoperatively the template fitted on the bone surface and screw insertion was completed successfully. Postoperative CT scans confirmed that the inserted pedicle screw reached the virtually planned position (Fig 2.).

## Conclusion:

The navigation provided by the patient specific screw-guiding template allows the surgeon to insert the screw into its optimal position considering the local bone material property and the challenging geometrical situation. Its advantages compared to the conventional surgical navigation techniques are the relatively low cost, minimized intraoperative X-ray exposure.

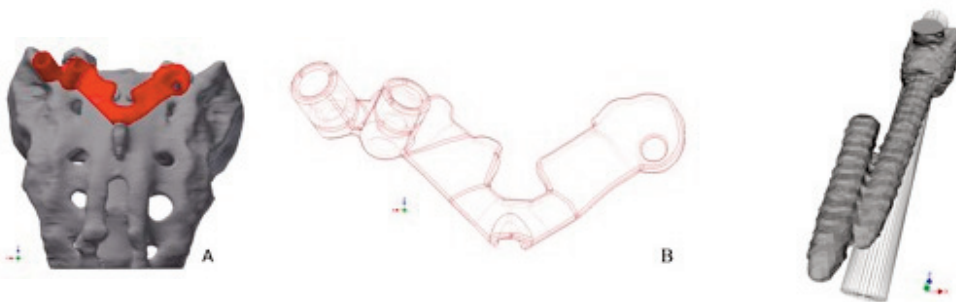


Fig 1. A. 3D representation of the patient specific surgical template (red). B. Wireframe representation of the surgical template.

Fig 2. 3D model of the broken screw and the new pedicle screw, the cylinder represents the preoperative virtual position of the revision screw.

## BIOMECHANICAL GAIT ASSESSMENT ON A PATIENT UNDERGOING SURGICAL CORRECTION OF KYPHOSIS FROM SEVERE ANKYLOSING SPONDYLITIS - A CASE STUDY

**Ram Haddas<sup>1</sup>, Theodore Belanger<sup>2</sup>**

*1 Texas Back Institute Research Foundation, Plano, United States, 2 Texas Back Institute, Rockwall, United States*

Ankylosing spondylitis is a chronic inflammatory disease primarily affecting the axial skeleton, including the sacroiliac joints and the spine. Clinical gait analysis is the process by which quantitative information is collected to aid in understanding the etiology of gait abnormalities and in treatment decision-making. Objective motor performance measures, especially gait analysis, could improve evaluation of spine disorder surgeries.

A 20 year-old male presented with severe ankylosing spondylitis, resulting severe sagittal imbalance and inability to stand erect. He presented with thoracic kyphosis of 70°, lumbar kyphosis of 25°, and pelvic incidence of 43°. The patient had a complex spinal reconstruction with 84° of sagittal correction, normalizing his sagittal alignment.

Gait analysis was performed the day before surgery and one month post surgery. Reflective markers were incorporated to collect full body 3D kinematics at a sampling rate of 100 Hz. Ground reaction forces were measured at 2000 Hz using force plates. Electromyography data from bilateral trunk and lower extremities were measured using preamplified surface at 2000 Hz. All raw data were exported from the Vicon Nexus system and imported into a custom Matlab program for processing. Three-dimensional joint rotation angle and muscles activity at the spine and lower extremity were analyzed using the custom algorithm.

Normalization of spinal alignment increased walking speed and cadence. The trunk muscles were activated earlier in the post surgery condition compared to the pre surgery condition. Lower extremity muscles did not show change in muscle activation time. Postoperatively, trunk flexion, neck extension and head orientation angles decreased at initial contact compared with preoperative values. Lower extremity angles were not symmetrical even one month post surgery.

Surgical correction of spinal alignment improved lower extremity function and efficiency. Changes in gait abnormality parameters observed imply that the patient used less energy to ambulate after surgery than before surgery. Formal gait and motion analysis can provide a method to assess the impact of severe spinal deformity on function and changes after treatment.



*Figure Caption: Pre (sitting) and post (standing) surgery radiographs*

## GENERATION OF ANATOMICAL MODELS FOR BIOMECHANICAL SIMULATION OF TRANSSEPTAL PUNCTURE

Pedro Morais<sup>1</sup>, João Vilaça<sup>2</sup>, Sandro Queiros<sup>3</sup>, Jan D'hooge<sup>4</sup>, Joao Tavares<sup>5</sup>

<sup>1</sup> Instituto de Ciência e Inovação Em Engenharia Mecânica e Engenharia Industrial, Faculdade de Engenharia, Universidade Do Porto, Porto, Portugal,

<sup>2</sup> Icv3/3b's - Pt Government Associate Laboratory, Digarc - Polytechnic Institute of Cávado and Ave, Guimarães, Portugal,

<sup>3</sup> Algoritmi Center, School of Engineering, University of Minho, Guimarães, Portugal,

<sup>4</sup> Lab on Cardiovascular Imaging & Dynamics, Department of Cardiovascular Sciences, University of Leuven, Leuven, Belgium,

<sup>5</sup> Faculdade de Engenharia, Universidade Do Porto, Instituto de Ciência e Inovação Em Engenharia Mecânica e Engenharia Industrial, Porto, Portugal

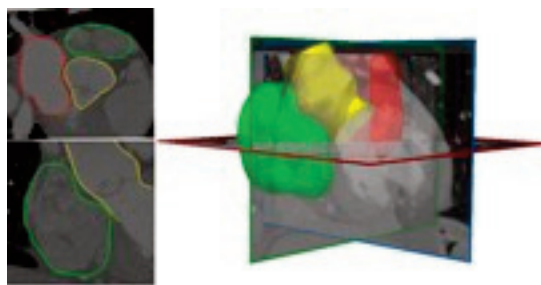
Access to the left atrium (LA) is required for several minimally invasive cardiac interventions of the left heart, such as catheter ablation for atrial fibrillation. Hereto, the septum is punctured using a catheter inserted in the right atrium (RA) via the venous system using fluoroscopy. Although this approach has been used for many years, complications and procedural failure are common.

This project aims therefore to develop technologies to assist the physician in performing atrial transseptal punctures. The goal is to use a subject-specific biomechanical approach to identify the optimal puncture position and consequently plan the entire procedure. Thus, a methodology to accurately obtain patient-specific atrial models from cardiac computed-tomography (CT) images is required. As such, here is presented the methodology used to generate these anatomical models.

The B-spline Explicit Active Surface framework was used to semi-automatically segment the LA, RA and aorta [1]. The segmentation process requires an initialization obtained through a manual definition of the desired structures (mitral valve, aortic valve, tricuspid valve and vena cava) and their boundaries. Then, a contour evolution strategy is used to delineate the entire cardiac chambers automatically.

The proposed methodology was tested on 8 CT datasets and the results compared against manual landmarks. APD errors of  $1.48 \pm 0.26$ ,  $1.56 \pm 0.52$  and  $2.51 \pm 0.87$  and DICE values of  $91.50 \pm 1.31$ ,  $89.54 \pm 2.95$ ,  $82.24 \pm 3.98$  were obtained for the LA, RA and aorta, respectively, which is very promising.

*Figure Caption: Result obtained with the semi-automatic segmentation approach.*



### Acknowledgments:

This work was supported by “Fundação para a Ciência e a Tecnologia” through the PhD grants SFRH/BD/95438/2013 and SFRH/BD/93443/2013. Authors gratefully acknowledge the funding of Project NORTE-01-0145-FEDER-000022 - SciTech - Science and Technology for Competitive and Sustainable Industries, cofinanced by “Programa Operacional Regional do Norte”, through “Fundo Europeu de Desenvolvimento Regional”.

### References:

[1] D. Barbosa et al.: B-spline explicit active surfaces: An efficient framework for real-time 3-D region-based segmentation. *Image Processing, IEEE Transactions on* 2012; 21:241-251.

# COMPUTATIONAL MODELING OF ELECTROMAGNETIC AND (FOCUSED-) ULTRASOUND THERMAL THERAPIES: APPLICATION TO APPLICATOR DESIGN, PERSONALIZED TREATMENT PLANNING/OPTIMIZATION, AND THERAPEUTIC INNOVATION

**Esra Neufeld<sup>1</sup>, Niels Kuster<sup>2</sup>**

*1 It's Foundation for Research on Information Technologies in Society, Zurich, Switzerland,*

*2 It's Foundation for Research on Information Technologies in Society, Swiss Federal Institute of Technology (Ethz), Zurich, Switzerland*

A comprehensive and validated simulation platform for computational modeling of thermal therapies has been developed. It includes functionality for image-based generation of personalized models (anatomy and tissue inhomogeneity/anisotropy), a population of predefined and parameterized high resolution human models, a data-base of tissue properties and their variability, applicator design functionality, interactive and verifiable patient/applicator placement tools (incl. automatic generation of rapid-prototyping fixation masks), high-performance-computing enhanced physics solvers for the simulation of acoustic and electromagnetic wave propagation within the human body, multi-scale thermo-physiological models of tissue temperature evolution considering the impact of perfusion and thermoregulation, biological effect estimation, multi-goal and interactive field optimization techniques to focus energy to target location while avoiding exposure of healthy tissues and compensating for organ motion, visualization and scripting interfaces, and functionality for automation in clinical environments.

The platform has been successfully applied to design a novel, closed-loop-controlled, modular hyperthermia applicator for superficial and deep hyperthermia therapy of tumors, a dedicated applicator for hyperthermia in the head&neck, multiple focused ultrasound ablation transducers, and a magnetic field applicator for nano-particle hyperthermia. It is being used for personalized treatment planning in hyperthermic oncology, RF-ablation, and focused ultrasound therapies (functional neurosurgery and tumor ablation), with recent pilot studies showing highly promising results (strong tumor volume reduction in previously untreatable animal patients, selective transcranial ablation of targets deep in the brain for chronic pain treatment...). The platform has also been applied to assess safety and efficacy of novel therapeutic approaches.



*Figure Caption: Modeling of acoustic (left) and radiofrequency (right) ablation of liver tumors.*

## Acknowledgments:

We gratefully acknowledge financial support by the Swiss Commission for Technology and Innovation CTI and by the Swiss National Centre of Competence in Research (NCCR) CO-ME, and major clinical input by the Erasmus Medical Center, the University Hospital Zurich, the Children Hospital Zurich, and the Kantonsspital Aarau.

# NEW METHOD FOR RADIOGRAPHIC SPINAL RECONSTRUCTION USING PROBABILISTIC PRINCIPAL COMPONENT ANALYSIS (PPCA)

**Olivier Moal<sup>1</sup>, Bertrand Moal<sup>2</sup>, Schwab Frank<sup>1</sup>, Virginie Lafage<sup>1</sup>**

<sup>1</sup> Hospital for Special Surgery, New York, United States,

<sup>2</sup> Nemaris, Hospital for Special Surgery, New York, United States

## Introduction:

With the development of radiographic analysis and surgery simulation in the setting of adult spinal deformity(ASD), spinal reconstructions are keys for patient treatment but are still time consuming. The aim of this work was to present data-driven models for faster and accurate sagittal and coronal spine reconstruction based on a few manually identified landmarks.

## Method:

Sagittal and coronal radiographic reconstructions of operated and non-operated ASD patients were analyzed by defining 72 anatomical landmarks each: femoral head centers, sacral endplate, and four corners of the lumbar and thoracic vertebrae. After identifying an initial set of 8 landmarks (femoral head centers, sacral plate, L1 and T1 superior endplates), both coronal and sagittal models were trained to predict the intermediaries vertebral corners using PPCA. Improvement of prediction was evaluated by manually identifying additional vertebral corners. The number of additional landmarks to obtain an RMSE below 10% and 5% for 95% of the tested reconstruction was calculated. RMSE errors were expressed in percentage of the L1 superior endplate length.

## Results:

The sagittal and the coronal model were respectively built with 2271 and 2187 ASD radiographic reconstructions and tested on 562 and 541 radiographs. After identifying the initial set of landmarks, the RMSE was  $15.7\% \pm 6.3$  for the sagittal model and  $14.0\% \pm 7.0$  for the coronal. For both Sagittal and coronal models, respectively 4 and 3 additional landmarks were needed to reach  $RMSE < 10\%$  for 95% of the tested reconstruction and 12 and 10 for an  $RMSE < 5\%$ .

## Conclusion:

Those models permits prediction of vertebral endplates from T1 to S1 based on the identification of only 12 of the 72 landmarks for both coronal and sagittal radiographs. Those models permit expeditious and accurate full spine reconstruction.

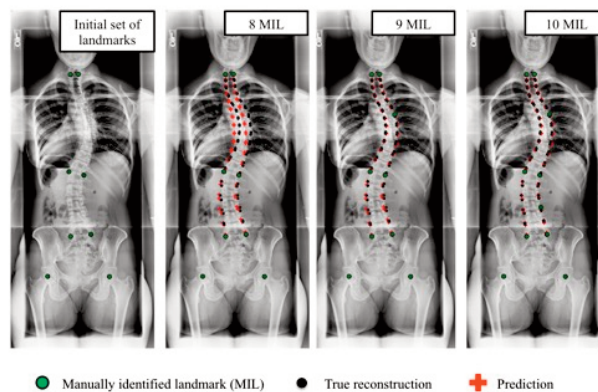


Figure Caption: Coronal model - Identification of the initial set of landmarks and prediction with the initial set of landmarks and additional landmarks to reach a RMSE below 5% of L1

## Acknowledgments:

Authors thanks for their support Menpo team: <http://www.menpo.org>

# PREDICTION OF ALIGNMENT AFTER SURGICAL TREATMENT OF ADULT SPINAL DEFORMITY (ASD) WITH PROBABILISTIC PRINCIPAL COMPONENT ANALYSIS

**Bertrand Moal<sup>1</sup>, Olivier Moal<sup>2</sup>, Schwab Frank<sup>2</sup>, Virginie Lafage<sup>2</sup>**

<sup>1</sup> Nemeris, Hospital for Special Surgery, New York, United States,

<sup>2</sup> Hospital for Special Surgery, New York, United States

## Introduction:

Sagittal plane malalignment is recognized as a key driver of disability and pain in ASD. However, prediction of postoperative sagittal alignment after vertebrae fusion, including changes in unfused vertebrae and pelvic version (pelvic tilt [PT]) remains challenging. Recent advances in machine learning algorithms and the availability of large spine reconstruction databases may offer new means to predict postoperative spino-pelvic alignment. The aim of this work was to present a data-driven model to predict postoperative spinal alignment using preoperative reconstruction and postoperative fused part.

## Method:

Radiographic sagittal reconstructions at baseline and 1 year after surgery for ASD patients fused from the sacrum up to between L1 and T4 were prospectively collected. Probabilistic principal component analysis model was used to build a model based on pre- and postoperative spine reconstruction. The unfused thoracic portion and the PT were then predicted. Model performance was evaluated based on the root-mean-square error (RMSE) between the prediction and the actual postoperative endplate location and on the absolute error of the PT and the thoracic kyphosis (TK). RMSE was expressed in percentage of L1 endplate length.

## Results:

The model was trained with 250 patients and tested on 60. The average RMSE related to the prediction of the location of the unfused endplate corners was  $26\% \pm 20$ . The error in term of PT and TK was respectively  $3.6^\circ \pm 3.0$  and  $8.5^\circ \pm 6.3$ .

## Conclusion:

The model permits prediction of vertebral endplates and provided good postoperative PT prediction but higher error for prediction of the unfused thoracic spine. Combining the pre-operative surgical planning/simulation with modeling can offer patient-specific prediction of postoperative alignment to substantially improve surgical effectiveness.

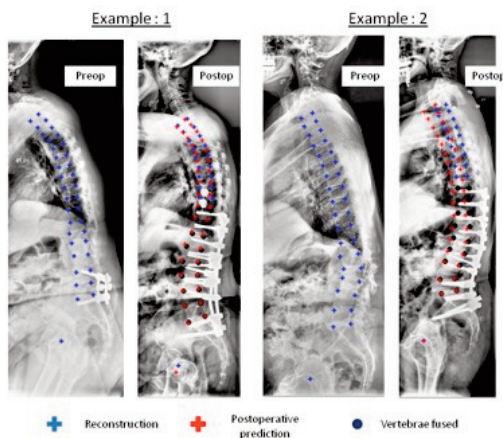


Figure Caption: Pre-operative reconstruction and post-operative reconstruction including prediction for two adults with spinal deformation.

## Acknowledgments:

Authors thanks for their support Menpo team ; "Menpo: A comprehensive platform for parametric image alignment and visual deformable models", In Proceedings of the ACM International Conference on Multimedia, MM '14, pages 679-682, New York, NY, USA, 2014. ACM.

# STATISTICAL SHAPE MODELING TO ANALYSE THE TALUS IN PEDIATRIC CLUBFOOT

Yixuan Feng<sup>1</sup>, Aaron Bishop<sup>1</sup>, Joseph Mitchell<sup>1</sup>, Xiaoping Qian<sup>1</sup>, Heidi-Lynn Ploeg<sup>2</sup>

<sup>1</sup> University of Wisconsin Madison, Madison, United States,

<sup>2</sup> University of Wisconsin-Madison, Madison, United States

## Purpose:

Serial Ponseti casting fails to completely correct idiopathic clubfoot deformities in up to 20% of pediatric patients<sup>1</sup>. In addition, recurrence of deformity occurs in up to 20% to 30% of clubfeet treated nonoperatively<sup>2</sup>. Statistical shape modeling (SSM) considers the entire set of shape features simultaneously and may provide a more accurate assessment of differences in bone morphology between two groups<sup>3</sup>. The purpose of this study was to compare the shape of the talus in normal and clubfeet using direct measurements and SSM.

## Methods:

Magnetic resonance image data from 16 children (average age 4.7 years) with residual deformity were compared with 10 age-matched, control ankles. 23 measurements were obtained from 3D models generated via reverse engineering (Mimics v17, Materialise, Leuven, Belgium). SSM, using non-rigid shape registration and principal component analysis, was conducted on 26 talar models.

## Results:

The talus width in clubfeet was 2.3 - 2.8 mm less than controls ( $p < 0.05$ ). The average neck angle was greater in clubfeet (132-154 degrees) than in controls (126-141 degrees,  $p < 0.05$ ). The talar neck depth was decreased in the clubfeet (2.2-2.3 mm) in comparison to the control group (3.6-3.8 mm,  $p < 0.01$ ). The relative contributions of the first five modes were 27.7%, 12.6%, 9.75%, 7.16% and 5.66% respectively (Figure 1). The mean ( $\pm$  standard deviation) of the first five standardized principal component (Std PC) scores for the control group were  $-0.47 \pm 0.98$ ,  $0.09 \pm 0.29$ ,  $-0.21 \pm 0.86$ ,  $0.63 \pm 0.68$  and  $0.35 \pm 0.91$ . For the clubfoot group, they were  $0.29 \pm 0.92$ ,  $-0.05 \pm 1.27$ ,  $0.13 \pm 1.09$ ,  $-0.40 \pm 0.97$  and  $-0.22 \pm 1.02$  (Figure 2).

## Conclusion:

Direct measurements and SSM found significant differences between the control and clubfoot groups. The mean value differences of 1st and 4th Std PC scores between two groups were significant. The standard deviation of 2nd Std PC scores in the clubfoot group was larger.

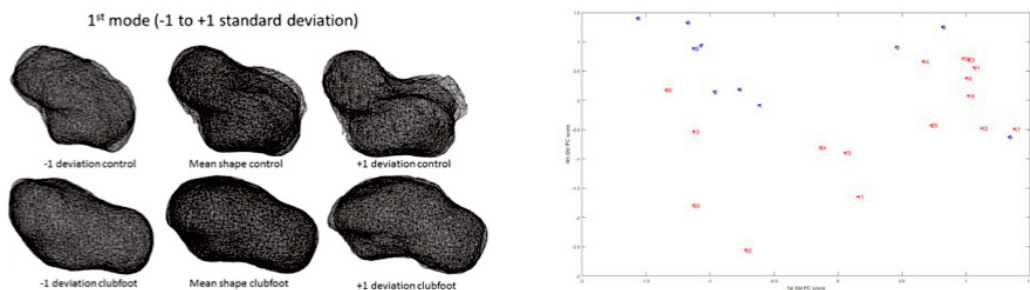


Figure 1: The 1st mode with scaling from -1, 0 to +1 standard deviation among 10 normal shapes (top) and 16 clubfoot shapes (bottom). Figure 2: The 1st Std PC scores versus 4th Std PC scores among 10 normal talus bones (Number 1 to 10 in blue) and 16 clubfeet (Number 11 to 26 in red).

## Acknowledgments:

The authors thank Dr. Kenneth Noonan from American Family Children's Hospital for his guidance and persistent help.

## References:

1. Docquier P.L., Leemrijse T., and Rombouts J.J.: Clinical and radiographic features of operatively treated stiff clubfeet after skeletal maturity: etiology of the deformities and how to prevent them. *Foot Ankle Int* 2006; 27: pp. 29-37
2. Uglow, M. G. & Kurup, H. V. Residual Clubfoot in Children. *Foot Ankle Clin.* 15, 245-264 (2010).
3. Golland, P., Grimson, W. E. L., Shenton, M. E. & Kikinis, R. Detection and analysis of statistical differences in anatomical shape. *Med. Image Anal.* 9, 69-86 (2005).